ADDITIONAL MATERIALS AVAILABLE ON THE HEI WEBSITE

Research Report 203
Mortality–Air Pollution Associations in Low-Exposure Environments (MAPLE)

Michael Brauer et al.

Additional Materials 2. Publications Resulting from This Research

Appendix A: Meng et al. 2019. Estimated long-term (1981–2016) concentrations of ambient fine particulate matter across North America from chemical transport modeling, satellite remote sensing, and ground-based measurements. Environ Sci Technol 53:5071–5079. (Reprinted from Meng et al with permission from American Chemical Society [ACS]. Further permissions related to this article should be directed to ACS.)

Appendix B: Latimer and Martin. 2019. Interpretation of measured aerosol mass scattering efficiency over North America using a chemical transport model. Atmos Chem Phys 19:2635–2653. (Distributed under Creative Commons Attribution 4.0 License.)

Appendix C: Pappin et al. 2019. Examining the shape of the association between low levels of fine particulate matter and mortality across three cycles of the Canadian Census Health and Environment Cohort. Environ Health Perspect 127. (Reprinted from Environmental Health Perspectives.)

Appendix D: Christidis et al. 2019. Low concentrations of fine particle air pollution and mortality in the Canadian Community Health Survey cohort. Environ Health doi:10.1186/s12940-019-0518-y. (This article is distributed under the terms of the Creative Commons Attribution 4.0 International License [http://creativecommons.org/licenses/by/4.0/].)

Appendix E: Erickson et al. 2019. Evaluation of a method to indirectly adjust for unmeasured covariates in the association between fine particulate matter and mortality. Environ Res 175:108–116. (Reprinted with permission from Elsevier.)

Appendix F: Pinault et al. 2017. Associations between fine particulate matter and mortality in the 2001 Canadian Census Health and Environment Cohort. Environ Res 159:406–415. (Reprinted with permission from Elsevier.)

These Additional Materials were not formatted or edited by HEI. These documents were part of the HEI Low-Exposure Epidemiology Review Panel's review process.

Correspondence may be addressed to Dr. Michael Brauer, University of British Columbia, School of Population and Public Health, 366A – 2206 East Mall, Vancouver, BC V6T1Z3, Canada; e-mail: *michael.brauer@ubc.ca.*

Although this document was produced with partial funding by the United States Environmental Protection Agency under Assistance Award CR–83467701 to the Health Effects Institute, it has not been subjected to the Agency's peer and administrative review and therefore may not necessarily reflect the views of the Agency, and no official endorsement by it should be inferred. The contents of this document also have not been reviewed by private party institutions, including those that support the Health Effects Institute; therefore, it may not reflect the views or policies of these parties, and no endorsement by them should be inferred.

Environmental Science & Technology

Article

Cite This: Environ. Sci. Technol. 2019, 53, 5071−5079

pubs.acs.org/est

Estimated Long-Term (1981−2016) Concentrations of Ambient Fine Particulate Matter across North America from Chemical Transport Modeling, Satellite Remote Sensing, and Ground-Based Measurements

Jun Meng,*[,†] Chi Li,[†] Randall V. Martin,[†,‡] Aaron van Donkelaar,[†] Perry Hystad,[§] and Michael Brauer[∥]

[†]Department of Physics and Atmospheric Science, Dalhousie University, Halifax, Nova Scotia B3H 4R2, Canada

[‡]Smithsonian Astrophysical Observatory, Harvard-Smithsonian Center for Astrophysics, Cambridge, Massachusetts 02138, United States

[§]College of Public Health and Human Sciences, Oregon State University, Corvallis, Oregon 97331, United States

[∥]School of Population and Public Health, The University of British Columbia, 2206 East Mall, Vancouver, British Columbia V6T 1Z3, Canada

Supporting Information

ABSTRACT: Accurate data concerning historical fine particulate matter ($PM_{2.5}$) concentrations are needed to assess long-term changes in exposure and associated health risks. We estimated historical $PM_{2.5}$ concentrations over North America from 1981 to 2016 for the first time by combining chemical transport modeling, satellite remote sensing, and ground-based measurements. We constrained and evaluated our estimates with direct ground-based $PM_{2.5}$ measurements when available and otherwise with historical estimates of $PM_{2.5}$ from PM_{10} measurements or total suspended particle (TSP) measurements. The estimated $PM_{2.5}$ concentrations were generally consistent with direct ground-based $PM_{2.5}$ measurements over their duration from 1988 onward (R^2 = 0.6 to 0.85) and to a lesser extent with $PM_{2.5}$ inferred from PM_{10} measurements from 1985 to 1998 (R^2 = 0.5 to 0.6). The collocated comparison of the trends of population-weighted annual average $PM_{2.5}$ from our estimates and ground-based measurements was highly consistent (RMSD = 0.66 μg m^{-3}). The population-weighted annual average $PM_{2.5}$ over North America decreased from 22 ± 6.4 μg m^{-3} in 1981, to 12 ± 3.2 μg m^{-3} in 1998, and to 7.9 ± 2.1 μg m^{-3} in 2016, with an overall trend of −0.33 μg m^{-3} yr^{-1} (95% CI: −0.35, −0.31).

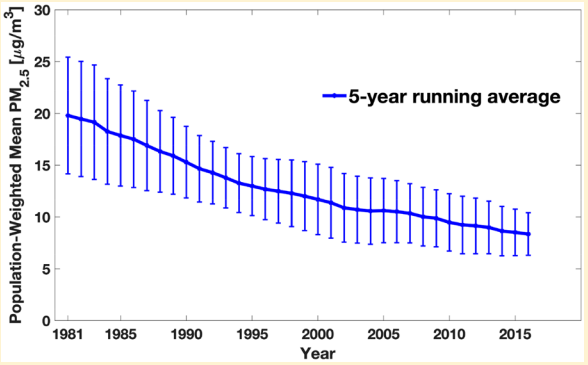

1. INTRODUCTION

Ambient fine particulate matter with aerodynamic diameter less than 2.5 μm ($PM_{2.5}$) is recognized as the leading environmental risk factor for the global burden of disease, with an estimated 4.1 million (3.6 to 4.6 million) attributable deaths in 2016.[1] Long-term exposure to high $PM_{2.5}$ adversely affects human health.[2−8] Several epidemiological studies reported adverse effects from long-term exposure at levels of $PM_{2.5}$ concentrations[9−12] below the World Health Organization (WHO) guideline (10 μg m^{-3} annual average), the United States standard (12 μg m^{-3} annual average), and the Canadian standard (10 μg m^{-3} annual average, to be reduced to 8.8 μg m^{-3} in 2020). However, the shape of the concentration−response function at these low $PM_{2.5}$ concentrations remains uncertain. Information about historical $PM_{2.5}$ concentrations across Canada and the United States is needed to understand long-term changes in exposure and their implications for health effects research.

Understanding historical long-term exposure is complicated by the paucity of $PM_{2.5}$ monitoring sites across North America before the late 1990s and by the spatial variation of monitoring sites over time. Ground-based monitoring provides historical time series at specific points for $PM_{2.5}$, PM_{10}, and total suspended particles (TSP). Several cohort studies have attempted to infer historical PM estimates using monitoring data for urban areas in later years.[4,13,14] A recent study by Kim et al.[15] demonstrated that historical measurements of PM_{10} and TSP offer valuable information for the prediction of

Received: December 6, 2018
Revised: April 8, 2019
Accepted: April 17, 2019
Published: April 17, 2019

DOI: 10.1021/acs.est.8b06875
Environ. Sci. Technol. 2019, 53, 5071−5079

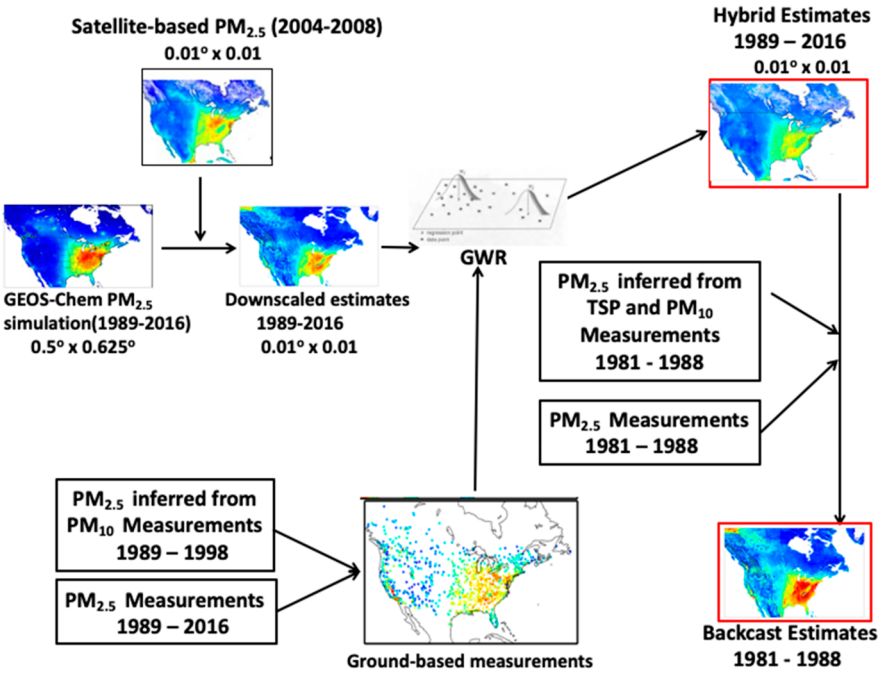

Figure 1. Overview of the estimation method.

historical $PM_{2.5}$ concentrations across the continental United States.

Additional sources of data are available to inform estimates of historical $PM_{2.5}$ spatial and temporal variations to improve the overall representativeness. Chemical transport modeling offers additional valuable information about historical $PM_{2.5}$ concentrations through the representation of atmospheric processes with historical emission inventories.[16−18] Satellite remote sensing offers a powerful additional constraint on $PM_{2.5}$ spatial distributions,[19,20] especially after 2002, when both the Terra and Aqua satellites were in orbit. Some studies[21,22] have developed prediction models to estimate historical $PM_{2.5}$ by backcasting using the ratio between $PM_{2.5}$ and PM_{10} or TSP observations. Other studies[19,23−25] use land-use regression, which includes predictor variables derived from geographic information systems or combines information from other PM measurements or satellite data. However, those studies focused on either smaller regions[21,25] or shorter durations.[19]

In this Article, we present historical estimates of $PM_{2.5}$ across North America by combining information from chemical transport modeling, satellite-derived $PM_{2.5}$ estimates, and ground-based monitoring from 1981 to 2016. These estimates can be used to assess long-term health impacts associated with low levels of $PM_{2.5}$ throughout North America.

2. MATERIALS AND METHODS

Figure 1 provides an overview of our method to develop estimates of historical $PM_{2.5}$ concentrations across North America by incorporating information from ground-based monitoring, chemical transport modeling, and satellite-derived $PM_{2.5}$. We started with a fine-resolution chemical transport model (GEOS-Chem) simulation across North America for 1989−2016. We downscaled the simulation to $0.01^\circ \times 0.01^\circ$ using a satellite-derived $PM_{2.5}$ data set.[20] We applied geographically weighted regression (GWR) to the downscaled simulation to incorporate information from ground-based measurements into the estimates. For 1981−1988, we relied on information on interannual variation from ground-based measurements to backcast the gridded $PM_{2.5}$ concentrations. Each step is described further below.

2.1. Historical Particulate Matter Monitoring Data. We collected ground-based measurements for 1981−2016 across Canada and the United States. Canadian PM data were obtained from the National Air Pollutant Surveillance (NAPS) (http://maps-cartes.ec.gc.ca/rnspa-naps/data.aspx?lang=en). This database includes continuous PM measurement data, dichotomous sampler (dichot, PM_{10}, and $PM_{2.5}$) data, and TSP data. Instrument-specific calibrations were applied as recommended by the Canadian Council of Ministers of the Environment (CCME).[26] Daily PM data for the United States were obtained from the United States Air Quality System Data Mart for PM_{10} and $PM_{2.5}$ (https://aqs.epa.gov/aqsweb/airdata/download_files.html). In addition, data from the inhalable particle network (IPN), which consisted of $PM_{2.5}$ measurements in the early 1980s, were included. Table S1 summarizes the available monitoring data by measurement type in the selected years (1981−2016). In Canada, dichot $PM_{2.5}$ and PM_{10} sampling began in the mid-1980s, followed by continuous $PM_{2.5}$ monitoring in the late 1990s. In the United States, most PM_{10} sampling began in the late 1980s, followed by widespread $PM_{2.5}$ monitoring in 1999. Limited $PM_{2.5}$ measurements were available prior to 1999. Separate predictive models based on the uniform method were created for Canadian and United States monitoring data because the larger number of monitoring stations in the United States would overwhelm the Canadian dataset. Detailed information about the predictive models of inferring monthly $PM_{2.5}$ concentrations from the historical PM_{10} and TSP measurements is provided in the Supporting Information SI.1

2.2. Estimated Historical Gridded $PM_{2.5}$ Data. *2.2.1. GEOS-Chem Chemical Transport Model.* We use the GEOS-Chem chemical transport model (version 11-01, http://www.geos-chem.org), with updated historical emissions inventories and meteorological data, to consistently simulate

DOI: 10.1021/acs.est.8b06875
Environ. Sci. Technol. 2019, 53, 5071−5079

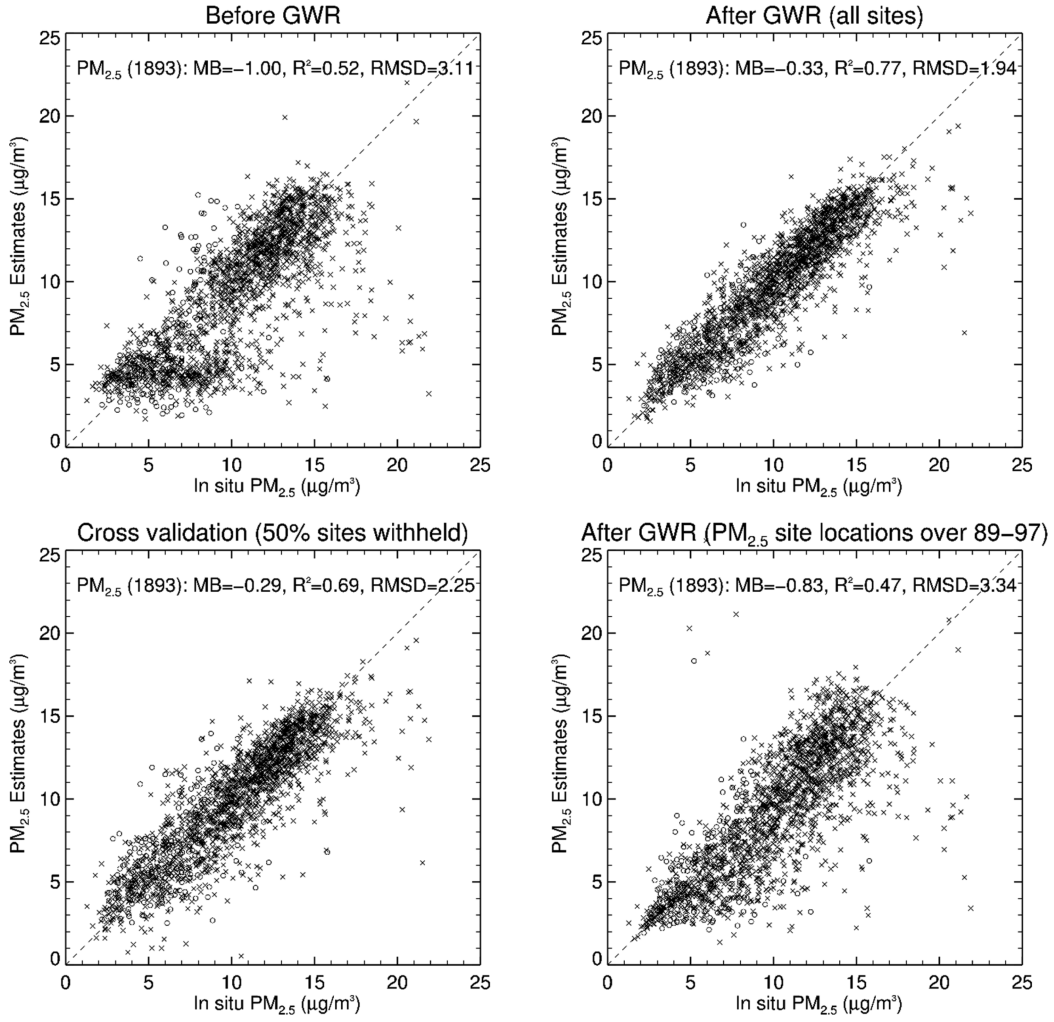

Figure 2. Comparison over 2004−2008 of mean $PM_{2.5}$ estimates with in situ measurements before (top left) and after GWR adjustment using all sites (top right), using cross-validation sites using 50% random holdout (bottom left), and using $PM_{2.5}$ sites present over 1989−1997 (bottom right). Open circles are Canadian sites, and crosses are United States sites. The number of sites is shown in brackets. Statistics shown are mean bias (MB, in $\mu g\ m^{-3}$), coefficient of determination (R^2), and root-mean-square difference (RMSD, in $\mu g\ m^{-3}$).

$PM_{2.5}$ concentrations across North America for 1989−2016. GEOS-Chem includes detailed aerosol−oxidant chemistry.[27,28] The simulation of concentrations of $PM_{2.5}$ components includes the sulfate−nitrate−ammonium (SNA) aerosol system,[28,29] mineral dust,[30] sea salt,[31] and carbonaceous aerosol,[32] with updates to black carbon[33] and secondary organic aerosol (SOA),[34,35] including an aqueous-phase mechanism for SOA from isoprene.[35] Our simulation used a relative-humidity-dependent and composition-dependent fixed size distribution following Martin et al.,[36] with updates to organics[37] and mineral dust.[38] We drove the simulation using MERRA-2 meteorological data from NASA's Global Modeling and Assimilation Office (GMAO) with a nested resolution at 0.5° × 0.625° over North America for 1989−2016 for which updated historical emissions were available. Anthropogenic emissions over North America were from the 2011 National Emissions Inventory (NEI2011, http://www.epa.gov/air-emissions-inventories) for the United States and the Criteria Air Contaminants (CAC, http://www.ec.gc.ca/inrp-npri/) for Canada, with historical scale factors applied to each simulating year. Black carbon (BC) and organic carbon (OC) emissions were calculated by applying sector-specific OC and BC to $PM_{2.5}$ emission ratios.[18,39,40] Open fire emissions were from GFED4[41] for 1997−2016 and from the RETRO fire emission inventory[42] for earlier years.

2.2.2. Creation of Historical Gridded $PM_{2.5}$ Data Set. Given our objective of a consistent data set over the entire 1989−2016 period and the lack of satellite aerosol optical depth (AOD) for the entire period, we used the 5-year average from near the middle of the period (2004−2008) of geophysical satellite-based $PM_{2.5}$ estimates (referred to as PM_{sat}),[20] derived from both the Terra and Aqua satellites, to downscale the GEOS-Chem model simulation (1989−2016) to a resolution relevant for exposure at 0.01° × 0.01° following Li et al.[18] We calculated the ratio between PM_{sat} and the 5 yr average (2004−2008) of GEOS-Chem simulations. Then, we used this ratio to downscale simulations in all years from 1989 to 2016. The downscaling process does not change the simulated relative temporal variation of $PM_{2.5}$ because the same scale factor was applied to all years. This downscaled estimate (referred to as PM_{scl}) contained fine-scale spatial information from satellite-derived $PM_{2.5}$ estimates (PM_{sat}) and long-term temporal information from the GEOS-Chem simulation. We evaluate the approach by excluding the satellite-based estimates.

DOI: 10.1021/acs.est.8b06875
Environ. Sci. Technol. 2019, 53, 5071−5079

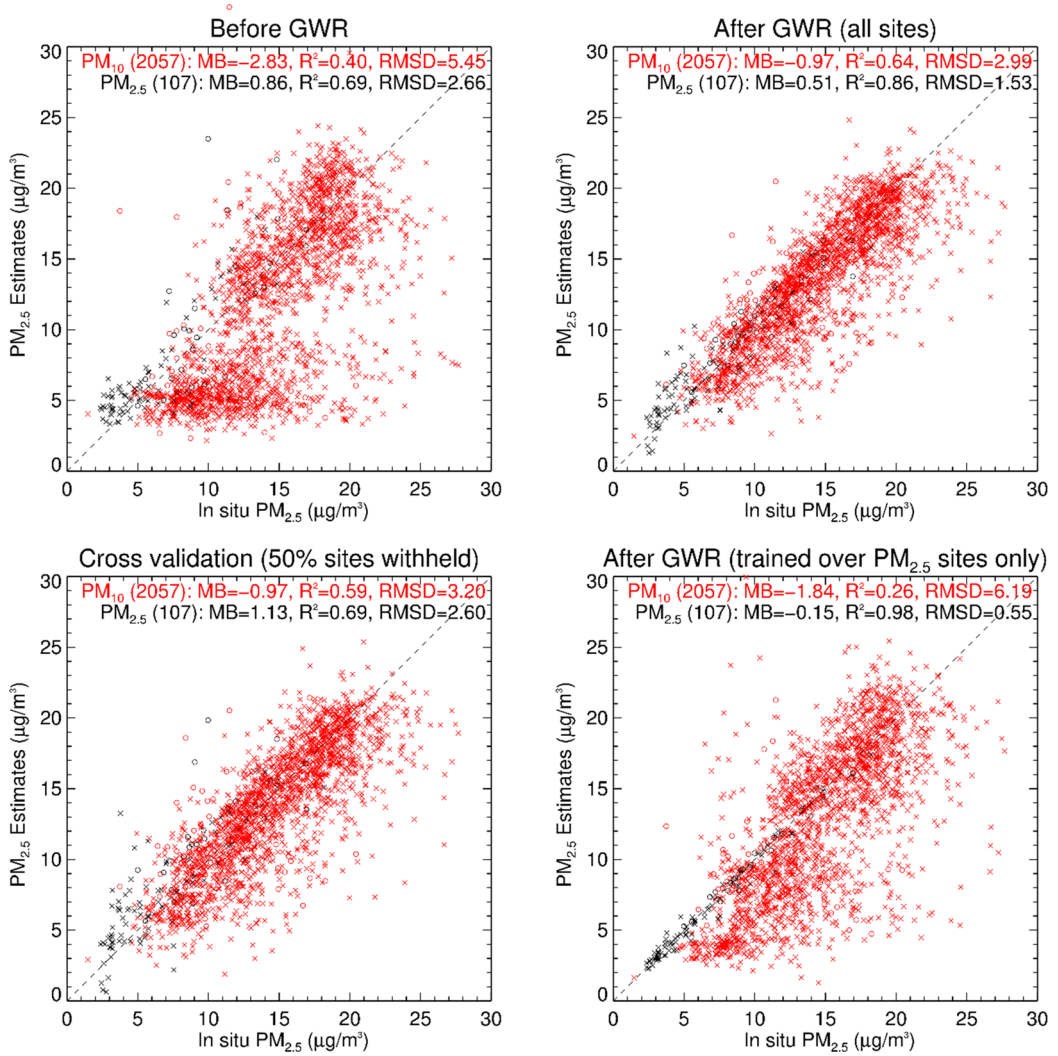

Figure 3. Comparison over 1992−1996 of mean $PM_{2.5}$ estimates with in situ measurements before (top left) and after GWR adjustment using all sites (top right), using cross validation using 50% random holdout (bottom left), and using only $PM_{2.5}$ sites (bottom right). Open circles are Canadian sites, and crosses are United States sites. Number of sites is shown in brackets. Comparison of $PM_{2.5}$ (black) and PM_{10} (red) sites is shown separately. Statistics shown are mean bias (MB, in $\mu g\ m^{-3}$), coefficient of determination (R^2), and root-mean-square difference (RMSD, in $\mu g\ m^{-3}$).

Ground-based monitoring offers reliable information on $PM_{2.5}$ when and where available. We used this information to constrain our estimates. We included monitor information across both the United States and Canada to produce a continuous surface for North America. Following van Donkelaar et al.,[20] we applied GWR to PM_{scl} over 1989−2016 using available $PM_{2.5}$ observations and $PM_{2.5}$ concentrations inferred from PM_{10} observations. GWR[43] is a multiple regression, an extension of least-squares regression, to allow predictor coefficients to vary by choosing different spatial weighting function at several geographic locations according to their inverse-squared distance from individual observation sites. We used GWR to regress the spatial relationship between multiple predictors and the bias between $PM_{2.5}$ estimates and $PM_{2.5}$ measurements. Our predictors in GWR include urban land cover (ULC), subgrid elevation difference (SED), and aerosol chemical composition from GEOS-Chem simulation. We fit the GWR model at the same resolution ($0.01° \times 0.01°$) as the downscaled $PM_{2.5}$ estimates, which was scaled by satellite-driven $PM_{2.5}$ following eq 1

$$\begin{aligned}(\text{measured } PM_{2.5} - \text{estimated } PM_{2.5}) &= \alpha_1 \text{ULC} + \alpha_2 \text{SED} + \alpha_3 \text{SUL} + \alpha_4 \text{NIT} + \alpha_5 \text{PrC} \\ &+ \alpha_6 \text{SOA} + \alpha_7 \text{DST} + \varepsilon \end{aligned} \quad (1)$$

where α_1 to α_7 represented the spatial weighted predictor coefficients for each predictor and ε is the error. ULC is the percent of urban land cover from the 500 m spatial resolution MODIS land cover type product.[44] The SED is the difference between the site elevations, which are from the ETOPO1 Global Relief Model of the National Geophysical Data Center,[45] and the annual mean elevation of the GEOS-Chem grid cell. SUL, NIT, PrC, SOA, and DST are sulfate, nitrate, primary carbon, secondary carbon, and dust, respectively, as simulated with GEOS-Chem. We conducted sensitivity tests by changing the weight of PM_{10} observations in the GWR regression and found that a reduction by 75% of the weight of PM_{10} best represented its uncertainty compared with direct $PM_{2.5}$ measurements from ground-based measurements, GEOS-Chem transport model simulations, and satellite remote sensing.

DOI: 10.1021/acs.est.8b06875
Environ. Sci. Technol. 2019, 53, 5071−5079

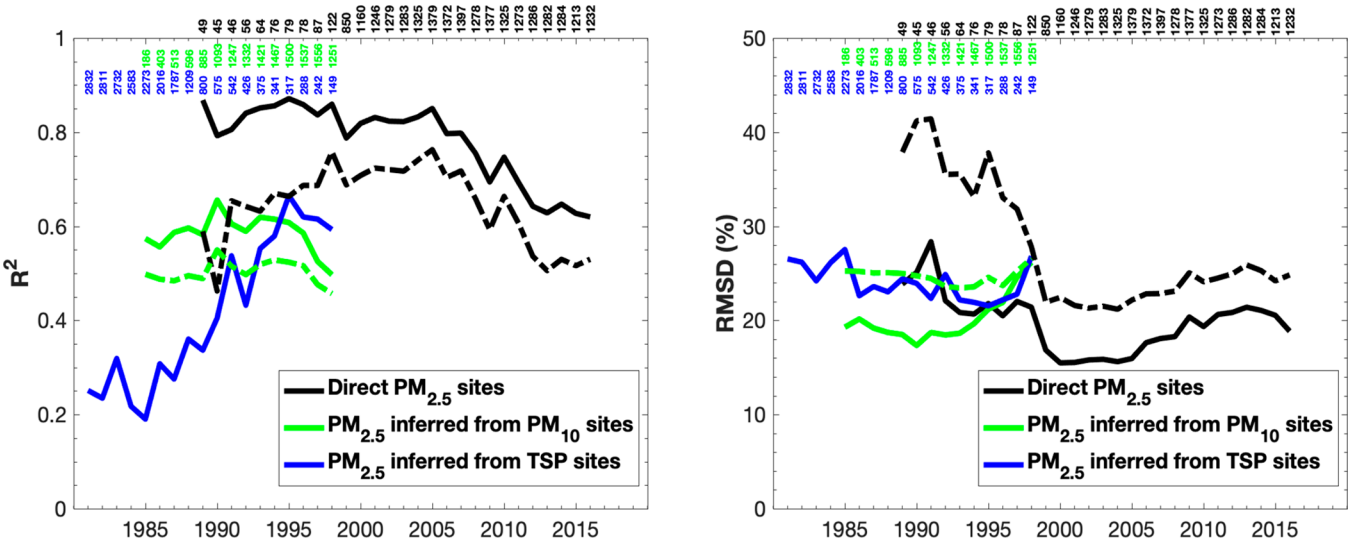

Figure 4. Statistics (R^2 and RMSD) of estimated $PM_{2.5}$ against ground-based measurements from 1981 to 2016. Solid lines indicate the performance of base estimates. Dashed lines indicate the performance of sensitivity estimates that exclude satellite remote sensing information (no blue dashed line). Numbers at the top of each panel indicate the number of monitors of direct $PM_{2.5}$ (black), $PM_{2.5}$ inferred from PM_{10} (green), and $PM_{2.5}$ inferred from TSP (blue).

For 1981−1988, reliable emission inventories were not available for the GEOS-Chem simulation. Instead, we used the information on interannual variation from ground-based measurements to backcast the gridded $PM_{2.5}$ concentrations following previous studies.[21,22] Ground-based measurements include TSP measurements, PM_{10} measurements, and $PM_{2.5}$ measurements. Ground-based $PM_{2.5}$ concentrations inferred from TSP measurements were included for this time period because fewer than 200 PM_{10} sites existed before 1986, and even fewer $PM_{2.5}$ monitoring sites existed. For each year (e.g., 1988), we calculated the ratio between the annual mean $PM_{2.5}$ of this year and the following 3-year mean $PM_{2.5}$ (e.g., 1989−1991) for each ground-based monitoring site. We used the ratios from TSP sites as the basis, which were overwritten by the ratios from PM_{10} sites and then by the ratios from $PM_{2.5}$ sites. This ratio field from ground-based measurements was then interpolated to other grids using distance-weighted interpolation. Finally, we applied this gridded ratio field to the following 3-year mean $PM_{2.5}$ estimates to get the estimated $PM_{2.5}$ for each year. The process is described by eq 2

$$Y(t) = \gamma[Y(t+1) + Y(t+2) + Y(t+3)]/3 \quad (2)$$

where $Y(t)$ represents the $PM_{2.5}$ estimates in year t and γ is the gridded ratio field.

We evaluated the backcasting method by repeating the procedure for 2001−2008 using measurements from 2001 to 2011 for comparison with our estimates from 2001 to 2008 (Table S5).

We calculated the overall root-mean-square difference (RMSD) between the estimates and measurements for each year over 1981−2016 as a measure of uncertainty.

3. RESULTS AND DISCUSSION

We first evaluated the approach in the years when only $PM_{2.5}$ stations were used for GWR adjustment to statistically incorporate information from ground-based observations into the downscaled model results. Figure 2 shows scatter plots of 2004−2008 mean $PM_{2.5}$ from the downscaled simulation (PM_{scl}) before and after GWR adjustment versus in situ $PM_{2.5}$. As found by van Donkelaar et al.,[20] the GWR model significantly reduces the mean bias (MB) and RMSD over both Canada and the United States Out-of-sample cross validation using 50% of randomly selected sites to train the GWR model exhibits significantly improved performance (R^2 = 0.69; RMSD = 2.3 $\mu g\ m^{-3}$) (bottom left panel) compared with the base case (R^2 = 0.52; RMSD = 3.1 $\mu g\ m^{-3}$). In such a holdback analysis, GWR parameter coefficients are trained using only 50% of available ground-based monitors. The withheld sites provide an independent data set with which to evaluate the quality of fused $PM_{2.5}$ estimates in areas without ground-based observation. The improvement at these independent sites suggests improvement in the GWR-adjusted surface, even at locations away from ground-based observation. The bottom right panel of Figure 2 shows the 2004−2008 mean performance of GWR-adjusted values made using only the $PM_{2.5}$ sites that were also available before 1998 (<70 sites in total), consisting mostly of remote and rural United-States-based sites. Limiting the GWR-based adjustment to only these earlier vailable $PM_{2.5}$ sites provided no improvement in agreement compared with the initial estimates without GWR. The negative MB in PM_{scl} ($-1.00\ \mu g\ m^{-3}$) (top left panel) is not corrected in the adjusted estimates ($-0.83\ \mu g\ m^{-3}$) (bottom right panel) due to a lack of representative urban and Eastern sites, which generally have higher $PM_{2.5}$ levels. Complementary information from PM_{10} sites that are representative of urban environments is necessary for early years.

Figure 3 shows scatter plots for the 1992−1996 time period to evaluate the performance of $PM_{2.5}$ inferred from PM_{10}. The top panels show that the performance of the scaled geophysical estimate is promising, with an R^2 versus $PM_{2.5}$ monitors of 0.69 that increases to 0.86 after GWR adjustment. The RMSD decreases from 2.7 to 1.5 $\mu g\ m^{-3}$ over ~100 $PM_{2.5}$ sites in the adjusted estimates. For ~2000 PM_{10} sites, significantly improved agreement is also found after GWR adjustment. Cross validation with 50% out-of-sample sites (bottom left) further confirms the overall robustness of the approach. As found in the 2004−2008 period, using only $PM_{2.5}$ sites for

DOI: 10.1021/acs.est.8b06875
Environ. Sci. Technol. 2019, 53, 5071−5079

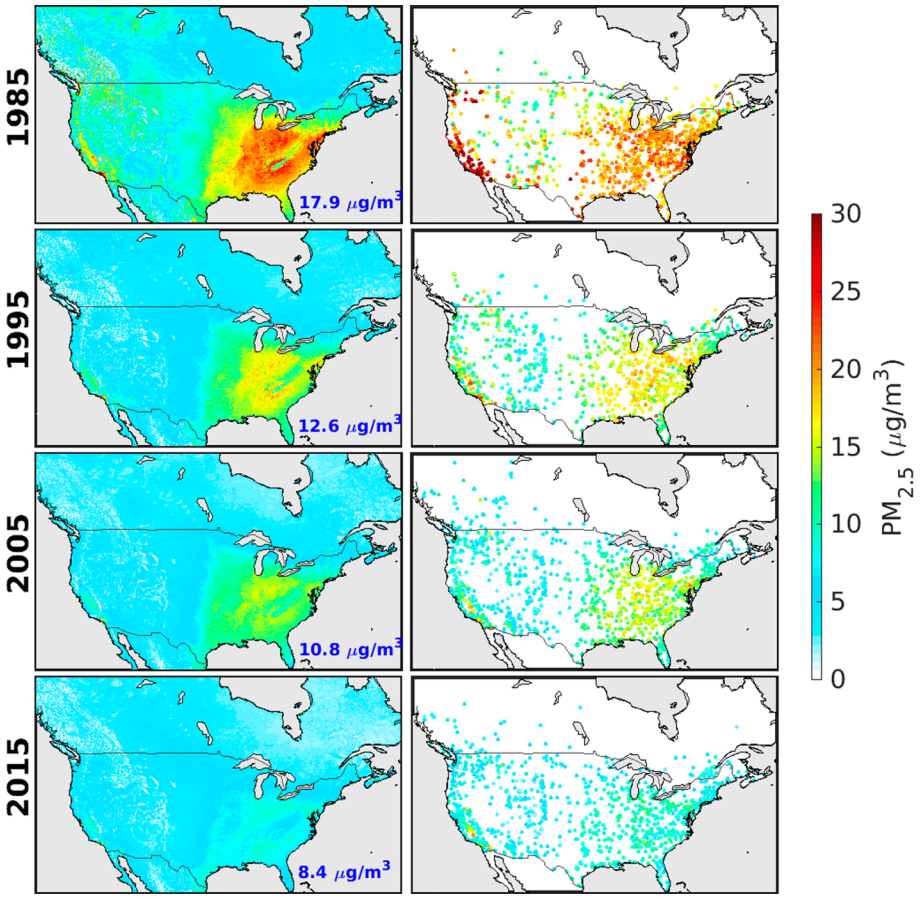

Figure 5. Estimated fine particulate matter annual means in 1985, 1995, 2005, and 2015 over North America. Left panels are estimated $PM_{2.5}$. Inset values in the left panel are the population-weighted average $PM_{2.5}$ mass. Right panels indicate $PM_{2.5}$ derived from ground-based measurements of $PM_{2.5}$, PM_{10}, and TSP.

GWR modeling does not improve the overall representation of the estimates, especially for PM_{10} sites in urban areas.

Figure 4 shows the R^2 and RMSD for each year (1981−2016) of the estimates versus ground-based measurements to provide an overall assessment of uncertainty. Only $PM_{2.5}$ data are used over 1999−2016 because sufficient $PM_{2.5}$ measurements are available after 1999. Because the number of PM_{10} sites significantly decreases prior to 1989 (~1000 in 1989, ~600 in 1988, ~400 sites in 1986, and <50 sites in 1984), the backcasting from 1985 to 1981 is primarily based on the trend information from TSP-based estimates and is expected to be more uncertain. The R^2 increases with the increase in PM_{10} sites for 1985−1990. The R^2 is ~0.8 for 1989−2005 compared with $PM_{2.5}$ sites. The relative RMSD at only $PM_{2.5}$ sites drops from 30% in the early 1990s to <20% prior to 1999, when the $PM_{2.5}$ measurements became more widespread. The decrease in R^2 after 2008 reflects weaker spatial $PM_{2.5}$ gradients in recent years as $PM_{2.5}$ levels decrease across North America. Higher RMSD errors are expected before 1999 due to more uncertainties in emission inventories as well as larger uncertainties in the monitor data used in GWR adjustments. Overall, the GWR-adjusted $PM_{2.5}$ estimates yield an estimated error of <20% since 1999 and <30% from 1981 to 1998.

We tested how the satellite-derived $PM_{2.5}$ data used for downscaling affected the performance of the estimated data set. Supporting Information SI.3 describes sensitivity estimates of $PM_{2.5}$ data without satellite remote sensing. The R^2 values of these sensitivity estimates are between 0.1 and 0.2 lower than our base estimate across all years, with larger differences in years preceding 1999 when fewer $PM_{2.5}$ measurements were available. The relative RMSDs of the sensitivity estimates at direct observed $PM_{2.5}$ sites are higher than the base estimates by 10 to 20%. This analysis indicates the significance of the constraints on $PM_{2.5}$ spatial distributions offered by satellite remote sensing.

Figure 5 shows the distribution of $PM_{2.5}$ estimates and ground-based measurements for 1985, 1995, 2005, and 2015 from this study. Enhancements in both the GWR -adjusted estimates and ground-based measurements are apparent across the Eastern United States and California. The estimated $PM_{2.5}$ is generally consistent with ground-based measurements (Figure 4), especially with the direct $PM_{2.5}$ measurements. $PM_{2.5}$ concentrations decreased dramatically during the last three decades, especially in the Eastern United States

Figure 6 shows the time series of population-weighted annual average $PM_{2.5}$ concentrations across North America. We used gridded population estimates from the Socio-economic Data and Applications Center[46,47] for calculating the population-weighted average (Supporting Information SI.3). The population-weighted annual average $PM_{2.5}$ over North America decreased from 22 ± 6.4 $\mu g\ m^{-3}$ in 1981 to 7.9 ± 2.1 $\mu g\ m^{-3}$ in 2016. The linear tendency over this period is −0.33 ± 0.2 $\mu g\ m^{-3}\ yr^{-1}$. Both time series of the in situ measurements and estimates of population-weighted annual mean $PM_{2.5}$ exhibit minor peaks in 2005 and 2007. The collocated comparison of the trends of population-weighted

DOI: 10.1021/acs.est.8b06875
Environ. Sci. Technol. 2019, 53, 5071−5079

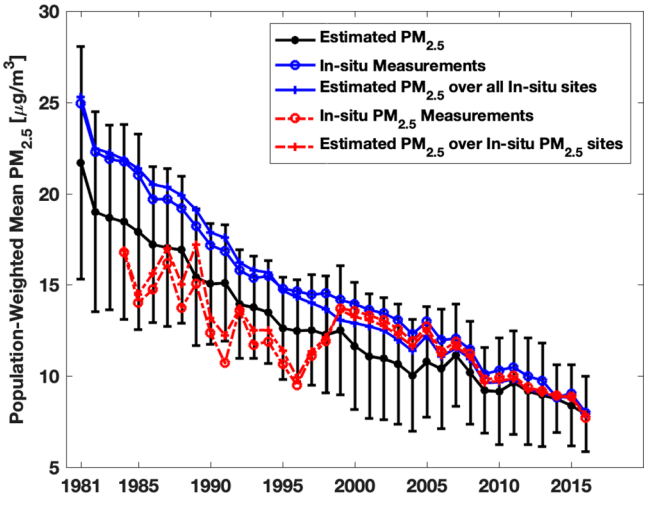

Figure 6. Time series of population-weighted average annual $PM_{2.5}$ concentrations across North America. Error bars are included for population-weighted annual mean estimated $PM_{2.5}$ concentrations.

annual average $PM_{2.5}$ from our estimates and ground-based measurements is highly consistent (RMSD = 0.66 $\mu g\ m^{-3}$) over 1985−1995. The population-weighted annual average $PM_{2.5}$ calculated from direct $PM_{2.5}$ sites is 20% lower than that calculated from all in situ sites, illustrating the effects of changes in monitor placement over time when assessing long-term changes in ambient $PM_{2.5}$ and the value of spatiotemporally continuous $PM_{2.5}$ estimates from this work. Larger error bars prior to 1990 reflect greater uncertainty in the TSP data set.

Figure S5 shows regional time series of the population-weighted annual average $PM_{2.5}$. Figure S6 shows regional time series of the relative percentage change of population-weighted annual average $PM_{2.5}$ concentrations using 2016 as the reference year. Northwestern North America has the most dramatic decrease for population-weighted average $PM_{2.5}$ concentrations with a factor of 2.7 decrease over 1981−2016, followed by Southeastern and Northeastern North America, with a factor of 2.4 decrease over 1981−2016. The relative changes in North Central, South Central, and Southwestern North America are similar, with a factor of 1.6 to 2.0 decrease in population-weighted $PM_{2.5}$ over 1981−2016. Overall, the spatially resolved historical $PM_{2.5}$ data set across North America reveals a factor of 1.7 decrease in population-weighted $PM_{2.5}$ over 1981−2016.

The comparison with previous estimates of historical $PM_{2.5}$ concentrations is instructive. Our estimated historical $PM_{2.5}$ concentrations from 1982−1991 in the Southeastern United States indicate a decrease of 3.9 $\mu g\ m^{-3}$, similar to the reported decrease of 3−5 $\mu g\ m^{-3}$ found by Parkhurst et al.[21] We find similar large-scale reductions in historical $PM_{2.5}$ concentrations from 1981−2000, as found by Lall et al.,[22] albeit with smoother temporal trends in the present study that are more consistent with Kim et al.[15] The primary difference with our prior historical $PM_{2.5}$ estimates[48−50] is that our current study spans a time period (1981−2016) that is about twice as long as our prior work by including more trend information from our GEOS-Chem simulation and includes historical ground-based measurements prior to 1999. Nonetheless, the population-weighted trends from our current data set remain within 0.03 $\mu g\ m^{-3}\ yr^{-1}$ of our prior work, indicating overall consistency, as further discussed in the Supporting Information SI.4.

■ ASSOCIATED CONTENT

Supporting Information

The Supporting Information is available free of charge on the ACS Publications website at DOI: 10.1021/acs.est.8b06875.

Detailed description of prediction of monitoring historical $PM_{2.5}$ from measured PM_{10} and TSP, sensitivity test of estimated $PM_{2.5}$ data set without satellite remote sensing information, population data and further discussion of population-weighted $PM_{2.5}$ trends, and supporting figures for Section 3 (PDF)

■ AUTHOR INFORMATION

Corresponding Author

*Phone: (902) 932-3886; e-mail: Jun.Meng@dal.ca.

ORCID

Jun Meng: 0000-0001-9716-1051

Chi Li: 0000-0002-8992-7026

Aaron van Donkelaar: 0000-0002-2998-8521

Michael Brauer: 0000-0002-9103-9343

Notes

The authors declare no competing financial interest.

The annual mean estimated $PM_{2.5}$ for 1981−2016 across the North America data set has been deposited in the Zenodo Digital Repository (DOI: 10.5281/zenodo.2616769).[51]

■ ACKNOWLEDGMENTS

This research was supported by research agreement 4952-RFA14-3/16-3 with the Health Effects Institute (HEI), an organization jointly funded by the United States Environmental Protection Agency (EPA) (Assistance Award No. R-82811201) and certain motor vehicle and engine manufacturers. The contents of this article do not necessarily reflect the views of HEI, or its sponsors, nor do they necessarily reflect the views and policies of the EPA or motor vehicle and engine manufacturers. We are grateful to the Atlantic Computational Excellence Network and Compute Canada for computing resources.

■ REFERENCES

(1) Gakidou, E.; Afshin, A.; Abajobir, A. A.; Abate, K. H.; Abbafati, C.; Abbas, K. M.; Abd-Allah, F.; Abdulle, A. M.; Abera, S. F.; Aboyans, V.; et al. Global, Regional, and National Comparative Risk Assessment of 84 Behavioural, Environmental and Occupational, and Metabolic Risks or Clusters of Risks, 1990−2016: A Systematic Analysis for the Global Burden of Disease Study 2016. *Lancet* **2017**, *390* (10100), 1345−1422.

(2) Beelen, R.; Raaschou-Nielsen, O.; Stafoggia, M.; Andersen, Z. J.; Weinmayr, G.; Hoffmann, B.; Wolf, K.; Samoli, E.; Fischer, P.; Nieuwenhuijsen, M.; et al. Effects of Long-Term Exposure to Air Pollution on Natural-Cause Mortality: An Analysis of 22 European Cohorts within the Multicentre ESCAPE Project. *Lancet* **2014**, *383* (9919), 785−795.

(3) Boldo, E.; Medina, S.; LeTertre, A.; Hurley, F.; Mücke, H.-G.; Ballester, F.; Aguilera, I. Apheis: Health Impact Assessment of Long-Term Exposure to $PM_{2.5}$ in 23 European Cities. *Eur. J. Epidemiol.* **2006**, *21* (6), 449−458.

(4) Caiazzo, F.; Ashok, A.; Waitz, I. A.; Yim, S. H. L.; Barrett, S. R. H. Air Pollution and Early Deaths in the United States. Part I: Quantifying the Impact of Major Sectors in 2005. *Atmos. Environ.* **2013**, *79*, 198−208.

(5) Schwartz, J. Harvesting and Long Term Exposure Effects in the Relation between Air Pollution and Mortality. *Am. J. Epidemiol.* **2000**, *151* (5), 440−448.

DOI: 10.1021/acs.est.8b06875
Environ. Sci. Technol. 2019, 53, 5071−5079

(6) Weichenthal, S.; Villeneuve, P. J.; Burnett, R. T.; van Donkelaar, A.; Martin, R. V.; Jones, R. R.; DellaValle, C. T.; Sandler, D. P.; Ward, M. H.; Hoppin, J. A. Long-Term Exposure to Fine Particulate Matter: Association with Nonaccidental and Cardiovascular Mortality in the Agricultural Health Study Cohort. *Environ. Health Perspect.* **2014**, *122* (6), 609−615.
(7) Zhang, Y.; West, J. J.; Mathur, R.; Xing, J.; Hogrefe, C.; Roselle, S. J.; Bash, J. O.; Pleim, J. E.; Gan, C.-M.; Wong, D. C. Long-Term Trends in the Ambient $PM_{2.5}$- and O_3-Related Mortality Burdens in the United States under Emission Reductions from 1990 to 2010. *Atmos. Chem. Phys.* **2018**, *18* (20), 15003−15016.
(8) Pope, C. A.; Ezzati, M.; Dockery, D. W. Fine-Particulate Air Pollution and Life Expectancy in the United States. *N. Engl. J. Med.* **2009**, *360* (4), 376−386.
(9) Crouse, D. L.; Peters, P. A.; van Donkelaar, A.; Goldberg, M. S.; Villeneuve, P. J.; Brion, O.; Khan, S.; Atari, D. O.; Jerrett, M.; Pope, C. A.; Brauer, M.; Brook, J. R.; Martin, R. V.; Stieb, D.; Burnett, R. T. Risk of Nonaccidental and Cardiovascular Mortality in Relation to Long-Term Exposure to Low Concentrations of Fine Particulate Matter: A Canadian National-Level Cohort Study. *Environ. Health Perspect.* **2012**, *120* (5), 708−714.
(10) Hales, S.; Blakely, T.; Woodward, A. Air Pollution and Mortality in New Zealand: Cohort Study. *J. Epidemiol. Community Health* **2012**, *66* (5), 468−473.
(11) Schwartz, J.; Bind, M.-A.; Koutrakis, P. Estimating Causal Effects of Local Air Pollution on Daily Deaths: Effect of Low Levels. *Environ. Health Perspect.* **2017**, *125* (1), 23−29.
(12) Shi, L.; Zanobetti, A.; Kloog, I.; Coull, B. A.; Koutrakis, P.; Melly, S. J.; Schwartz, J. D. Low-Concentration $PM_{2.5}$ and Mortality: Estimating Acute and Chronic Effects in a Population-Based Study. *Environ. Health Perspect.* **2016**, *124* (1), 46−52.
(13) Beelen, R.; Hoek, G.; van den Brandt, P. A.; Goldbohm, R. A.; Fischer, P.; Schouten, L. J.; Jerrett, M.; Hughes, E.; Armstrong, B.; Brunekreef, B. Long-Term Effects of Traffic-Related Air Pollution on Mortality in a Dutch Cohort (NLCS-AIR Study). *Environ. Health Perspect.* **2008**, *116* (2), 196−202.
(14) Lepeule, J.; Laden, F.; Dockery, D.; Schwartz, J. Chronic Exposure to Fine Particles and Mortality: An Extended Follow-up of the Harvard Six Cities Study from 1974 to 2009. *Environ. Health Perspect.* **2012**, *120* (7), 965−970.
(15) Kim, S.-Y.; Olives, C.; Sheppard, L.; Sampson, P. D.; Larson, T. V.; Keller, J. P.; Kaufman, J. D. Historical Prediction Modeling Approach for Estimating Long-Term Concentrations of $PM_{2.5}$ in Cohort Studies before the 1999 Implementation of Widespread Monitoring. *Environ. Health Perspect.* **2017**, *125* (1), 38−46.
(16) Hoesly, R. M.; Smith, S. J.; Feng, L.; Klimont, Z.; Janssens-Maenhout, G.; Pitkanen, T.; Seibert, J. J.; Vu, L.; Andres, R. J.; Bolt, R. M.; et al. Historical (1750−2014) Anthropogenic Emissions of Reactive Gases and Aerosols from the Community Emissions Data System (CEDS). *Geosci. Model Dev.* **2018**, *11* (1), 369−408.
(17) EPA. *Air Quality Improves as America Grows*, 2017. https://gispub.epa.gov/air/trendsreport/2017/ (accessed Nov 11, 2018).
(18) Li, C.; Martin, R. V.; van Donkelaar, A.; Boys, B. L.; Hammer, M. S.; Xu, J.-W.; Marais, E. A.; Reff, A.; Strum, M.; Ridley, D. A.; Crippa, M.; Brauer, M.; Zhang, Q. Trends in Chemical Composition of Global and Regional Population-Weighted Fine Particulate Matter Estimated for 25 Years. *Environ. Sci. Technol.* **2017**, *51* (19), 11185−11195.
(19) Ma, Z.; Hu, X.; Sayer, A. M.; Levy, R.; Zhang, Q.; Xue, Y.; Tong, S.; Bi, J.; Huang, L.; Liu, Y. Satellite-Based Spatiotemporal Trends in $PM_{2.5}$ Concentrations: China, 2004−2013. *Environ. Health Perspect.* **2016**, *124* (2), 184−192.
(20) van Donkelaar, A.; Martin, R. V.; Spurr, R. J. D.; Burnett, R. T. High-Resolution Satellite-Derived $PM_{2.5}$ from Optimal Estimation and Geographically Weighted Regression over North America. *Environ. Sci. Technol.* **2015**, *49* (17), 10482−10491.
(21) Parkhurst, W. J.; Tanner, R. L.; Weatherford, F. P.; Valente, R. J.; Meagher, J. F. Historic $PM_{2.5}/PM_{10}$ Concentrations in the Southeastern United States - Potential Implications of the Revised Particulate Matter Standard. *J. Air Waste Manage. Assoc.* **1999**, *49* (9), 1060−1067.
(22) Lall, R.; Kendall, M.; Ito, K.; Thurston, G. D. Estimation of Historical Annual $PM_{2.5}$ Exposures for Health Effects Assessment. *Atmos. Environ.* **2004**, *38* (31), 5217−5226.
(23) Beckerman, B. S.; Jerrett, M.; Serre, M.; Martin, R. V.; Lee, S.-J.; van Donkelaar, A.; Ross, Z.; Su, J.; Burnett, R. T. A Hybrid Approach to Estimating National Scale Spatiotemporal Variability of $PM_{2.5}$ in the Contiguous United States. *Environ. Sci. Technol.* **2013**, *47* (13), 7233−7241.
(24) Eeftens, M.; Beelen, R.; de Hoogh, K.; Bellander, T.; Cesaroni, G.; Cirach, M.; Declercq, C.; Dèdelè, A.; Dons, E.; de Nazelle, A.; et al. Development of Land Use Regression Models for $PM_{2.5}PM_{2.5}$ Absorbance, PM_{10} and PM_{Coarse} in 20 European Study Areas; Results of the ESCAPE Project. *Environ. Sci. Technol.* **2012**, *46* (20), 11195−11205.
(25) Li, L.; Wu, A. H.; Cheng, I.; Chen, J.-C.; Wu, J. Spatiotemporal Estimation of Historical $PM_{2.5}$ Concentrations Using PM_{10}Meteorological Variables, and Spatial Effect. *Atmos. Environ.* **2017**, *166*, 182−191.
(26) *Ambient Air Monitoring Protocol for $PM_{2.5}$ and Ozone: Canada-Wide Standards for Particulate Matter and Ozone*; Canadian Council of Ministers of the Environment (CCME): Winnipeg, Canada, 2011. https://www.ccme.ca/files/Resources/air/pm_ozone/pm_oz_cws_monitoring_protocol_pn1456_e.pdf (accessed Oct 24, 2018).
(27) Bey, I.; Jacob, D. J.; Yantosca, R. M.; Logan, J. A.; Field, B. D.; Fiore, A. M.; Li, Q.; Liu, H. Y.; Mickley, L. J.; Schultz, M. G. Global Modeling of Tropospheric Chemistry with Assimilated Meteorology: Model Description and Evaluation. *J. Geophys. Res. Atmospheres* **2001**, *106* (D19), 23073−23095.
(28) Park, R. J.; Jacob, D. J.; Field, B.; Yantosca, R. M.; Chin, M. Natural and Transboundary Pollution Influences on Sulfate-Nitrate-Ammonium Aerosols in the United States: Implications for Policy. *J. Geophys. Res.* **2004**, *109* (D15), D15204.
(29) Fountoukis, C.; Nenes, A. ISORROPIA II: A Computationally Efficient Thermodynamic Equilibrium Model for K^+-Ca^{2+}-Mg^{2+}-NH_4^+-Na^+-SO_4^{2-}-NO_3^--Cl^--H_2O Aerosols. *Atmos. Chem. Phys.* **2007**, *7* (17), 4639−4659.
(30) Fairlie, T. D.; Jacob, D. J.; Park, R. J. The Impact of Transpacific Transport of Mineral Dust in the United States. *Atmos. Environ.* **2007**, *41* (6), 1251−1266.
(31) Jaeglé, L.; Quinn, P. K.; Bates, T. S.; Alexander, B.; Lin, J.-T. Global Distribution of Sea Salt Aerosols: New Constraints from in Situ and Remote Sensing Observations. *Atmos. Chem. Phys.* **2011**, *11* (7), 3137−3157.
(32) Park, R. J.; Jacob, D. J.; Chin, M.; Martin, R. V. Sources of Carbonaceous Aerosols over the United States and Implications for Natural Visibility. *J. Geophys. Res.* **2003**, *108* (D12), 4355.
(33) Wang, Q.; Jacob, D. J.; Spackman, J. R.; Perring, A. E.; Schwarz, J. P.; Moteki, N.; Marais, E. A.; Ge, C.; Wang, J.; Barrett, S. R. H. Budget and Radiative Forcing of Black Carbon Aerosol: Constraints from Pole-to-Pole (HIPPO) Observations across the Pacific. *J. Geophys. Res. Atmospheres* **2014**, *119*, 195−206.
(34) Pye, H. O. T.; Chan, A. W. H.; Barkley, M. P.; Seinfeld, J. H. Global Modeling of Organic Aerosol: The Importance of Reactive Nitrogen (NOx and NO_3). *Atmos. Chem. Phys.* **2010**, *10* (22), 11261−11276.
(35) Marais, E. A.; Jacob, D. J.; Jimenez, J. L.; Campuzano-Jost, P.; Day, D. A.; Hu, W.; Krechmer, J.; Zhu, L.; Kim, P. S.; Miller, C. C.; Fisher, J. A.; Travis, K.; Yu, K.; Hanisco, T. F.; Wolfe, G. M.; Arkinson, H. L.; Pye, H. O. T.; Froyd, K. D.; Liao, J.; McNeill, V. F. Aqueous-Phase Mechanism for Secondary Organic Aerosol Formation from Isoprene: Application to the Southeast United States and Co-Benefit of SO_2 Emission Controls. *Atmos. Chem. Phys.* **2016**, *16* (3), 1603−1618.
(36) Martin, R. V.; Jacob, D. J.; Yantosca, R. M.; Chin, M.; Ginoux, P. Global and Regional Decreases in Tropospheric Oxidants from Photochemical Effects of Aerosols. *J. Geophys. Res. Atmospheres* **2003**, *108* (D3), 4097.

DOI: 10.1021/acs.est.8b06875
Environ. Sci. Technol. 2019, 53, 5071−5079

(37) Drury, E.; Jacob, D. J.; Spurr, R. J. D.; Wang, J.; Shinozuka, Y.; Anderson, B. E.; Clarke, A. D.; Dibb, J.; McNaughton, C.; Weber, R. Synthesis of Satellite (MODIS), Aircraft (ICARTT), and Surface (IMPROVE, EPA-AQS, AERONET) Aerosol Observations over Eastern North America to Improve MODIS Aerosol Retrievals and Constrain Surface Aerosol Concentrations and Sources. *J. Geophys. Res.* **2010**, *115* (D14), D14204.
(38) Ridley, D. A.; Heald, C. L.; Ford, B. North African Dust Export and Deposition: A Satellite and Model Perspective. *J. Geophys. Res. Atmospheres* **2012**, *117*, D02202.
(39) Reff, A.; Bhave, P. V.; Simon, H.; Pace, T. G.; Pouliot, G. A.; Mobley, J. D.; Houyoux, M. Emissions Inventory of $PM_{2.5}$ Trace Elements across the United States. *Environ. Sci. Technol.* **2009**, *43* (15), 5790−5796.
(40) Ridley, D. A.; Heald, C. L.; Ridley, K. J.; Kroll, J. H. Causes and Consequences of Decreasing Atmospheric Organic Aerosol in the United States. *Proc. Natl. Acad. Sci. U. S. A.* **2018**, *115* (2), 290−295.
(41) Giglio, L.; Randerson, J. T.; van der Werf, G. R. Analysis of Daily, Monthly, and Annual Burned Area Using the Fourth-Generation Global Fire Emissions Database (GFED4). *J. Geophys. Res.: Biogeosci.* **2013**, *118* (1), 317−328.
(42) Schultz, M. G.; Heil, A.; Hoelzemann, J. J.; Spessa, A.; Thonicke, K.; Goldammer, J. G.; Held, A. C.; Pereira, J. M. C.; van het Bolscher, M. Global Wildland Fire Emissions from 1960 to 2000. *Glob. Biogeochem. Cycles* **2008**, *22* (2), GB2002.
(43) Brunsdon, C.; Fotheringham, A. S.; Charlton, M. E. Geographically Weighted Regression: A Method for Exploring Spatial Nonstationarity. *Geogr. Anal.* **1996**, *28* (4), 281−298.
(44) Friedl, M. A.; Sulla-Menashe, D.; Tan, B.; Schneider, A.; Ramankutty, N.; Sibley, A.; Huang, X. MODIS Collection 5 Global Land Cover: Algorithm Refinements and Characterization of New Datasets. *Remote Sens. Environ.* **2010**, *114* (1), 168−182.
(45) National Centers for Environmental Information (NCEI). *ETOPO1 1 Arc-Minute Global Relief Model*. https://data.nodc.noaa.gov/cgi-bin/iso?id=gov.noaa.ngdc.mgg.dem:316 (accessed Nov 9, 2018).
(46) SEDAC. *Global Population Count Grid Time Series Estimates, v1: Population Dynamics*. http://sedac.ciesin.columbia.edu/data/set/popdynamics-global-pop-count-time-series-estimates (accessed Aug 8, 2018).
(47) SEDAC. *Gridded Population of the World (GPW), v4*. http://sedac.ciesin.columbia.edu/data/collection/gpw-v4 (accessed Aug 8, 2018).
(48) Boys, B. L.; Martin, R. V.; van Donkelaar, A.; MacDonell, R. J.; Hsu, N. C.; Cooper, M. J.; Yantosca, R. M.; Lu, Z.; Streets, D. G.; Zhang, Q.; Wang, S. Fifteen-Year Global Time Series of Satellite-Derived Fine Particulate Matter. *Environ. Sci. Technol.* **2014**, *48* (19), 11109−11118.
(49) van Donkelaar, A.; Martin, R. V.; Brauer, M.; Boys, B. L. Use of Satellite Observations for Long-Term Exposure Assessment of Global Concentrations of Fine Particulate Matter. *Environ. Health Perspect.* **2015**, *123* (2), 135−143.
(50) van Donkelaar, A.; Martin, R. V.; Li, C.; Burnett, R. T. Regional Estimates of Chemical Composition of Fine Particulate Matter Using a Combined Geoscience-Statistical Method with Information from Satellites, Models, and Monitors. *Environ. Sci. Technol.* **2019**, *53* (5), 2595−2611.
(51) Meng, J.; Li, C.; Martin, R. V.; van Donkelaar, A.; Hystad, P.; Brauer, M. *Historical PM2.5 Dataset across North America*, 2019. DOI: 10.5281/zenodo.2616769

DOI: 10.1021/acs.est.8b06875
Environ. Sci. Technol. 2019, 53, 5071−5079

Atmos. Chem. Phys., 19, 2635–2653, 2019
https://doi.org/10.5194/acp-19-2635-2019

Atmospheric Chemistry and Physics
Open Access
EGU

Interpretation of measured aerosol mass scattering efficiency over North America using a chemical transport model

Robyn N. C. Latimer[1] **and Randall V. Martin**[1,2]

[1]Department of Physics and Atmospheric Science, Dalhousie University, Halifax, B3H 4R2, Canada
[2]Harvard-Smithsonian Center for Astrophysics, Cambridge, MA 02138, USA

Correspondence: Robyn N. C. Latimer (robyn.latimer3@gmail.ca) and Randall V. Martin (randall.martin@dal.ca)

Received: 9 May 2018 – Discussion started: 19 July 2018
Revised: 29 October 2018 – Accepted: 23 January 2019 – Published: 28 February 2019

Abstract. Aerosol mass scattering efficiency affects climate forcing calculations, atmospheric visibility, and the interpretation of satellite observations of aerosol optical depth. We evaluated the representation of aerosol mass scattering efficiency (α_{sp}) in the GEOS-Chem chemical transport model over North America using collocated measurements of aerosol scatter and mass from IMPROVE network sites between 2000 and 2010. We found a positive bias in mass scattering efficiency given current assumptions of aerosol size distributions and particle hygroscopicity in the model. We found that overestimation of mass scattering efficiency was most significant in dry (RH <35 %) and midrange humidity (35 % < RH <65 %) conditions, with biases of 82 % and 40 %, respectively. To address these biases, we investigated assumptions surrounding the two largest contributors to fine aerosol mass, organic (OA) and secondary inorganic aerosols (SIA). Inhibiting hygroscopic growth of SIA below 35 % RH and decreasing the dry geometric mean radius, from 0.069 µm for SIA and 0.073 µm for OA to 0.058 µm for both aerosol types, significantly decreased the overall bias observed at IMPROVE sites in dry conditions from 82 % to 9 %. Implementation of a widely used alternative representation of hygroscopic growth following κ-Kohler theory for secondary inorganic (hygroscopicity parameter $\kappa = 0.61$) and organic ($\kappa = 0.10$) aerosols eliminated the remaining overall bias in α_{sp}. Incorporating these changes in aerosol size and hygroscopicity into the GEOS-Chem model resulted in an increase of 16 % in simulated annual average α_{sp} over North America, with larger increases of 25 % to 45 % in northern regions with high RH and hygroscopic aerosol fractions, and decreases in α_{sp} up to 15 % in the southwestern U.S. where RH is low.

1 Introduction

The interaction of atmospheric aerosols with radiation has substantial implications for the direct radiative effects of atmospheric aerosols, atmospheric visibility, and satellite retrievals of aerosol optical properties. The direct radiative effects of aerosols remain a major source of uncertainty in radiative forcing (Myhre et al., 2013). Atmospheric visibility affects the appearance of landscape features, which is of particular concern in national parks and wilderness areas (Malm et al., 1994). Gaining insight into the concentration and composition of atmospheric aerosols via interpretation of satellite retrievals of aerosol optical depth (AOD) also relies heavily on an understanding of the interaction of aerosols with radiation (Kahn et al., 2005). Analysis of collocated measurements of aerosol scatter, mass, and composition could offer valuable insight into aerosol optical properties.

Mass scattering efficiency is a complex function of aerosol size, composition, hygroscopicity, and mixing state (Hand and Malm, 2007; Malm and Kreidenweis, 1997; White, 1986). Current chemical transport models and global circulation models often calculate atmospheric extinction due to aerosols from speciated aerosol mass concentrations using a composition- and size-dependent mass extinction efficiency (α_{ext}, $m^2\,g^{-1}$). Many of these models use aerosol optical and physical properties defined by the Global Aerosol Data Set (GADS), compiled from measurements and models from 1970 to 1995 (Koepke et al., 1997). The subsequent expansion in long-term aerosol monitoring offers an exciting possibility to further improve model representation of aerosol physical and optical properties. The Interagency Monitoring of Protected Visual Environments (IMPROVE) network offers long-term collocated measurements since 1987 of par-

ticle scatter (b_{sp}), relative humidity (RH), particulate mass concentrations less than 10 µm (PM_{10}) and less than 2.5 µm ($PM_{2.5}$), as well as $PM_{2.5}$ chemical composition at sites across the United States and Canada (Malm et al., 1994, 2004). These collocated measurements provide direct estimates of mass scattering efficiency (α_{sp}) across North America that are useful to evaluate and improve the mass scattering efficiency currently used in models.

Several prior studies have analysed mass scattering efficiencies. Hand et al. (2007) performed an extensive review that examined and compared mass scattering efficiencies calculated from ground-based measurements from approximately 60 mostly short-term studies from 1990 to 2007. In this review, the importance of long-term measurements was emphasized. Malm and Hand (2007) applied IMPROVE network data between 1987 and 2003 to evaluate mass scattering efficiency of organic and inorganic aerosols at 21 IMPROVE sites. A couple of more recent examples of short-term studies of mass scattering efficiency are Titos et al. (2012) and Tao et al. (2014). Many other long-term multi-site studies have investigated aerosol optical properties (e.g. Andrews et al., 2011; Collaud Coen et al., 2013; Pandolfi et al., 2017), but few include measurements of aerosol mass concentrations and therefore do not provide information on mass scattering efficiencies. Our study builds upon previous studies of mass scattering efficiency by reducing initial assumptions regarding size and hygroscopicity of inorganic and organic aerosols and by using measurements of particle speciation, mass, and scatter to inform the representation of these properties. We interpret long-term measurement data to obtain a representation of mass scattering efficiency that can be used across an array of conditions and locations to facilitate incorporation into chemical transport models.

Here we interpret collocated measurements of $PM_{2.5}$, PM_{10}, b_{sp}, and RH from the IMPROVE network to understand factors affecting the representation of mass scattering efficiency. Section 2 provides a description of IMPROVE network measurements, of the GEOS-Chem chemical transport model, and of an alternative aerosol hygroscopic growth scheme. In Sect. 3, we present an analysis of the current representation of mass scattering efficiency in the GEOS-Chem model, and identify changes that improve the consistency with observations. The impacts of these changes on GEOS-Chem-simulated mass scattering efficiency, as well as on agreement between the GEOS-Chem model and observations from the IMPROVE network, are described in Sect. 4.

2 Methods

2.1 IMPROVE network measurements

The IMPROVE network (Malm et al., 1994) is a long-term monitoring program established in 1987 to monitor visibility trends in national parks and wilderness areas in the United States. The network offers measurements of $PM_{2.5}$ speciation, $PM_{2.5}$ and PM_{10} gravimetric mass, and collocated measurements of b_{sp} and RH at a subset of sites that we interpret to understand mass scattering efficiency.

The IMPROVE particle sampler collects $PM_{2.5}$ and PM_{10} on filters. Sampling occurs over a 24 h period every third day. Collected $PM_{2.5}$ is analysed for fine gravimetric mass, elemental concentrations (including Al, Si, Ca, Fe, Ti), ions (SO_4^{2-}, NO_3^-, NO_2^-, Cl^-), and organic and elemental carbon. Collected PM_{10} undergoes gravimetric analysis for total particulate mass less than 10 µm, allowing for the determination of coarse mass ($PM_{10} - PM_{2.5}$) (Malm et al., 1994).

Particle scatter (b_{sp}) is measured at 550 nm at a subset of IMPROVE sites using OPTEC NGN-2 open air integrating nephelometers (Malm et al., 1994; Malm and Hand, 2007; Molenar, 1997). b_{sp} is reported hourly at ambient air temperature and relative humidity; all three parameters are recorded. We filter b_{sp} data to exclude measurements likely affected by meteorological interference such as fog. These conditions include an RH threshold of 95 %, a maximum b_{sp} threshold of 5000 Mm^{-1}, and an hourly rate of change threshold for b_{sp} of 50 Mm^{-1}, following IMPROVE filtering protocols (IMPROVE, 2004).

The IMPROVE network collects collocated samples at a subset of sites, which can provide insight into precision errors associated with the measurements of major species. Hyslop and White (2008) and Solomon et al. (2014) found mean collocated precision errors ranging from 6 % to 11 % for particulate mass measured by IMPROVE. Typical uncertainties in IMPROVE b_{sp} measurements are in the range of 5 %–15 % (Gebhart et al., 2001). Due to nephelometer truncation errors, uncertainties in measured b_{sp} increase as particle size distributions increase, and coarse particle scattering can be underestimated (Molenar, 1997).

For this study, we select sites where fine aerosol mass and speciation measurements are collocated with IMPROVE nephelometers between 2000 and 2010. We exclude data after 2010 to address concerns about variable laboratory RH for PM_{10} measurement after 2010. Sea salt aerosols are excluded from the analysis from 2000 to 2004, as reliable estimates of sea salt concentrations were not reported during this period. We exclude coastal sites during this period, as sea salt can contribute significantly to b_{sp} in coastal conditions of high RH due to its highly hygroscopic nature (Lowenthal and Kumar, 2006). We use only days with coincident mass and scatter measurements, and a minimum of 23 hourly measurements per day, to reduce influence of meteorological interference. Additionally, only sites with a minimum of 90 days of measurements are included in the analysis.

Figure 1 shows at the 28 sites used in this study the average hourly b_{sp} at ambient RH and the average 24 h PM_{10} and $PM_{2.5}$ measured between 2000 and 2010. Measured b_{sp} values vary by a factor of 7, with scatter below 20 Mm^{-1} across the southwestern U.S. and scatter above 50 Mm^{-1} across the southeastern U.S. Measured PM_{10} concentrations vary by a

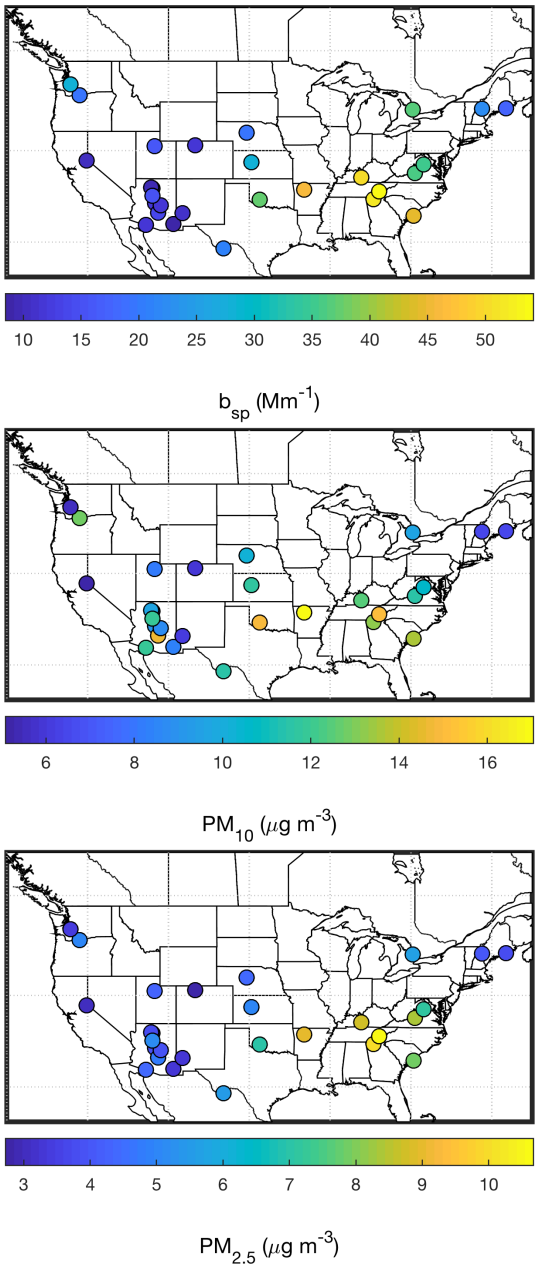

Figure 1. Map of IMPROVE sites with collocated scatter (b_{sp}) at 550 nm and ambient relative humidity, PM_{10}, and $PM_{2.5}$ measurements in North America between 2000 and 2010.

factor of 3, with values below 6 µg m^{-3} in the west to above 14 µg m^{-3} in the southeast. Measured $PM_{2.5}$ concentrations also vary by a factor of 3, with values below 3 µg m^{-3} in the west to above 9 µg m^{-3} in the southeast.

2.2 GEOS-Chem simulation

We simulate hourly $PM_{2.5}$ and PM_{10} mass concentrations and particle scatter using the global chemical transport model GEOS-Chem (version 11-02, http://geos-chem.org, last access: 7 September 2017). The GEOS-Chem model is driven by assimilated meteorology from the Goddard Earth Observation System (GEOS MERRA-2, Gelaro et al., 2017) of the NASA Global Modeling and Assimilation Office (GMAO). Our simulation for North America is conducted at 2° × 2.5° resolution over 47 vertical levels.

The majority of our analysis focuses on the accuracy of the GEOS-Chem parameterization of mass scattering efficiency based on optical parameters given in Table A1. These default aerosol physical and optical properties are defined by the Global Aerosol Data Set (GADS) (Koepke et al., 1997), as implemented by Martin et al. (2003), with modifications to dry size distributions (Drury et al., 2010) and dust mass partitioning (Ridley et al., 2012). After evaluating and improving this parameterization, implications are examined using the full GEOS-Chem simulation in Sect. 3.3.

GEOS-Chem simulates detailed aerosol-oxidant chemistry (Bey et al., 2001; Park et al., 2004). The aerosol simulation includes the sulfate–nitrate–ammonium system (Park et al., 2004), primary (Park et al., 2003; Wang et al., 2014) and secondary (Pye et al., 2010) carbonaceous aerosols, mineral dust (Fairlie et al., 2007, 2010; Zhang et al., 2013), and sea salt (Jaeglé et al., 2011). Organic matter (OM) is estimated from primary organic carbon (OC) using spatially and seasonally varying OM / OC ratios at 0.1° × 0.1° resolution (Philip et al., 2014b). The thermodynamic equilibrium model ISORROPIA-II (Fountoukis and Nenes, 2007), implemented by Pye et al. (2009), is used to calculate gas–aerosol partitioning. Total PM_{10} is calculated following van Donkelaar et al. (2010), but at 40 % RH here for consistency with the IMPROVE network gravimetric analysis in the range of 30 %–50 % RH (Solomon et al., 2014). Particle scatter and aerosol optical depth are calculated at modelled ambient RH based on dry species mass concentrations and aerosol physical and optical properties. The GEOS-Chem aerosol simulation has been extensively evaluated with observations of mass (van Donkelaar et al., 2015; Li et al., 2016), composition (Achakulwisut et al., 2017; Kim et al., 2015; Marais et al., 2016; Philip et al., 2014a; Ridley et al., 2017; Zhang et al., 2013), and scatter (Drury et al., 2010).

We conduct a simulation for the year 2006, to represent the period of greatest measurement density of collocated b_{sp} and PM sites over North America. We archive model fields every hour over North America. We simulate PM_{10}, $PM_{2.5}$, and b_{sp}, allowing for the comparison of model mass scattering efficiency coincident with that measured at IMPROVE network sites over the same time period over North America.

2.3 Determining mass scattering efficiency (α_{sp})

One method of determining mass scattering efficiencies from measurements involves b_{sp} measurements and particle mass concentration measurements (M_{meas}). Mass scattering efficiency of a given aerosol population can be defined as the

ratio of particle scatter to mass.

$$\alpha_{sp,\,\mathrm{meas}} = \frac{b_{sp,\,\mathrm{meas}}}{M_{\mathrm{meas}}} \tag{1}$$

Hourly mass scattering efficiencies are determined using collocated measurements of b_{sp} and mass concentrations from the IMPROVE network, treating IMPROVE mass concentrations as constant over each 24 h sampling period. Total scatter is typically dominated by fine-mode aerosols, but in certain conditions coarse dust can also make a significant contribution (White et al., 1994). Thus, measured PM_{10} mass is used in the denominator of Eq. (1).

Multiple definitions of α_{sp} exist. We define α_{sp} operationally here based on optical measurements at ambient RH, and PM measurements at controlled RH (treated as 40 % RH for consistency with IMPROVE protocols prior to 2011). At 40 % RH, hygroscopic components of PM_{10} will have associated water, and thus measured PM_{10} mass is not treated as dry. We compare these measured α_{sp} with calculated α_{sp} based on species-specific mass scattering efficiencies ($\alpha_{\mathrm{GC},\,j}$) used in GEOS-Chem, constrained with mass concentrations (M_j) and PM_{10} mass measured by IMPROVE.

$$\alpha_{sp,\,\mathrm{calc}} = \frac{b_{sp,\,\mathrm{calc}}}{\mathrm{PM}_{10,\,\mathrm{meas}}} = \frac{\sum_j \alpha_{\mathrm{GC},\,j} M_j}{\mathrm{PM}_{10,\,\mathrm{meas}}} \tag{2}$$

To reduce the impacts of meteorological variation on the comparison of measured and calculated mass scattering efficiency, we perform averages of hourly $b_{sp,\,\mathrm{calc}}$, $b_{sp,\,\mathrm{meas}}$, and PM_{10} over the entire sampling period at each IMPROVE site i. Equation (3) is then used to obtain average calculated and measured mass scattering efficiency at each site.

$$\alpha_{sp,\,\mathrm{avg},\,i} = \frac{b_{sp,\,\mathrm{avg},\,i}}{\mathrm{PM}_{10,\,\mathrm{avg},\,i}} \tag{3}$$

Although the OPTEC open air nephelometer reduces truncation error compared with other nephelometers, truncation error can be significant for coarse particles (Hand and Malm, 2007; Lowenthal and Kumar, 2006). Thus our analysis below focuses on conditions dominated by fine-mode aerosols, and mechanisms affecting fine-mode aerosols.

Appendix A describes the calculation of mass scattering efficiency in more detail. This approach enables isolation of the mass scattering efficiencies used in GEOS-Chem from the species concentrations.

2.4 Introducing an alternate hygroscopic growth scheme

We examine for GEOS-Chem the use of a widely adopted alternate hygroscopic growth scheme, in which aerosol hygroscopic growth is defined by a single parameter, κ (Petters and Kreidenweis 2007, 2008, 2013). This representation of water uptake by aerosols was originally developed for supersaturated CCN conditions, but in recent years has been used extensively in subsaturated conditions (Dusek et al., 2011; Hersey et al., 2013).

The hygroscopic parameter κ is defined by

$$\frac{1}{a_{\mathrm{w}}} = 1 + \kappa \frac{V_{\mathrm{d}}}{V_{\mathrm{w}}}, \tag{4}$$

where V_{d} is dry particulate matter volume, V_{w} is the water volume, and a_{w} is water activity (Petters and Kreidenweis, 2013), which is unity for secondary inorganic aerosols (SIA) and organic aerosols (OA). The diameter growth factor ($\mathrm{GF} = D/D_{\mathrm{d}}$) can be expressed (Snider et al., 2016) as

$$\mathrm{GF} = \left(1 + \kappa \frac{\mathrm{RH}}{100 - \mathrm{RH}}\right)^{1/3}, \tag{5}$$

where D is the wet aerosol radius and D_{d} is the dry aerosol radius. Typically, κ is in the range of 0.5–0.7 for SIA (Hersey et al., 2013; Kreidenweis et al., 2008; Petters and Kreidenweis, 2007) and 0–0.2 for OA (Duplissy et al., 2011; Kreidenweis et al., 2008; Rickards et al., 2013; Snider et al., 2016).

3 Results

3.1 Understanding the current representation of α_{sp}

Figure 2 (left) shows measured vs. calculated mass scattering efficiency using GEOS-Chem default optical tables. Each point represents the average α_{sp} over the entire sampling period at each IMPROVE site. A significant correlation ($r = 0.94$) is apparent; however, a bias in α_{sp} is evident. A positive correlation between average mass scattering efficiency and RH is apparent; sites with low average RH have low average α_{sp} and vice versa. (Panel (b) of Fig. 2 is discussed below.)

To further investigate the RH dependence of this bias, we separate our analysis of calculated α_{sp} into three relative humidity groupings: 0 %–35 % (low), 35 %–65 % (mid), and 65 %–95 % (high). The IMPROVE data are divided among the RH groupings using IMPROVE measurements of hourly RH. Within each grouping, average calculated and measured mass scattering efficiencies are obtained for each site using Eq. (3). The blue dots in Fig. 3 show average calculated vs. measured α_{sp} for each RH range. In the low RH case, a significant overestimation of mass scattering efficiency is apparent at most sites, with a bias of 82 % indicated by the slope. In the mid RH case, overestimation of α_{sp} is less significant but still apparent, with a bias of 40 % indicated by the slope. At high RH, bias is weak.

To further understand the source of the bias in calculated mass scattering efficiency, we now examine calculated α_{sp} in conditions dominated by different aerosol types. Using IMPROVE measurements of 24 hr $PM_{2.5}$ mass and speciation and PM_{10} mass, the IMPROVE data are grouped based

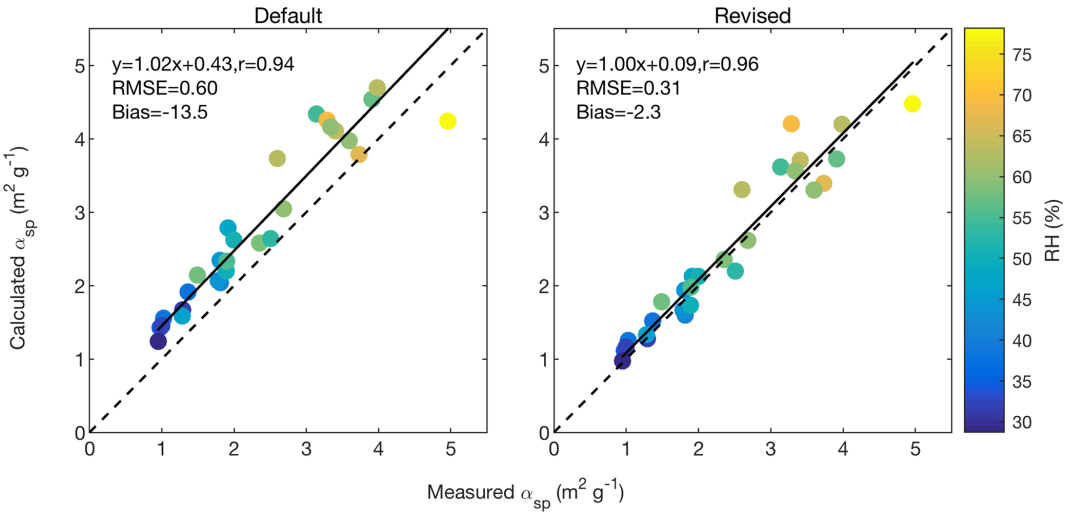

Figure 2. Average measured vs. calculated α_{sp} at 550 nm at IMPROVE sites between 2000 and 2010 using GEOS-Chem default optical tables and revised optical tables. The colour of each point corresponds to the average relative humidity at the site. The 1 : 1 line is black. Slope, offset, and correlation coefficient are inset.

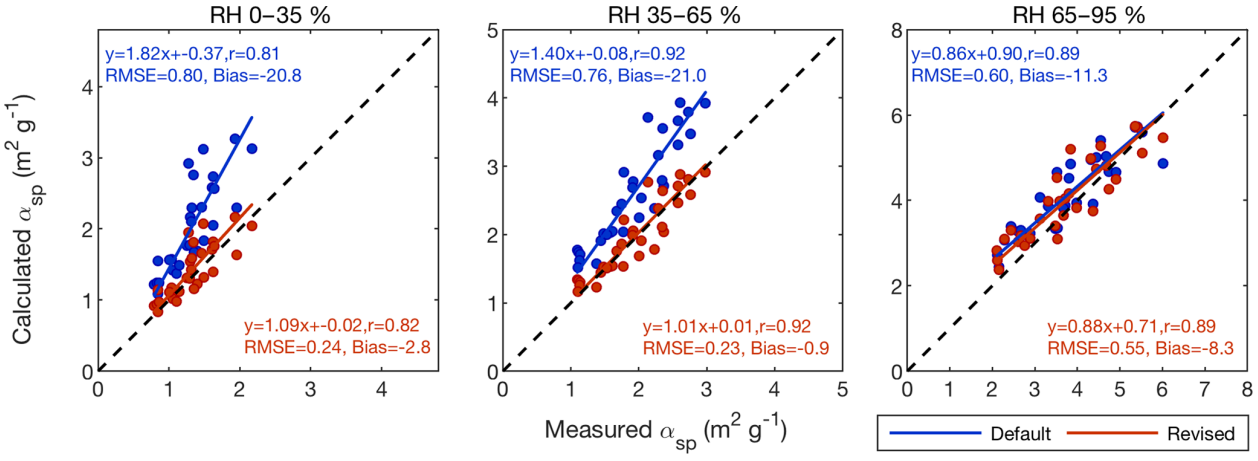

Figure 3. Average measured vs. calculated α_{sp} at 550 nm at IMPROVE sites between 2000 and 2010 using GEOS-Chem default and revised optical tables (Table A1) for measurements taken in 0 %–35 %, 35 %–65 %, and 65 %–95 % RH conditions. The 1 : 1 line is black. Slope, offset, and correlation coefficient are inset.

on dominant aerosol type. Within each group, average calculated and measured mass scattering efficiency is obtained for each site using Eq. (3). Figure 4 shows in blue average measured vs. calculated α_{sp} using default optical tables for conditions where measured $PM_{2.5}$ is dominated (>60 %) by secondary inorganic aerosol, organic aerosol, and fine dust, as well as conditions where PM_{10} is dominated (>60 %) by PM_{coarse} (PM_{10}–$PM_{2.5}$). The scatterplot in the SIA-dominant case resembles the overall relationship shown in Fig. 2. α_{sp} is overestimated at most sites, with significant correlation ($r = 0.88$) and a bias evident in the offset of 0.70. Where OA is the dominant component of $PM_{2.5}$, the slope is close to unity (1.02), but the large offset of 0.80 m^{2}g^{-1} results in α_{sp} being largely overestimated. Where dust is the dominant fine aerosol, correlation is significant ($r = 0.89$) and mass scattering efficiency is accurately calculated at the vast majority of sites, despite a prominent outlier at a site in the Columbia River Gorge, Washington. The PM_{coarse}-dominant case shows significant correlation ($r = 0.88$) and a slight tendency for overestimation of α_{sp}. As this case is not independent of the other cases, this overestimation is likely linked to the overestimation in the OA- and SIA-dominant cases as demonstrated below.

These results indicate that the bias in calculated mass scattering efficiency arises mostly due to the representation of the physical and optical properties of secondary inorganic and organic aerosols. The following will focus on improving the

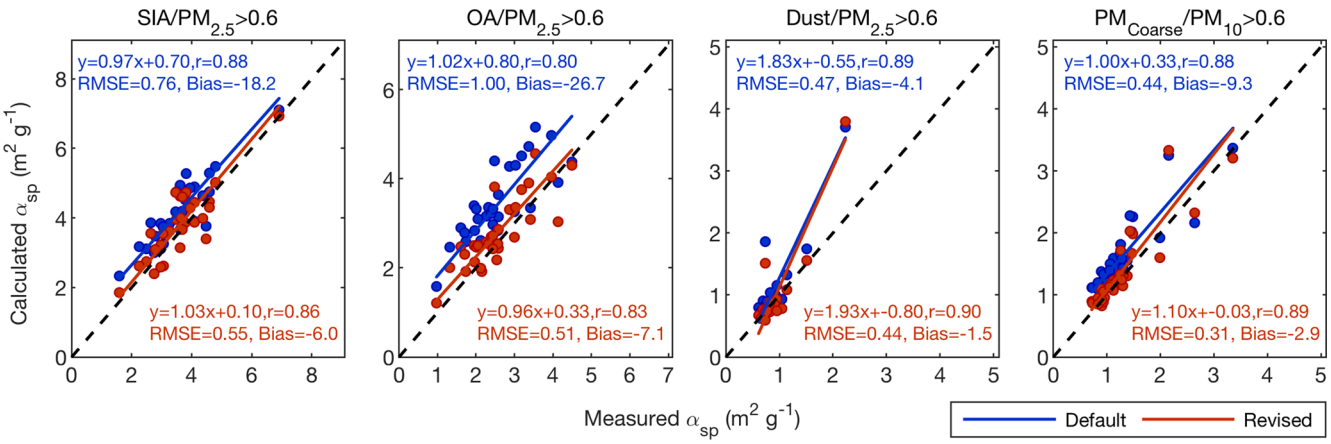

Figure 4. Average measured vs. calculated α_{sp} (550 nm) at IMPROVE sites between 2000 and 2010 using GEOS-Chem default and revised optical tables for measurements taken in conditions dominated by secondary inorganic aerosols (SIA), organic aerosols (OA), fine dust, and PM_{coarse} (PM_{10}–$PM_{2.5}$). The 1 : 1 line is black. Slope, offset, and correlation coefficient are inset.

representation of physical and optical properties of these two aerosol types.

3.2 Changing the physical properties of SIA and OA

Figure 5 shows mass scattering efficiency as a function of aerosol size for secondary inorganic (orange) and organic (blue) aerosols for dry aerosols (solid) and aerosols at 80 % RH (dashed lines) as calculated using a Mie algorithm (Mishchenko et al., 1999). Water uptake at 80 % RH for OA and SIA is calculated using default hygroscopic growth factors from GEOS-Chem. The uptake of water increases aerosol scatter, decreases aerosol density, and decreases the refractive index. The increase in aerosol scatter with increasing ambient RH drives the increase in α_{sp}.

The points in Fig. 5 represent the current mass scattering efficiency values of OA and SIA in GEOS-Chem. For dry aerosols, $\alpha_{sp} = 4.4\,m^2\,g^{-1}$ for OA and $\alpha_{sp} = 3.2\,m^2\,g^{-1}$ for SIA. In a review of ground-based estimates of aerosol mass scattering efficiencies, Hand et al. (2007) found dry α_{sp} values of $2.5\,m^2\,g^{-1}$ for ammonium sulfate, $2.7\,m^2\,g^{-1}$ for ammonium nitrate, and $3.9\,m^2\,g^{-1}$ for particulate organic matter. These values suggest that the default optical tables in GEOS-Chem currently overestimate mass scattering efficiency of SIA and OA in dry conditions. This reaffirms the overestimation of α_{sp} in dry conditions evident in panel (a) of Fig. 3. As aerosol size is the strongest determinant of dry mass scattering efficiency, we begin by examining the dry sizes of SIA and OA in GEOS-Chem.

The current dry sizes of SIA and OA in GEOS-Chem were informed by measurements from several aircraft campaigns over eastern North America during the summer of 2004 (Drury et al., 2010) as part of the International Consortium for Atmospheric Research on Transport and Transformation (ICARTT) (Fehsenfeld et al., 2006; Singh et al., 2006). Aerosol surface area and volume distributions fluctuate seasonally in the northeastern U.S., with summer maxima and winter minima (Stanier et al., 2004). We divide our analysis at low RH by season, in an effort to discern a seasonal pattern in the overestimation of α_{sp}.

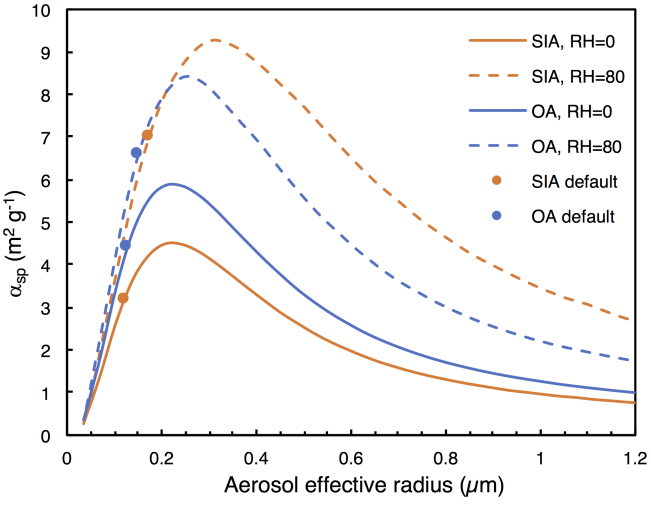

Figure 5. Mass scattering efficiency (α_{sp}) at 550 nm as a function of aerosol wet effective radius for organic aerosol and secondary inorganic aerosol. Solid lines show α_{sp} for dry aerosol (RH = 0 %); dashed lines show α_{sp} for aqueous aerosols (RH = 80 %). Points represent the default size in GEOS-Chem.

Figure 6 (blue) shows seasonal measured vs. calculated mass scattering efficiency in dry conditions using default optical tables (Table A1). Estimations of α_{sp} are most accurate in the summer, consistent with the dry sizes chosen by Drury et al. (2010) which were informed by summertime size distribution measurements. The larger overestimation of α_{sp} in all other seasons, most notably in winter, is consistent with the

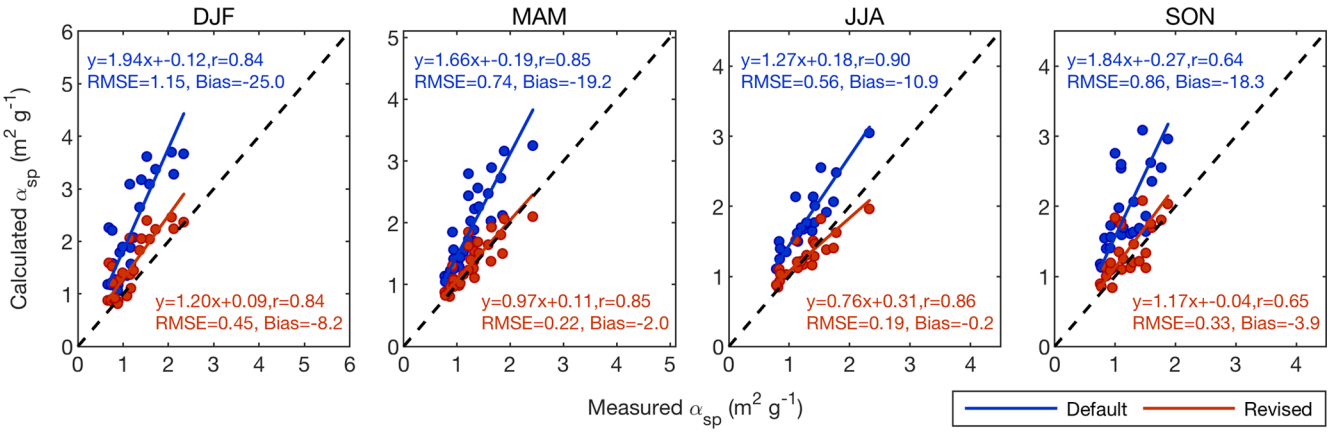

Figure 6. Average measured vs. calculated α_{sp} (550 nm) at IMPROVE sites between 2000 and 2010 using GEOS-Chem default and revised optical tables for measurements taken in dry conditions (RH <35 %) in winter, spring, summer, and fall. The 1 : 1 line is black. Slope, offset, and correlation coefficient are inset.

seasonality in aerosol size distributions observed by Stanier et al. (2004).

3.2.1 Efflorescence relative humidity

To address the overestimation of mass scattering efficiency in dry conditions illustrated in Figs. 3 and 6, we begin by accounting for efflorescence transitions in secondary inorganic aerosols. Efflorescence phase transitions are characterized by nucleation of the crystalline phase followed by rapid evaporation of water. Field measurements have found evidence for these transitions (Martin et al., 2008). The efflorescence relative humidity (ERH) of ammonium sulfate reported in several experimental studies ranges from 35 % to 40 % (Ciobanu et al., 2010). Laboratory tests have shown that mixtures of sulfate–nitrate–ammonium particles will undergo efflorescence when the ammonium sulfate fraction is high (Dougle et al., 1998; Martin et al., 2003). This condition is true at most global measurement sites, with the possible exception of Europe, where particles are nitrate rich (Martin et al., 2003).

We therefore define the hygroscopic growth factor for SIA as unity for RH $\leq$ 35 %, linearly increasing between 35 % and 40 % RH from unity to $GF_{40\,\%}$ (calculated by Eq. 5), and following the default (or κ-Kohler) growth curve for RH $\geq$ 40 %.

Incorporating an ERH for SIA and consequently inhibiting hygroscopic growth of SIA below 35 % RH significantly reduce the overestimation of mass scattering efficiency in dry conditions. In the case of default hygroscopic growth in GEOS-Chem, the overall dry bias in α_{sp} is reduced from 82 % to 48 %.

3.2.2 Aerosol dry size

To address the remaining overestimation of mass scattering efficiency in dry conditions, we explore different dry sizes of secondary inorganic and organic aerosols. Effective variance may also be important (Chin et al., 2002), but given insufficient information to simultaneously constrain size and variance, we focus on size. Figure 7 shows the slope of the average measured vs. calculated α_{sp} plot for RH <35 % for dry radii ranging from 0.048 to 0.074 µm at intervals of 0.001 µm, assuming SIA and OA have the same dry size. The slope of the best fit line acts as an indicator of the appropriate dry size for each season. Sensitivity tests exploring alternative error metrics (RMSE, MSE) yielded similar results. The slope decreases steadily as dry radius is decreased in all seasons. Using the dry radius which gives a slope of unity, we find that aerosols are largest in summer ($r = 0.067$ µm), smallest in winter ($r = 0.051$ µm), and in between in spring and fall (0.059 and 0.054 µm, respectively). The spring and summer radii are consistent with accumulation-mode size distribution measurements performed by Levin et al. (2009) in the spring and summer of 2006. Averaging the sizes from all four seasons results in an annual representative dry radius of 0.058 µm. This annual radius is smaller than the GEOS-Chem default sizes of SIA and OA that were informed by summertime measurements alone (Drury et al., 2010).

Figure 6 (red) shows seasonal measured vs. calculated α_{sp} in dry conditions using a new representative annual geometric mean radius of 0.058 µm for SIA and OA. This change in geometric mean radius reduces the overestimation of α_{sp} in all seasons, with the largest improvements in fall (slope decreases from 1.84 to 1.17) and winter (slope decreases from 1.94 to 1.20). Changes in correlation are minor. For the remainder of the analysis, this new dry radius of 0.058 µm is implemented for SIA and OA.

3.2.3 Aerosol hygroscopicity

We now examine the implementation of the widely adopted κ-Kohler hygroscopic growth scheme described in Sect. 2.4.

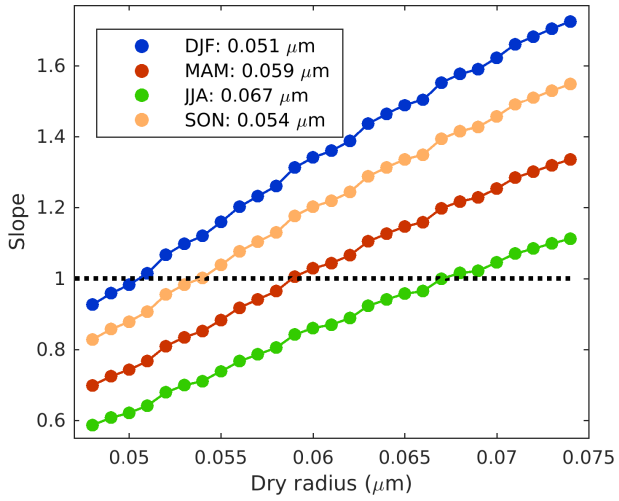

Figure 7. Slope of measured vs. calculated α_{sp} plot vs. dry geometric mean aerosol radius, by season. Winter (DJF) is in blue, spring (MAM) in red, summer (JJA) in green, and fall (SON) in orange. The line slope = 1 is shown in black. Numbers in the legend represent the dry radius for which the slope = 1 for each season.

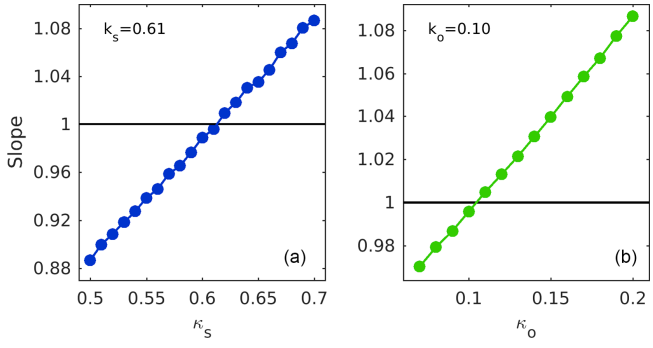

Figure 8. Slope of measured vs. calculated α_{sp} plot as a function of the κ of secondary inorganic aerosols (κ_s, **a**) and the κ of organic aerosols (κ_o, **b**). The line slope = 1 is shown in black. κ_s and κ_o values for which slope = 1 are inset.

A range of measured κ values for SIA (κ_s) and OA (κ_o) exist in the literature. We explore the range of possible κ values, using the slope of the measured vs. calculated α_{sp} plot as an indicator of the appropriate values.

Figure 8 shows the slope of the measured vs. calculated α_{sp} plot for κ values for SIA (κ_s) ranging from 0.5 to 0.7 and for OA (κ_o) ranging from 0.08 to 0.20. Slope increases steadily as κ_s and κ_o increase. A slope of unity identifies representative values of $\kappa_s = 0.61$ and $\kappa_o = 0.10$. These values are in the middle of the range of measured κ values (Duplissy et al., 2011; Hersey et al., 2013; Kreidenweis et al., 2008; Petters and Kreidenweis, 2007; Rickards et al., 2013).

Figure 9 shows the diameter growth factor as a function of relative humidity following κ-Kohler theory, as well as GADS hygroscopic growth for both SIA and OA used in the default GEOS-Chem model. Hygroscopic growth from the Aerosol Inorganic Model (AIM) at $T = 298$ K (Wexler and Clegg, 2002) and laboratory measurements (Wise et al., 2003) are also shown for ammonium sulfate (Snider et al., 2016). The GADS hygroscopic growth schemes used in the default GEOS-Chem simulation are characterized by larger growth at low RH and smaller growth at high RH for both secondary inorganic and organic aerosols. The κ-Kohler scheme exhibits greater consistency with both AIM and laboratory hygroscopic growth for SIA.

Using the revised dry size of 0.058 µm and the κ-Kohler theory of hygroscopic growth, we calculate revised physical and optical properties for SIA and OA over a range of RH values. Table A1 contains geometric mean radius, extinction efficiency, and single scattering albedo for the revised optical tables at eight relative humidity values.

Figure 2 (right) shows the measured vs. calculated mass scattering efficiency using these revised optical tables for SIA and OA. The overestimation of mass scattering efficiency has been eliminated with these revised aerosol properties, with a slope of 1.00 and an offset of 0.09. Correlation remains significant at $r = 0.96$.

Figure 4 (red) shows measured vs. calculated α_{sp} in conditions dominated by different aerosol types using the revised optical tables. The overestimation of α_{sp} in SIA-dominant conditions using the default optical tables has been eliminated, with a slope of 1.03 and a decreased offset (0.70 to 0.1). The large overestimation of α_{sp} that was apparent in OA-dominant conditions has been reduced by a factor of 2. α_{sp} remains accurately estimated at the majority of dust-dominant sites, with the outlier at the Columbia River Gorge site in Washington still skewing the best fit line. The slight overestimation of α_{sp} that was present in the PM_{coarse}-dominant case using default optical tables has been eliminated using the revised tables (offset 0.33 to 0.03). Slight increases in correlation coefficients are apparent in all cases except for the SIA-dominant case, where it decreased by 0.02.

Figure 3 (red) shows measured vs. calculated α_{sp} using revised optical tables. The overestimation in α_{sp} has been significantly reduced in the low RH case (slope = 1.82 to slope = 1.09) and in the mid RH case (slope = 1.40 to slope = 1.01) compared to when default optical tables were used. The slight overestimation in high RH conditions present in the default case has also been reduced, as shown by the decreased offset (0.90 to 0.71).

3.3 Changes in GEOS-Chem-simulated α_{sp}

Here, we examine how these changes to aerosol properties impact both GEOS-Chem simulation of mass scattering efficiency over North America and the fit between modelled and measured α_{sp} at IMPROVE sites. These simulations rely on GEOS-Chem simulations of aerosol composition using GEOS RH fields.

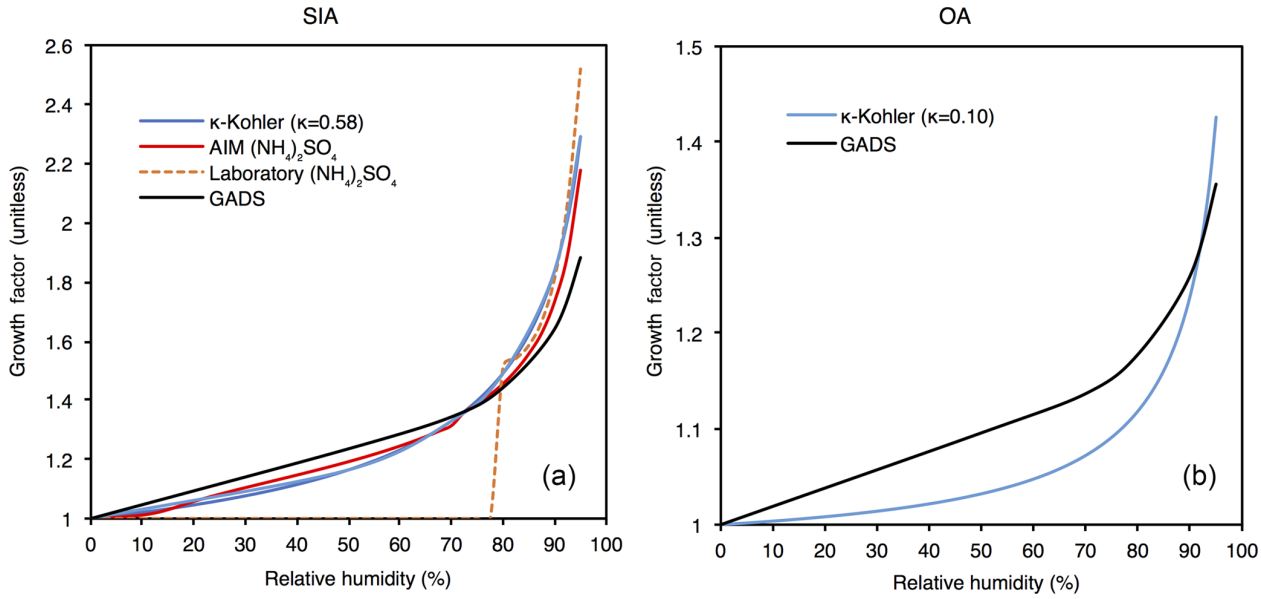

Figure 9. Hygroscopic growth factor curves for secondary inorganic aerosols (SIA, **a**) and organic aerosols (OA, **b**). GADS (Global Aerosol Data Set) hygroscopic growth from empirical data and κ-Kohler hygroscopic growth are shown for both SIA and OA. For ammonium sulfate, AIM (Aerosol Inorganic Model) hygroscopic growth at $T = 298$ K (Wexler and Clegg, 2002) and laboratory hygroscopic growth with a deliquesence point of RH = 80 % (Wise et al., 2003) are also shown.

Figure 10 shows the relative and absolute change in mass scattering efficiency when switching from the default to revised optical tables. Continental mean α_{sp} increased by 16 %. Increases in α_{sp} range from 25 % to 45 % in northeastern regions of North America, corresponding to an increase of 1.5–3.5 $m^2\,g^{-1}$. These larger changes reflect the higher RH and SIA fractions. Decreases in α_{sp} of up to 15 % or $-0.5\,m^2 g^{-1}$ are found in the southwest where RH is low and mineral dust dominates.

Figure 11 shows GEOS-Chem annual average mass scattering efficiency using default (top) and revised (bottom) optical tables over North America for the year 2006. The overlaying circles represent average measured α_{sp} at IMPROVE network sites for the year 2006, and the outer rings show the coincident simulated α_{sp} for each site. We exclude sites within 1° of the coast, where sea salt affects α_{sp}, as well as sites where elevation differs from average gridbox elevation by more than 1500 m. These criteria result in a decrease from 24 to 19 in the number of sites available for the analysis in 2006.

Using default optical tables, simulated continental mean α_{sp} is $5.4\,m^2\,g^{-1}$. A maximum α_{sp} of $10\,m^2\,g^{-1}$ occurs in British Columbia, and a minimum α_{sp} of $1.7\,m^2\,g^{-1}$ occurs in the southwestern United States. Using revised optical tables, simulated continental mean α_{sp} is $6.3\,m^2\,g^{-1}$, with a maximum of $12.5\,m^2\,g^{-1}$ in the northwest and a minimum of $1.5\,m^2\,g^{-1}$ in the southwest. The elevated mass scattering efficiencies in the northwest can be attributed in part to the high average RH in this region of 83 %.

Figure 12 (left) shows coincident measured vs. simulated mass scattering efficiency at the 19 IMPROVE sites, using default optical tables. Correlation is significant ($r = 0.88$), but a bias in simulated α_{sp} is apparent (slope = 0.83). Simulated α_{sp} is notably biased low at sites in the southeastern United States where average α_{sp} is largest, and simulated α_{sp} is notably biased high at sites in the southwestern United States where average mass scattering efficiency is lowest. Sites with the lowest average RH correspond to those with the lowest average mass scattering efficiency and vice versa. The tendency of mass scattering efficiency to be overestimated at low RH reflects the tendency that was originally seen in Fig. 4.

Figure 12 (right) shows coincident measured vs. simulated α_{sp} using revised optical tables. Correlation remains significant ($r = 0.89$), and a decrease in bias is evident from the increase in slope (0.83 to 0.93) and decrease in offset (0.47 to 0.08). Most sites now lie closer to the 1 : 1 line. The overestimation of simulated α_{sp} in the southwest, where RH is low, has been reduced or eliminated at all sites.

3.4 Comparison with AERONET measurements

Appendix B investigates changes to simulated AOD, and compares measured and simulated AOD at AERONET sites. Although large relative increases upwards of 60 % in average AOD are evident in large parts of northern high latitudes where absolute AOD is small, absolute AOD generally changes by less than 0.1 (Fig. B1). Comparisons with AERONET AOD reveal that the revised optical properties

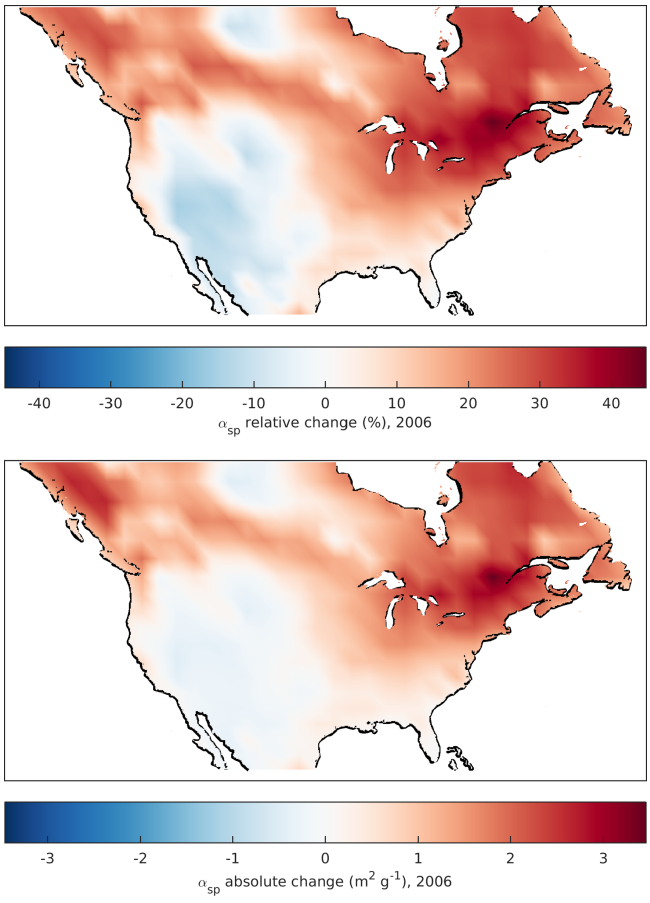

Figure 10. Average relative and absolute change in GEOS-Chem mass scattering efficiency over North America for the year 2006 after implementing revised optical tables for secondary inorganic and organic aerosols.

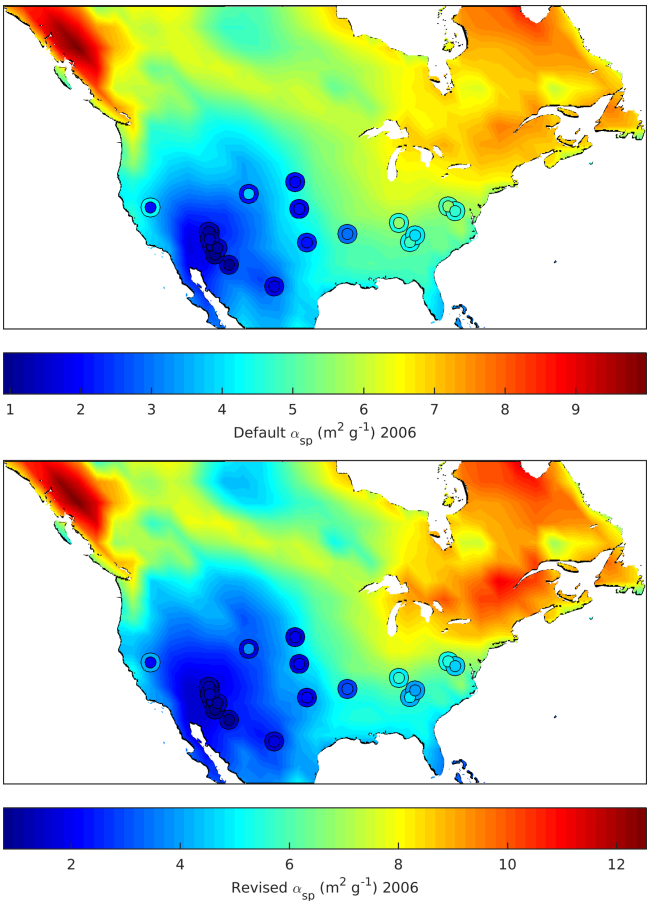

Figure 11. GEOS-Chem annual average mass scattering efficiency (at 550 nm) for the year 2006 using default and revised sizes and hygroscopicity for secondary inorganic and organic aerosols. Overlaying inner circles represent annual averages of α_{sp} at IMPROVE network sites for the year 2006. Outer rings represent coincident average simulated α_{sp}.

slightly improve the simulation of AOD worldwide (slope decreases from 1.08 to 1.00) despite the large influence of other factors (e.g. ambient aerosol concentrations) upon AOD.

4 Conclusions

The current representation of mass scattering efficiency in the GEOS-Chem global chemical transport model was evaluated using collocated ground-based measurements of particle mass, speciation, scatter, and relative humidity from the IMPROVE network.

Calculated mass scattering efficiency had a positive bias using default physical and optical properties used in the GEOS-Chem model. This bias was most significant when $PM_{2.5}$ mass was dominated by secondary inorganic (SIA) or organic aerosols (OA). Mass scattering efficiency in $PM_{2.5}$ dust and coarse particulate matter dominant conditions was accurately represented at the majority of IMPROVE sites.

Relative humidity played an important role in the severity of the bias in mass scattering efficiency. Mean α_{sp} was overestimated by 82 % in dry conditions (RH <35 %). This bias was largest in the winter (94 %) and smallest in the summer (27 %). Implementing an efflorescence relative humidity for SIA and thus inhibiting hygroscopic growth below 35 % RH decreased the dry bias by 34 %. An annual representative dry geometric mean radius of 0.058 µm for SIA and OA decreased the dry mass scattering efficiency of these aerosols, and subsequently further reduced the bias in dry conditions to 9 %.

κ-Kohler theory was implemented for the hygroscopic growth of SIA and OA, which is characterized by smaller growth factors at low RH and larger growth factors at high RH compared to default growth factors in GEOS-Chem. κ values of 0.61 for SIA and 0.10 for OA eliminated the overall bias in calculated mass scattering efficiency.

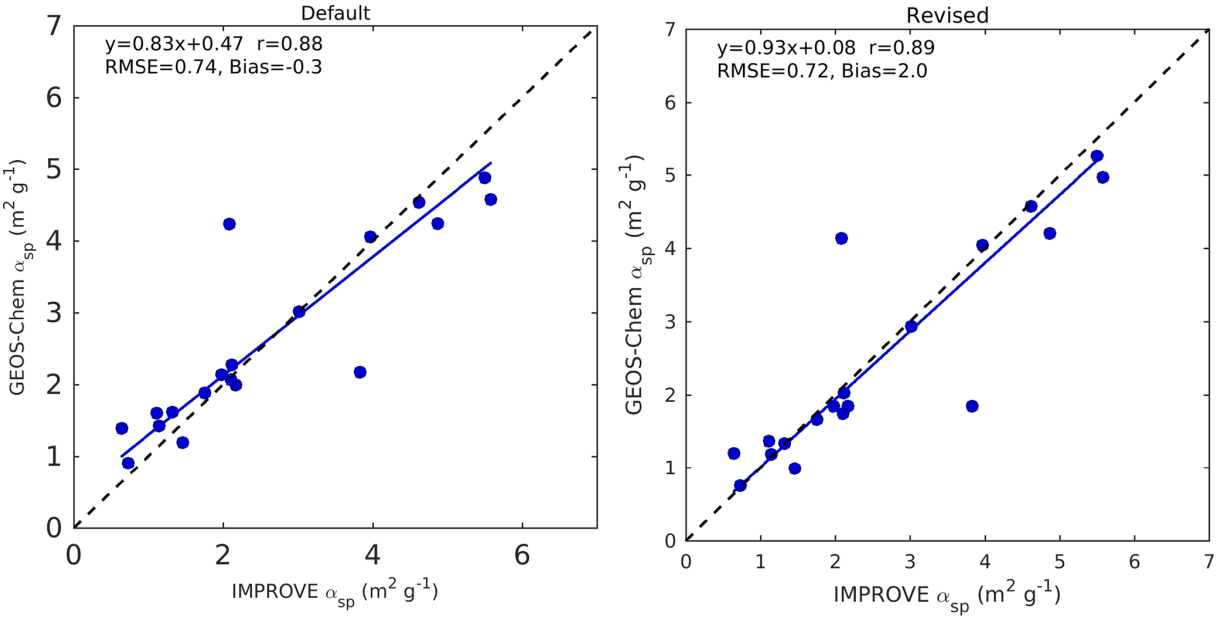

Figure 12. Coincident simulated vs. measured average mass scattering efficiency at 550 nm for the year 2006, using default and revised optical tables. Slope, offset, and correlation coefficient are inset.

These changes to SIA and OA optical tables resulted in a continental mean increase in GEOS-Chem-simulated mass scattering efficiency of 16 %. Northeastern regions of North America exhibited the largest increases (25 %–45 %) due to high RH and SIA fractions, while southwestern regions of the continent exhibited decreases in α_{sp} of up to 15 % due to low RH and high dust fractions. These changes to the GEOS-Chem optical tables improved the fit between measured and simulated mass scattering efficiency at IMPROVE sites, reflected in the changes to the slope (0.83 to 0.93) and the offset (0.47 to 0.08).

Future work should examine the implications of these changes for satellite-derived estimates of fine particulate matter that depend on the relationship of AOD with $PM_{2.5}$. Future work should also expand analysis of the representation of mass scattering efficiency for other years, and by incorporating measurements from other ground-based measurement networks such as the Surface PARTiculate MAtter network (SPARTAN), which provides measurements of particulate mass, speciation, and scatter in populated regions worldwide (Snider et al., 2015, 2016). Such comparisons may also be useful to evaluate and improve prognostic simulations of aerosol size (Mann et al., 2010; Spracklen et al., 2005; Trivitayanurak et al., 2008; Yu and Luo, 2009). Representation of particle RH history may also be important (Wang et al., 2008).

Data availability. IMPROVE network data for 2000–2010 can be accessed at http://vista.cira.colostate.edu/Improve/improve-data/ (last access: 3 October 2018). The GEOS-Chem chemical transport model used here is available at http://www.geos-chem.org (last access: 7 September 2017).

Appendix A

A1 b_{sp} and α_{sp} calculations in GEOS-Chem

In GEOS-Chem, surface-level b_{sp} is calculated using model particle mass concentrations and local relative humidity, as well as predefined mass densities and aerosol optical properties for each aerosol component following

$$b_{sp} = \sum_{species,\, i} \frac{\frac{3}{4} \cdot \left(\frac{R_{w,\,i}}{R_{d,\,i}}\right)^2 \cdot M_{d,\,i} \cdot Q_{w,\,i} \cdot SSA_{w,\,i}}{\rho_{d,\,i} \cdot R_{d,\,i}}, \quad \text{(A1)}$$

where ρ_d is the dry particle mass density, R_w is the effective radius (defined as the ratio of the third to second moments of an aerosol size distribution), R_d is the dry effective radius, M_d is the dry surface-level mass concentration, Q_w is the extinction efficiency, and SSA_w is the single scattering albedo. Parameters with subscript w indicate values at ambient RH. Species included in this calculation are SO_4^{2-}, NH_4^+, NO_3^-, BC, OM, and fine and coarse dust and sea salt.

Dividing Eq. (A1) by total surface-level PM_{10} results in the following equation for mass scattering efficiency:

$$\alpha_{sp} = \frac{B_{sp}}{PM_{10}} = \frac{\sum_{species,\, i} \frac{\frac{3}{4} \cdot \left(\frac{R_{w,\,i}}{R_{d,\,i}}\right)^2 \cdot \frac{M_{d,\,i}}{PM_{10}} \cdot Q_{w,\,i} \cdot SSA_{w,\,i}}{\rho_{d,\,i} \cdot R_{d,\,i}}}{PM_{10}}. \quad \text{(A2)}$$

The effective radius, extinction efficiency, and single scattering albedo in Eqs. (A1) and (A2) are obtained from GEOS-Chem optical tables for the ambient RH values measured by IMPROVE. Dry mass density ρ_d is specified for each aerosol species in GEOS-Chem (Table A2). $M_{d,\,i}$ and PM_{10} are obtained from IMPROVE network measurements of aerosol mass and composition. α_{sp} calculated by Eq. (A2) is compared to α_{sp} directly measured by the IMPROVE network.

Mass scattering efficiency is dependent on particle density, refractive index, and particle size. Mass scattering efficiency is typically most dependent on aerosol size, which is dictated by both the dry size distribution chosen to represent a given aerosol species and the hygroscopic growth scheme used to represent aerosol water uptake for hydrophilic species.

A2 Incorporating IMPROVE network measurements

The IMPROVE network measures every 3 days $PM_{2.5}$ mass and speciation and PM_{10} mass. The IMPROVE particle sampler consists of four independent modules with separate inlets and pumps. The first three modules (A, B, and C) collect only fine particulate matter ($PM_{2.5}$), while the fourth module (D) collects both fine and coarse particles (PM_{10}). Module A collects $PM_{2.5}$ on a Teflon filter, which undergoes gravimetric analysis for total $PM_{2.5}$ mass and X-ray florescence for elemental concentrations (including Al, Si, Ca, Fe, and Ti). The nylon filter in module B undergoes ion chromatography analysis for SO_4^{2-}, NO_3^-, NO_2^-, and Cl^-. Module C contains a quartz filter that is analysed for organic and elemental carbon via thermal optical reflectance. The Teflon filter in module D undergoes gravimetric analysis for PM_{10} mass (Malm et al., 1994, 2004). Prior to gravimetric analysis, filters A and D undergo equilibration at 30 %–50 % RH and 20–25 °C for several minutes (Solomon et al., 2014).

The GEOS-Chem model partitions OM into hydrophilic and hydrophobic fractions, so the same is done for OM measured by IMPROVE to enable isolation of mass scattering efficiency in our comparisons. OM in remote regions tends to be highly oxidized, and oxidation level of organics has been shown to positively correlate with hygroscopicity (Duplissy et al., 2011; Jimenez et al., 2009; Ng et al., 2010). We treat measured OM as 90 % hydrophilic, due to the rural nature of IMPROVE sites. EC is treated as 50 % hydrophilic. As speciation of coarse material is unavailable, we treat all coarse material as crustal in origin, an assumption that may break down at coastal sites. We partition fine and coarse dust measured by the IMPROVE network into the GEOS-Chem size bins using the dust particle size distribution (PSD) described by Zhang et al. (2013).

Table A1. Default and revised aerosol size and optical properties for secondary inorganic aerosols (SIA) and organic aerosols (OA) at 550 nm at eight relative humidity values. Columns indicate geometric mean radius (r_g), effective radius (r_{eff}), extinction efficiency (Q), and single scattering albedo (SSA). κ_s and κ_o represent the hygroscopic growth parameters for SIA and OA, respectively.

		Default				Revised ($\kappa_s = 0.61$; $\kappa_o = 0.10$)			
Aerosol	RH	r_g (µm)	r_{eff} (µm)	Q	SSA	r_g (µm)	r_{eff} (µm)	Q	SSA
SIA	0	0.069	0.121	0.902	0.965	0.058	0.101	0.603	0.959
	35	0.081	0.141	0.965	0.975	0.058	0.101	0.603	0.959
	50	0.086	0.149	0.992	0.979	0.068	0.118	0.656	0.972
	70	0.093	0.163	1.062	0.983	0.078	0.135	0.742	0.981
	80	0.100	0.174	1.137	0.986	0.088	0.152	0.847	0.987
	90	0.114	0.198	1.301	0.991	0.108	0.188	1.116	0.993
	95	0.131	0.227	1.517	0.994	0.135	0.234	1.500	0.997
	99	0.175	0.304	1.2725	0.993	0.229	0.397	2.570	0.999
OA	0	0.073	0.127	1.007	0.966	0.058	0.101	0.603	0.959
	35	0.078	0.135	0.965	0.972	0.059	0.103	0.608	0.965
	50	0.080	0.139	0.947	0.975	0.060	0.104	0.610	0.963
	70	0.083	0.145	0.947	0.978	0.063	0.108	0.622	0.966
	80	0.086	0.149	0.955	0.980	0.065	0.113	0.639	0.970
	90	0.092	0.159	0.990	0.984	0.073	0.125	0.696	0.977
	95	0.099	0.171	1.053	0.988	0.084	0.144	0.811	0.985
	99	0.117	0.203	1.273	0.993	0.132	0.223	1.463	0.996

Table A2. Current microphysical properties of each aerosol species in GEOS-Chem. r_g represents the dry geometric mean radius (µm) and σ the geometric standard deviation of the lognormal size distributions assumed for each species. ρ_d represents the dry mass densities of each species (g cm^{-3}).

Component	r_g (µm)	σ	ρ_d (g cm^{-3})
Sulfate–nitrate–ammonium	0.070	1.6	1.7
Organic carbon	0.073	1.6	1.3
Black carbon	0.020	1.6	1.8
Sea salt (fine)	0.085	1.5	2.2
Sea salt (coarse)	0.401	1.8	2.2
Brown carbon	0.073	1.6	1.3
Dust 1 a–d	0.030–0.170	2.2	2.5
Dust 2	0.265	2.2	2.65
Dust 3	0.530	2.2	2.65
Dust 4	0.845	2.2	2.65

Appendix B

The *Ae*rosol *Ro*botics *Net*work (AERONET) is a long-term network of ground-based sun photometers that provides continuous, cloud-screened measurements of aerosol optical depth (AOD) at several fixed wavelengths in the visible and near infrared (Holben et al., 1998). The calculation of AOD in GEOS-Chem is performed using simulated mass concentrations of aerosol species and mass extinction efficiencies, summed over all vertical layers. Our analysis of mass scattering efficiency can therefore be extended globally by comparing GEOS-Chem-calculated AOD to AOD measured at AERONET sites. During our simulation year of 2006, AERONET consisted of 231 sites across the globe.

Here we examine how the changes to SIA and OA properties impact GEOS-Chem simulated AOD globally. Figure B1 shows the relative (top) and absolute (bottom) changes in AOD. Global mean AOD increases by 19 %. Relative changes in AOD are most pronounced in northern regions where mean relative humidity is high, with increases in simulated AOD ranging from 50 % to 90 %. Decreases in AOD between 0 % and 20 % are present in most of the Southern Hemisphere, in part due to the lower average RH. Absolute changes in AOD show a similar tendency, with slight increases in AOD of up to 0.2 in northern regions, and slight decreases of up of −0.09 in southern regions. An exception to this is seen over parts of China, where AOD increases by 0.5 due to the elevated SIA and OA concentrations.

Figure B2 shows coincident measured (inner circles) and simulated (outer rings) AOD for the year 2006 using default optical tables (top) and revised optical tables (bottom). We exclude sites within 1° of the coast, as well as sites where elevation differs from average gridbox elevation by more than 1500 m. We also exclude sites where average $PM_{2.5}$ is dominated by dust (dust / $PM_{2.5}$ > 0.6), to focus on the representation of the optical properties of SIA and OA. Across the globe, we see that AOD is both overestimated and underestimated. AOD is overestimated at most sites in Africa, with the most notable overestimation at the site in Nigeria. AOD is moderately overestimated at sites in Australia. Underestimation of AOD occurs at most sites in South America, as well as at sites in southern North America and southern Asia.

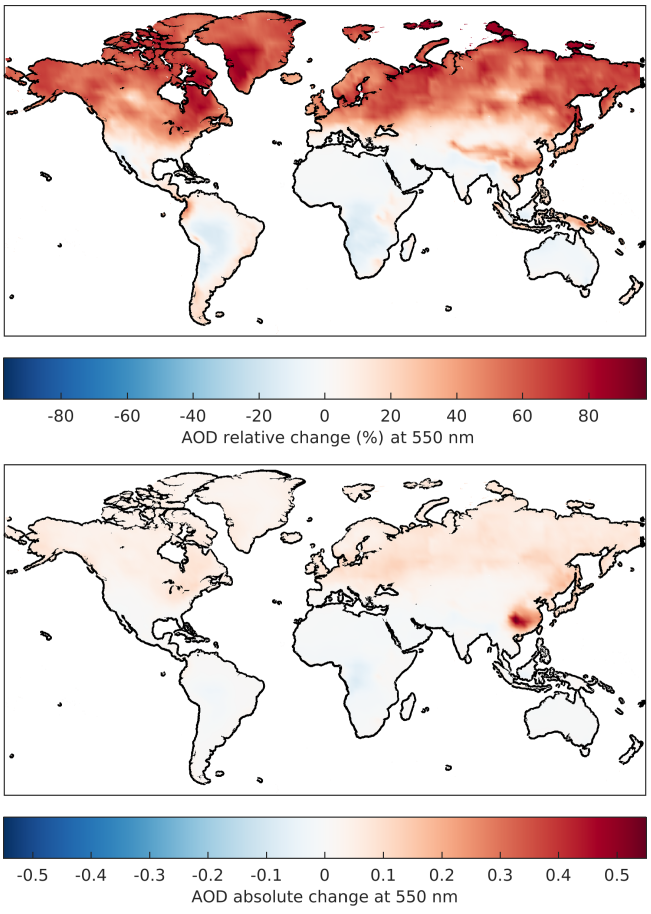

Figure B1. Average relative and absolute change in GEOS-Chem aerosol optical depth at 550 nm globally for the year 2006 after implementing revised optical tables for SIA and OA.

Figure B3 shows coincident measured vs. simulated AOD at AERONET sites for default (left) and revised (right) optical tables. The correlation coefficient ($r = 0.80$ to $r = 0.78$) changes insignificantly, while the slope decreases from 1.08 to 1.00 when switching to the revised optical tables. In summary, the revised optical properties developed for North America slightly improve the representation of AOD at the global scale, despite the large influence of other factors (e.g. ambient aerosol concentrations and composition) upon AOD.

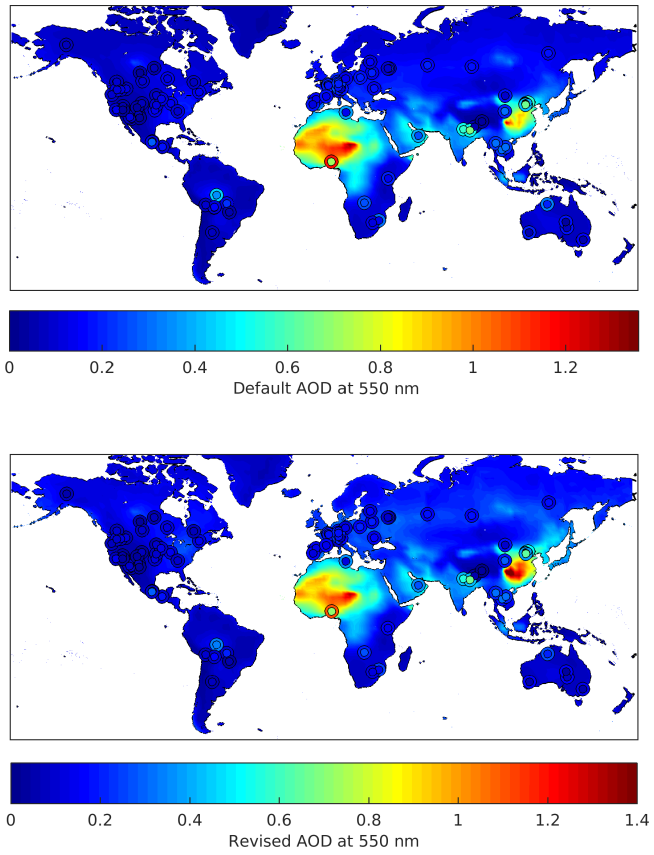

Figure B2. Global comparison for the year 2006 of AERONET AOD (inner circles) and GEOS-Chem coincident simulated AOD (outer rings) using default optical tables.

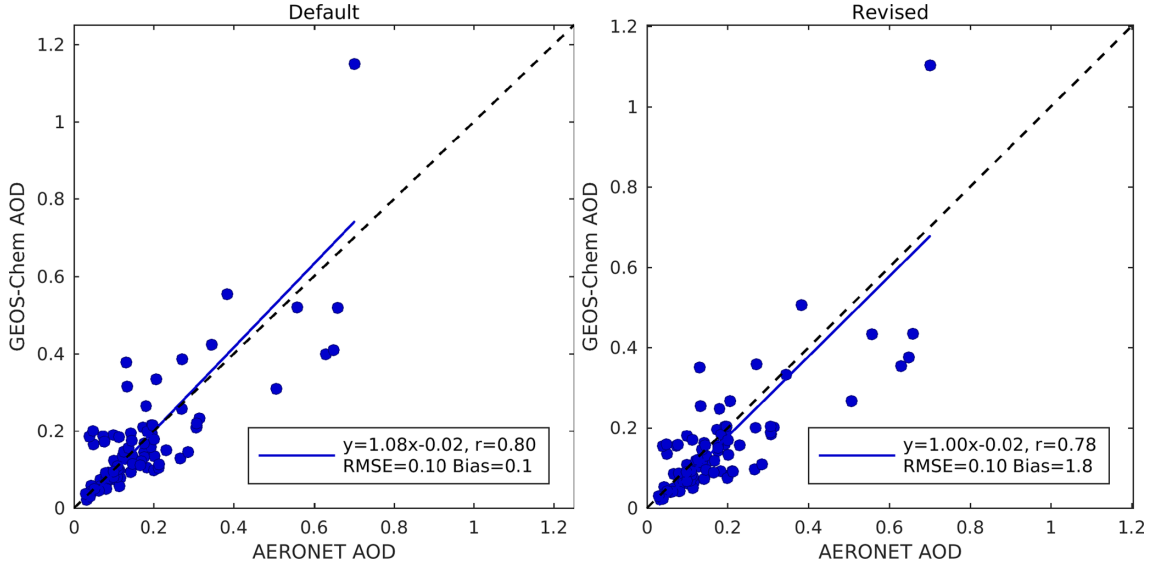

Figure B3. Coincident simulated vs. measured AOD at 550 nm at AERONET sites for the year 2006, using default and revised sizes and hygroscopicity. Slope, offset, and correlation coefficient are inset. The 1 : 1 line is shown in black.

Author contributions. RNCL and RVM conceived the study. RNCL conducted the analysis. RNCL and RVM prepared the paper.

Competing interests. The authors declare that they have no conflict of interest.

Acknowledgements. Research described in this article was conducted under contract to the Health Effects Institute (HEI), an organization jointly funded by the United States Environmental Protection Agency (EPA) (Assistance Award No. R-82811201) and certain motor vehicle and engine manufacturers. The contents of this article do not necessarily reflect the views of HEI, or its sponsors, nor do they necessarily reflect the views and policies of the EPA or motor vehicle and engine manufacturers.

IMPROVE is a collaborative association of state, tribal, and federal agencies, and international partners. The US Environmental Protection Agency is the primary funding source, with contracting and research support from the National Park Service. The Air Quality Group at the University of California, Davis is the central analytical laboratory, with ion analysis provided by the Research Triangle Institute, and carbon analysis provided by the Desert Research Institute.

We thank Environment and Climate Change Canada for providing nephelometer data at the site in Egbert, Ontario.

Edited by: Ashu Dastoor
Reviewed by: two anonymous referees

References

Achakulwisut, P., Shen, L., and Mickley, L. J.: What Controls Springtime Fine Dust Variability in the Western United States? Investigating the 2002–2015 Increase in Fine Dust in the U.S. Southwest, J. Geophys. Res.-Atmos., 122, 12449–12467, https://doi.org/10.1002/2017JD027208, 2017.

Andrews, E., Ogren, J. A., Bonasoni, P., Marinoni, A., Cuevas, E., Rodríguez, S., Sun, J. Y., Jaffe, D. A., Fischer, E. V., Baltensperger, U., Weingartner, E., Coen, M. C., Sharma, S., Macdonald, A. M., Leaitch, W. R., Lin, N. H., Laj, P., Arsov, T., Kalapov, I., Jefferson, A., and Sheridan, P.: Climatology of aerosol radiative properties in the free troposphere, Atmos. Res., 102, 365–393, https://doi.org/10.1016/j.atmosres.2011.08.017, 2011.

Bey, I., Jacob, D. J., Yantosca, R. M., Logan, J. A., Field, B. D., Fiore, A. M., Li, Q.-B., Liu, H.-Y., Mickley, L. J., and Schultz, M. G.: Global Modeling of Tropospheric Chemistry with Assimilated Meteorology: Model Description and Evaluation, J. Geophys. Res., 106, 73–95, https://doi.org/10.1029/2001JD000807, 2001.

Chin, M., Ginoux, P., Kinne, S., Torres, O., Holben, B. N., Duncan, B. N., Martin, R. V., Logan, J. A., Higurashi, A., and Nakajima, T.: Tropospheric Aerosol Optical Thickness from the GOCART Model and Comparisons with Satellite and Sun Photometer Measurements, J. Atmos. Sci., 59, 461–483, https://doi.org/10.1175/1520-0469(2002)059<0461:TAOTFT>2.0.CO;2, 2002.

Ciobanu, V. G., Marcolli, C., Krieger, U. K., Zuend, A., and Peter, T.: Efflorescence of ammonium sulfate and coated ammonium sulfate particles: Evidence for surface nucleation, J. Phys. Chem. A, 114, 9486–9495, https://doi.org/10.1021/jp103541w, 2010.

Collaud Coen, M., Andrews, E., Asmi, A., Baltensperger, U., Bukowiecki, N., Day, D., Fiebig, M., Fjaeraa, A. M., Flentje, H., Hyvärinen, A., Jefferson, A., Jennings, S. G., Kouvarakis, G., Lihavainen, H., Lund Myhre, C., Malm, W. C., Mihapopoulos, N., Molenar, J. V., O'Dowd, C., Ogren, J. A., Schichtel, B. A., Sheridan, P., Virkkula, A., Weingartner, E., Weller, R., and Laj, P.: Aerosol decadal trends – Part 1: In-situ optical measurements at GAW and IMPROVE stations, Atmos. Chem. Phys., 13, 869–894, https://doi.org/10.5194/acp-13-869-2013, 2013.

Dougle, P. G., Veefkind, J. P., and ten Brink, H. M. : Crystallisation of mixtures of ammonium nitrate, ammonium sulphate and soot, J. Aerosol. Sci., 29, 375–386, https://doi.org/10.1016/S0021-8502(97)10003-9, 1998.

Drury, E., Jacob, D. J., Spurr, R. J. D., Wang, J., Shinozuka, Y., Anderson, B. E., Clarke, A. D., Dibb, J., McNaughton, C., and Weber, R.: Synthesis of satellite (MODIS), aircraft (ICARTT), and surface (IMPROVE, EPA-AQS, AERONET) aerosol observations over eastern North America to improve MODIS aerosol retrievals and constrain surface aerosol concentrations and sources, J. Geophys. Res.-Atmos., 115, 1–17, https://doi.org/10.1029/2009JD012629, 2010.

Duplissy, J., DeCarlo, P. F., Dommen, J., Alfarra, M. R., Metzger, A., Barmpadimos, I., Prevot, A. S. H., Weingartner, E., Tritscher, T., Gysel, M., Aiken, A. C., Jimenez, J. L., Canagaratna, M. R., Worsnop, D. R., Collins, D. R., Tomlinson, J., and Baltensperger, U.: Relating hygroscopicity and composition of organic aerosol particulate matter, Atmos. Chem. Phys., 11, 1155–1165, https://doi.org/10.5194/acp-11-1155-2011, 2011.

Dusek, U., Frank, G. P., Massling, A., Zeromskiene, K., Iinuma, Y., Schmid, O., Helas, G., Hennig, T., Wiedensohler, A., and Andreae, M. O.: Water uptake by biomass burning aerosol at sub- and supersaturated conditions: closure studies and implications for the role of organics, Atmos. Chem. Phys., 11, 9519–9532, https://doi.org/10.5194/acp-11-9519-2011, 2011.

Fairlie, D. T., Jacob, D. J., and Park, R. J.: The impact of transpacific transport of mineral dust in the United States, Atmos. Environ., 41, 1251–1266, https://doi.org/10.1016/j.atmosenv.2006.09.048, 2007.

Fairlie, T. D., Jacob, D. J., Dibb, J. E., Alexander, B., Avery, M. A., van Donkelaar, A., and Zhang, L.: Impact of mineral dust on nitrate, sulfate, and ozone in transpacific Asian pollution plumes, Atmos. Chem. Phys., 10, 3999–4012, https://doi.org/10.5194/acp-10-3999-2010, 2010.

Fehsenfeld, F. C., Ancellet, G., Bates, T. S., Goldstein, A. H., Hardesty, R. M., Honrath, R., Law, K. S., Lewis, A. C., Leaitch, R., McKeen, S., Meagher, J., Parrish, D. D., Pszenny, A. A. P., Russell, P. B., Schlager, H., Seinfeld, J., Talbot, R., and Zbinden, R.: International Consortium for Atmospheric Research on Transport and Transformation (ICARTT): North America to Europe – Overview of the 2004 summer field study, J. Geophys. Res.-Atmos., 111, D23S01, https://doi.org/10.1029/2006JD007829, 2006.

Fountoukis, C. and Nenes, A.: ISORROPIA II: a computationally efficient thermodynamic equilibrium model for K^+-Ca^{2+}-Mg^{2+}-NH_4^+-Na^+-SO_4^{2-}-NO_3^--Cl^--H_2O aerosols, At-

mos. Chem. Phys., 7, 4639–4659, https://doi.org/10.5194/acp-7-4639-2007, 2007.

Gebhart, K. A., Copeland, S., and Malm, W. C.: Diurnal and seasonal patterns in light scattering, extinction, and relative humidity, Atmos. Environ., 35, 5177–5191, https://doi.org/10.1016/S1352-2310(01)00319-3, 2001.

Gelaro, R., McCarty, W., Suárez, M. J., Todling, R., Molod, A., Takacs, L., Randles, C. A., Darmenov, A., Bosilovich, M. G., Reichle, R., Wargan, K., Coy, L., Cullather, R., Draper, C., Akella, S., Buchard, V., Conaty, A., da Silva, A. M., Gu, W., Kim, G. K., Koster, R., Lucchesi, R., Merkova, D., Nielsen, J. E., Partyka, G., Pawson, S., Putman, W., Rienecker, M., Schubert, S. D., Sienkiewicz, M., and Zhao, B.: The modern-era retrospective analysis for research and applications, version 2 (MERRA-2), J. Climate, 30, 5419–5454, https://doi.org/10.1175/JCLI-D-16-0758.1, 2017.

Hand, J. L. and Malm, W. C.: Review of aerosol mass scattering efficiencies from ground-based measurements since 1990, J. Geophys. Res.-Atmos., 112, D16203, https://doi.org/10.1029/2007JD008484, 2007.

Hersey, S. P., Craven, J. S., Metcalf, A. R., Lin, J., Lathem, T., Suski, K. J., Cahill, J. F., Duong, H. T., Sorooshian, A., Jonsson, H. H., Shiraiwa, M., Zuend, A., Nenes, A., Prather, K. A., Flagan, R. C., and Seinfeld, J. H.: Composition and hygroscopicity of the Los Angeles Aerosol: CalNex, J. Geophys. Res.-Atmos., 118, 3016–3036, https://doi.org/10.1002/jgrd.50307, 2013.

Holben, B. N., Eck, T. F., Slutsker, I., Tanré, D., Buis, J. P., Setzer, A., Vermote, E., Reagan, J. A., Kaufman, Y. J., Nakajima, T., Lavenu, F., Jankowiak, I., and Smirnov, A.: AERONET – A Federated Instrument Network and Data Archive for Aerosol Characterization, Remote Sens. Environ., 66, 1–16, https://doi.org/10.1016/S0034-4257(98)00031-5, 1998.

Hyslop, N. P. and White, W. H.: An evaluation of interagency monitoring of protected visual environments (IMPROVE) collocated precision and uncertainty estimates, Atmos. Environ., 42, 2691–2705, https://doi.org/10.1016/j.atmosenv.2007.06.053, 2008.

Jaeglé, L., Quinn, P. K., Bates, T. S., Alexander, B., and Lin, J.-T.: Global distribution of sea salt aerosols: new constraints from in situ and remote sensing observations, Atmos. Chem. Phys., 11, 3137–3157, https://doi.org/10.5194/acp-11-3137-2011, 2011.

Jimenez, J. L., Canagaratna, M. R., Donahue, N. M., Prevot, A. S. H., Zhang, Q., Kroll, J. H., Decarlo, P. F., Allan, J. D., Coe, H., Ng, N. L., Aiken, A. C., Docherty, K. S., Ulbrich, I. M., Grieshop, A. P., Robinson, A. L., Duplissy, J., Smith, J. D., Wilson, K. R., Lanz, V. A., Hueglin, C., Sun, Y. L., Tian, J., Laaksonen, A., Raatikainen, T., Rautiainen, J., Vaattovaara, P., Ehn, M., Kulmala, M., Tomlinson, J. M., Collins, D. R., Cubison, M. J., Dunlea, J., Huffman, J. A., Onasch, T. B., Alfarra, M. R., Williams, P. I., Bower, K., Kondo, Y., Schneider, J., Drewnick, F., Borrmann, S., Weimer, S., Demerjian, K., Salcedo, D., Cottrell, L., Griffin, R., Takami, A., Miyoshi, T., Hatakeyama, S., Shimono, A., Sun, J. Y, Zhang, Y. M., Dzepina, K., Kimmel, J. R., Sueper, D., Jayne, J. T., Herndon, S. C., Trimborn, A. M., Williams, L. R., Wood, E. C., Middlebrook, A. M., Kolb, C. E., Baltensperger, U., and Worsnop, D. R.: Evolution of Organic Aerosols in the Atmosphere, Science, 326, 1525–1529, https://doi.org/10.1126/science.1180353, 2009.

Kahn, R. A., Gaitley, B. J., Martonchik, J. V., Diner, D. J., Crean, K. A., and Holben, B.: Multiangle Imaging Spectroradiometer (MISR) global aerosol optical depth validation based on 2 years of coincident Aerosol Robotic Network (AERONET) observations, J. Geophys. Res., 110, D10S04, https://doi.org/10.1029/2004JD004706, 2005.

Kim, P. S., Jacob, D. J., Fisher, J. A., Travis, K., Yu, K., Zhu, L., Yantosca, R. M., Sulprizio, M. P., Jimenez, J. L., Campuzano-Jost, P., Froyd, K. D., Liao, J., Hair, J. W., Fenn, M. A., Butler, C. F., Wagner, N. L., Gordon, T. D., Welti, A., Wennberg, P. O., Crounse, J. D., St. Clair, J. M., Teng, A. P., Millet, D. B., Schwarz, J. P., Markovic, M. Z., and Perring, A. E.: Sources, seasonality, and trends of southeast US aerosol: an integrated analysis of surface, aircraft, and satellite observations with the GEOS-Chem chemical transport model, Atmos. Chem. Phys., 15, 10411–10433, https://doi.org/10.5194/acp-15-10411-2015, 2015.

Koepke, P., Hess M., Schult I., and Shettle E.P.: Global Aerosol Data Set, Report No. 243, Max-Planck-Institut für Meteorologie, Hamburg, ISSN 0937-1060, 1997.

Kreidenweis, S. M., Petters, M. D., and DeMott, P. J.: Single-parameter estimates of aerosol water content, Environ. Res. Lett., 3, 035002, https://doi.org/10.1088/1748-9326/3/3/035002, 2008.

Levin, E. J. T., Kreidenweis, S. M., McMeeking, G. R., Carrico, C. M., Collett, J. L., and Malm, W. C.: Aerosol physical, chemical and optical properties during the Rocky Mountain Airborne Nitrogen and Sulfur study, Atmos. Environ., 43, 1932–1939, https://doi.org/10.1016/j.atmosenv.2008.12.042, 2009.

Li, Y., Henze, D. K., Jack, D., and Kinney, P. L.: The influence of air quality model resolution on health impact assessment for fine particulate matter and its components, Air Qual. Atmos. Hlth., 9, 51–68, https://doi.org/10.1007/s11869-015-0321-z, 2016.

Lowenthal, D. and Kumar, N.: Light scattering from sea-salt aerosols at interagency monitoring of protected visual environments (IMPROVE) sites, J. Air Waste Manage., 56, 636–642, https://doi.org/10.1080/10473289.2006.10464478, 2006.

Malm, C., Sisler, J. F., and Cahill, A.: Spatial and seasonal trends in particle concentration and optical extinction in the United States, J. Geophys. Res., 99, 1347–1370, 1994.

Malm, W. C.: Spatial and monthly trends in speciated fine particle concentration in the United States, J. Geophys. Res., 109, D03306, https://doi.org/10.1029/2003JD003739, 2004.

Malm, W. C. and Kreidenweis, S. M.: The effects of models of aerosol hygroscopicity on the apportionment of extinction, Atmos. Environ., 31, 1965–1976, https://doi.org/10.1016/S1352-2310(96)00355-X, 1997.

Malm, W. C. and Hand, J. L.: An examination of the physical and optical properties of aerosols collected in the IMPROVE program, Atmos. Environ., 41, 3407–3427, https://doi.org/10.1016/j.atmosenv.2006.12.012, 2007.

Mann, G. W., Carslaw, K. S., Spracklen, D. V., Ridley, D. A., Manktelow, P. T., Chipperfield, M. P., Pickering, S. J., and Johnson, C. E.: Description and evaluation of GLOMAP-mode: a modal global aerosol microphysics model for the UKCA composition-climate model, Geosci. Model Dev., 3, 519–551, https://doi.org/10.5194/gmd-3-519-2010, 2010.

Marais, E. A., Jacob, D. J., Jimenez, J. L., Campuzano-Jost, P., Day, D. A., Hu, W., Krechmer, J., Zhu, L., Kim, P. S., Miller, C. C., Fisher, J. A., Travis, K., Yu, K., Hanisco, T. F., Wolfe, G. M., Arkinson, H. L., Pye, H. O. T., Froyd, K. D., Liao, J., and McNeill, V. F.: Aqueous-phase mechanism for secondary or-

ganic aerosol formation from isoprene: application to the southeast United States and co-benefit of SO_2 emission controls, Atmos. Chem. Phys., 16, 1603–1618, https://doi.org/10.5194/acp-16-1603-2016, 2016.

Martin, R. V.: Global and regional decreases in tropospheric oxidants from photochemical effects of aerosols, J. Geophys. Res., 108, 4097, https://doi.org/10.1029/2002JD002622, 2003.

Martin, S. T., Schlenker, J. C., Malinowski, A., and Hung, H.: Crystallization of atmospheric sulfate-nitrate-ammonium particles, Geophys. Res. Lett., 30, 2102, https://doi.org/10.1029/2003GL017930, 2003.

Martin, S. T., Rosenoern, T., Chen, Q., and Collins, D. R.: Phase changes of ambient particles in the Southern Great Plains of Oklahoma, Geophys. Res. Lett., 35, 1–5, https://doi.org/10.1029/2008GL035650, 2008.

Mishchenko, M. I., Dlugach, J. M., Yanovitskij, E. G., and Zakharova, N. T.: Bidirectional reflectance of flat, optically thick particulate layers: An efficient radiative transfer solution and applications to snow and soil surfaces, J. Quant. Spectrosc. Ra., 63, 409–432, https://doi.org/10.1016/S0022-4073(99)00028-X, 1999.

Molenar, J. V.: Analysis of the Real World Performance of the Optec NGN-2 Ambient Nephelometer, in: Visual Air Quality: Aerosols and Global Radiation Balance, Air & Waste Management Association, Pittsburgh, 243–265, 1997.

Myhre, G., Shindell, D., Bréon, F.-M., Collins, W., Fuglestvedt, J., Huang, J., Koch, D., Lamarque, J.-F., Lee, D., Mendoza, B., Nakajima, T., Robock, A., Stephens, G., Takemura, T., and Zhang, H.: Anthropogenic and Natural Radiative Forcing, in: Climate Change 2013: The Physical Science Basis, Contribution of Working Group I to the Fifth Assessment Report of the Intergovernmental Panel on Climate Change, 659–740, https://doi.org/10.1017/CBO9781107415324.018, 2013.

Ng, N. L., Canagaratna, M. R., Zhang, Q., Jimenez, J. L., Tian, J., Ulbrich, I. M., Kroll, J. H., Docherty, K. S., Chhabra, P. S., Bahreini, R., Murphy, S. M., Seinfeld, J. H., Hildebrandt, L., Donahue, N. M., DeCarlo, P. F., Lanz, V. A., Prévôt, A. S. H., Dinar, E., Rudich, Y., and Worsnop, D. R.: Organic aerosol components observed in Northern Hemispheric datasets from Aerosol Mass Spectrometry, Atmos. Chem. Phys., 10, 4625–4641, https://doi.org/10.5194/acp-10-4625-2010, 2010.

Petters, M. D. and Kreidenweis, S. M.: A single parameter representation of hygroscopic growth and cloud condensation nucleus activity – Part 2: Including solubility, Atmos. Chem. Phys., 8, 6273–6279, https://doi.org/10.5194/acp-8-6273-2008, 2008.

Pandolfi, M., Alados-Arboledas, L., Alastuey, A., Andrade, M., Angelov, C., Artiñano, B., Backman, J., Baltensperger, U., Bonasoni, P., Bukowiecki, N., Collaud Coen, M., Conil, S., Coz, E., Crenn, V., Dudoitis, V., Ealo, M., Eleftheriadis, K., Favez, O., Fetfatzis, P., Fiebig, M., Flentje, H., Ginot, P., Gysel, M., Henzing, B., Hoffer, A., Holubova Smejkalova, A., Kalapov, I., Kalivitis, N., Kouvarakis, G., Kristensson, A., Kulmala, M., Lihavainen, H., Lunder, C., Luoma, K., Lyamani, H., Marinoni, A., Mihalopoulos, N., Moerman, M., Nicolas, J., O'Dowd, C., Petäjä, T., Petit, J.-E., Pichon, J. M., Prokopciuk, N., Putaud, J.-P., Rodríguez, S., Sciare, J., Sellegri, K., Swietlicki, E., Titos, G., Tuch, T., Tunved, P., Ulevicius, V., Vaishya, A., Vana, M., Virkkula, A., Vratolis, S., Weingartner, E., Wiedensohler, A., and Laj, P.: A European aerosol phenomenology – 6: scattering properties of atmospheric aerosol particles from 28 ACTRIS sites, Atmos. Chem. Phys., 18, 7877–7911, https://doi.org/10.5194/acp-18-7877-2018, 2018.

Park, R. J.: Sources of carbonaceous aerosols over the United States and implications for natural visibility, J. Geophys. Res., 108, 4355, https://doi.org/10.1029/2002JD003190, 2003.

Park, R. J., Jacob, D. J., Field, B. D., Yantosca, R. M., and Chin, M.: Natural and transboundary pollution influences on sulfate-nitrate-ammonium aerosols in the United States: Implications for policy, J. Geophys. Res.-Atmos., 109, D15204, https://doi.org/10.1029/2003JD004473, 2004.

Petters, M. D. and Kreidenweis, S. M.: A single parameter representation of hygroscopic growth and cloud condensation nucleus activity, Atmos. Chem. Phys., 7, 1961–1971, https://doi.org/10.5194/acp-7-1961-2007, 2007.

Petters, M. D. and Kreidenweis, S. M.: A single parameter representation of hygroscopic growth and cloud condensation nucleus activity – Part 3: Including surfactant partitioning, Atmos. Chem. Phys., 13, 1081–1091, https://doi.org/10.5194/acp-13-1081-2013, 2013.

Philip, S., Martin, R. V., van Donkelaar, A., Lo, J. W.-H., Wang, Y., Chen, D., Zhang, L., Kasibhatla, P. S., Wang, S., Zhang, Q., Lu, Z., Streets, D. G., Bittman, S., and Macdonald, D. J.: Global Chemical Composition of Ambient Fine Particulate Matter for Exposure Assessment, Environ. Sci. Technol., 48, 13060–13068, https://doi.org/10.1021/es502965b, 2014a.

Philip, S., Martin, R. V., Pierce, J. R., Jimenez, J. L., Zhang, Q., Canagaratna, M. R., Spracklen, D. V., Nowlan, C. R., Lamsal, L. N., Cooper, M. J., and Krotkov, N. A.: Spatially and seasonally resolved estimate of the ratio of organic mass to organic carbon, Atmos. Environ., 87, 34–40, https://doi.org/10.1016/j.atmosenv.2013.11.065, 2014b.

Pye, H. O. T., Liao, H., Wu, S., Mickley, L. J., Jacob, D. J., Henze, D. J., and Seinfeld, J. H.: Effect of changes in climate and emissions on future sulfate-nitrate-ammonium aerosol levels in the United States, J. Geophys. Res.-Atmos., 114, 1–18, https://doi.org/10.1029/2008JD010701, 2009.

Pye, H. O. T., Chan, A. W. H., Barkley, M. P., and Seinfeld, J. H.: Global modeling of organic aerosol: the importance of reactive nitrogen (NO_x and NO_3), Atmos. Chem. Phys., 10, 11261–11276, https://doi.org/10.5194/acp-10-11261-2010, 2010.

Rickards, A. M. J., Miles, R. E. H., Davies, J. F., Marshall, F. H., and Reid, J. P.: Measurements of the sensitivity of aerosol hygroscopicity and the κ parameter to the O/C ratio, J. Phys. Chem. A, 117, 14120–14131, https://doi.org/10.1021/jp407991n, 2013.

Ridley, D. A., Heald, C. L., and Ford, B.: North African dust export and deposition: A satellite and model perspective, J. Geophys. Res.-Atmos., 117, 1–21, https://doi.org/10.1029/2011JD016794, 2012.

Ridley, D. A., Heald, C. L., Ridley, K. J., and Kroll, J. H.: Causes and consequences of decreasing atmospheric organic aerosol in the United States, P. Natl. Acad. Sci. USA, 201700387, 115, 290–295, https://doi.org/10.1073/pnas.1700387115, 2017.

Singh, H. B., Brune, W. H., Crawford, J. H., Jacob, D. J., and Russell, P. B.: Overview of the summer 2004 Intercontinental Chemical Transport Experiment-North America (INTEX-A), J. Geophys. Res.-Atmos., 111, 0148–0227, https://doi.org/10.1029/2006JD007905, 2006.

Snider, G., Weagle, C. L., Martin, R. V., van Donkelaar, A., Conrad, K., Cunningham, D., Gordon, C., Zwicker, M., Akoshile, C., Artaxo, P., Anh, N. X., Brook, J., Dong, J., Garland, R. M., Greenwald, R., Griffith, D., He, K., Holben, B. N., Kahn, R., Koren, I., Lagrosas, N., Lestari, P., Ma, Z., Vanderlei Martins, J., Quel, E. J., Rudich, Y., Salam, A., Tripathi, S. N., Yu, C., Zhang, Q., Zhang, Y., Brauer, M., Cohen, A., Gibson, M. D., and Liu, Y.: SPARTAN: a global network to evaluate and enhance satellite-based estimates of ground-level particulate matter for global health applications, Atmos. Meas. Tech., 8, 505–521, https://doi.org/10.5194/amt-8-505-2015, 2015.

Snider, G., Weagle, C. L., Murdymootoo, K. K., Ring, A., Ritchie, Y., Stone, E., Walsh, A., Akoshile, C., Anh, N. X., Balasubramanian, R., Brook, J., Qonitan, F. D., Dong, J., Griffith, D., He, K., Holben, B. N., Kahn, R., Lagrosas, N., Lestari, P., Ma, Z., Misra, A., Norford, L. K., Quel, E. J., Salam, A., Schichtel, B., Segev, L., Tripathi, S., Wang, C., Yu, C., Zhang, Q., Zhang, Y., Brauer, M., Cohen, A., Gibson, M. D., Liu, Y., Martins, J. V., Rudich, Y., and Martin, R. V.: Variation in global chemical composition of $PM_{2.5}$: emerging results from SPARTAN, Atmos. Chem. Phys., 16, 9629–9653, https://doi.org/10.5194/acp-16-9629-2016, 2016.

Solomon, P. A., Crumpler, D., Flanagan, J. B., Jayanty, R. K. M., Rickman, E. E., and McDade, C. E.: U.S. National $PM_{2.5}$ Chemical Speciation Monitoring Networks-CSN and IMPROVE: Description of Networks, J. Air Waste Manage., 64, 1410–1438, https://doi.org/10.1080/10962247.2014.956904, 2014.

Spracklen, D. V., Pringle, K. J., Carslaw, K. S., Chipperfield, M. P., and Mann, G. W.: A global off-line model of size-resolved aerosol microphysics: I. Model development and prediction of aerosol properties, Atmos. Chem. Phys., 5, 2227–2252, https://doi.org/10.5194/acp-5-2227-2005, 2005.

Stanier, C. O., Khlystov, A. Y., and Pandis, S. N.: Ambient aerosol size distributions and number concentrations measured during the Pittsburgh Air Quality Study (PAQS), Atmos. Environ., 38, 3275–3284, https://doi.org/10.1016/j.atmosenv.2004.03.020, 2004.

Tao, J., Zhang, L., Ho, K., Zhang, R., Lin, Z., Zhang, Z., Lin, M., Cao, J., Liu, S., and Wang, G.: Impact of $PM_{2.5}$ chemical compositions on aerosol light scattering in Guangzhou – the largest megacity in South China, Atmos. Res., 135–136, 48–58, https://doi.org/10.1016/j.atmosres.2013.08.015, 2014.

Titos, G., Foyo-Moreno, I., Lyamani, H., Querol, X., Alastuey, A., and Alados-Arboledas, L.: Optical properties and chemical composition of aerosol particles at an urban location: An estimation of the aerosol mass scattering and absorption efficiencies, J. Geophys. Res.-Atmos., 117, 1–12, https://doi.org/10.1029/2011JD016671, 2012.

Trivitayanurak, W., Adams, P. J., Spracklen, D. V., and Carslaw, K. S.: Tropospheric aerosol microphysics simulation with assimilated meteorology: model description and intermodel comparison, Atmos. Chem. Phys., 8, 3149–3168, https://doi.org/10.5194/acp-8-3149-2008, 2008.

van Donkelaar, A., Martin, R. V., Brauer, M., Kahn, R., Levy, R., Verduzco, C., and Villeneuve, P. J.: Global estimates of ambient fine particulate matter concentrations from satellite-based aerosol optical depth: Development and application, Environ. Health Perspect., 118, 847–855, https://doi.org/10.1289/ehp.0901623, 2010.

van Donkelaar, A., Martin, R. V., Spurr, R. J. D., and Burnett, R. T.: High-Resolution Satellite-Derived $PM_{2.5}$ from Optimal Estimation and Geographically Weighted Regression over North America, Environ. Sci. Technol., 49, 10482–10491, https://doi.org/10.1021/acs.est.5b02076, 2015.

Wang, J., Hoffmann, A. A., Park, R. J., Jacob, D. J., and Martin, S. T.: Global distribution of solid and aqueous sulfafte aerosols: Effect of the hysteresis of particle phase transitions, J. Geophys. Res.-Atmos., 113, 1–11, https://doi.org/10.1029/2007JD009367, 2008.

Wang, Q., Jacob, D. J., Spackman, J. R., Perring, A. E., Schwarz, J. P., Moteki, N., Marais, E. A., Ge, C., Wang, J., and Barrett, S. R. H.: Global budget and radiative forcing of black carbon aerosol: Constraints from pole-to-pole (HIPPO) observations across the Pacific, 119, 195–206, https://doi.org/10.1002/2013JD020824, 2014.

Wexler, A. S. and Clegg, S. L.: Atmospheric aerosol models for systems including the ions H^+, NH_4^+, Na^+, SO_4^{2-}, NO_3^-, Cl^-, Br^-, and H_2O, J. Geophys. Res., 107, 4207, https://doi.org/10.1029/2001JD000451, 2002.

White, W. H.: On the theoretical and empirical basis for apportioning extinction by aerosols: A critical review, Atmos. Environ., 20, 1659–1672, https://doi.org/10.1016/0004-6981(86)90113-7, 1986.

White, W. H., Macias, E. S., Nininger, R. C., and Schorran, D.: Size-resolved measurements of light scattering by ambient particles in the southwestern U.S.A., Atmos. Environ., 28, 909–921, https://doi.org/10.1016/1352-2310(94)90249-6, 1994.

Wise, M. E.: Hygroscopic growth of ammonium sulfate/dicarboxylic acids, J. Geophys. Res., 108, 4638, https://doi.org/10.1029/2003JD003775, 2003.

Yu, F. and Luo, G.: Simulation of particle size distribution with a global aerosol model: contribution of nucleation to aerosol and CCN number concentrations, Atmos. Chem. Phys., 9, 7691–7710, https://doi.org/10.5194/acp-9-7691-2009, 2009.

Zhang, L., Kok, J. F., Henze, D. K., Li, Q., and Zhao, C.: Improving simulations of fine dust surface concentrations over the western United States by optimizing the particle size distribution, Geophys. Res. Lett., 40, 3270–3275, https://doi.org/10.1002/grl.50591, 2013.

A Section 508–conformant HTML version of this article is available at https://doi.org/10.1289/EHP5204.

Examining the Shape of the Association between Low Levels of Fine Particulate Matter and Mortality across Three Cycles of the Canadian Census Health and Environment Cohort

Amanda J. Pappin,[1] Tanya Christidis,[1] Lauren L. Pinault,[1] Dan L. Crouse,[2,3] Jeffrey R. Brook,[4] Anders Erickson,[5] Perry Hystad,[6] Chi Li,[7] Randall V. Martin,[7,8,9] Jun Meng,[7,9] Scott Weichenthal,[10,11] Aaron van Donkelaar,[7,9] Michael Tjepkema,[1] Michael Brauer,[5] and Richard T. Burnett[12]*

[1]Health Analysis Division, Statistics Canada, Ottawa, Ontario, Canada
[2]Department of Sociology, University of New Brunswick, Fredericton, New Brunswick, Canada
[3]New Brunswick Institute for Research, Data, and Training, Fredericton, New Brunswick, Canada
[4]Dalla Lana School of Public Health, University of Toronto, Toronto, Ontario, Canada
[5]School of Population and Public Health, University of British Columbia, Vancouver, British Columbia, Canada
[6]College of Public Health and Human Sciences, Oregon State University, Corvallis, Oregon, USA
[7]Department of Physics and Atmospheric Science, Dalhousie University, Halifax, Nova Scotia, Canada
[8]Harvard-Smithsonian Center for Astrophysics, Cambridge, Massachusetts, USA
[9]Department of Energy, Environmental & Chemical Engineering, Washington University in St. Louis, St. Louis, Missouri, United States
[10]Department of Epidemiology, Biostatistics & Occupational Health, McGill University, Montreal, Quebec, Canada
[11]Air Health Science Division, Health Canada, Ottawa, Ontario, Canada
[12]Population Studies Division, Health Canada, Ottawa, Ontario, Canada

Background: Ambient fine particulate air pollution with aerodynamic diameter $\leq 2.5\,\mu m$ ($PM_{2.5}$) is an important contributor to the global burden of disease. Information on the shape of the concentration–response relationship at low concentrations is critical for estimating this burden, setting air quality standards, and in benefits assessments.

Objectives: We examined the concentration–response relationship between $PM_{2.5}$ and nonaccidental mortality in three Canadian Census Health and Environment Cohorts (CanCHECs) based on the 1991, 1996, and 2001 census cycles linked to mobility and mortality data.

Methods: Census respondents were linked with death records through 2016, resulting in 8.5 million adults, 150 million years of follow-up, and 1.5 million deaths. Using annual mailing address, we assigned time-varying contextual variables and 3-y moving-average ambient $PM_{2.5}$ at a 1×1 km spatial resolution from 1988 to 2015. We ran Cox proportional hazards models for $PM_{2.5}$ adjusted for eight subject-level indicators of socioeconomic status, seven contextual covariates, ozone, nitrogen dioxide, and combined oxidative potential. We used three statistical methods to examine the shape of the concentration–response relationship between $PM_{2.5}$ and nonaccidental mortality.

Results: The mean 3-y annual average estimate of $PM_{2.5}$ exposure ranged from 6.7 to 8.0 $\mu g/m^3$ over the three cohorts. We estimated a hazard ratio (HR) of 1.053 [95% confidence interval (CI): 1.041, 1.065] per 10-$\mu g/m^3$ change in $PM_{2.5}$ after pooling the three cohort-specific hazard ratios, with some variation between cohorts (1.041 for the 1991 and 1996 cohorts and 1.084 for the 2001 cohort). We observed a supralinear association in all three cohorts. The lower bound of the 95% CIs exceeded unity for all concentrations in the 1991 cohort, for concentrations above 2 $\mu g/m^3$ in the 1996 cohort, and above 5 $\mu g/m^3$ in the 2001 cohort.

Discussion: In a very large population-based cohort with up to 25 y of follow-up, $PM_{2.5}$ was associated with nonaccidental mortality at concentrations as low as 5 $\mu g/m^3$. https://doi.org/10.1289/EHP5204

Introduction

Exposure to ambient fine particulate air pollution with aerodynamic diameter $\leq 2.5\,\mu m$ ($PM_{2.5}$) consistently ranks among the leading risk factors for premature death and disease worldwide (Burnett et al. 2018; GBD 2017 Risk Factors Collaborators 2018; Lim et al. 2012). A number of studies supporting this work have found that the relationship between $PM_{2.5}$ concentrations and mortality risk (for various causes) was supralinear across the global range (Burnett et al. 2014; Pope et al. 2009, 2011; Yin et al. 2017). In a detailed examination of the shape of the $PM_{2.5}$–mortality association in 15 of the world's largest cohorts (Burnett et al. 2018), 12 displayed a supralinear association. A supralinear concentration–response curve is characterized by a positively sloped curve of decreasing steepness, such that risk initially rises rapidly with a decreasing slope as concentrations increase. Studies that specifically characterize the shape of concentration–response relationships at low-$PM_{2.5}$ mass concentrations offer great value given the steady decline in $PM_{2.5}$ levels over recent decades in North America (ECCC 2017). Further, a substantial proportion of the global $PM_{2.5}$ disease burden is from relatively low level exposures (Apte et al. 2015). Canada is an ideal setting to conduct such analyses, given the availability of large, national cohorts with sufficient sample sizes and detailed exposure information at low $PM_{2.5}$ concentrations.

Canadian cohort studies have shown consistent positive associations between $PM_{2.5}$ and mortality from various causes at low $PM_{2.5}$ concentrations (i.e., annual concentrations generally below 20 $\mu g/m^3$ even in large urban areas) (Crouse et al. 2012, 2015; Nasari et al. 2016; Pinault et al. 2016b, 2017; Weichenthal et al. 2017). Crouse et al. (2012) used the 1991 Canadian Census Health and Environment Cohort (CanCHEC) to conduct the first nationwide cohort analysis and identified a hazard ratio (HR) for nonaccidental mortality of 1.07 [95% confidence interval (CI): 1.06, 1.08] per 10-$\mu g/m^3$ change in $PM_{2.5}$ among nonimmigrant

Address correspondence to Dan L Crouse, PhD, Dept. of Sociology, University of New Brunswick, 9 Macaulay Lane, Tilley Hall, Room 20, Fredericton, New Brunswick, Canada E3B 5A3. Telephone: (506) 458-7436. Email: Dlcrouse@gmail.com

*Current affiliation of Amanda J. Pappin is Air Health Effects Assessment Division, Health Canada, Ottawa, Ontario, Canada.

Supplemental Material is available online (https://doi.org/10.1289/EHP5204).

The authors declare they have no actual or potential competing financial interests.

Received 15 February 2019; Revised 18 September 2019; Accepted 18 September 2019; Published 22 October 2019.

adults. In a recent analysis of the 2001 CanCHEC, Pinault et al. (2017) reported a larger HR of 1.18 (95% CI: 1.15, 1.21) for $PM_{2.5}$ and nonaccidental mortality. While these studies made important contributions to the evidence base for mortality risks at low $PM_{2.5}$ levels, they also had several important limitations. For example, with the exception of Pinault et al. (2017), past studies used coarser-resolution $PM_{2.5}$ models (i.e., 10×10 km) to assign exposures to census respondents. Furthermore, most of the previous studies excluded immigrants, although this group represents nearly 20% of the Canadian population. Additionally, most of these studies had only 10 y of follow-up.

The present study specifically investigated the shape of the concentration–response function between $PM_{2.5}$ and nonaccidental mortality at low levels of exposure among Canadian adults. We examined data from the 1991, 1996, and 2001 CanCHECs with follow-up until 2016. We address a number of limitations of previous cohort studies in Canada by extending the period of follow-up to 25 y (i.e., for individuals in the 1991 cohort), including all but recent immigrants in the analysis, using annual 1 km^2 $PM_{2.5}$ estimates from 1988–2015, using time-varying contextual covariates over the duration of follow-up, and applying a validated marginalization index to represent four orthogonal dimensions of neighborhood- or community-level socioeconomic status. We examined the shape of associations at low levels of $PM_{2.5}$ exposure by applying restricted cubic splines (RCS) (Harrell 2015), monotonically increasing smoothing splines (MISS) (Pya and Wood 2015), and the Shape Constrained Health Impact Function (SCHIF) (Nasari et al. 2016).

Methods

Analytical Cohort

We created three new, separate analytical cohorts from the 1991, 1996, and 2001 CanCHECs. Briefly, the CanCHECs are population-based, administrative data cohorts that link eligible census respondents (i.e., noninstitutional respondents to the mandatory Statistics Canada long-form census questionnaire that is distributed to 20% of all Canadian households) to their annual mailing address (1981–2016) and follow subjects for mortality. Information on a number of variables capturing the social and economic status of the subjects was available from the long-form census (Table 1).

The linkage was approved by Statistics Canada (linkage requests 037-2016 and 045-2015) and is governed by the Directive on Microdata Linkage (Statistics Canada 2017a). Eligible respondents were first linked probabilistically to tax records using sex, date of birth, postal code (PC), and spousal date of birth (if available).

Table 1. $PM_{2.5}$ Distribution by cohort with lowest (2nd percentile) and highest (98th percentile) knot values for restricted cubic spline.

	2001	1996	1991
100% max	18.50	20.00	20.00
99%	12.30	15.00	17.26
98% (highest knot)	11.70	13.97	17.03
95%	10.70	12.20	14.63
90%	9.80	10.70	12.60
75% Q3	8.23	8.84	9.83
50% median	6.40	6.75	7.40
25% Q1	4.87	5.04	5.38
10%	3.97	4.10	4.26
5%	3.57	3.67	3.80
2% (lowest knot)	3.00	3.29	3.43
1%	3.00	3.05	3.13
0% min	0.37	0.37	0.37
Mean	6.68	7.18	7.95
SD	2.24	2.70	3.28

Note: SD, standard deviation.

This initial linkage was necessary since linkage to the mortality database is based on the social insurance number (SIN), a unique personal identifier. The long form censuses did not capture the SIN, but they are available on tax records. The linkage rate to tax records near the time of cohort inception was approximately 80%, of which 99% were determined to be accurate matches (Christidis et al. 2018; Pinault et al. 2016a; Wilkins et al. 2008).

Mortality and PC history data were attached to the census-tax cohorts using Statistics Canada's Social Data Linkage Environment (SDLE) Derived Record Depository (DRD) (Statistics Canada 2017b), a dynamic relational database. About 99.8% of all deaths that occurred in Canada between 1991 and 2016 were linked to the DRD before being linked to eligible census respondents. From this linkage, we obtained death date and underlying cause of death if it occurred between census day and 31 December 2016. Mortality data were coded by underlying cause of death according to the *International Classification of Diseases, 9th Revision*, prior to 2000 (ICD-9; WHO 1977), and *10th Revision* post-2000 (ICD-10; WHO 2016).

We enhanced the cohort with a number of data elements characterizing the environment in which each subject lived, using PC histories from tax records, of which the primary source was income tax filings (1981 to 2016). We assigned a representative point (latitude and longitude) to each PC (Statistics Canada 2017c). In large cities, PCs often correspond to a single block face, though in rural areas, they can range over much larger areas. Similarly, the point estimates of PCs are accurate within 0.2 km in urban centers and 5.6 km in rural areas (Khan et al. 2018). These point estimates were used to derive estimates of air pollution and location-based contextual risk factors.

We note that these three linked cohorts are newly created using an enhanced linkage environment (SDLE) and thus are not identical to the CanCHEC cohorts used in previous publications (Crouse et al. 2015; Pinault et al. 2017).

Outdoor Air Pollution Concentrations

We used annual ambient $PM_{2.5}$ surfaces as our main exposure of interest at a $0.01^\circ \times 0.01^\circ$ resolution (~ 1 km^2) over North America for 1981–2016 (Meng et al. 2019; van Donkelaar et al. 2015). $PM_{2.5}$ estimates for the years 1998–2012 were developed by relating satellite-based retrievals of total column aerosol optical depth to near-surface $PM_{2.5}$ concentrations using the geophysical relationship simulated by a chemical transport model (CTM). These estimates were constrained using ground-based monitoring from the National Air Pollution Surveillance (NAPS) program stations, along with other North America–based measurements, land-use information, and simulated composition in a geographically weighted regression (V4.NA.01; van Donkelaar et al. 2015). For years outside this period, we used $PM_{2.5}$ surfaces developed using a backcasting method (Meng et al. 2019) that applied observed annual trends in ground monitoring data for $PM_{2.5}$ and coarser size fractions to adjust pregridded $PM_{2.5}$ estimates backwards or forwards in time. We estimated a 3-y moving-average exposure window with 1-y lag for assigning $PM_{2.5}$ exposures for consistency with previous studies, as ambient $PM_{2.5}$ is regulated based on a 3-y time window in Canada (CCME 2012).

We assigned estimates of exposures to ambient ozone (O_3; as a May–September daily maximum 8-h average) and nitrogen dioxide (NO_2; annual) for inclusion in multipollutant models. Additionally, we estimated a measure of the combined oxidant capacity of O_3 and NO_2, expressed as $O_x = 2/3\,O_3 + 1/3\,NO_2$ (Weichenthal et al. 2017). We estimated a 3-y average with 1-y lag for each of O_3, NO_2, and O_x for inclusion in the hazard models. Modeled O_3 surfaces at 21-km spatial resolution were developed by Environment and Climate Change Canada (ECCC) for

2002–2015 using chemical transport modeling informed by surface observations (Robichaud and Ménard 2014; Robichaud et al. 2016). Estimates of ambient NO_2 were based on a national land-use regression model (LUR) developed for 2006 (Hystad et al. 2011) with a spatial resolution of 100 m. The LUR estimates were built using satellite-derived NO_2 (with 10-km resolution), distances to highways and major roads, and roadway kernel density gradients as predictive variables.

We temporally adjusted the O_3 and NO_2 models to obtain exposure estimates over our study period (i.e., 1988–2015). Our adjustment was based on observed trends in ground monitoring data for NO_2 and O_3 from the NAPS in Canada. For each of 24 census divisions (CDs) that had monitoring data available, we estimated yearly adjustment factors from the ratio of observed CD-average concentration in a specific year to the reference year(s) for which the original surfaces were estimated (i.e., 2006 for NO_2 and 2002–2015 average for O_3). We assigned adjustment factors for each PC from the closest CD.

Contextual Covariates

We assigned contextual risk factors describing neighborhood-level characteristics and geographic identifiers using residential PC and data from the closest census (every 5 y from 1991 through 2016). We included in our analysis the Canadian Marginalization Index (CAN-Marg), population size of home community or city, an indicator of urban form, and regional airshed to capture risk factors beyond those captured at the subject level. We assigned these four categories of contextual covariates to residential PCs linked to census geography for each census year.

CAN-Marg is a publicly available index of neighborhood marginalization in Canada that was developed by Matheson et al. (2012) using an analysis of the 2001 and 2006 long-form census cycles. CAN-Marg consists of four dimensions that aim to capture different aspects of marginalization: material deprivation, residential instability, ethnic concentration, and dependency. Following the methodology of Matheson et al. (2012), we developed CAN-Marg using the 1991 and 1996 censuses. We assigned CAN-Marg to PC locations and then created quintiles (based on the cohort distribution) of the continuous values in the four Can-MARG dimensions in order to account for any potentially nonlinear associations with mortality.

We used a variable to describe the population size of a subject's community (Pinault et al. 2017) (Table 2). We categorized geographic locations into the following: census metropolitan areas (CMAs) or census agglomerations (CAs; Statistics Canada 2003) with a population exceeding 1.5 million; 500,000–1.49 million; 100,000–499,999; 30,000–99,999; or 10,000–29,999, as well as non-CMAs/CAs. We note that although non-CMA/CAs are always rural areas, CMAs cover both the urban core of a city and the urban–rural fringe, such that some rural locations fall within a CMA/CA. As such, this variable does not perfectly delineate subjects living in rural vs. urban settings.

To further differentiate between the kinds of built environments and neighborhoods within communities, we created an urban form variable following the methodology developed by Gordon and Janzen (2013). This measure of urban form is informed by population density and the most frequently reported mode of transportation (active or transit) in each census tract as reported on each census cycle. The categories of this variable include an active urban core, transit-reliant suburb, car-reliant suburb, exurban, and non-CMA/CA. We note that mode of commute was not reported on the 1991 census cycle and was derived from the 1996 census.

We included airshed as a geographic covariate in our analysis (Crouse et al. 2016). Airsheds divide Canada into six regions (Western, Prairie, West Central, Southern Atlantic, East Central, and Northern) based on large-scale differences in air masses and meteorology. Airsheds can also be used to represent regional differences in mortality rates across Canada that remain uncaptured by other geographic covariates.

Exclusion of Person-Years of Follow-Up

PC history was not available for each person in every year of follow-up, either because they did not file a tax return or from gaps in administrative data. Any gaps in PCs that had the same PC prior to and after the gap were assigned that PC for all years of the gap. After this imputation, 87.8% of person-years had an available PC. We imputed an additional 2.1% of person-years of missing PCs if the bounding PCs shared the first two characters (Finès et al. 2017; Pinault et al. 2017), totaling 89.9% of person-years with a PC.

After imputation, person-years were excluded if they did not have an assigned PC. Further exclusions of person-years occurred due to: immigrated to Canada less than 10 y before survey date (9,364,400 person-years), age during follow-up period exceeded 89 y (7,357,200), could not be linked to air pollution values (17,814,400), could not be linked to CAN-Marg values (25,973,900), could not be linked to CMA/CA size (25,613,100), could not be linked to airshed (25,545,500), 3-y moving average being informed by only 1 y of exposure (20,056,400), and year after subject death (17,936,100). The above are not mutually exclusive numbers of exclusions. The total available person-years for analyses were 150,996,500 after all exclusions (Figure S1).

Statistical Analysis

Our primary statistical model relating exposure to mortality was the Cox proportional hazards model (Cox 1972). Participants were at least 25 y of age at the beginning of each cohort, and the time axis was the year of follow-up until 2016. Person-years before a census year and after a subject's death year were excluded from analysis. Events were determined by year of death for nonaccidental causes. The Cox model baseline hazard function was stratified by age (5-y groups), sex, and immigrant status (yes or no). This latter strata variable was included since immigrants to Canada live longer, on average, than do Canadian-born citizens (Ng 2011). We excluded immigrants living in Canada for less than 10 y at cohort commencement due to the healthy immigrant effect (Ng 2011) and lack of knowledge of their historical air pollution exposures. Each subject was censored at 89 y of age, either at the start of each cohort or during follow-up, due to evidence suggesting an increased mismatch between home address and the tax return mailing address with increasing age (Bérard-Chagnon 2017). We postulate that relatives of elderly people were completing their tax returns. Each of the three CanCHEC cohorts (1991, 1996, and 2001) was examined separately. Estimates of the cohort-specific hazard ratios were then pooled to form a single summary hazard ratio. We also conducted a test for differences in the hazard ratios between cohorts (Cochran 1950).

We fit two covariate adjustment models for each cohort. The first was based on a directed acyclic graph (DAG; Figure S2) and consisted of all the geographically based predictors: CAN-Marg (four dimensions), airshed, urban form, and CMA/CA size. The second model, denoted as "Full," additionally included the subject-level predictors (income, education, occupational class, Indigenous status, visible minority status, employment status, and marital status), which are not *a priori* causes of outdoor $PM_{2.5}$ concentrations, but which may contribute to confounding owing to a chance imbalance across the $PM_{2.5}$ distribution.

We also conducted analysis by categories of: immigrant status (yes or no), sex (male or female), and age during follow-up (<65, 65–74, or ≥75 y) for each cohort separately, again pooling the

Table 2. Descriptive statistics of 1991, 1996, and 2001 Canadian Census Health and Environment Cohort (CanCHEC) study cohorts.

	1991 CanCHEC				1996 CanCHEC				2001 CanCHEC			
	Person-years		$PM_{2.5}$ concentration ($\mu g/m^3$)		Person-years		$PM_{2.5}$ concentration ($\mu g/m^3$)		Person-years		$PM_{2.5}$ concentration ($\mu g/m^3$)	
Covariate	*n*	%	Mean	SD	*n*	%	Mean	SD	*n*	%	Mean	SD
Total	54,042,100	100.0%	8.10	3.44	54,082,700	100.0%	7.18	2.70	42,871,700	100.0%	6.68	2.24
Sex												
Male	27,769,300	51.4	8.14	3.43	28,240,300	52.2	7.23	2.69	22,308,500	52.0	6.72	2.24
Female	26,272,800	48.6	8.06	3.45	25,842,400	47.8	7.13	2.70	20,563,200	48.0	6.64	2.24
Age group												
24–34 y	3,540,300	6.6	10.56	3.96	3,170,900	5.9	8.37	3.18	2,659,100	6.2	7.18	2.52
35–44 y	10,088,100	18.7	8.75	3.58	10,368,100	19.2	7.37	2.82	8,518,300	19.9	6.64	2.29
45–54 y	14,381,600	26.6	7.72	3.25	14,364,600	26.6	6.99	2.61	11,112,700	25.9	6.58	2.21
55–64 y	11,986,800	22.2	7.55	3.19	11,839,400	21.9	6.93	2.56	9,401,200	21.9	6.57	2.17
65–74 y	8,227,800	15.2	7.84	3.32	8,259,400	15.3	7.12	2.64	6,335,700	14.8	6.69	2.21
75–89 y	5,817,700	10.8	7.88	3.13	6,080,300	11.2	7.26	2.55	4,844,600	11.3	6.90	2.20
Immigrant status												
Nonimmigrant	45,568,900	84.3	7.82	3.34	45,280,200	83.7	6.94	2.62	35,465,100	82.7	6.46	2.20
Immigrant, 11–20 y	2,711,900	5.0	9.48	3.48	2,114,600	3.9	8.40	2.60	1,871,300	4.4	7.82	2.00
Immigrant, 21–30 y	2,585,500	4.8	9.57	3.57	3,148,000	5.8	8.45	2.69	2,055,200	4.8	7.69	2.06
Immigrant, >30 y	3,175,800	5.9	9.63	3.74	3,539,800	6.6	8.47	2.84	3,480,100	8.1	7.69	2.23
Visible minority status												
No	51,309,700	94.9	8.02	3.42	51,075,900	94.4	7.10	2.69	37,791,200	88.2	6.69	2.22
Yes	2,732,400	5.1	9.61	3.40	3,006,700	5.6	8.56	2.49	5,080,500	11.9	6.60	2.41
Indigenous status												
No	51,920,400	96.1	8.17	3.43	51,916,000	96.0	7.28	2.68	40,921,000	95.5	6.78	2.22
Yes	2,121,800	3.9	6.28	3.06	2,166,700	4.0	4.90	1.99	1,950,700	4.6	4.61	1.69
Marital status												
Never married/not common-law	6,776,600	12.5	8.52	3.49	6,597,000	12.2	7.57	2.74	5,233,700	12.2	7.05	2.29
Common-law	4,035,500	7.5	7.73	3.24	5,066,100	9.4	6.81	2.50	4,693,200	11.0	6.50	2.15
Married	37,316,200	69.1	7.95	3.40	36,029,200	66.6	7.07	2.68	27,590,800	64.4	6.57	2.22
Separated	1,275,500	2.4	8.46	3.53	1,323,000	2.5	7.49	2.78	1,032,800	2.4	6.89	2.29
Divorced	2,524,900	4.7	8.62	3.46	2,861,000	5.3	7.65	2.68	2,404,100	5.6	7.09	2.21
Widowed	2,113,400	3.9	9.11	3.76	2,206,300	4.1	7.83	2.91	1,917,000	4.5	7.09	2.37
Educational attainment												
<High school graduation	17,025,100	31.5	8.00	3.55	16,190,200	29.9	7.01	2.80	11,564,900	27.0	6.50	2.34
High school, with or without trades certificate	20,516,400	38.0	8.00	3.39	19,575,600	36.2	7.11	2.65	15,491,200	36.1	6.60	2.22
Postsecondary nonuniversity	8,940,200	16.5	8.11	3.35	10,185,400	18.8	7.23	2.63	8,542,100	19.9	6.71	2.17
University degree	7,560,400	14.0	8.55	3.38	8,131,400	15.0	7.64	2.62	7,273,600	17.0	7.08	2.16
Income inadequacy												
Q1 (lowest income)	8,373,700	15.5	8.25	3.61	8,693,400	16.1	7.21	2.81	7,216,300	16.8	6.76	2.36
Q2	9,989,100	18.5	8.22	3.50	9,949,900	18.4	7.28	2.75	8,078,000	18.8	6.74	2.28
Q3	11,417,600	21.1	8.09	3.42	11,248,900	20.8	7.21	2.69	8,772,600	20.5	6.70	2.23
Q4	12,023,900	22.3	8.03	3.37	11,875,400	22.0	7.15	2.65	9,194,600	21.5	6.64	2.19
Q5 (highest income)	12,237,800	22.6	7.97	3.34	12,315,200	22.8	7.08	2.62	9,610,200	22.4	6.58	2.17
Employment status												
Employed	38,679,600	71.6	8.00	3.36	36,133,000	66.8	7.13	2.64	28,781,900	67.1	6.65	2.20
Unemployed	3,380,300	6.3	7.65	3.42	3,018,000	5.6	6.72	2.71	1,739,800	4.1	6.06	2.29
Not in labor force	11,982,200	22.2	8.53	3.63	14,931,700	27.6	7.41	2.82	12,350,000	28.8	6.82	2.32
Occupational class												
Management	4,811,500	8.9	8.17	3.36	4,107,400	7.6	7.25	2.62	3,806,700	8.9	6.75	2.18
Professional	6,718,300	12.4	8.25	3.35	6,598,700	12.2	7.39	2.62	5,593,100	13.1	6.87	2.17
Skilled, technical, and supervisory	14,058,800	26.0	7.77	3.33	12,379,800	22.9	6.89	2.61	10,290,500	24.0	6.45	2.18
Semi-skilled	14,023,100	26.0	7.99	3.40	13,401,200	24.8	7.11	2.67	9,410,200	22.0	6.62	2.22
Unskilled	4,339,400	8.0	7.92	3.46	4,091,000	7.6	6.95	2.72	2,996,100	7.0	6.46	2.29
Not applicable	10,090,900	18.7	8.64	3.66	13,504,600	25.0	7.47	2.82	10,775,000	25.1	6.88	2.33
Residential instability (CAN-Marg)												
Q1 (lowest marginalization)	12,129,000	22.4	7.28	3.19	12,537,400	23.2	6.50	2.53	10,200,700	23.8	6.06	2.09
Q2	13,959,900	25.8	7.46	3.29	14,328,200	26.5	6.63	2.61	11,519,100	26.9	6.20	2.16
Q3	11,234,900	20.8	8.18	3.56	11,059,600	20.5	7.23	2.79	8,645,800	20.2	6.69	2.29
Q4	9,674,400	17.9	8.86	3.41	9,488,700	17.5	7.92	2.62	7,407,900	17.3	7.37	2.14
Q5 (highest marginalization)	7,044,000	13.0	9.58	3.25	6,668,800	12.3	8.53	2.37	5,098,300	11.9	7.97	1.95
Dependence (CAN-Marg)												
Q1 (lowest marginalization)	8,881,200	16.4	8.30	3.48	8,958,200	16.6	7.14	2.68	7,416,500	17.3	6.44	2.12
Q2	9,310,000	17.2	8.44	3.43	8,908,400	16.5	7.38	2.65	6,938,000	16.2	6.73	2.11
Q3	9,079,900	16.8	8.67	3.55	8,702,200	16.1	7.65	2.75	6,663,500	15.5	7.06	2.25
Q4	11,665,500	21.6	8.22	3.43	11,497,400	21.3	7.36	2.71	8,882,800	20.7	6.93	2.31

Note: CA, census agglomeration; CAN-Marg, Canadian Marginalization Index; CMA, census metropolitan area; Pop, population; SD, standard deviation.

Table 2. (*Continued.*)

	1991 CanCHEC				1996 CanCHEC				2001 CanCHEC			
	Person-years		$PM_{2.5}$ concentration ($\mu g/m^3$)		Person-years		$PM_{2.5}$ concentration ($\mu g/m^3$)		Person-years		$PM_{2.5}$ concentration ($\mu g/m^3$)	
Covariate	*n*	%	Mean	SD	*n*	%	Mean	SD	*n*	%	Mean	SD
Q5 (highest marginalization)	15,105,600	28.0	7.32	3.22	16,016,500	29.6	6.72	2.62	12,970,900	30.3	6.41	2.27
Material deprivation (CAN-Marg)												
Q1 (lowest marginalization)	11,497,200	21.3	7.59	3.07	10,947,700	20.2	7.00	2.52	8,651,800	20.2	6.61	2.04
Q2	12,268,900	22.7	8.18	3.24	11,270,800	20.8	7.29	2.49	8,383,500	19.6	6.86	2.06
Q3	10,965,300	20.3	8.46	3.43	10,652,500	19.7	7.44	2.63	8,375,900	19.5	6.85	2.16
Q4	8,826,900	16.3	8.59	3.49	9,190,500	17.0	7.61	2.73	7,335,900	17.1	7.08	2.29
Q5 (highest marginalization)	10,483,800	19.4	7.76	3.88	12,021,200	22.2	6.70	2.98	10,124,600	23.6	6.15	2.47
Ethnic concentration (CAN-Marg)												
Q1 (lowest marginalization)	15,066,600	27.9	6.81	3.20	17,014,800	31.5	6.08	2.38	14,272,200	33.3	5.71	1.96
Q2	12,404,500	23.0	7.79	3.22	13,274,500	24.5	7.02	2.54	10,882,100	25.4	6.57	2.16
Q3	9,435,300	17.5	8.37	3.33	9,457,600	17.5	7.48	2.63	7,569,000	17.7	6.93	2.22
Q4	8,678,400	16.1	9.18	3.34	7,620,700	14.1	8.26	2.66	5,616,300	13.1	7.71	2.16
Q5 (highest marginalization)	8,457,300	15.7	9.43	3.48	6,715,100	12.4	8.65	2.64	4,532,100	10.6	8.28	1.80
CMA/CA size												
Pop: > 1,500,000	15,000,000	27.8	10.07	3.32	14,932,200	27.6	8.85	2.36	12,159,300	28.4	8.13	1.83
Pop: 500,000–1,499,999	8,747,700	16.2	8.16	2.82	8,679,700	16.1	7.40	2.18	6,991,200	16.3	6.95	1.81
Pop: 100,000–499,999	9,759,400	18.1	8.68	3.56	9,751,700	18.0	7.83	2.92	7,826,800	18.3	7.16	2.42
Pop: 30,000–99,999	5,510,600	10.2	7.66	3.27	5,267,500	9.7	6.68	2.42	4,081,700	9.5	6.14	1.98
Pop: 10,000–29,000	2,111700	3.9	6.44	2.51	2,107,400	3.9	5.73	1.88	1,699,900	4.0	5.27	1.42
Non-CMA/CA	12,912,700	23.9	5.78	2.33	13,344,100	24.7	5.13	1.72	10,112,800	23.6	4.83	1.39
Urban form												
Active urban core	4,152,200	7.7	10.02	3.26	4,006,700	7.4	8.95	2.40	3,220,700	7.5	8.32	1.92
Transit-reliant suburb	3,490,900	6.5	10.50	3.26	3,405,600	6.3	9.31	2.30	2,689,000	6.3	8.58	1.69
Car-reliant suburb	21,595,500	40.0	9.16	3.30	21,787,500	40.3	8.18	2.50	17,930,300	41.8	7.53	2.00
Exurban	2,951,100	5.5	6.57	2.59	3,000,100	5.6	5.98	2.06	2,471,500	5.8	5.68	1.72
Non-CMA/CA	21,852,400	40.4	6.50	2.87	21,882,700	40.5	5.70	2.16	16,560,200	38.6	5.27	1.74
Airshed												
Western	6,532,200	12.1	7.92	3.44	6,404,500	11.8	6.58	2.08	5,137,600	12.0	5.95	1.55
Prairie	6,942700	12.9	6.45	2.07	7,016,900	13.0	5.92	1.73	5,675,500	13.2	5.61	1.54
West Central	3,205,600	5.9	5.86	1.73	3,322,900	6.1	5.30	1.41	2,589,400	6.0	5.01	1.25
Southern Atlantic	5,312,600	9.8	5.41	1.87	5,324,000	9.8	4.80	1.30	4,044,400	9.4	4.54	1.05
East Central	31,626,600	58.5	9.23	3.48	31,439,700	58.1	8.25	2.71	24,932,700	58.2	7.65	2.17
Northern	422,300	0.8	4.19	1.37	574,600	1.1	3.80	1.11	492,100	1.2	3.67	1.05

cohort-specific hazard ratio estimates among the three cohorts. In addition, we examined the $PM_{2.5}$ association, adjusting for O_3, NO_2, or O_x by cohort.

Shape of the Association between $PM_{2.5}$ and Mortality

The main purpose of the current study was to describe the association between $PM_{2.5}$ and mortality in a manner that can be used for risk and benefits assessment. The standard approach is the log-linear (LL) model that relates the logarithm of the hazard ratio to exposure in a linear manner: $logHR(PM_{2.5}) = \beta PM_{2.5}$. Here, β represents a change in relative risk per unit change in concentration estimated using the Cox model. Nasari et al. (2016) developed the SCHIF in order to extend the LL model to nonlinear transformations of exposure, $T(PM_{2.5})$, with the form: $SCHIF(PM_{2.5}) = \theta T(PM_{2.5})$. Nasari et al. (2016) proposed a specific family of transformations based on a sigmodal function that could accommodate a variety of shapes they suggested would be suitable for risk and benefits assessment. Here, θ represents a change in risk per unit change in $T(\mathrm{PM}_{2.5})$. The SCHIF can then be used in benefits assessment in a manner similar to the LL model after a suitable transformation of concentration.

The SCHIF approach has two major limitations: The first is in defining an appropriate number of transformations of a sigmodal function that can capture all shapes of interest; the second is that the method requires considerable computational capacity if the selected family is very large. This can be a serious limitation when cohort sizes are very large, such as with the CanCHECs.

Spline methods have also been proposed to characterize the shape. RCS with a few knots have been used (Beelen et al. 2014) in addition to smoothing splines (Di et al. 2017). However, the manner in which splines are presented by graphic representation of the mean predictions and uncertainty bounds over the concentration range limits their use in risk and benefits assessment, as these assessments typically require a differentiable algebraic function in addition to a quantitative estimate of uncertainty by concentration.

We developed and applied a new method that combines the flexibility of splines and the ease of use of the SCHIF in benefits assessment. Our method involves three steps. The first step is a data reduction step in which we fit a RCS with a large number of knots in order to characterize the shape of the concentration–response relationship in sufficient detail. RCS can easily be fit to large cohorts, as they only involve a series of transformations of concentration. Here, we have converted millions of person-years of data into a few hundred observations of RCS predictions over the observed concentration range. In step 2, we smooth the potential erratic predictions due to the large number of knots using a MISS, and in step 3, we fit our SCHIF function to the MISS predictions. In addition, we model the uncertainty in the spline fit as a cubic polynomial in concentration in a manner that assigns all uncertainty to the θ parameter in the SCHIF model, but unlike the LL model, uncertainty can vary with concentration. We now have a differentiable algebraic function of both relative risk and its uncertainty by concentration. This approach also allows for visualization of the SCHIF as well as its representation of the underlying data (as summarized by the RCS).

Specifically, we selected 15 knots defined at the 2nd, 4th, 10th, 14th, 18th, 22nd, 26th, 50th, 74th, 78th, 82nd, 86th, 90th, 94th, and 98th percentiles of the $PM_{2.5}$ person-year distribution. We selected a large number of knots covering both the lower and upper quartiles in order to capture a variety of desired shapes. From this first step, we obtain estimates of the logarithm of the RCS hazard ratio (logRCS) and the associated standard error at several hundred concentrations between the minimum and the 99th percentile of the exposure distribution. We do not include predictions above the 99th percentile, since RCS are linear beyond the highest knot concentration. This linear form can have some influence on the shape of the SCHIF throughout the concentration range, and especially over the higher concentrations, since the SCHIF is a single algebraic function. We also fixed the logRCS to zero at the minimum concentration, and its associated standard error was also set to zero.

In step 2, we smooth the potentially erratic logRCS predictions with a MISS in order to obtain predictions suitable to model with the SCHIF algebraic function, which itself is monotonically increasing (Pya and Wood 2015). The SCHIF hazard ratio function has the form:

$$logSCHIF(z) = \theta f(z) l(z)$$

with $l(z) = \frac{1}{\left[1 + \exp\left(\frac{z-\mu}{\tau r}\right)\right]}$ a logistic function in concentration. Here, $\theta, \mu,$ and τ are unknown parameters to be estimated from the data, r is the range in the translated exposure, and $z = PM_{2.5} - \min(PM_{2.5})$ such that $logSCHIF(0) = 0$. The function $f(z)$ can take two forms: $f(z) = z$ (linear) and $f(z) = log(z+1)$ (log). We have constructed the SCHIF to be similar to the LL model, $logLL(z) = \beta z$, by writing: $logSCHIF(z) = \theta T(z)$, where $T(z) = f(z)l(z)$ is a specific transformation of concentration.

The linear form $f(z) = z$ can model both linear and sublinear associations, while the log form $f(z) = log(z+1)$ can model supralinear associations with mortality. Both forms can accommodate S-shaped functions through $l(z)$. Sets of values (μ,τ) are selected that define the shape of $l(z)$. Larger values of μ result in larger ranges of concentration for which a sublinear association is modeled at lower concentrations due to the property of the logistic function. Larger values of τ generate shapes for $l(z)$ with less curvature. By limiting the ranges for (μ,τ), we can limit the amount of curvature in the SCHIF.

A linear regression model was constructed using each transformation as the single predictor and the MISS prediction as the response. Using the MISS predictions, we were then able to select a wide range of values of the parameters to examine a wide variety of shapes that is not possible by modeling the subject-level cohort data. We selected values of μ ranging from 0 to r by integers, and τ ranging from 0.1 to 1 by 0.1 increments. For each set of parameters and the two forms of $f(z)$, we obtained an estimate of θ and its standard error. We then created a single SCHIF curve by a weighted average of all the SCHIF curves examined, with weights determined by the fit of each curve on the MISS values. However, as the model averaged predictions at each concentration are themselves a potentially complicated function, these predictions can be summarized as a single algebraic function. Specifically, we fit a generalization of the SCHIF model

$$logSCHIF(z) = \frac{\theta \log\left(\frac{z}{\alpha} + 1\right)}{1 + \exp\left[-(z-\mu)/v\right]}$$

to the mean SCHIF predicted curve over the concentration range. We added an additional parameter α to model the combination of the linear and log forms of $f(z)$ used in the fitting step. The function $\log\left(\frac{z}{\alpha} + 1\right)$ is nearly linear in z for large values of α. We collapse the product τr into a single parameter v to simplify the reporting of the parameter estimates.

In the LL model, all uncertainty in the hazard ratio is assigned to the single unknown parameter, β. We aim to make a similar characterization of uncertainty in the SCHIF predictions, where all the uncertainty is ascribed to the parameter θ. We do this by considering a model of the standard error in the RCS predictions. However, unlike the LL model, RCS standard errors can vary in a nonlinear manner with concentration. We therefore consider a model for the standard error as a function of concentration of the form: $se_{RCS}(z) = se_\theta(z) \times T(z)$, with $se_\theta(z)$ denoting our standard error model of θ, dependent on concentration. We select a general model that can accommodate a variety of shapes such as a cubic polynomial with the form: $se_\theta(z) = \sigma_0 + \sigma_1 z + \sigma_2 z^2 + \sigma_3 z^3$.

Finally, we construct pooled SCHIF models among the three cohorts in the following manner: Let $v_c(z)$ be the variance of the logarithm of the SCHIF prediction, $logSCHIF_c(z)$, at concentration z for cohort $c = 1,2,3$. We construct a meta-analytic summary of the SCHIF predictions among the three cohorts as:

$$logSCHIF_{Pooled}(z) = \sum_{c=1}^{3} w_c \, logSCHIF_c(z),$$

where $w_c(z) = [1/v_c(z)] / \sum_{c=1}^{3} 1/v_c(z)$. For the variance of $logSCHIF_{Pooled}(z)$, we include the variation in predictions among the cohorts in addition to the sampling uncertainty for each cohort as:

$$\sum_{c=1}^{3} w_c^2(z)\{v_c(z) + [logSCHIF_c(z) - logSCHIF_{Pooled}(z)]^2\}.$$

In order to obtain an algebraic function for the pooled SCHIF, we used nonlinear regression to estimate the SCHIF parameters, with $logSCHIF_{Pooled}(z)$ defining the data for the regression. We also modeled the standard error of the pooled SCHIF in a manner similar to that for each cohort separately. The variance of the pooled SCHIFs is a function of both the variance of each cohort-specific SCHIF prediction and the squared difference between the cohort-specific SCHIF predictions and the pooled SCHIF prediction. This latter term captures the uncertainty in both the shape and magnitude of the hazard ratio predictions among the three cohorts.

Results

Main Analysis

$PM_{2.5}$ by cohort and covariate categories. Table 1 presents percentiles of the $PM_{2.5}$ distribution based on person-years for each of the three cohorts separately. Concentrations were highest for the 1991 cohort, moderate for the 1996 cohort, and lowest for the 2001 cohort. Concentration differences were well within 1 $\mu g/m^3$ between cohorts for median and lower percentiles, with greater differences for the higher percentiles, suggesting that greater declines in exposure were observed in locations with higher levels. The spatial distribution of $PM_{2.5}$ across Canada is presented for selected 3-y averages (Figure 1). Concentrations declined over time in the heavily populated areas of Southern Ontario and Quebec. Moderate concentrations were observed in the earlier time periods for Northern Canada and the Prairies. These levels declined through the 1990s but then increased during the latter part of our cohort follow-up period.

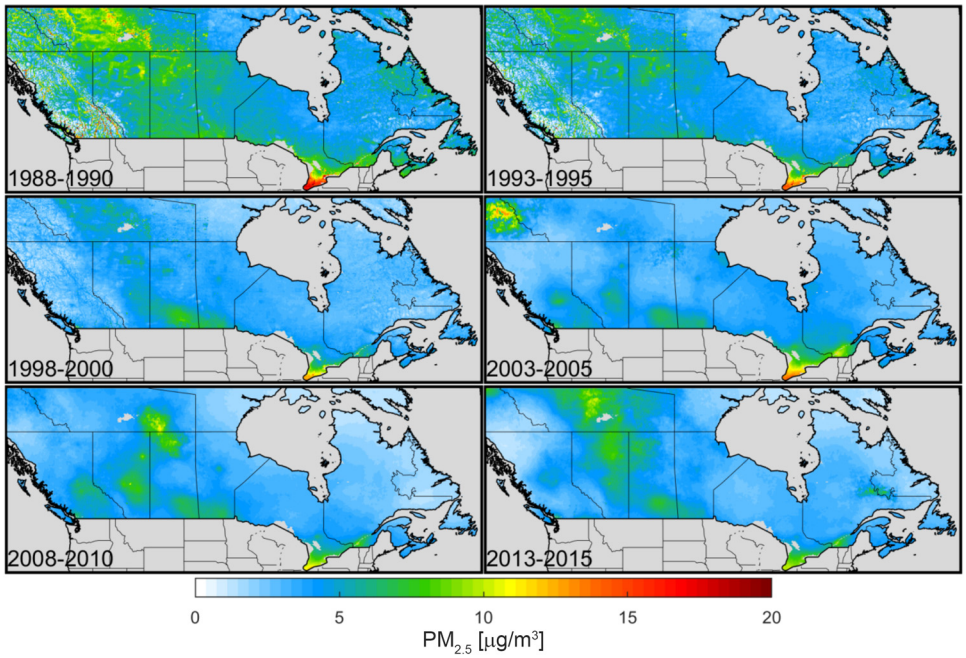

Figure 1. Spatial distribution of particulate matter with aerodynamic diameter ≤2.5 μm ($PM_{2.5}$) across Canada for selected 3-y averages: 1998–2000 (first exposure assigned to the 1991 cohort), 1993–1995 (first exposure assigned to 1996 cohort), 1998–2000 (first exposure assigned to 2001 cohort), 2003–2005, 2008–2010, and 2013–2015 (exposure assigned to last year of follow-up, 2015).

Table 2 reports both the number of person-years and percentages among the categories of mortality predictors for each cohort separately, in addition to the mean and standard deviation of $PM_{2.5}$ assigned to each category. Males tended to be assigned higher concentrations than females in all three cohorts, although the difference was very small (<1 $\mu g/m^3$). There was a U-shaped pattern with age at cohort commencement for all three cohorts, with concentration declining with age up to the 55- to 64-y-old group and then increasing. Immigrants were consistently assigned higher concentrations than nonimmigrants; however, concentrations were similar over the length an immigrant subject lived in Canada. Subjects who defined themselves as visible minorities had higher assigned concentrations than those subjects who did not in the 1991 and 1996 cohorts. Subjects of Indigenous identity had lower concentrations. Married and common-law subjects had lower assigned exposures compared to other marital categories in all cohorts. Exposure monotonically increased with educational attainment in all cohorts. However, exposure monotonically declined with income. Employed subjects at the time of interview had higher exposures compared to those unemployed subjects. Exposure tended to decline over the occupational class categories moving from management/professional to semi- and unskilled workers. Note that the "not in the labor force" and "not-applicable occupational class" categories had the highest exposures, possibly to due to older subjects who tended to have higher than average exposures. There was a tendency for exposure to increase over the quintiles of three of the CAN-Marg dimensions: residential instability, material deprivation, and ethnic concentration, with no clear trend for the fourth dimension, dependence. Outdoor concentrations increased with CMA/CA size and for the inner-city categories of urban form. Of the six airsheds, the East Central contained 58% of person-years and had the highest concentrations. Based on the associations between several geographic and subject based covariates, there is some potential that adjustment for these variables could influence the magnitude of our estimates of the $PM_{2.5}$–mortality association.

Hazard ratio estimates. Table 3 reports the hazard ratio and 95% confidence limits per 10-$\mu g/m^3$, for each cohort separately and pooled among the three cohorts by categories of immigrant status, age, and sex, for both the DAG and Full models. There was a tendency for the hazard ratio to be larger under the Full model compared to the DAG for the 1991 and 1996 cohorts, but smaller for the 2001 cohort. Consequently, there was less variation among the hazard ratios between cohorts under the Full compared to the DAG models. The Full model was a better predictor of mortality compared to the DAG model based on its much lower Akaike Information Criterion/Schwarz's Bayesian Criterion values (see Table S1). We therefore focus our interpretation on the results using the Full model.

When all subjects were considered together, hazard ratio estimates were similar for the 1991 and 1996 cohorts (HR = 1.041), with a larger estimate observed for the 2001 cohort (HR = 1.084). The pooled cohort HR estimate was 1.053 (95% CI: 1.041, 1.065). Hazard ratio estimates for nonimmigrants were higher than for immigrants in the 1991 and 1996 cohorts, but lower in the 2001 cohort. Hazard ratio estimates for males were higher than for females in the 1991 and 1996 cohorts but lower in the 2001 cohort. Hazard ratio estimates declined with age in all three cohorts, however.

Hazard ratio estimates based on interquartile range changes in concentrations were larger for O_x compared to O_3, and lowest for NO_2 (Table 3). The $PM_{2.5}$ HR estimate was moderately sensitive to adjustment for NO_2, declining from 1.053 to 1.043 per 10-$\mu g/m^3$, but very sensitive to adjustment for either O_3, declining to 0.982, and O_x, declining to 0.955.

Shape of $PM_{2.5}$–mortality association. The shape of the association between $PM_{2.5}$ concentrations and mortality for the Full model is displayed in Figure 2 for each of the three cohorts separately and pooled among cohorts using the SCHIF. MISS predictions (dashed black line) and RCS predictions (dashed red line) over the concentration range are also displayed. A similar shape is observed in each cohort for the MISS, with a steep increase below 5 $\mu g/m^3$ followed by a much shallower increase for higher concentrations. The SCHIF predictions also display a supralinear association with concentration. Note that the SCHIF predictions display much less curvature than the MISS; a design feature of

Table 3. Hazard ratio (HR) estimates and 95% confidence intervals (CIs) for the association between $PM_{2.5}$ and nonaccidental mortality, as well as for copollutants (NO_2, Ozone, oxidative potential), within the Canadian Health and Environment Cohorts (CanCHECs) from 1991, 1996, 2001, and pooled cohorts. Effect modification analyses by immigrant status, sex, and age, and multi-pollutant models are also provided.

		1991 Cohort			1996 Cohort			2001 Cohort			Pooled results[a]			
Subgroup/model	Model form	HR	95% CI		HR	95% CI		HR	95% CI		HR	95% CI		p-Value
All subjects														
—	DAG[b]	0.982	0.959	1.006	1.033	1.016	1.051	1.120	1.096	1.146	1.044	1.031	1.056	<0.01
—	Full[c]	1.041	1.016	1.066	1.041	1.024	1.059	1.084	1.060	1.108	1.053	1.041	1.065	<0.01
Immigrant status[d]														
No	DAG	0.975	0.951	1.000	1.024	1.005	1.043	1.105	1.078	1.133	1.032	1.019	1.045	<0.01
No	Full	1.049	1.022	1.076	1.058	1.039	1.078	1.089	1.062	1.116	1.064	1.050	1.078	0.09
Yes	DAG	1.016	0.945	1.092	1.082	1.040	1.125	1.190	1.131	1.253	1.104	1.073	1.136	<0.01
Yes	Full	1.006	0.935	1.081	1.027	0.987	1.068	1.109	1.053	1.167	1.049	1.019	1.079	0.03
Sex[d]														
Female	DAG	0.956	0.921	0.993	1.001	0.976	1.026	1.121	1.084	1.160	1.022	1.004	1.040	<0.01
Female	Full	1.009	0.972	1.048	1.008	0.983	1.034	1.093	1.056	1.130	1.031	1.013	1.050	<0.01
Male	DAG	0.993	0.963	1.024	1.055	1.032	1.078	1.116	1.083	1.150	1.055	1.039	1.071	<0.01
Male	Full	1.053	1.021	1.086	1.062	1.039	1.086	1.071	1.040	1.104	1.062	1.046	1.079	0.74
Age during follow-up[d]														
<65 y	DAG	1.022	0.971	1.075	1.057	1.019	1.097	1.176	1.119	1.236	1.078	1.051	1.106	<0.01
<65 y	Full	1.079	1.026	1.136	1.095	1.056	1.136	1.165	1.108	1.225	1.109	1.081	1.137	0.07
65–74 y	DAG	0.984	0.939	1.031	1.079	1.044	1.116	1.176	1.122	1.232	1.077	1.052	1.103	<0.01
65–74 y	Full	1.069	1.020	1.120	1.092	1.057	1.130	1.130	1.078	1.184	1.096	1.070	1.122	0.25
>75 y	DAG	0.929	0.899	0.961	0.986	0.964	1.009	1.062	1.031	1.094	0.994	0.978	1.010	<0.01
>75 y	Full	0.972	0.940	1.005	0.985	0.963	1.008	1.031	1.001	1.062	0.995	0.979	1.011	0.02
Single pollutant														
NO_2	DAG	1.009	1.004	1.015	0.997	0.993	1.001	1.003	0.998	1.008	1.002	0.999	1.004	<0.01
NO_2	Full	1.015	1.009	1.020	1.001	0.997	1.005	1.003	0.998	1.009	1.005	1.002	1.008	<0.01
O_3	DAG	1.016	1.006	1.027	1.035	1.029	1.041	1.041	1.034	1.049	1.034	1.030	1.038	<0.01
O_3	Full	1.044	1.033	1.055	1.076	1.069	1.082	1.081	1.073	1.088	1.073	1.068	1.077	<0.01
O_x	DAG	1.030	1.018	1.043	1.037	1.029	1.044	1.049	1.040	1.058	1.040	1.035	1.045	0.03
O_x	Full	1.068	1.056	1.081	1.086	1.078	1.093	1.094	1.085	1.103	1.086	1.080	1.091	<0.01
Two pollutant														
Adjusted for NO_2[e]														
$PM_{2.5}$	DAG	0.966	0.942	0.991	1.038	1.02	1.057	1.115	1.089	1.142	1.040	1.028	1.053	<0.01
NO_2	DAG	1.010	1.004	1.015	0.997	0.993	1.001	1.003	0.998	1.009	1.002	0.999	1.005	<0.01
$PM_{2.5}$	Full	1.014	0.989	1.041	1.039	1.021	1.058	1.078	1.052	1.104	1.043	1.030	1.056	<0.01
NO_2	Full	1.015	1.010	1.021	1.001	0.997	1.006	1.004	0.998	1.009	1.006	1.003	1.009	<0.01
Adjusted for O_3[e]														
$PM_{2.5}$	DAG	0.969	0.944	0.994	0.996	0.978	1.014	1.073	1.048	1.098	1.011	0.998	1.024	<0.01
O_3	DAG	1.016	1.006	1.026	1.034	1.028	1.04	1.040	1.033	1.047	1.033	1.029	1.037	<0.01
$PM_{2.5}$	Full	1.003	0.978	1.029	0.963	0.946	0.981	0.996	0.973	1.020	0.982	0.970	0.994	0.01
O_3	Full	1.043	1.033	1.054	1.074	1.068	1.08	1.079	1.072	1.086	1.071	1.067	1.075	<0.01
Adjusted for O_x[e]														
$PM_{2.5}$	DAG	0.950	0.925	0.977	0.988	0.97	1.007	1.056	1.031	1.083	0.998	0.985	1.011	<0.01
O_x	DAG	1.028	1.017	1.039	1.034	1.027	1.04	1.045	1.037	1.053	1.037	1.032	1.041	0.03
$PM_{2.5}$	Full	0.967	0.941	0.994	0.941	0.923	0.959	0.970	0.946	0.994	0.955	0.943	0.968	0.10
O_x	Full	1.062	1.051	1.074	1.078	1.071	1.085	1.086	1.077	1.094	1.078	1.073	1.083	<0.01

Note: —, no data; NO_2, nitrogen dioxide; O_x, combined oxidant capacity of O_3 and NO_2; O_3, ambient ozone; $PM_{2.5}$, particulate matter with aerodynamic diameter ≤2.5 μm.
[a]Tests for heterogeneity of hazard ratio among cohorts: $^{*}p < 0.05$, $^{**}p < 0.01$.
[b]Directed acyclic graph (DAG) model is stratified by 5-y age groups by age at baseline, sex, and immigrant status and included the following geographic-based covariates: four Canadian Marginalization Index dimensions, urban form, CMA/CA size and airshed.
[c]Full model is stratified by 5-y age groups by age at baseline, sex, and immigrant status and included the geographic based covariates: four Canadian Marginalization Index dimensions, urban form, CMA/CA size and airshed, and the subject-based covariates: marital status, education, income quintile, Indigenous status, visible minority status, employment status, and occupational class.
[d]Note that the models by immigrant status are not stratified by immigrant status. The models by sex are not stratified by sex.
[e]$PM_{2.5}$ always uses 10 units, copollutants use: O_3, 10.20 ppb; NO_2, 6.63 ppb; O_x, 8.05 ppb.

constraining the shape of the SCHIF. The SCHIF 95% CIs (gray-shaped area) are clearly widest in the 2001 cohort, as it had the shortest follow-up time (15 y) and lowest concentrations (Table 1) compared to the 1991 and 1996 cohorts. The steepness of the increase in the HR below 5 $\mu g/m^3$ appears to dampen between the 1991 to 1996 to 2001 cohorts, with the SCHIF predictions of the MISS improving over these lower concentrations as the start date of the cohorts increased. The lower bound of the CIs exceeded unity for all concentrations for the 1991 cohort, above 2 $\mu g/m^3$ for the 1996 cohort, and above 5 $\mu g/m^3$ for the 2001 cohort.

We display the association between both θ and its standard error and show that association varies with concentration by the ratio $N(z) = \theta / se_\theta(z)$ in Figure 3. Here, $N(z)$ represents the signal-to-noise ratio by concentration. This ratio increases with concentration for all three cohorts, exceeding the 1.96 value (dashed black line) for all concentrations in the 1991 cohort, above 2 $\mu g/m^3$ in the 1996 cohort, and above 5 $\mu g/m^3$ in the 2001 cohort. For the pooled SCHIF, the ratio increases for concentrations less than 7 $\mu g/m^3$ and then is relatively stable for higher concentrations. This pattern is due to the additional variation between the SCHIF values among the three cohorts at higher levels. The parameter estimates for both the SCHIF and its standard error are given in Table 4.

Discussion

The three CanCHEC cohorts included 8.5 million adults with 150 million person-years of follow-up and nearly 1.5 million deaths,

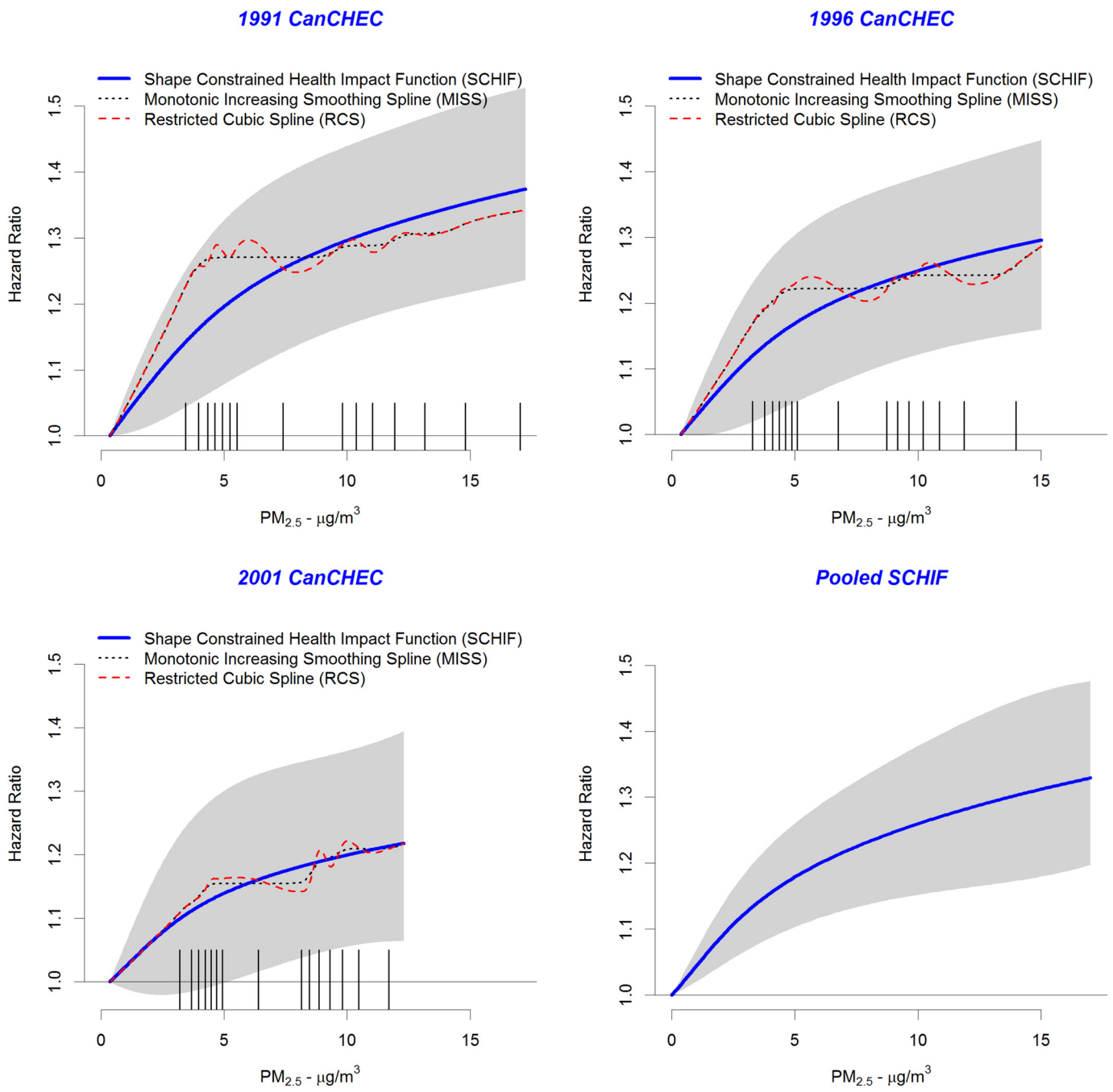

Figure 2. Shape Constrained Health Impact Function (SCHIF) (solid blue line), monotonically increasing smoothing spline (MISS) (dotted black line), and restricted cubic spline (RCS) (dashed red line) predictions by particulate matter with aerodynamic diameter $\leq 2.5\,\mu m$ ($PM_{2.5}$) concentration and Canadian Census Health and Environment Cohort (CanCHEC) (1991, 1996, and 2001). Hazard ratio predictions based on pooling cohort-specific SCHIFs are also presented. Uncertainty bounds are displayed as gray shaded area. Tick marks on $PM_{2.5}$ axis represent the 15-RCS knot locations.

representing one of the largest population-based air pollution cohort analyses conducted to date. We found a HR of 1.053 (95% CI: 1.041, 1.065) per 10-$\mu g/m^3$ change in $PM_{2.5}$ after pooling the three cohort-specific hazard ratios. Hazard ratio estimates based on a LL model do not fully characterize the relationship between $PM_{2.5}$ exposure and mortality, as in each cohort, a supralinear association was observed (Figure 1).

We found variation in the sensitivity of covariate model specification. The full model yielded larger hazard ratio estimates compared to the DAG model for both the 1991 and 1996 cohorts, with the opposite pattern observed in the 2001 cohort. It is not completely clear why such patterns occur, as the change in exposure among the categories of the covariates was similar in all three cohorts (Table 1), although the differences in exposure among the categories decreases with more recent cohort start dates due to generally declining concentrations over time.

We observed an increase in the hazard ratio for the immigrant population over time, starting with the weakest association for the 1991 cohort (HR = 1.006; 95% CI: 0.935, 1.081), a slightly stronger association in the 1996 cohort (HR = 1.027; 95% CI: 0.987, 1.068), with the strongest association in the 2001 cohort (HR = 1.109; 95% CI: 1.053, 1.167). We previously also observed no association in the 1991 cohort (Crouse et al. 2015) for immigrants to Canada. There also appeared to be little evidence

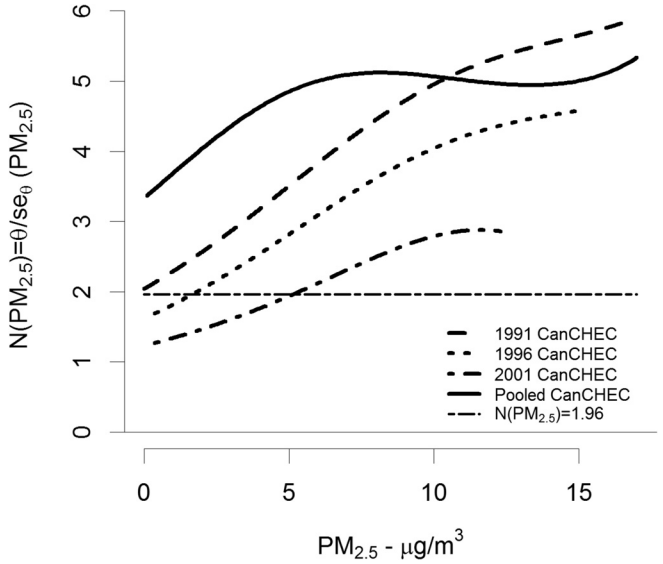

Figure 3. Signal-to-noise ratio, $N(z) = \theta/se_\theta(z)$, by concentration and Canadian Census Health and Environment Cohort (CanCHEC; 1991, 1996, 2001). Dashed-dotted horizontal black line represents a ratio of 1.96.

of an association for females in the 1991 and 1996 cohorts, with much stronger evidence for males. However, the association was similar for males and females in the 2001 cohort (Table 3).

The observation that the $PM_{2.5}$ hazard ratio can be partially explained by NO_2 and fully explained by O_3 also supports previously reported results (Crouse et al. 2015). As these gaseous pollutants may exhibit varying correlations with different components of $PM_{2.5}$, these multipollutant results can provide insight into the source components of $PM_{2.5}$ that are most influential in the relationship between $PM_{2.5}$ mass and mortality. That is, the results of our models with NO_2 and O_3 may, in part, reflect differences in the mixture/composition of $PM_{2.5}$ across space and time. Earlier work has shown that the distribution of components, such as sulfate, organic matter, and black carbon, vary by total mass concentration in Canada (van Donkelaar et al. 2019). Using this spatial variation, Crouse et al. (2016) showed that inclusion of components in addition to total mass improved the prediction of mortality in the 1991 cohort. Mortality from ischemic heart disease has been shown to vary by source of $PM_{2.5}$ in the U.S.-based American Cancer Society (ACS) cohort (Thurston et al. 2016). Therefore, differences over time in the component distribution could explain some of the differences in our hazard ratio estimates between cohorts. However, the empirical evidence for such temporal changes in the component distribution is not supported by our recent modeling efforts (van Donkelaar et al. 2019), which suggest that the proportion of components is relatively stable over time, even as total mass concentrations have clearly declined.

Table 4. Shape-constrained health impact function and standard error parameter estimates by Canadian Census Health and Environment Cohort (CanCHEC) cohorts.

	Shape-constrained health impact function parameters			
Cohort	θ	α	μ	ν
1991	0.1102	1	0	1.688
1996	0.0942	1	0	1.465
2001	0.0703	1	0	1.193
Pooled	0.1126	1.477	−0.233	1.165
	Standard error parameters			
	$\sigma_0 \times 10^{-2}$	$\sigma_1 \times 10^{-3}$	$\sigma_2 \times 10^{-4}$	$\sigma_3 \times 10^{-6}$
1991	5.639	−6.608	4.148	−9.179
1996	5.835	−6.942	4.411	−9.747
2001	6.267	−5.330	1.183	6.406
Pooled	3.383	−3.640	3.593	−11.13

We find a substantially lower hazard ratio estimate based on the LL model than in previous CanCHEC analyses. There are a number of possible explanations for these differences. First, this new version of the cohort includes an improved death and mobility linkage with updated methodology. Second, the period of follow-up in our analysis ranges from 15 to 25 y (up to 2016). Our analysis further differs from previous CanCHEC studies (e.g., Crouse et al. 2012; Pinault et al. 2017; Weichenthal et al. 2017) in our inclusion of immigrants in the analytical cohort. Immigrants generally have lower mortality rates than the Canadian-born population due to screening criteria for immigration into Canada (Newbold 2005; Ng 2011). Immigrants also tend to live in cities with higher $PM_{2.5}$ concentrations, leading to different risks of air pollution exposure. Our methods of $PM_{2.5}$ averaging at the PC level and imputation differed slightly from previous analyses. Specifically, we required a minimum of a two-digit PC (e.g., K1) to assign a $PM_{2.5}$ value based on a population-weighted average of the geographic area. Some previous analyses assigned the national average $PM_{2.5}$ value in absence of any PC information. We also removed all person-years that resulted in missing environmental ($PM_{2.5}$, O_3, or NO_2) or contextual covariates that may have informed previous analyses, while in previous analyses, we either imputed all missing person-years or included dummy variables for geographically based predictors. Finally, these analyses employ updated $PM_{2.5}$ estimates for the 2012–2016 period based on enhancements to the satellite retrievals (van Donkelaar et al. 2019) and backcasted estimates prior to 2000 that were not available previously. We do note, however, that the relationship between $PM_{2.5}$ and mortality, in both shape and magnitude, is similar to that previously reported for the 1991 (Crouse et al. 2015) and 2001 (Pinault et al. 2017) cohorts. This observation suggests that caution is required in interpreting the magnitude of an association solely based on the LL model without further consideration of the shape of the association.

This work supports observations of a supralinear concentration–response between $PM_{2.5}$ exposure and risk of nonaccidental mortality similar to that reported in Crouse et al. (2012, 2015) for the 1991 cohort and Pinault et al. (2017) for the 2001 cohort in more limited analyses. Most of the previous major cohort studies on $PM_{2.5}$ did not examine the shape of the concentration–mortality association at the low levels that are observed in our cohort, in which the 25th percentile is 5.1 $\mu g/m^3$, and the median is 6.9 $\mu g/m^3$ among all person-years of the three cohorts combined. For example, the lower end of the exposure distribution in the Medicare cohort was 6.2 $\mu g/m^3$ (minimum; Di et al. 2017), the National Health Interview Survey cohort (NHIS) was 7.6 $\mu g/m^3$ (minimum; Pope et al. 2018), and the ACS Cancer Prevention Study II cohort was 6.7 $\mu g/m^3$ (first percentile; Turner et al. 2016). Our mortality HR estimate of 1.053 (95% CI: 1.041, 1.065) is slightly below estimates of U.S. cohorts such as the Medicare cohort (HR = 1.073; 95% CI: 1.071, 1.075), NHIS cohort (HR = 1.056; 95% CI: 1.005, 1.110), and the ACS cohort (HR = 1.07; 95% CI: 1.06, 1.09). Our estimate for the 2001 cohort—the only CanCHEC cohort that did not require backcasted exposure data—was slightly higher than the U.S. cohorts at 1.084 (95% CI: 1.060, 1.108).

Strengths and Limitations

Our study has a number of strengths and limitations. These analyses include a large number of deaths (nearly 1.5 million); population representativeness; a number of subject-level mortality predictors, such as occupation, income, and education, that are

often not available in such large administrative-based cohorts (Di et al. 2017); and annual location information through linkage to income tax filings back to 1981. Our temporally resolved air pollution estimates could then be assigned to each year of follow-up. We also developed a method to combine the flexibility of splines to characterize the shape of the relationship between $PM_{2.5}$ and mortality with the usefulness of the SCHIF in risk and benefits assessments. This new approach is feasible with respect to computing resources for very large cohort studies.

Despite these important strengths, the study includes a number of limitations. Specifically, the cohorts lack individual information on behavioral mortality risk factors such as smoking, diet, and obesity. We have previously examined the influence of further adjustment for these missing risk factors using statistical methods of indirect adjustment (Crouse et al. 2015; Erickson et al. 2019; Shin et al. 2014) and direct adjustment in a cohort based on annual health surveys in Canada where such information was available (Pinault et al. 2016b). For both of these approaches, we found that the $PM_{2.5}$–mortality association remained positive. These observations indicate that it is unlikely that the positive associations we observed are entirely due to lack of inclusion of missing risk factors.

We captured information on social and economic status of each subject only at cohort inception. Thus, information on marital status, income, education, occupation, and employment may have changed over time, and we were not able to model any potential influence of such changes on the $PM_{2.5}$–mortality association. The 1991 cohort may have been most influenced by this lack of temporal adjustment given its 25 y of follow-up.

As we examined a 3-y moving-average $PM_{2.5}$ exposure window lagged by 1 y in all analyses, for the 2001 cohort, the initial exposure window assigned to the 2001 follow-up year was a 1998–2000 average and thus did not include backcasted exposures. The 1991 cohort used more years of backcasted exposures (1988–1997) than the 1996 cohort (1993–1997). Backcasted predictions may have induced greater exposure error in the two earlier cohorts.

We employed three very different exposure models for $PM_{2.5}$, NO_2, and O_3. The $PM_{2.5}$ exposure model included remote sensing information coupled with CTM predictions. Land-use information informed any bias in the CTM predictions for the chemical components of total mass, but were not included as direct predictors of ground measurement data. The NO_2 model used both land-use and remote sensing information, while the O_3 model fused ground data with CTM predictions. The spatial resolution of the models was also different, with NO_2 having the finest resolution of 100 m and $PM_{2.5}$ at 1 km, while the O_3 model was at a resolution of 21 km. It was therefore difficult to directly compare the associations with mortality between pollutants and even more difficult with multiple-pollutant models subject to potential differential exposure error. However, the observed stronger associations with O_3 may be due to a lower exposure error in both the original surfaces and the temporal adjustments, since O_3 is known to be more spatially homogenous than $PM_{2.5}$, while NO_2 is known to have the largest spatial variation. Additionally, although the quantitative estimates presented here reflect the large and diverse geographic area of Canada, they may not apply to places around the world with notably different sources and compositions of $PM_{2.5}$, for example, in areas where a much higher proportion of the $PM_{2.5}$ is from dust and sand.

In summary, we found positive associations between $PM_{2.5}$ and mortality in all three cohorts, and a similar supralinear concentration–response relationship. Lower uncertainty bounds were elevated above unity for all concentrations in the 1991 cohort, above 2 $\mu g/m^3$ in the 1996 cohort, and above 5 $\mu g/m^3$ in the 2001 cohort, suggesting our confidence in identifying concentrations where there exists a positive response is declining as concentrations decline over time. Therefore, interest exists in examining subsequent CanCHEC cohorts as they become available with the administration of more recent long form censuses.

Acknowledgments

Research described in this article was conducted under contract to the Health Effects Institute (HEI), an organization jointly funded by the U.S. Environmental Protection Agency (EPA; Assistance Award No. R-82811201) and certain motor vehicle and engine manufacturers. The contents of this article do not necessarily reflect the views of HEI or its sponsors, nor do they necessarily reflect the views and policies of the EPA or motor vehicle and engine manufacturers.

We would like to thank the Canadian Urban Environmental Health Research Consortium (CANUE) for providing PC-level ozone surfaces to support the multipollutant modeling conducted here. We also thank Dr. Hong Chen for his support in running the SCHIF code.

References

Apte JS, Marshall JD, Cohen A, Brauer M. 2015. Addressing global mortality from ambient $PM_{2.5}$. Environ Sci Technol 49(13):8057–8066, PMID: 26077815, https://doi.org/10.1021/acs.est.5b01236.

Beelen R, Raaschou-Nielsen O, Stafoggia M, Andersen ZJ, Weinmayr G, Hoffmann B, et al. 2014. Effects of long-term exposure to air pollution on natural-cause mortality: an analysis of 22 European cohorts within the multicentre ESCAPE project. Lancet 383(9919):785–795, PMID: 24332274, https://doi.org/10.1016/S0140-6736(13)62158-3.

Bérard-Chagnon J. 2017. Comparison of Place of Residence between the T1 Family File and the Census: Evaluation using record linkage. Ottawa, Canada: Statistics Canada, Catalogue no. 91F0015M — No. 13.

Burnett R, Chen H, Szyszkowicz M, Fann N, Hubbell B, Pope CA 3rd, et al. 2018. Global estimates of mortality associated with long-term exposure to outdoor fine particulate matter. Proc Natl Acad Sci USA 115(38):9592–9597, PMID: 30181279, https://doi.org/10.1073/pnas.1803222115.

Burnett RT, Pope CA 3rd, Ezzati M, Olives C, Lim SS, Mehta S, et al. 2014. An integrated risk function for estimating the global burden of disease attributable to ambient fine particulate matter exposure. Environ Health Perspect 122(4):397–403, PMID: 24518036, https://doi.org/10.1289/ehp.1307049.

CCME (Canadian Council of Ministers of the Environment). 2012. *Guidance Document on Achievement Determination Canadian Ambient Air Quality Standards for Fine Particulate Matter and Ozone*. 978-1-896997-91-9 PDF. Winnipeg, Manitoba, Canada: Canadian Council of Ministers of the Environment.

Christidis T, Labrecque-Synnott F, Pinault L, Saidi A, Tjepkema M. 2018. *The 1996 CanCHEC: Canadian Census Health and Environment Cohort Profile*. Canada No. 11-633-X no. 013. Ottawa, Ontario, Canada: Statistics Canada.

Cochran WG. 1950. The comparison of percentages in matched samples. Biometrika 37(3–4):256–266, PMID: 14801052, https://doi.org/10.1093/biomet/37.3-4.256.

Cox DR. 1972. Regression models and life tables. J R Stat Soc B 34(2):187–202, https://doi.org/10.1111/j.2517-6161.1972.tb00899.x.

Crouse DL, Peters PA, Hystad P, Brook JR, van Donkelaar A, Martin RV, et al. 2015. Ambient $PM_{2.5}$, O_3, and NO_2 exposures and associations with mortality over 16 years of follow-up in the Canadian Census Health and Environment Cohort (CanCHEC). Environ Health Perspect 123(11):1180–1186, PMID: 26528712, https://doi.org/10.1289/ehp.1409276.

Crouse DL, Peters PA, van Donkelaar A, Goldberg MS, Villeneuve PJ, Brion O, et al. 2012. Risk of nonaccidental and cardiovascular mortality in relation to long-term exposure to low concentrations of fine particulate matter: a Canadian national-level cohort study. Environ Health Perspect 120(5):708–714, PMID: 22313724, https://doi.org/10.1289/ehp.1104049.

Crouse DL, Philip S, van Donkelaar A, Martin RV, Jessiman B, Peters PA, et al. 2016. A new method to jointly estimate the mortality risk of long-term exposure to fine particulate matter and its components. Sci Rep 6(1):18916, https://doi.org/10.1038/srep18916.

Di Q, Wang Y, Zanobetti A, Wang Y, Koutrakis P, Choirat C, et al. 2017. Air pollution and mortality in the Medicare population. N Engl J Med 376(26):2513–2522, PMID: 28657878, https://doi.org/10.1056/NEJMoa1702747.

ECCC (Environment and Climate Change Canada). 2017. *Canadian Environmental Sustainability Indicators: Air Pollutant Emissions*. En4-144/22-2017E-PDF. Gatineau, Quebec, Canada: Environment and Climate Change Canada.

Erickson AC, Brauer M, Christidis T, Pinault L, Crouse DL, van Donkelaar A, et al. 2019. Evaluation of a method to indirectly adjust for unmeasured covariates in the association between fine particulate matter and mortality. Environ Res 175:108–116, PMID: 31108354, https://doi.org/10.1016/j.envres.2019.05.010.

Finès P, Pinault L, Tjepkema M. 2017. *Imputing Postal Codes to Analyze Ecological Variables in Longitudinal Cohorts: Exposure To Particulate Matter in the Canadian Census Health and Environment Cohort Database*. Catalogue no. 11-633-X—No. 006. Ottawa, Ontario, Canada: Statistics Canada.

GBD 2017 Risk Factors Collaborators. 2018. Global, regional, and national comparative risk assessment of 84 behavioural, environmental and occupational, and metabolic risks or clusters of risks for 195 countries and territories, 1990–2017: a systematic analysis for the Global Burden of Disease Study 2017. Lancet 392(10159):1923–1994, PMID: 30496105, https://doi.org/10.1016/S0140-6736(18)32225-6.

Gordon DLA, Janzen M. 2013. Suburban nation? Estimating the size of Canada's suburban population. J Archit Plann Res 30(3):197–220.

Harrell FE. 2015. *Regression Modeling Strategies with Applications to Linear Models, Logistic and Ordinal Regression, and Survival Analysis*. 2nd ed. New York, NY: Springer.

Hystad P, Setton E, Cervantes A, Poplawski K, Deschenes S, Brauer M, et al. 2011. Creating national air pollution models for population exposure assessment in Canada. Environ Health Perspect 119(8):1123–1129, PMID: 21454147, https://doi.org/10.1289/ehp.1002976.

Khan S, Pinault L, Tjepkema M, Wilkins R. 2018. Positional accuracy of geocoding from residential postal codes versus full street addresses. Health Rep 29(2):3–9, PMID: 29465738.

Lim SS, Vos T, Flaxman AD, Danaei G, Shibuya K, Adair-Rohani H, et al. 2012. A comparative risk assessment of burden of disease and injury attributable to 67 risk factors and risk factor clusters in 21 regions, 1990–2010: a systematic analysis for the Global Burden of Disease Study 2010. Lancet 380(9859):2224–2260, PMID: 23245609, https://doi.org/10.1016/S0140-6736(12)61766-8.

Matheson FI, Dunn JR, Smith KLW, Moineddin R, Glazier RH. 2012. Development of the Canadian Marginalization Index: a new tool for the study of inequality. Can J Public Health 103(8 Suppl 2):S12–S16, PMID: 23618065, https://doi.org/10.1007/BF03403823.

Meng J, Li C, Martin RV, van Donkelaar A, Hystad P, Brauer M, et al. 2019. Estimated long-term (1981–2016) concentrations of ambient fine particulate matter across North America from chemical transport modeling, satellite remote sensing, and ground-based measurements. Environ Sci Technol 53(9):5071–5079, PMID: 30995030, https://doi.org/10.1021/acs.est.8b06875.

Nasari MM, Szyszkowicz M, Chen H, Crouse D, Turner MC, Jerrett M, et al. 2016. A class of non-linear exposure-response models suitable for health impact assessment applicable to large cohort studies of ambient air pollution. Air Qual Atmos Health 9(8):961–972, PMID: 27867428, https://doi.org/10.1007/s11869-016-0398-z.

Newbold KB. 2005. Self-rated health within the Canadian immigrant population: risk and the healthy immigrant effect. Soc Sci Med 60(6):1359–1370, PMID: 15626530, https://doi.org/10.1016/j.socscimed.2004.06.048.

Ng E. 2011. The healthy immigrant effect and mortality rates. Health Rep 22(4):25–29, PMID: 22352149.

Pinault LL, Weichenthal S, Crouse DL, Brauer M, Erickson A, Donkelaar AV, et al. 2017. Associations between fine particulate matter and mortality in the 2001 Canadian Census Health and Environment Cohort. Environ Res 159:406–415, PMID: 28850858, https://doi.org/10.1016/j.envres.2017.08.037.

Pinault L, Finès P, Labrecque-Synnott F, Saidi A, Tjepkema M. 2016a. *The 2001 Canadian Census-Tax-Mortality Cohort: A 10-Year Follow-Up*. No. 11-633-X no. 003. Ottawa, Ontario, Canada: Statistics Canada.

Pinault L, Tjepkema M, Crouse DL, Weichenthal S, van Donkelaar A, Martin RV, et al. 2016b. Risk estimates of mortality attributed to low concentrations of ambient fine particulate matter in the Canadian community health survey cohort. Environ Health 15(1):18–31, PMID: 26864652, https://doi.org/10.1186/s12940-016-0111-6.

Pope CA 3rd, Burnett RT, Krewski D, Jerrett M, Shi Y, Calle EE, et al. 2009. Cardiovascular mortality and exposure to airborne fine particulate matter and cigarette smoke: shape of the exposure-response relationship. Circulation 120(11):941–948, PMID: 19720932, https://doi.org/10.1161/CIRCULATIONAHA.109.857888.

Pope CA 3rd, Burnett RT, Turner MC, Cohen A, Krewski D, Jerrett M, et al. 2011. Lung cancer and cardiovascular disease mortality associated with ambient air pollution and cigarette smoke: shape of the exposure-response relationships. Environ Health Perspect 119(11):1616–1621, PMID: 21768054, https://doi.org/10.1289/ehp.1103639.

Pope CA 3rd, Ezzati M, Cannon JB, Allen RT, Jerrett M, Burnett RT III. 2018. Mortality risk and $PM_{2.5}$ air pollution in the USA: an analysis of a national prospective cohort. Air Qual Atmos Health 11(3):245–252, https://doi.org/10.1007/s11869-017-0535-3.

Pya N, Wood SN. 2015. Shape constrained additive models. Stat Comput 25(3):543–559, https://doi.org/10.1007/s11222-013-9448-7.

Robichaud A, Ménard R. 2014. Multi-year objective analyses of warm season ground-level ozone and $PM_{2.5}$ over North America using real-time observations and Canadian operational air quality models. Atmos Chem Phys 14(4):1769–1800, https://doi.org/10.5194/acp-14-1769-2014.

Robichaud A, Ménard R, Zaïtseva Y, Anselmo D. 2016. Multi-pollutant surface objective analyses and mapping of air quality health index over North America. Air Qual Atmos Health 9(7):743–759, PMID: 27785157, https://doi.org/10.1007/s11869-015-0385-9.

Shin HH, Cakmak S, Brion O, Villeneuve P, Turner MC, Goldberg MS, et al. 2014. Indirect adjustment for multiple missing variables applicable to environmental epidemiology. Environ Res 134:482–487, PMID: 24972508, https://doi.org/10.1016/j.envres.2014.05.016.

Statistics Canada. 2003. *2001 Census Dictionary*. 92-378-XIE. Ottawa, Ontario, Canada: Statistics Canada.

Statistics Canada. 2017a. Directive on Microdata Linkage. https://www.statcan.gc.ca/eng/record/policy4-1 [accessed 8 February 2019].

Statistics Canada. 2017b. Social Data Linkage Environment (SDLE). https://www.statcan.gc.ca/eng/sdle/index [accessed 28 January 2019].

Statistics Canada. 2017c. *Postal Code^{OM} Conversion File Plus (PCCF+) Version 7A, Reference Guide: June 2017 Postal Codes^{OM}*. Ottawa, Ontario, Canada: Statistics Canada.

Thurston GD, Burnett RT, Turner MC, Shi Y, Krewski D, Lall R, et al. 2016. Ischemic heart disease mortality and long-term exposure to source-related components of U.S. fine particle air pollution. Environ Health Perspect 124(6):785–794, PMID: 26629599, https://doi.org/10.1289/ehp.1509777.

Turner MC, Jerrett M, Pope CA 3rd, Krewski D, Gapstur SM, Diver WR, et al. 2016. Long-term ozone exposure and mortality in a large prospective study. Am J Respir Crit Care Med 193(10):1134–1142, PMID: 26680605, https://doi.org/10.1164/rccm.201508-1633OC.

van Donkelaar A, Martin RV, Spurr RJD, Burnett RT. 2015. High resolution satellite-derived $PM_{2.5}$ for optical estimation and geographically-weighted regression over North America. Environ Sci Technol 49(17):10482–10491, PMID: 26261937, https://doi.org/10.1021/acs.est.5b02076.

van Donkelaar A, Martin RV, Li C, Burnett RT. 2019. Regional estimates of chemical composition of fine particulate matter using a combined geoscience-statistical method with information from satellites, models, and monitors. Environ Sci Technol 53(5):2595–2611, PMID: 30698001, https://doi.org/10.1021/acs.est.8b06392.

Weichenthal S, Pinault LL, Burnett RT. 2017. Impact of oxidant gases on the relationship between outdoor fine particulate air pollution and nonaccidental, cardiovascular, and respiratory mortality. Sci Rep 7(1):16401, PMID: 29180643, https://doi.org/10.1038/s41598-017-16770-y.

WHO (World Health Organization). 1977. *Manual of the International Statistical Classification of Diseases, Injuries, and Causes of Death: Based on the Recommendations of the Ninth Revision Conference, 1975, and Adopted by the Twenty-Ninth World Health Assembly, 1975 Revision*. http://www.who.int/iris/handle/10665/40492 [accessed 12 February 2019].

WHO. 2016. *International Statistical Classification of Diseases and Related Health Problems, 10th Revision*. https://www.who.int/classifications/icd/ICD10Volume2_en_2010.pdf [accessed 12 February 2019].

Wilkins R, Tjepkema M, Mustard C, Choinière R. 2008. The Canadian census mortality follow-up study, 1991 through 2001. Health Rep 19(3):25–43, PMID: 18847143.

Yin P, Brauer M, Cohen A, Burnett RT, Liu J, Liu Y, et al. 2017. Long-term fine particulate matter exposure and nonaccidental and cause-specific mortality in a large national cohort of Chinese men. Environ Health Perspect 125(11):117002, PMID: 29116930, https://doi.org/10.1289/EHP1673.

Christidis et al. Environmental Health (2019) 18:84
https://doi.org/10.1186/s12940-019-0518-y

Environmental Health

RESEARCH Open Access

Low concentrations of fine particle air pollution and mortality in the Canadian Community Health Survey cohort

Tanya Christidis[1*], Anders C. Erickson[2], Amanda J. Pappin[1,13], Daniel L. Crouse[3], Lauren L. Pinault[1], Scott A. Weichenthal[4,5], Jeffrey R. Brook[6,12], Aaron van Donkelaar[7,11], Perry Hystad[8], Randall V. Martin[7,9,11], Michael Tjepkema[1], Richard T. Burnett[10] and Michael Brauer[2]

Abstract

Background: Approximately 2.9 million deaths are attributed to ambient fine particle air pollution around the world each year ($PM_{2.5}$). In general, cohort studies of mortality and outdoor $PM_{2.5}$ concentrations have limited information on individuals exposed to low levels of $PM_{2.5}$ as well as covariates such as smoking behaviours, alcohol consumption, and diet which may confound relationships with mortality. This study provides an updated and extended analysis of the Canadian Community Health Survey-Mortality cohort: a population-based cohort with detailed $PM_{2.5}$ exposure data and information on a number of important individual-level behavioural risk factors. We also used this rich dataset to provide insight into the shape of the concentration-response curve for mortality at low levels of $PM_{2.5}$.

Methods: Respondents to the Canadian Community Health Survey from 2000 to 2012 were linked by postal code history from 1981 to 2016 to high resolution $PM_{2.5}$ exposure estimates, and mortality incidence to 2016. Cox proportional hazard models were used to estimate the relationship between non-accidental mortality and ambient $PM_{2.5}$ concentrations (measured as a three-year average with a one-year lag) adjusted for socio-economic, behavioural, and time-varying contextual covariates.

Results: In total, 50,700 deaths from non-accidental causes occurred in the cohort over the follow-up period. Annual average ambient $PM_{2.5}$ concentrations were low (i.e. 5.9 $\mu g/m^3$, s.d. 2.0) and each 10 $\mu g/m^3$ increase in exposure was associated with an increase in non-accidental mortality (HR = 1.11; 95% CI 1.04–1.18). Adjustment for behavioural covariates did not materially change this relationship. We estimated a supra-linear concentration-response curve extending to concentrations below 2 $\mu g/m^3$ using a shape constrained health impact function. Mortality risks associated with exposure to $PM_{2.5}$ were increased for males, those under age 65, and non-immigrants. Hazard ratios for $PM_{2.5}$ and mortality were attenuated when gaseous pollutants were included in models.

Conclusions: Outdoor $PM_{2.5}$ concentrations were associated with non-accidental mortality and adjusting for individual-level behavioural covariates did not materially change this relationship. The concentration-response curve was supra-linear with increased mortality risks extending to low outdoor $PM_{2.5}$ concentrations.

Keywords: $PM_{2.5}$, Air pollution, Canada, Cohort study, Fine particulate matter, Mortality, Fine particle air pollution

* Correspondence: tanya.christidis@canada.ca
[1]Health Analysis Division, Statistics Canada, 100 Tunney's Pasture Driveway, Ottawa, Ontario K1A 0T6, Canada
Full list of author information is available at the end of the article

Background

Exposure to ambient fine particle air pollution ($PM_{2.5}$) is responsible for an estimated 2.9 million deaths annually and 83 million disability-adjusted life years lost [1], with several large epidemiological cohort studies linking long-term exposure to $PM_{2.5}$ to all-cause and cause-specific mortality [2–4]. Even in settings with relatively low concentrations of air pollution, such as Canada, the relationships persist [5, 6]. Despite these findings, there remain two key areas of potential bias and uncertainty that past work has been unable to address simultaneously. The first is the inability to directly adjust for individual-level behavioural risk factors associated with chronic disease mortality, such as smoking, diet, and exercise, or health measures such as body mass index; various indirect methods for adjustment have been applied elsewhere [7, 8]. The second regards the shape of the concentration-response curve for $PM_{2.5}$ and mortality. This issue has become increasingly pertinent as clean air regulations have succeeded in reducing $PM_{2.5}$ concentrations across North America and elsewhere, and thus a better understanding of the shape of the $PM_{2.5}$-mortality associations at low concentrations are required for cost-benefit assessments of future reduction efforts.

The purpose of this study was to provide an updated and extended analysis of the Canadian Community Health Survey-Mortality cohort [9] including [1]: additional years of follow-up to 2016 [2]; improvements in the resolution of $PM_{2.5}$ exposure (approximately $1km^2$ grid) [3]; annual residential history from 1981 to 2016 for all cohort members from a linkage to postal code records [4]; time-varying contextual covariates [5]; inclusion of immigrants to Canada, and [6] an improved linkage between survey respondents and death records. We examine the shape of the concentration-response curves using a Shape Constrained Health Impact Function (SCHIF) [10] and perform sensitivity analyses.

Methods

CCHS-mortality cohort

The Canadian Community Health Survey (CCHS) is a national cross-sectional survey of the Canadian population that collects information related to health status, health care utilization, and health determinants. From 2000 to 2007 the survey was administered every 2 years to approximately 130,000 respondents; from 2007 onwards, data has been collected on an ongoing basis from 65,000 respondents per year and released annually with response rates declining over time (Fig. 1) [11–16]. The

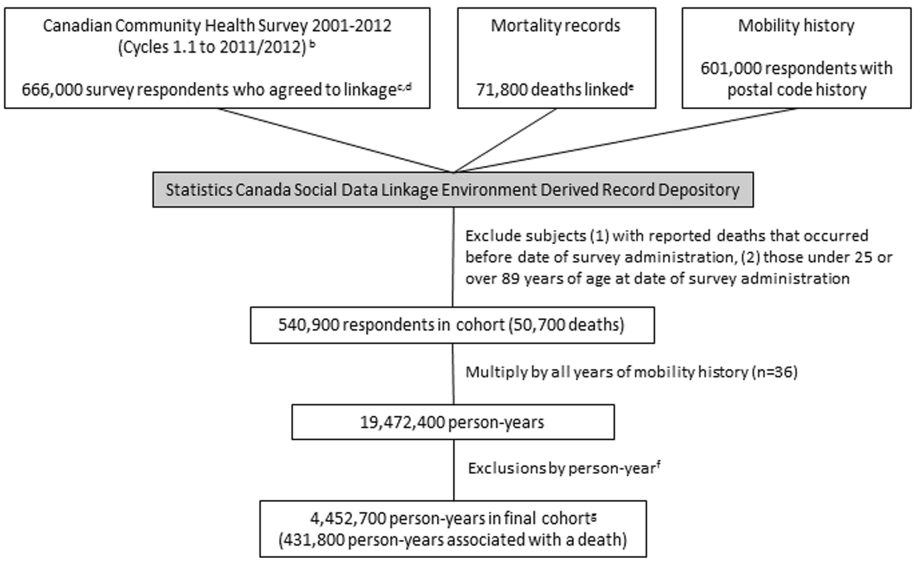

Fig. 1 Flowchart of CCHS-Mortality cohort creation from linkage of survey to mortality and mobility history to person-year based analytical file[a]. [a]numbers rounded to the nearest 100 for confidentiality. [b]response rates: 2000/2001 (Cycle 1.1) 84.7%, 2003 (Cycle 2.1) 80.7%, 2005 (Cycle 3.1) 78.9%, 2007/2008 (Cycle 4.1) 76.4%, 2009/2010 72.3%, 2011/2012 68.4%. [c]respondents who agreed to data linkage: 2000/2001 (Cycle 1.1) $n = 117,800$, 2003 (Cycle 2.1) $n = 112,900$, 2005 (Cycle 3.1) $n = 113,900$, 2007/2008 (Cycle 4.1) n = 112,700, 2009/2010 $n = 104,700$, 2011/2012 n = 104,100. [d]linkage rate of respondents who agreed to linkage to the SDLE DRD: 95.2%. [e]linkage rate of relevant deaths to the SDLE DRD: 99.8%. [f]see methods for list of exclusion criteria, totals will exceed number of deleted person-years given that more than one exclusion criteria may apply to a single person-year; immigrated to Canada less than 10 years before survey date $n = 541,600$, age during follow-up period exceeds 89 years $n = 161,000$, no postal code n = 5,009,900, could not be linked to air pollution values n = 5,711,600, could not be linked to Can-MARG values $n = 7,668,000$, could not be linked to Census Metropolitan Area/Census Agglomeration size $n = 4,800,600$, could not be linked to airshed $n = 3500$, 3-year moving average being informed by only 1 year of exposure $n = 4,321,500$, year after subject death $n = 343,600$, year before survey interview date $n = 13,570,300$. [g]from 452,700 unique individuals

CCHS data are sampled from approximately 98% of the Canadian population aged 12 and older living in private dwellings within the 115 Heath Regions covering all provinces and territories. Individuals living on Indian Reserves and on Crown Land, institutional residents, full-time members of the Canadian Forces, and residents of certain remote regions are excluded.

Consent to record linkage and data sharing was obtained at time of survey (Fig. 1) and only those CCHS respondents who agreed were linked to death records and residential history through Statistics Canada's Social Data Linkage Environment (SDLE) [17]. The linkage was approved by Statistics Canada [18] and is governed by the Directive on Microdata Linkage [19]. The linkage occurred within the Derived Record Depository, a highly secure linkage environment comprised of a national dynamic relational database of basic personal identifiers. Survey and administrative data are linked to the Derived Record Depository using a SAS-based generalized record linkage software (G-link) that supports deterministic and probabilistic linkage based on the mathematical theory of record linkage developed at Statistics Canada [20]. Mortality linkage to the Derived Record Depository between 2000 and 2016 was 99.8% [21]. A list of linked unique individuals is created through linkages that are deterministic (matching records based on unique identifiers) and probabilistic (matching records based on non-unique identifiers such as names, sex, date of birth, and postal code and estimating the likelihood that records are referring to the same entity). For the CCHS cycles considered, there was a linkage rate to the Derived Record Depository of 95.2% and a false error rate for the CCHS to SDLE linkage of 0.4% [22].

There were 666,000 CCHS respondents who agreed to data linkage (Fig. 1), reduced to 540,900 after excluding subjects with death dates prior to survey response dates (i.e. either the death record or linkage must be incorrect) or who were below the age of 25 or above 89 at time of survey as they are less likely to reside at the same postal code as their income tax mailing address [23]. The CCHS to SDLE linkage rates across key indicators were consistently high, ranging from 94.4% for the 20–29 age group to 96.2% for the 80–89 age group, 95.5 and 95.3% for males and females respectively, and by province/territory from 91.8% for the Yukon to 96.7% for Newfoundland and Labrador [22].

After linkage, we stacked the CCHS cycles into one data file. We standardized the variable categorizations when discrepancies between cycles existed. The covariates (listed, along with categorizations in Table 1) included socio-economic, behavioural, and contextual measures. More information about the definitions and classifications of these variables can be found elsewhere [9]. Provincially standardized deciles were calculated according to the distribution of residents in each province and the ratio of their total household income to the low-income cut-off for their corresponding household and community size. As this measure excluded subjects living in territories, we took the mean income within each decile and used these as cut-offs to categorize subjects living in territories by income into deciles. Once all subjects were placed in deciles, we merged groups to create quintiles.

Postal code history was complete from 1981 to 2016 for 35.0% of respondents and 12.6% of respondents had no postal code history. There were gaps in postal code histories for 52.4% of respondents, which is to be expected, as taxes may not have been filed for various reasons (e.g immigration, death, or age). We imputed complete or partial postal codes only when bookended by postal codes with sufficient similarity before and after the gap [24]. For example, if a postal code in 2008 was K1A 0T6 and then K1A 0K9 in 2012, a partial postal code of K1A 0** would be imputed for the four missing years from 2009 to 2011. We did not impute postal codes if a gap existed at the beginning or end of the follow-up period or after a person's death; full or partial postal codes (two to five digits) were imputed for 1.5% of person-years.

We organised the cohort into a person-year file with each year of exposure (1981–2016) per person representing a row of data. Subsequently we excluded specific person-years [1] once they turned age 90 during follow-up [2], if the person had immigrated to Canada less than 10 years prior to survey interview [3], if there was no postal code [4], if the postal code could not be linked to air pollution or contextual covariates [5], if the $PM_{2.5}$ three-year moving average with a one-year lag was calculated by fewer than 2 years of exposure data, or [6] if the person-year was before survey interview date or after a person's death (Fig. 1). We excluded recent immigrants to Canada (10 years or less) since they have spent the majority of their lives outside of Canada with unknown exposure, and this time exceeds the number of years in Canada where exposure can be estimated.

Exposure file and analytical file

The task of linking contextual covariates and air pollution values to the cohort required the creation of a master list of postal codes with their respective points of latitude and longitude and census geography. We produced this list from Statistics Canada's June 2017 Postal Code Conversion File and the two previous versions (August 2015 and May 2011) to ensure coverage of retired postal codes [25–27]. Since census geography does not align with postal code locations, a single postal code can have multiple points of latitude and longitude. Each can represent the centroid of a blockface (i.e. a

Table 1 Descriptive statistics of the cohort and $PM_{2.5}$ O_3, and NO_2 exposure, with Cox proportional hazard ratios

Covariate	Person-years[a]	HR	95% CI		$PM_{2.5}$	S.D.	O_3	S.D.	NO_2	S.D.
			Lower	Upper						
All	4,452,700	–	–	–	5.9	2.0	36.0	7.5	8.6	5.9
Sex										
Male	1,995,100	–	–	–	5.9	2.0	35.9	7.6	8.5	5.9
Female	2,457,600	–	–	–	6.0	2.0	36.0	7.5	8.6	5.9
Age group (years)										
25 to 29	381,100	–	–	–	5.9	2.0	35.7	7.6	8.8	5.9
30 to 39	869,300	–	–	–	5.9	2.0	35.9	7.7	8.7	5.9
40 to 49	887,000	–	–	–	5.9	2.0	35.8	7.6	8.7	6.0
50 to 59	918,100	–	–	–	5.8	2.0	35.8	7.4	8.2	5.7
60 to 69	753,800	–	–	–	5.9	2.0	36.2	7.3	8.3	5.8
70 to 79	497,100	–	–	–	6.1	2.1	36.4	7.4	8.9	6.1
80 to 89	146,200	–	–	–	6.2	2.1	36.3	7.6	9.6	6.3
Immigrant status										
Non-immigrants	3,945,800	1.00	–	–	5.8	2.0	35.7	7.4	8.1	5.6
In Canada for 30+ years	317,900	0.86	0.83	0.88	6.8	2.1	38.5	8.0	11.2	6.5
In Canada for 20–29 years	92,300	0.74	0.68	0.80	7.0	2.0	37.4	8.0	13.2	7.0
In Canada for 10–19 years	96,800	0.62	0.56	0.69	7.2	1.9	37.6	7.7	14.5	7.0
Visible minority identity										
Not a visible minority	4,119,200	1.00	–	–	5.9	2.0	36.1	7.4	8.4	5.7
Visible Minority	244,900	0.89	0.84	0.93	6.6	2.1	34.9	8.9	12.8	7.2
Missing (dummy variable)	88,600	1.48	1.37	1.59	4.9	1.6	31.7	8.3	6.5	4.3
Indigenous identity										
Non-Indigenous or not stated	4,295,500	1.00	–	–	6.0	2.0	36.2	7.4	8.6	5.9
Indigenous	146,000	1.58	1.50	1.67	4.9	1.7	30.3	8.8	6.9	4.7
Missing (dummy variable)	11,300	1.16	0.99	1.35	5.6	1.8	35.0	7.5	8.2	5.6
Marital status										
Married or Common-law	2,823,000	1.00	–	–	5.8	2.0	36.1	7.6	8.1	5.5
Separated, Widowed, or Divorced	945,100	1.42	1.39	1.45	6.1	2.1	36.1	7.5	9.1	6.2
Single	681,400	1.57	1.52	1.62	6.2	2.1	35.4	7.5	9.8	6.8
Missing (dummy variable)	3200	1.58	1.20	2.07	5.9	1.9	34.5	8.0	9.4	6.1
Educational attainment										
No high school diploma	980,900	1.00	–	–	5.7	2.1	35.2	7.5	7.8	5.8
High School	757,200	0.82	0.80	0.84	6.0	2.0	36.6	7.7	8.6	5.8
Any post-secondary	1,926,400	0.77	0.75	0.78	5.9	2.0	36.0	7.5	8.4	5.7
University	752,100	0.55	0.54	0.57	6.2	2.0	36.4	7.4	10.1	6.5
Missing (dummy variable)	36,000	0.98	0.91	1.06	5.9	2.0	35.6	7.7	8.8	5.8
Employment status										
Employed	2,701,800	1.00	–	–	5.9	2.0	36.0	7.6	8.7	5.8
Unemployed	115,100	1.67	1.54	1.82	5.8	2.1	34.9	7.7	8.4	6.3
Not in work force	1,630,100	2.02	1.96	2.08	6.0	2.1	36.0	7.4	8.5	6.0
Missing (dummy variable)	5800	1.62	1.24	2.12	5.5	1.8	34.0	7.2	8.8	5.4
Income quintile										
Q1 (lowest income)	788,200	1.00	–	–	6.1	2.1	35.6	7.4	9.2	6.5

Table 1 Descriptive statistics of the cohort and $PM_{2.5}$ O_3, and NO_2 exposure, with Cox proportional hazard ratios *(Continued)*

Covariate	Person-years[a]	HR	95% CI		$PM_{2.5}$	S.D.	O_3	S.D.	NO_2	S.D.
			Lower	Upper						
Q2	788,700	0.76	0.74	0.78	6.0	2.0	36.1	7.4	8.7	6.1
Q3	808,500	0.64	0.62	0.66	6.0	2.0	36.3	7.4	8.5	5.8
Q4	828,500	0.53	0.52	0.55	5.9	2.0	36.2	7.5	8.4	5.7
Q5 (highest income)	909,000	0.44	0.43	0.46	5.7	1.9	35.9	7.7	8.2	5.5
Missing (dummy variable)	329,800	0.74	0.72	0.77	5.8	2.0	35.5	8.0	8.6	5.8
Alcohol consumption										
Never drinker	392,400	1.00	–	–	5.8	2.0	35.8	7.3	8.0	5.9
Occasional drinker	840,300	0.84	0.81	0.86	5.8	2.0	35.7	7.6	8.3	5.8
Regular drinker, binging unknown	1,332,300	0.64	0.62	0.66	6.1	2.0	36.7	7.3	9.1	6.0
Regular, non-binge drinker	1,169,600	0.69	0.67	0.72	5.8	2.0	35.8	7.5	8.4	5.7
Regular, binge drinker	260,400	1.08	1.03	1.14	5.9	2.0	35.8	7.8	8.1	5.8
Former drinker	447,500	1.10	1.07	1.14	5.9	2.1	35.3	8.0	8.8	6.2
Missing (dummy variable)	10,200	0.93	0.81	1.07	5.6	1.9	34.8	7.5	8.5	5.5
Smoking behaviours										
Never smoker	1,293,700	1.00	–	–	6.0	2.0	36.4	7.5	9.0	6.1
Occasional smoker	177,200	2.11	2.00	2.23	6.0	2.0	35.6	7.7	9.0	6.3
Smoke under 10 cigarettes/day	263,000	2.45	2.35	2.55	5.9	2.1	35.3	7.9	8.7	6.2
Smoke 11–20 cigarettes /day	398,900	2.76	2.66	2.86	5.9	2.0	35.6	7.7	8.3	5.8
Smoke 20+ cigarettes /day	255,300	3.69	3.55	3.82	5.9	2.1	36.0	7.6	8.2	5.9
Former smoker	2,058,700	1.32	1.29	1.35	5.9	2.0	35.9	7.4	8.4	5.8
Missing (dummy variable)	6100	1.51	1.26	1.80	5.7	1.8	35.6	7.4	8.3	5.7
Fruit and vegetable consumption										
Under 5 servings/day	2,411,900	1.00	–	–	5.9	2.0	36.0	7.7	8.6	5.9
5–10 servings/day	1,450,300	0.82	0.80	0.83	6.0	2.0	36.6	7.5	8.8	5.9
10+ servings/day	132,700	0.82	0.77	0.87	6.1	2.0	36.6	7.5	8.9	6.0
Missing (dummy variable)	457,900	1.19	1.16	1.23	5.6	1.9	33.6	5.8	7.9	6.1
Leisure exercise frequency										
Active	1,005,700	1.00	–	–	5.9	2.0	36.1	7.6	8.6	5.7
Moderate	1,123,600	1.10	1.07	1.14	5.9	2.0	36.1	7.5	8.6	5.8
Inactive	2,224,700	1.70	1.65	1.74	5.9	2.0	35.9	7.5	8.5	6.0
Missing (dummy variable)	98,700	2.49	2.39	2.60	5.9	2.1	35.2	7.8	9.0	6.2
Body mass index (BMI)										
Normal weight (18.5–24.9)	1,425,400	1.00	–	–	6.1	2.0	36.1	7.4	9.1	6.2
Overweight (25.0–29.9)	1,671,700	0.81	0.80	0.83	5.9	2.0	36.0	7.5	8.5	5.8
Obese 1 (30.0–34.9)	800,500	0.93	0.90	0.95	5.8	2.0	35.9	7.6	8.1	5.6
Obese 2 (≥ 35)	355,300	1.33	1.28	1.37	5.7	2.0	35.7	7.7	7.9	5.5
Underweight (< 18.5)	57,700	2.13	2.00	2.26	6.2	2.1	36.0	7.4	9.7	6.5
Missing	142,200	1.61	1.53	1.68	5.8	2.0	35.8	7.8	8.2	5.5
Residential Instability										
Q1 (lowest marginalization)	993,500	1.00	–	–	5.3	1.8	36.9	7.8	7.1	4.8
Q2	1,231,300	0.98	0.95	1.00	5.6	1.9	36.7	7.9	7.1	4.8
Q3	957,500	0.98	0.95	1.01	5.9	2.0	34.6	7.7	8.6	5.5

Table 1 Descriptive statistics of the cohort and $PM_{2.5}$ O_3, and NO_2 exposure, with Cox proportional hazard ratios *(Continued)*

Covariate	Person-years[a]	HR	95% CI		$PM_{2.5}$	S.D.	O_3	S.D.	NO_2	S.D.
			Lower	Upper						
Q4	780,100	0.96	0.93	0.99	6.5	2.0	35.7	6.8	10.0	6.2
Q5 (highest marginalization)	490,300	1.04	1.01	1.07	7.2	1.9	35.5	6.1	13.0	7.6
Dependency										
Q1 (lowest marginalization)	701,400	1.00	–	–	5.7	1.9	33.4	8.7	10.0	6.2
Q2	601,900	0.96	0.92	0.99	6.1	1.9	35.8	7.3	9.9	6.0
Q3	602,400	0.92	0.89	0.95	6.3	2.1	37.4	7.5	9.7	6.1
Q4	945,800	0.90	0.87	0.93	6.2	2.1	37.6	7.5	8.6	5.8
Q5 (highest marginalization)	1,601,300	0.88	0.86	0.91	5.7	2.0	35.7	6.7	7.0	5.3
Material deprivation										
Q1 (lowest marginalization)	713,600	1.00	–	–	6.0	1.8	37.7	7.4	9.8	5.2
Q2	777,700	1.03	1.00	1.06	6.2	1.9	38.0	8.0	9.4	5.4
Q3	897,400	1.04	1.01	1.07	6.2	1.9	37.5	7.3	8.8	5.5
Q4	783,800	1.08	1.04	1.11	6.2	2.1	35.7	7.5	9.2	6.3
Q5 (highest marginalization)	1,280,200	1.15	1.12	1.19	5.3	2.0	32.9	6.4	6.8	6.2
Ethnic concentration										
Q1 (lowest marginalization)	1,839,100	1.00	–	–	5.2	1.7	35.7	6.9	5.9	3.8
Q2	1,211,600	1.02	1.00	1.04	6.0	2.0	36.7	8.0	8.0	4.8
Q3	749,900	1.01	0.99	1.04	6.3	2.0	35.5	7.8	10.1	5.7
Q4	409,500	1.04	1.00	1.07	7.0	2.1	35.7	8.2	14.2	6.9
Q5 (highest marginalization)	242,600	0.98	0.94	1.02	7.7	1.7	36.4	7.5	17.7	6.2
Census Metropolitan Area/Census Agglomeration size										
Not applicable (non-CMA/CA)	1,485,900	1.00	–	–	4.7	1.3	33.9	7.1	4.9	2.7
10,000–29,999	355,900	1.03	0.99	1.06	5.0	1.3	31.6	7.9	6.0	3.1
30,000–99,999	570,900	1.03	1.00	1.06	5.8	1.8	36.6	6.9	7.1	3.3
100,000–499,999	872,600	1.00	0.98	1.03	6.8	2.2	39.5	8.0	8.9	4.6
500,000-1,499,999	506,400	0.94	0.91	0.97	6.7	1.7	36.5	6.2	13.2	6.2
> 1,500,000	661,000	0.91	0.89	0.94	7.5	1.7	37.4	6.5	15.5	6.9
Urban form										
Active urban core	304,800	1.00	–	–	7.6	1.9	36.7	7.1	14.5	7.1
Transit-reliant suburb	179,500	0.98	0.93	1.04	7.8	1.7	36.7	7.1	16.1	7.4
Car-reliant suburb	1,242,700	0.81	0.78	0.84	7.0	1.9	38.3	7.0	12.1	6.0
Exurban	216,400	0.83	0.78	0.87	5.5	1.6	38.7	7.0	6.8	3.6
Non-CMA/CA	2,509,400	0.93	0.90	0.96	5.1	1.6	34.4	7.5	5.7	3.2
Airshed										
East Central	2,041,500	1.00	–	–	7.0	2.1	41.3	6.0	9.9	6.6
Northern	117,800	1.18	1.11	1.27	3.9	1.2	26.0	7.0	4.7	2.6
Southern Atlantic	711,700	1.11	1.08	1.13	4.4	1.0	30.7	3.1	3.9	2.6
Prairie	666,900	1.00	0.97	1.02	5.2	1.4	34.1	5.7	9.5	4.9
West Central	397,100	1.07	1.03	1.10	4.9	1.1	31.3	5.0	8.0	4.9
Western	517,600	1.04	1.01	1.07	5.7	1.5	30.6	5.9	9.8	5.0

Columns 6, 8, and 10 are mean values

[a]numbers rounded to the nearest 100 for confidentiality

street block), dissemination block (i.e. an area bounded on all sides by roads), or dissemination area (i.e. adjacent dissemination blocks that collectively contain 400 to 700 persons) within a postal code.

We developed and used annual exposure estimates of $PM_{2.5}$ from 1998 to 2012 by relating satellite retrievals of aerosol optical depth (AOD) to near-surface $PM_{2.5}$ concentrations using the geophysically-based relationship simulated by a chemical transport model [28]. Ground monitoring data from the National Air Pollution Surveillance (NAPS) network were then incorporated, along with other North American-based measurements, to constrain these $PM_{2.5}$ estimates with geographically weighted regression. The resulting ambient $PM_{2.5}$ surface provided estimates for North America at about a $1km^2$ resolution [28]. Spatial variation from this surface was used with simulated $PM_{2.5}$ and consistently constrained with local ground-based monitors to extend our $PM_{2.5}$ coverage to 2015 [29].

The ambient warm season daily-maximum eight-hour average O_3 surfaces were developed by Environment and Climate Change Canada for 2002–2015 using chemical transport modelling informed by surface observations as hourly estimates from 2002 to 2015 [30–32]. Estimates of NO_2 were created using a national land use regression model (LUR) informed by on satellite-derived NO_2 (10 km resolution), distances to highways and major roads, and roadway kernel density gradients [33]. Ozone and NO_2 values were back-casted to obtain exposures for 1981–2015 using ground monitoring data from the Canadian National Air Pollution Surveillance program. Annual adjustment factors were calculated at a census division level from the ratio of observed concentration to the values in the surface for the reference year (see Pinault et al. for more detail [9]).

We linked postal codes to $PM_{2.5}$ in ArcGIS Desktop 10.5.1 using the points of latitude and longitude from the master postal code list and the air pollutant surfaces. In cases where there were multiple points of latitude and longitude for a single urban postal code, we used equal weighting of the multiple air pollutant values to provide a singular value. In rural communities, we took the population-weighted average of the values associated with duplicate postal codes. We used population-weighing to average multiple values to create inputs for partial postal codes (2 to 5 digits).

Covariates

Contextual covariates were available at various census geographies and we merged these to individual person-years via postal codes (as described below). We created historic measures when possible to reflect neighbourhood-level changes over the time.

Regions of Canada that share air quality characteristics and movement patterns have been defined by the Air Quality Management System (AQMS) as six distinct airsheds [34]. By subdividing the country into large geographic areas, adjustment for the broad spatial variation in mortality rates can be performed [9, 34]. We assigned airshed to the cohort by postal code. We used a population weighted mode in cases where there were multiple points of latitude and longitude for a single postal code.

We developed a historic community size variable to account for different sizes of metropolitan regions and changes in population over time, classifying Census Metropolitan Areas (CMAs: major urban core, 100,000+ residents) and Census Agglomerations (CAs: smaller urban cores, 10,000+ residents) by population counts [35]. Since CMA/CAs cover large areas that can include farmland near the urban-rural fringe and residential enclaves of commuters to the city, we created a measure that accounts for differences in urban form within these CMA/CAs. We used population density measures (1991–2016) and frequencies for different modes of transportation at the neighbourhood level (1996–2016) to categorize census tracts as active urban core, transit-reliant suburb, car-reliant suburb, exurban, and non-CMA/CA [36]. Both CMA/CA size and urban form were attached to the postal code list via census geography before merging with the cohort. In cases where there were multiple points of latitude and longitude representing a postal code, we used a population-weighted mode to assign categories.

The Canadian Marginalization Index (Can-MARG) is a measure of community-level marginalization comprised of four factors: material deprivation (e.g. proportion of people living in dwellings in need of repair), residential instability (e.g. proportion of people who live in a dwelling that they do not own) dependency (e.g. proportion of seniors and youth compared to those who are not), and ethnic concentration (e.g. proportion of recent immigrants and self-reported visible minorities) [37]. We used historic census tract-level Can-MARG values in CMA/CAs, and a population-weighted aggregation of the dissemination area-level Can-MARG values at the census subdivision level in rural areas outside of CMA/CAs that are not covered by census tracts. We assigned Can-MARG values to points of latitude and longitude before quintiles were assigned.

Statistical analysis

We calculated for each individual and year of follow-up a three-year moving average for $PM_{2.5}$ with a one-year lag, (e.g. the exposure in 2002 is the average of exposures in 1999, 2000, and 2001).

We ran standard Cox proportional hazard models to assess the relationship between $PM_{2.5}$ exposure and non-accidental death (ICD-10 codes A to R) from survey interview year to the end of follow-up period or year of death. We started model building with a baseline hazard function for $PM_{2.5}$ stratified by five-year age groups, sex, and survey cycle to ensure that respondents within these strata would be broadly comparable. We calculated new

hazard ratios for models that included each socio-economic and behavioural covariate individually. We included covariates in the partially-adjusted model if the log difference between the new hazard ratio and the baseline was more than 10%. Subsequently, we added contextual covariates individually to the partially-adjusted model and included them in the final model using the same criteria (comparing to the partially-adjusted model that included socio-economic and behavioural covariates). All covariates considered for inclusion in the final model and the associated hazard ratios are found in Table 1.

We examined the shape of the association between $PM_{2.5}$ and mortality with a SCHIF [10]. This method is based on a construction of several transformations of concentration and fitting the transformed variable in a Cox model, estimating the log-hazard ratio for a unit change in the transformed variable and its standard error. An ensemble of all models examined was then constructed using a weighted average of the predicted log-hazard ratio and any concentration, with weights defined by the AIC of each model. The transformations are variations on a sigmoidal function which yields supra-linear, near linear, and sub-linear shapes.

Sensitivity analyses

We examined effect modification by select socio-economic and behavioural covariates, and by high- and low-exposure groups to the combined oxidant capacity of NO_2 and O_3 (henceforth: O_X) which is calculated as the redox-weighted oxidant capacity [38] i.e. a weighted average using redox potentials as the weights (O_x^{wt} = $[(1.07\ V \times NO_2) + (2.075\ V \times O_3)]/3.145\ V$) (Table 4). We examined multiple pollutant models to investigate whether the inclusion of other common pollutants (NO_2, O_3, and O_X) in the model may modify the $PM_{2.5}$-mortality relationship [5, 39].

Results

There were 4,452,700 person-years in the cohort after exclusion criteria were applied (Fig. 1) from 452,700 unique individuals. Entry into the cohort and length of the follow-up period varied by survey cycle, with the first cohort having up to 15 years of follow-up. For those who died, the average follow-up period was 5.1 years (s.d. 3.4); it was 6.5 years (s.d. 4.1) for those who survived the follow-up period. There were 50,700 non-accidental deaths. Of these, there were 7900 deaths from ischemic heart disease, 2800 from cerebrovascular disease, and 4300 from other cardiovascular diseases; 900 from pneumonia, 2800 from COPD, and 1100 from other respiratory diseases; 5500 from lung cancer, 1300 from colon cancer, 1300 from breast cancer, 1100 from pancreatic cancer, and 9900 from all other cancers. Further, there were 1700 deaths from diabetes, 3900 deaths from neuropsychiatric conditions, 2200 from digestive diseases, 1100 from genitourinary diseases and 3000 from all other non-accidental causes.

Exposure to $PM_{2.5}$ was higher in women, more recent immigrants, and non-Indigenous people. Being single, university educated, and in the poorest income quintile were also associated with higher exposures (Table 1). We observed higher exposure to $PM_{2.5}$ in people living in the largest CMAs and in the East Central airshed (which includes Toronto and Montreal). The distribution of exposure estimates for $PM_{2.5}$, NO_2, O_3, and O_X is found in Table 2.

The cohort was generally representative of the Canadian population, as seen through their mortality rates by subgroup (Table 1). Immigrants and non-Indigenous people had lower mortality rates compared to their counterparts. Being married, holding a university degree, and being employed were associated with a lower risk of mortality. As expected, there were clear trends in mortality risk with income, education, and immigrant status.

The unadjusted model had a hazard ratio of 0.96 (95% CI 0.92–1.00) which increased to 1.11 (95% CI 1.04–1.18) when adjusted by the socio-economic, behavioural, and contextual covariates that met the inclusion threshold (Table 3). All covariates except for body mass index (BMI), employment status, and urban form met the criteria and were included in the final model. When we added the behavioural covariates to a model that included only socio-economic covariates the hazard ratio increased from 1.05 (95% CI 1.00–1.09) to 1.09 (95% CI 1.05–1.15). Conversely, when we added the behavioural covariates to a model that included both the socio-economic and contextual covariates, they lowered the $PM_{2.5}$ hazard ratio from 1.13 (95% CI 1.06–1.21) to 1.11 (95% CI 1.04–1.18).

The SCHIF characterisation of the $PM_{2.5}$-mortality association (for all cohort members) displayed a supra-linear shape that rises in a steeper fashion compared to the standard log-linear model prediction for lower concentrations and changes in a more moderate manner for higher levels (Fig. 2). Note that the SCHIF displays wider uncertainty intervals compared to the log-linear model at low concentrations, in part due to the additional variation associated with model shape, a feature captured by the SCHIF but not the log-linear model. We observed a positive and statistically significant ($p < 0.05$) association

Table 2 Distribution of air pollutant values for all person-years

	mean	minimum	percentile					maximum
			5th	25th	50th	75th	95th	
$PM_{2.5}$	5.9	0.4	3.4	4.3	5.5	7.1	9.7	17.2
O_3	36.0	3.1	24.9	30.7	35.3	40.9	49.0	65.8
NO_2	8.6	0.0	2.3	4.4	6.9	11.1	20.5	69.1
O_X [a]	26.7	4.1	18.6	22.6	26.2	30.6	36.5	54.1

[a] the combined oxidant capacity of NO_2 and O_3

Table 3 Cox proportional hazard ratios for non-accidental mortality[a] and $PM_{2.5}$ exposure, all respondents, 10% inclusion threshold

Model		95% CI		
	HR	Lower	Upper	-2 LL
Unadjusted (stratified by age, sex, and cycle)	0.96	0.92	1.00	769,047.51
Socio-economic covariates (Unadjusted model +)				
Visible minority identity	0.98	0.93	1.02	768,923.2
Indigenous identity	0.98	0.94	1.03	768,812.8
Immigrant status	1.02	0.98	1.07	768,784.2
Educational attainment	1.05	1.01	1.10	767,553.7
Marital status	0.92	0.88	0.96	767,479.4
Income quintile	0.94	0.90	0.98	766,080.2
Adjusted by socio-economic covariates*	1.05	1.00	1.09	764,396.4
Behavioural level covariates (Unadjusted model +)				
Fruit and vegetable consumption	1.00	0.96	1.05	768,304.6
Leisure exercise frequency	1.00	0.96	1.05	768,304.6
Alcohol consumption	1.04	1.00	1.09	766,726.1
Smoking behaviours	0.97	0.93	1.02	762,432.6
Adjusted by all socio-economic + behavioural covariates	1.09	1.05	1.15	756,074.0
Contextual covariates (Adjusted by socio-economic covariates +)				
Ethnic concentration	1.00	0.95	1.05	764,411.6
Material deprivation	1.04	0.99	1.09	764,411.2
Residential instability	1.06	1.01	1.11	764,408.0
Census Metropolitan Area/Census Agglomeration size	1.04	0.98	1.09	764,401.7
Airshed	1.11	1.05	1.17	764,378.8
Dependency	1.03	0.98	1.08	764,314.1
Adjusted by all socio-economic + contextual covariates*	1.13	1.06	1.21	764,157.5
Contextual covariates (Adjusted by socio-economic + behavioural covariates +)				
Ethnic concentration	1.05	1.00	1.10	756,050.7
Material deprivation	1.12	1.07	1.17	756,049.0
Census Metropolitan Area/Census Agglomeration size	1.05	0.99	1.10	756,039.5
Dependency	1.08	1.03	1.13	755,985.4
Airshed	1.11	1.05	1.17	755,969.1
Residential instability	1.08	1.03	1.13	755,962.9
Final model (Adjusted by all socio-economic + behavioural + contextual covariates)	1.11	1.04	1.18	755,760.2

[a]due to a 10 μg/m^3 increase in $PM_{2.5}$ concentration

between $PM_{2.5}$ and non-accidental mortality for all concentrations examined as indicated by the SCHIF hazard ratio predictions.

We assessed effect modification within the $PM_{2.5}$-mortality relationship by separating the cohort by age, sex, immigrant status (i.e. immigrants who had been in Canada for 10 or more years vs. non-immigrants), and educational attainment, and comparing resulting hazard ratios with Cochrane's Q (Table 4). The hazard ratio was 4% higher for males (1.13 95% CI 1.03–1.23) than females (1.09 95% CI 0.99–1.19). When contrasted by age, the hazard ratio was 9% lower for those aged 75 years or more (1.04 95% CI 0.94–1.16) compared to those aged 65–74 (1.13 95% CI 1.01–1.27) and 10% lower compared to those aged 65 or less (1.14 95% CI 1.01–1.29). The hazard ratio for non-immigrants was higher than that of the final model (1.14

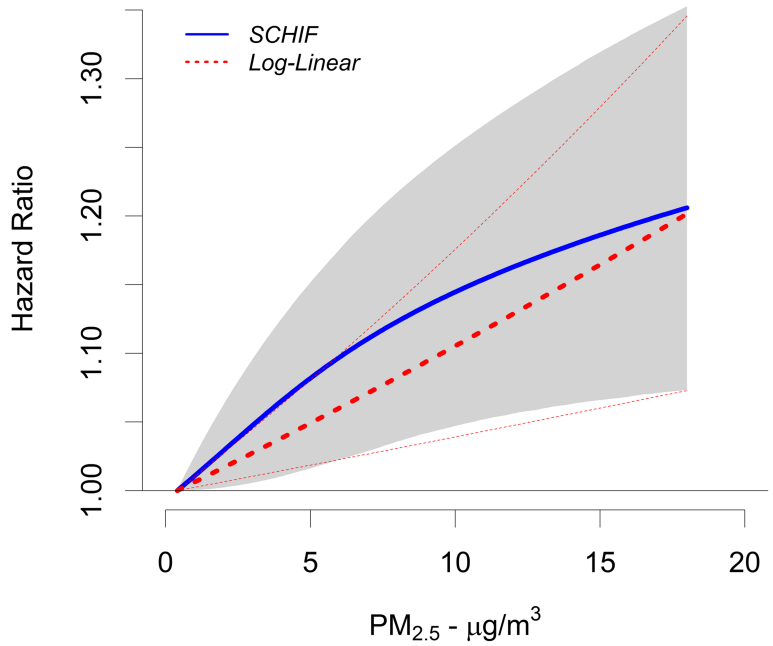

Fig. 2 SCHIF model of $PM_{2.5}$

95% CI 1.07–1.23) and the immigrant group had a null hazard ratio (0.98 95% CI 0.83–1.16). The hazard ratio for those without a high school diploma (1.08 95% CI 098–1.19) was lower than those who graduated from high school (1.14 95% CI 1.04–1.24). The Cochrane's Q *p*-values did not indicate that the above hazard ratios were significantly different between subgroups. We repeated the effect modification analyses for behavioural covariates. There was no significant difference between those who consumed fewer than five servings of fruits and vegetables per day compared to those who consumed five or more (1.10 95% CI 1.01–1.20 vs. 1.16 95% CI 1.04–1.30) although the hazard ratio was higher for those who consumed more fruits and vegetables. We found that hazard ratios were higher for regular drinkers (1.18 95% CI 1.09–1.28) and daily or occasional smokers (1.13 95% CI 0.99–1.27) compared to never or former drinkers (1.01 95% CI 0.90–1.12) or never or former smokers (1.11 95% CI 1.03–1.20), with a significant difference found between those who do and do not consume alcohol ($p < 0.05$). The HRs produced for each subgroup were pooled (Table 4), resulting in HRs that were similar to the full cohort final model. The high- and low- O_x groups had significantly different $PM_{2.5}$-mortality hazard ratios. The inclusion of other pollutants (O_3, NO_2, and O_X) attenuated the $PM_{2.5}$ hazard ratios and produced confidence intervals that include a null value, with the greatest reduction seen in the model that included $PM_{2.5}$, NO_2, and O_3 (1.00 95% CI 0.98–1.02, 1.03 95% CI 1.01–1.05, 1.05 95% CI 1.03–1.07 respectively) (Table 5).

Discussion

Using a cohort comprised of several cycles of a health survey with up to a 15-year follow-up period and high resolution exposure estimates, we found that exposure to $PM_{2.5}$ was associated with an 11% increase in non-accidental mortality per 10 µg/m^3 after extensive adjustment for socio-economic, behavioural, and contextual covariates.

The hazard ratio for the full cohort was similar to that of the Nurse's Health Study in the United States (1.13 95% CI 1.05–1.22) that adjusted for individual-level socio-economic and behavioural covariates [40] and a cohort from England (1.13 95% CI 1.00–1.25) that controlled for smoking, BMI, income, age, and sex [41]. Burnett and colleagues [42] report hazard ratio estimates for a 10 µg/m^3 change in long-term exposure to $PM_{2.5}$ and non-accidental mortality in 41 cohorts conducted globally, 36 of which included adjustment for behavioural risk factors. The pooled hazard ratio among these 36 cohorts was 1.09 (95% CI 1.05–1.12), a value similar to that observed in our current study (1.11 95% CI 1.04–1.18). A version of the 2001 CanCHEC census-based cohort produced a hazard ratio that is similar to this work (1.09 95% CI 1.07–1.11) [6].

The impact of individual-level behavioural risk factors on the $PM_{2.5}$-mortality association was assessed to address a common critique of many large administrative cohort studies examining the air pollution-mortality

Table 4 Examination of effect modification for non-accidental mortality[a] for the cohort through Cox proportional hazards models and Cochrane's Q

		95% CI	
	HR	Lower	Upper
Full cohort[b]	1.11	1.04	1.18
Sex			
Male	1.13	1.03	1.23
Female	1.09	0.99	1.19
Pooled HR	1.11	1.04	1.18
Age			
Under 65	1.14	1.01	1.29
65–74	1.13	1.01	1.27
75 or over	1.04	0.94	1.16
Pooled HR	1.10	1.03	1.17
Immigrant status			
Non-immigrants	1.14	1.07	1.23
Immigrants[b]	0.98	0.83	1.16
Pooled HR	1.12	1.05	1.19
Educational attainment			
No high school	1.08	0.98	1.19
High school graduate	1.14	1.04	1.24
Pooled HR	1.11	1.04	1.19
Fruit and vegetable consumption (servings per day)			
Less than five	1.10	1.01	1.20
Five or more	1.16	1.04	1.30
Pooled HR	1.12	1.05	1.20
Alcohol consumption			
Never or former drinker	1.01*	0.90	1.12
Occasional or regular drinker	1.18*	1.09	1.28
Pooled HR	1.12	1.05	1.19
Smoking behaviours			
Never or former smoker	1.11	1.03	1.20
Daily or occasional smoker	1.13	0.99	1.27
Pooled HR	1.12	1.05	1.19
Oxidant capacity[c]			
Low O_X	0.92*	0.81	1.04
High O_X	1.16*	1.07	1.26
Pooled HR	1.08	1.01	1.16

[a]due to a 10 μg/m^3 increase in $PM_{2.5}$ concentration
[b]excludes immigrants who have been living in Canada for fewer than ten years
[c]above or below the median value of Oxidant Capacity of all person-years (26.19 ppb)
*Cochrane's Q $p<0.05$

relationship. The inclusion of behavioural covariates to a model including socio-economic and ecological covariates lowered the $PM_{2.5}$ hazard ratio 2% (from 1.13 to 1.11). This modest change in the hazard ratio can be interpreted to indicate that the behavioural covariates were being adequately controlled for by the socio-economic and ecological covariates in the established relationship between $PM_{2.5}$ exposure and non-accidental mortality. This finding is similar to the previous CCHS cohort analysis and analysis of a Medicare-based cohort; both reported that adjustment for behavioural covariates had a minimal effect on hazard ratios [3, 7]. There is evidence (Tables 3 and 4) for a small increase in risk of $PM_{2.5}$-related mortality in occasional or regular drinkers but this may be masked by null effects from the inclusion of other behavioural covariates (fruit and vegetable consumption, smoking behaviours) and this confounding is likely the result of the spatial distribution of drinking behaviours, with binge drinkers having the largest mortality risk but lower $PM_{2.5}$ exposures. This study, through its inclusion of multiple covariates and an explicit a priori analysis approach for model building therefore provides the most extensive evidence to date that, in the Canadian context, missing data on behavioural risk factors for mortality have a minimal confounding bias on the $PM_{2.5}$-mortality association.

The increase in the $PM_{2.5}$ hazard ratio with the addition of the ecological covariates was largely driven by the addition of airsheds. Not only do these airsheds characterize broad air movement patterns, they also capture areas with similar composition of $PM_{2.5}$ (e.g., proportion of $PM_{2.5}$ composed of nitrate is highest in the Prairie airshed, whereas the Southern Atlantic airshed is composed of a notably higher proportion of black carbon) [34]. They also delineate general socio-cultural groups with distinct mortality risk factors beyond those captured by the typical socioeconomic census variables included in our survival models. The three airsheds with the largest hazard ratios, along with high material deprivation, all have the lowest levels of air pollutants which would account for the negative confounding effect observed in Table 3. Further, the largest airshed (East Central) contains both Toronto and Montreal, the two largest CMAs in Canada and significant population hubs. High $PM_{2.5}$ exposure and related mortality are largely driven by the population of Toronto (21% of the national population in 2006) where the mean $PM_{2.5}$ exposure is 9.33 μg/m^3 whereas the mean in the rest of the country is 7.68 μg/m^3 [43]. These results are consistent with a descriptive analysis of $PM_{2.5}$ exposure in 2006 long-form census respondents [9]. Although urban areas are the most common residence for both high income and highly educated Canadians, rural residences are more common among the high income earners than university graduates (i.e within the highest income quintile, 73.7% urban vs 26.3% urban fringe or rural; among those who are university educated, 82.6% urban vs. 17.3% urban fringe or rural). The greater

Table 5 Cox proportional hazard ratios for non-accidental mortality[a] and $PM_{2.5}$ NO_2, O_3, and O_X, and multiple-pollutant models

			95% CI				
	Pollutant	HR	Lower	Upper	-2 LL	SBC	AIC
$PM_{2.5}$	$PM_{2.5}$	1.03	1.01	1.05	755,760.2	756,453.5	755,888.2
O_3	O_3	1.05	1.03	1.07	755,742.1	756,435.4	755,870.1
NO_2	NO_2	1.03	1.02	1.05	755,756.9	756,450.3	755,884.9
O_X [b]	O_X	1.06	1.04	1.09	755,734.0	756,427.3	755,862.0
$PM_{2.5}$ and O_3	$PM_{2.5}$	1.01	1.00	1.03			
	O_3	1.05	1.03	1.07	755,740.0	756,444.2	755,870.0
$PM_{2.5}$ and NO_2	$PM_{2.5}$	1.02	1.00	1.04			
	NO_2	1.03	1.01	1.05	755,753.4	756,457.6	755,883.4
$PM_{2.5}$ and O_X [b]	$PM_{2.5}$	1.01	0.99	1.03			
	O_X	1.06	1.04	1.09	755,733.7	756,437.9	755,863.7
$PM_{2.5}$, O_3 and NO_2	$PM_{2.5}$	1.00	0.98	1.02			
	O_3	1.05	1.03	1.07			
	NO_2	1.03	1.01	1.05	755,732.5	756,447.5	755,864.5

[a]hazard ratios are per increase in inter-quartile range: $PM_{2.5}$ 2.80 μg/m^3, O_3 10.20 ppb, NO_2 6.63 ppb, O_X 8.05 ppb
[b]the combined oxidant capacity of NO_2 and O_3

tendency for high-income Canadians to live in rural areas is consistent with the findings in this paper. As a result, $PM_{2.5}$ exposure by income categories is a slightly more linear pattern than education in both of these studies.

We estimated the shape of the concentration-response (CR) function for the $PM_{2.5}$-mortality association. A slight supra-linear association (Fig. 2) was found, with a steep CR function at the low to median $PM_{2.5}$ range which levelled off slightly after approximately 10 μg/m^3. The SCHIF hazard ratio predictions indicated a positive and significant association between $PM_{2.5}$ and non-accidental mortality for all concentrations, suggesting risks to concentrations below 2 μg/m^3. Previous work using a CCHS-based cohort used a spline-based procedure and found that the shape of the relationship between non-accidental mortality and $PM_{2.5}$ was supra-linear in shape with a threshold of 4.5 μg/m^3, but was limited due to wide confidence intervals [9]. A study in China using a SCHIF function found non-linear relationships for multiple causes of death [44]. Such a relationship, when applied in a health impact framework, as in the Global Burden of Disease [45, 46] and in the recent Global Exposure Mortality Model [42] suggest benefits both from reducing $PM_{2.5}$ concentrations areas with the highest concentrations and from continuing to reduce them in relatively cleaner areas, including Canada, where it is estimated that the entire population now lives in areas with ambient $PM_{2.5}$ concentrations below the current WHO Guideline [47]. Worldwide it is estimated that small absolute reductions under 3 μg/m^3 could prevent hundreds of thousands of deaths in areas that comparatively have low levels of $PM_{2.5}$ [48].

The risk of non-accidental mortality from exposure to $PM_{2.5}$ was 4% higher in males over females (males 1.13, females 1.09), a pattern that has emerged in similar work. The hazard ratios from the current study are more aligned with the ESCAPE European pooled cohort (males 1.14 95% CI 1.04–1.24; females 0.99 95% CI 0.92–1.07) [2] albeit with a higher hazard ratio for women when compared to the previous version of CCHS-based cohort (males 1.34 95% CI 1.24–1.46; females 1.18 95% CI 1.09–1.28) [9]. Hazard ratios were lowest for members of the cohort aged 75 and older (1.04) and were similar for those aged 65 and under (1.14) and 65 to 75 (1.13); this is similar to the European study which found that risk decreases with age (< 60 years 1.16 95% CI 1.00–1.34; 60–75 years 1.10 95% CI 1.00–1.20; ≥75 years 1.03 95% CI 0.95–1.11). When we divided the cohort into immigrants (in Canada for 10 years or more) and non-immigrants, the $PM_{2.5}$-mortality association increased for non-immigrants and was null among the immigrant population. This result is consistent with prior Canadian census-based cohort studies [5] and is possibly the result of what is termed the "healthy immigrant effect" [49–53], likely intensified by the preferential settlement of immigrants into the largest cities which have higher $PM_{2.5}$ exposure. The hazard ratio for high school graduates (1.14) was higher than for those without a diploma (1.08) which is to be expected given that the latter is more likely to live in rural areas [43], and have a mean $PM_{2.5}$ exposure that is lower than other educational groups (Table 1) [43]. We examined effect modification by behavioural covariates (i.e., fruit and vegetable consumption, smoking behaviour, and alcohol consumption) and found significant difference in the resulting hazard ratios only in the case of alcohol consumption. Effect modification analyses on the

ESCAPE cohort also found no effect modification by fruit and vegetable consumption or smoking behaviour, but did not consider alcohol consumption [2].

The multiple pollutant models indicated that the relationship between non-accidental mortality and $PM_{2.5}$ exposure are attenuated when we included other pollutants (NO_2, O_3, and O_X) in the models. These findings indicate both that $PM_{2.5}$ is associated with mortality and that the inclusion of gaseous co-pollutants, O_x in particular, may better characterize the biologically active aspects of $PM_{2.5}$ and the overall air pollution mixture compared to the $PM_{2.5}$ mass concentration [5]. Weichenthal et al. looked at the effect modification of oxidant gases on $PM_{2.5}$ more specifically and found that spatial variations in O_x concentrations may act as surrogates for the presence or absence of harmful air pollutant mixtures that enhance $PM_{2.5}$ toxicity [42]. We examined the $PM_{2.5}$-mortality association in both low- and high- O_x person-years and found a 24% difference in risk. Our findings support these previous studies using different longitudinal Canadian cohorts and that knowledge of interactions between $PM_{2.5}$ and oxidant gases leading to adverse health will improve risk management activities and public health.

We performed this analysis on an extended and updated version of a cohort described in a previous study by Pinault et al. [9] with improvements to the exposure assessment and linkage to death, postal code history, environmental exposures, and contextual covariates. While some of the results are comparable to the previous cohort (e.g. socio-economic + behavioural covariate models are within a 1% margin), there are differences in the covariates included in the final models and the resulting hazard ratios. This is not unexpected since the contextual covariates addressing area-level marginalization in the two studies were created differently (area-level proportions of specific variables vs. a principle component analysis which resulted in four factors), and measured at different geographical units (census divisions vs. census tracts and census subdivisions). Another difference is that the updated cohort and current work includes immigrants who have lived in Canada for ten or more years whereas the previous work only included those who had been in Canada for 20 or more years. This newly included group of semi-recent immigrants (10–19 years in Canada) have substantially lower hazard ratios of mortality compared to the non-immigrant population (Table 1). Their inclusion in the current study acts to reduce the overall $PM_{2.5}$ hazard ratio (Table 4).

This large, national cohort is an extension and improvement to the previous CCHS-Mortality cohort, with an updated linkage and extended follow-up period for mortality and postal code history which now spans 36 years (1981 to 2016). More broadly the cohort has many strengths, including the fine resolution of the $PM_{2.5}$ estimates ($1km^2$), the ability to incorporate mobility across the follow-up years, an explicit a priori model building strategy, the inclusion of multiple time-varying contextual covariates to address spatial, neighbourhood- and city-level characteristics, and most uniquely the behavioural covariates such as smoking behaviours, alcohol consumption, diet, and exercise to control for health behaviours related to mortality that are not typically found on cohorts of this size.

This cohort and the analysis are limited by the data available. First, postal code history was derived from tax and administrative data. Historical postal codes reflect the mailing address as reported on a tax return and not necessarily a person's residence; in 92.9% of cases the postal code reflects the person's residence at time of survey [23]. Similarly, outdoor ambient levels of $PM_{2.5}$ at a person's residence may not reflect their actual exposure. Sensitivity analysis performed with the 2001 CanCHEC found that finer scale resolution ($1km^2$) estimates of $PM_{2.5}$ resulted in lower AIC values and higher hazard ratios in the $PM_{2.5}$-mortality model for non-accidental death compared to a $10km^2$ or $5km^2$ grid indicating that exposure estimates that are more specific to a person's residence are appropriate [54]. Gaps in postal code history are imputed under the assumption that the person did not leave the country or community during that time. In assigning contextual covariates by postal code, misclassification may occur from taking the mode or mean when estimating a single value to represent multiple points of latitude and longitude for a single postal code. Second, in contrast to the CanCHEC cohorts (Pappin AJ, Crouse DL, Christidis T, Pinault LL, Tjepkema M, Erickson A, Brauer M, Weichenthal S, van Donkelaar A, Martin RV, Brook J, Hystad P. Burnett RT. Associations between low levels of fine particulate matter andmortality within Canadian cohorts. Environ Health Persp., under review), this cohort does not completely represent the full Canadian population; the Canadian Community Health Survey is not a census of the population and survey weights were not used in this analysis. Further, in creating this cohort persons were removed if they did not consent to data linkage or if they could not be linked to the SDLE. The CCHS over-samples rural communities [55] which results in a disproportionate sample in areas with low levels of $PM_{2.5}$ and higher rates of mortality. The sampling framework and un-weighted analysis likely caused the null unadjusted hazard ratio which became positive as covariates were added to the model to address confounding. These results are consistent with the Agricultural Health study which examined non-accidental death related to $PM_{2.5}$ in rural communities in two American states (Iowa and North Carolina) and found a protective hazard ratio in minimally and

fully adjusted models [56]. Regardless, the protective unadjusted hazard ratio should not come as a surprise as contextual and socio-economic covariates are included in models because we know that they are related to both $PM_{2.5}$ and mortality and can act as confounders (see Table 1 for the mortality Hazard Ratios by individual covariates). Given that these factors covary with both mortality and $PM_{2.5}$ their inclusion in the models is crucial. We suggest that the unadjusted model is not reflective of the $PM_{2.5}$-mortality relationship and that the direction or magnitude should not be over-interpreted. Third, although this cohort includes behavioural covariates these are self-reported and in some cases there are missing responses. To avoid introducing bias into the cohort, we used dummy variables to code missing information rather than excluding non-respondents outright. Finally, the cohort itself is limited by follow-up and some persons have as few as 4 years of follow-up (with a maximum follow-up of 15 years).

Conclusions

We provided an update to the Canadian Community Health Survey-Mortality cohort, with a new linkage of the survey respondents to death records, inclusion of additional survey cycles, an extension of the annual residential history and mortality follow-up period, a finer scale of air pollution exposure, time-varying contextual covariates, and the inclusion of immigrants who have lived in Canada for 10–20 years (rather than only those who have been in Canada for 20+ years). The risk of non-accidental mortality from ambient $PM_{2.5}$ was found even at low levels although the hazard ratio was attenuated in models that included other pollutants (NO_2, O_3, and O_X). The $PM_{2.5}$-mortality association displayed a supra-linear concentration-response curve. The inclusion of behavioural covariates that could confound the $PM_{2.5}$-mortality association (fruit and vegetable consumption, leisure exercise frequency, alcohol consumption, and smoking behaviours) did not appear to impact hazard ratios. Hazard ratios were higher for males, those aged 65 or less, and non-immigrants.

Abbreviations

-2LL: (− 2) Log likelihood; AIC: Akaike information criterion; AOD: Aerosol optical depth; AQMS: Air quality management system; BMI: Body mass index; CA: Census agglomeration; CanCHEC: Canadian Census Health and Environment Cohort; Can-MARG: Canadian Marginalization Index; CCHS: Canadian Community Health Survey; CI: Confidence interval; CMA: Census Metropolitan Area; CR: Concentration-response; EPA: Environmental Protection Agency; HEI: Health Effects Institute; HR: Hazard ratio; ICD: International Classification of Diseases; NAPS: National Air Pollution Surveillance; O_X: Oxidant capacity; $PM_{2.5}$: Fine particle matter; ppb: Parts per billion; S.D.: Standard deviation; SBC: Schwarz Bayesian Criterion; SCHIF: Shape constrained health impact function; SDLE: Social data linkage environment

Acknowledgements

The authors would like to acknowledge the contribution of Hong Chen for his code to run the SCHIF and the Canadian Urban Environmental Health Research Consortium (CANUE) for supplying an ozone-postal code linked file.

Authors' contributions

TC linked the cohort and created the analytical file, conducted the analyses, and drafted the manuscript. AE led the establishment of the paper, provided support for covariate standardization and preparation, and writing of the introduction and discussion. AP created the postal code-exposure file and provided code that was used in analysis. LP provided support for covariate standardization and preparation and helped with conception of the analysis. DLC and SW participated in study design, provided feedback on analysis and the manuscript. JB, RVM, AVD, and PH provided air pollution models and guidance for use of these data in epidemiologic research. MT participated in the cohort linkage and study design, provided feedback on analysis and the manuscript. RTB participated in study design and statistics analysis, produced Fig. 2, and provided feedback on the analysis. MB led the conception of the paper and provided comments throughout the process on analysis and the manuscript. All authors read and approved the final manuscript.

Funding

Research described in this article was conducted under contract to the Health Effects Institute (HEI), an organization jointly funded by the United States Environmental Protection Agency (EPA; Assistance Award No. R-82811201) and certain motor vehicle and engine manufacturers. The contents of this article do not necessarily reflect the views of HEI, or its sponsors, nor do they necessarily reflect the views and policies of the EPA or motor vehicle and engine manufacturers.

Availability of data and materials

The datasets generated and analysed in this study are not publicly available due to privacy and confidentiality standards stated in the Statistics Act.

Ethics approval and consent to participate

Canadian Community Health Survey respondents who agreed to linkage of their survey responses with administrative and tax data were eligible. The linkage (007–2018) was approved by Statistics Canada's senior management (https://www.statcan.gc.ca/eng/record/2018) and is governed by the Directive on Microdata Linkage (https://www.statcan.gc.ca/eng/record/policy4–1).

Consent for publication

Not applicable.

Competing interests

The authors declare no competing interests.

Author details

[1]Health Analysis Division, Statistics Canada, 100 Tunney's Pasture Driveway, Ottawa, Ontario K1A 0T6, Canada. [2]School of Population and Public Health, The University of British Columbia, 2206 East Mall, Vancouver, British Columbia V6T 1Z3, Canada. [3]Department of Sociology, University of New Brunswick, PO Box 4400, Fredericton, New Brunswick E3B 5A3, Canada. [4]Department of Epidemiology, Biostatistics & Occupational Health, McGill University, 1110 Pine Ave West, Montreal, Quebec H3A 1A3, Canada. [5]Air Health Science Division, Health Canada, 269 Laurier Avenue West, Ottawa, Ontario K1A 0K0, Canada. [6]Dalla Lana School of Public Health, University of Toronto, 155 College Street, Toronto, Ontario M5T 1P8, Canada. [7]Department of Physics and Atmospheric Science, Dalhousie University, 6310 Coburg Road, PO Box 15000, Halifax, NS B3H 4R2, Canada. [8]College of Public Health and Human Sciences, Oregon State University, 2520 SW Campus Way, Corvallis, Oregon 97331, USA. [9]Harvard-Smithsonian Center for Astrophysics, 60 Garden St, Cambridge, MA 02138, USA. [10]Population Studies Division, Health Canada, 50 Columbine Driveway, Ottawa, Ontario K1A 0K9, Canada. [11]Department of Energy, Environmental & Chemical Engineering, Washington University in St. Louis, St. Louis, Missouri 63130, USA. [12]Department of Chemical Engineering and Applied Chemistry, University of Toronto, 223 College St., Toronto, ON M5T 1R4, Canada. [13]Safe Environments Directorate, Health Canada, 269 Laurier Avenue West, Ottawa, Ontario K1A 0K9, Canada.

Received: 14 February 2019 Accepted: 13 August 2019
Published online: 10 October 2019

References

1. GBD 2017 Risk Factor Collaborators. Global, regional, and national comparative risk assessment of 84 behavioural, environmental and occupational, and metabolic risks or clusters of risks for 195 countries and territories, 1990–2017: a systematic analysis for the Global Burden of Disease Study 2017. Lancet. 2018;392:1923–94.
2. Beelen R, Raaschou-Nielsen O, Stafoggia M, Andersen ZJ, Weinmayr G, Hoffmann B, Wolf K, Samoli E, Fischer P, Nieuwenhuijsen M. Effects of long-term exposure to air pollution on natural-cause mortality: an analysis of 22 European cohorts within the multicentre ESCAPE project. Lancet. 2014;383:785–95.
3. Di Q, Wang Y, Zanobetti A, Wang Y, Koutrakis P, Choirat C, Dominici F, Schwartz JD. Air pollution and mortality in the Medicare population. N Engl J Med. 2017;376:2513–22.
4. Pope CA III, Burnett RT, Thun MJ, Calle EE, Krewski D, Ito K, Thurston GD. Lung cancer, cardiopulmonary mortality, and long-term exposure to fine particulate air pollution. JAMA. 2002;287:1132–41.
5. Crouse DL, Peters PA, Hystad P, Brook JR, van Donkelaar A, Martin RV, Villeneuve PJ, Jerrett M, Goldberg MS, Pope CA III, Brauer M, Brook RD, Robichaud A, Menard R, Burnett RT. Ambient PM2.5, O3, and N2 exposures and associations with mortality over 16 years of follow-up in the Canadian census health and environment cohort (CanCHEC). Environ Health Persp. 2015;123:1180–6.
6. Pinault LL, Weichenthal S, Crouse DL, Brauer M, Erickson A, van Donkelaar A, Martin RV, Hystad P, Chen H, Finès P. Associations between fine particulate matter and mortality in the 2001 Canadian census health and environment cohort. Environ Res. 2017;159:406–15.
7. Erickson A, Brauer M, Christidis T, Pinault L, Crouse D, Donkelaar A, Weichenthal S, Pappin A, Tjepkema M, Martin R, Brook J, Hystad P, Burnett R. Evaluation of a method to indirectly adjust for unmeasured covariates in the association between fine particulate matter and mortality. Environ Res. 2019;175:108–116.
8. Shin HH, Cakmak S, Brion O, Villeneuve P, Turner MC, Goldberg MS, Jerrett M, Chen H, Crouse D, Peters P, Pope CA III. Indirect adjustment for multiple missing variables applicable to environmental epidemiology. Environ Res. 2014;134:482–7.
9. Pinault L, Tjepkema M, Crouse DL, Weichenthal S, van Donkelaar A, Martin RV, Brauer M, Chen H, Burnett RT. Risk estimates of mortality attributed to low concentrations of ambient fine particulate matter in the Canadian Community Health Survey cohort. Environ Health. 2016;15:1–15.
10. Nasari MM, Szyszkowicz M, Chen H, Crouse D, Turner MC, Jerrett M, Pope CA III, Hubbell B, Fann N, Cohen A. A class of non-linear exposure-response models suitable for health impact assessment applicable to large cohort studies of ambient air pollution. Air Qual Atmos Hlth. 2016;9:961–72.
11. Statistics Canada. Canadian Community Health Survey: Detailed information for 2001 (Cycle 1.1). 2007. http://www23.statcan.gc.ca/imdb/p2SV.pl?Function=getSurvey&Id=3359. Accessed 28 Jan 2019.
12. Statistics Canada. Canadian Community Health Survey (CCHS): Detailed information for 2003 (Cycle 2.1). 2007. http://www23.statcan.gc.ca/imdb/p2SV.pl?Function=getSurvey&Id=4995. Accessed 28 Jan 2019.
13. Statistics Canada. Canadian Community Health Survey (CCHS): Detailed information for 2005 (Cycle 3.1). 2007. http://www23.statcan.gc.ca/imdb/p2SV.pl?Function=getSurvey&Id=22642. Accessed 28 Jan 2019.
14. Statistics Canada. Canadian Community Health Survey (CCHS): Detailed information for 2007 (Cycle 4.1). 2008. http://www23.statcan.gc.ca/imdb/p2SV.pl?Function=getSurvey&Id=29539. Accessed 28 Jan 2019.
15. Statistics Canada. Canadian Community Health Survey (CCHS): detailed information for 2010. 2014. http://www23.statcan.gc.ca/imdb/p2SV.pl?Function=getSurvey&Id=81424. Accessed 28 Jan 2019.
16. Statistics Canada. Canadian Community Health Survey (CCHS): detailed information for 2012. 2012. http://www23.statcan.gc.ca/imdb/p2SV.pl?Function=getSurvey&Id=135927. Accessed 28 Jan 2019.
17. Statistics Canada. Social data linkage environment (SDLE). 2017. https://www.statcan.gc.ca/eng/sdle/index. Accessed 28 Jan 2019. Accessed 28 Jan 2019.
18. Statistics Canada. Linkage of the Canadian Community Health Survey (CCHS) to mortality, Cancer, hospital administrative files, and tax data (007–2018). 2019. https://www.statcan.gc.ca/eng/record/2018. Accessed 8 Feb 2019.
19. Statistics Canada. Directive on Microdata Linkage. 2017. https://www.statcan.gc.ca/eng/record/policy4–1. Accessed 8 Feb 2019.
20. Fellegi IP, Sunter AB. A theory for record linkage. J Am Stat Assoc. 1969;64:1183–210.
21. St-Jean H. SDLE production section. Social data linkage environment (SDLE) methodology report: linkage between the Canadian mortality database (CMDB 2015–16) and the SDLE derived record depository (version 18). Statistics Canada: Ottawa; 2018.
22. Judd P. SDLE production section. Social data linkage environment (SDLE) methodology report: external linkage between the Canadian Community Health Survey (2001 to 2014) and the SDLE derived record depository (version 5). Statistics Canada: Ottawa; 2017.
23. Bérard-Chagnon J. Comparison of Place of Residence between the T1 Family File and the Census: Evaluation using record linkage. Ottawa: Statistics Canada; 2017. Catalogue no. 91F0015M — No.13
24. Finès P, Pinault L, Tjepkema M. Imputing postal codes to analyze ecological variables in longitudinal cohorts: exposure to particulate matter in the Canadian Census Health and Environment Cohort Database. Ottawa: Statistics Canada; 2017. Catalogue no. 11–633-X — No. 006
25. Statistics Canada. Postal Code^{OM} Conversion File (PCCF). Ottawa: Statistics Canada; 2017. Catalogue no. 92–154-X
26. Statistics Canada. Postal Code^{OM} Conversion File (PCCF) Reference Guide August 2015. Ottawa: Statistics Canada; 2016. Catalogue no. 92–154-G
27. Statistics Canada. Postal Code^{OM} Conversion File (PCCF) November 2014. Ottawa: Statistics Canada; 2015. Catalogue no. 92–154-G
28. van Donkelaar A, Martin RV, Spurr RJ, Burnett RT. High-resolution satellite-derived PM2. 5 from optimal estimation and geographically weighted regression over North America. Environ Sci Technol. 2015;49:10482–91.
29. Meng J, Li C, Martin RV, van Donkelaar A, Hystad P, Brauer M. Estimated long-term (1981–2016) concentrations of ambient fine particulate matter across North America from chemical transport modeling, satellite remote sensing and ground-based measurements. Environ Sci Technol. 2019;53:5071–9.
30. Robichaud A, Ménard R, Zaïtseva Y, Anselmo D. Multi-pollutant surface objective analyses and mapping of air quality health index over North America. Air Qual Atmos Hlth. 2016;9:743–59.
31. Robichaud A, Ménard R. Multi-year objective analyses of warm season ground-level ozone and PM2.5 over North America using real-time observations and Canadian operational air quality models. Atmos Chem Phys. 2014;14:1769–800.
32. Environment and Climate Change Canada. CHRONOS_Ground-Level_O3_NA_2002.nc to CHRONOS_Ground-Level_O3_NA_2009.nc inclusive. Toronto: Air Quality Research Division; 2017. [generated July 2017]
33. Hystad P, Setton E, Cervantes A, Poplawski K, Deschenes S, Brauer M, van Donkelaar A, Lamsal L, Martin R, Jerrett M, Demers P. Creating national air pollution models for population exposure assessment in Canada. Environ Health Persp. 2011;119:1123–9.
34. Crouse DL, Philip S, Van Donkelaar A, Martin RV, Jessiman B, Peters PA, Weichenthal S, Brook JR, Hubbell B, Burnett RT. A new method to jointly estimate the mortality risk of long-term exposure to fine particulate matter and its components. Sci Rep. 2016;6:18916.
35. Statistics Canada. Illustrated Glossary. Ottawa: Statistics Canada; 2017. Catalogue no. 92–195-X
36. Gordon DL, Janzen M. Suburban nation? Estimating the size of Canada's suburban population. J Archit Plan Res. 2013;30:197–220.
37. Matheson FI, Dunn JR, Smith KL, Moineddin R, Glazier RH. Development of the Canadian marginalization index: a new tool for the study of inequality. C J Public Health. 2012;103(Suppl 2):12–6.
38. Bratsch SG. Standard electrode potentials and temperature coefficients in water at 298.15 K. J Phys Chem Ref Data. 1989;18:1–21.
39. Weichenthal S, Pinault LL, Burnett RT. Impact of oxidant gases on the relationship between outdoor fine particulate air pollution and nonaccidental, cardiovascular, and respiratory mortality. Sci Rep. 2017;7:16401.
40. Hart JE, Liao X, Hong B, Puett RC, Yanosky JD, Suh H, Kioumourtzoglou MA, Spiegelman D, Laden F. The association of long-term exposure to PM 2.5 on all-cause mortality in the nurses' health study and the impact of measurement-error correction. Environ Health. 2015;14:38.
41. Carey IM, Atkinson RW, Kent AJ, Van Staa T, Cook DG, Anderson HR. Mortality associations with long-term exposure to outdoor air pollution in a national English cohort. Am J Resp Crit Care. 2013;187:1226–33.
42. Burnett R, Chen H, Szyszkowicz M, Fann N, Hubbell B, Pope CA III, Apte JS, Brauer M, Cohen A, Weichenthal S, Coggins J. Global estimates of mortality

associated with long-term exposure to outdoor fine particulate matter. Proc Natl Acad Sci U S A. 2018;115:9592–7.
43. Pinault L, van Donkelaar A, Martin RV. Exposure to fine particulate matter air pollution in Canada. Health Rep. 2017;28:9.
44. Yin P, Brauer M, Cohen A, Burnett RT, Liu J, Liu Y, Liang R, Wang W, Qi J, Wang L, Zhou M. Long-term fine particulate matter exposure and nonaccidental and cause-specific mortality in a large national cohort of Chinese men. Environ Health Persp. 2017;125:117002.
45. Burnett RT, Pope CA III, Ezzati M, Olives C, Lim SS, Mehta S, Shin HH, Singh G, Hubbell B, Brauer M, Anderson HR. An integrated risk function for estimating the global burden of disease attributable to ambient fine particulate matter exposure. Environ Health Persp. 2014;122:397–403.
46. Cohen AJ, Brauer M, Burnett R, Anderson HR, Frostad J, Estep K, Balakrishnan K, Brunekreef B, Dandona L, Dandona R, Feigin V. Estimates and 25-year trends of the global burden of disease attributable to ambient air pollution: an analysis of data from the global burden of diseases study 2015. Lancet. 2017;389:1907–18.
47. Brauer M. PM2.5 air pollution, population exposed to levels exceeding WHO guideline value (% of total) for the Global Burden of Disease Study 2017 https://data.worldbank.org/indicator/EN.ATM.PM25.MC.ZS?end=2017&locations=CA&start=1990&view=chart. Accessed 24 May 2019.
48. Apte JS, Marshall JD, Cohen AJ, Brauer M. Addressing global mortality from ambient PM2. 5. Environ Sci Technol. 2015;49:8057–66.
49. Beiser M. The health of immigrants and refugees in Canada. C J Public Health. 2005;96(Suppl 2):30–44.
50. Ng E. The healthy immigrant effect and mortality rates. Health Rep. 2011;22:1–5.
51. Vang ZM, Sigouin J, Flenon A, Gagnon A. Are immigrants healthier than native-born Canadians? A systematic review of the healthy immigrant effect in Canada. Ethn Health. 2017;22:209–17.
52. Trovato F, Newbold KB. Understanding the healthy immigrant effect: evidence from Canada. In: Trovato F, editor. Migration, health and survival: international perspectives. Cheltenham: Edward Elgar Publishing Ltd; 2017. p. 15–30.
53. Omariba DW, Ross NA, Sanmartin C, Tu JV. Neighbourhood immigrant concentration and hospitalization: a multilevel analysis of cardiovascular-related admissions in Ontario using linked data. C J Public Health. 2014; 105:404–11.
54. Crouse DL, Christidis T, Erickson A, Pinault L, Martin RV, Tjepkema M, Hystad P, Pappin AJ, Burnett RT, Brauer M, Weichenthal S. Evaluating the Sensitivity of PM2.5-Mortality Associations to the Spatial and Temporal Scale of Exposure Assessment at Low Particle Mass Concentrations. Epidemiology. Accepted.
55. Statistics Canada. Canadian Community Health Survey (CCHS): Annual component User guide 2010 and 2009-2010 Microdata files. http://www23.statcan.gc.ca/imdb-bmdi/pub/document/3226_D7_T9_V8-eng.pdf. Accessed 23 May 2019.
56. Weichenthal S, Villeneuve PJ, Burnett RT, van Donkelaar A, Martin RV, Jones RR, DellaValle CT, Sandler DP, Ward MH, Hoppin JA. Long-term exposure to fine particulate matter: association with nonaccidental and cardiovascular mortality in the agricultural health study cohort. Environ Health Persp. 2014; 122:609–15.

Publisher's Note

Environmental Research 175 (2019) 108–116

Contents lists available at ScienceDirect

Environmental Research

journal homepage: www.elsevier.com/locate/envres

Evaluation of a method to indirectly adjust for unmeasured covariates in the association between fine particulate matter and mortality

Anders C. Erickson[a], Michael Brauer[a,*], Tanya Christidis[b], Lauren Pinault[b], Daniel L. Crouse[c], Aaron van Donkelaar[d], Scott Weichenthal[e], Amanda Pappin[b], Michael Tjepkema[b], Randall V. Martin[d], Jeffrey R. Brook[f], Perry Hystad[g], Richard T. Burnett[h]

[a] The University of British Columbia, Vancouver, British Columbia, Canada
[b] Health Analysis Division, Statistics Canada, Ottawa, Ontario, Canada
[c] University of New Brunswick, Fredericton, New Brunswick, Canada
[d] Department of Physics and Atmospheric Science, Dalhousie University, Halifax, NS, Canada
[e] McGill University, Montreal, Quebec, Canada
[f] University of Toronto, Toronto, ON, Canada
[g] Oregon State University, Corvallis, OR, USA
[h] Health Canada, Ottawa, Ontario, Canada

ARTICLE INFO

Keywords:
Air pollution
Indirect adjustment
Confounding
Survival analysis
Cohort study

ABSTRACT

Background: Indirect adjustment via partitioned regression is a promising technique to control for unmeasured confounding in large epidemiological studies. The method uses a representative ancillary dataset to estimate the association between variables missing in a primary dataset with the complete set of variables of the ancillary dataset to produce an adjusted risk estimate for the variable in question. The objective of this paper is threefold: 1) evaluate the method for non-linear survival models, 2) formalize an empirical process to evaluate the suitability of the required ancillary matching dataset, and 3) test modifications to the method to incorporate time-varying exposure data, and proportional weighting of datasets.

Methods: We used the association between fine particle air pollution ($PM_{2.5}$) with mortality in the 2001 Canadian Census Health and Environment Cohort (CanCHEC, N = 2.4 million, 10-years follow-up) as our primary dataset, and the 2001 cycle of the Canadian Community Health Survey (CCHS, N = 80,630) as the ancillary matching dataset that contained confounding risk factor information not available in CanCHEC (e.g., smoking). The main evaluation process used a gold-standard approach wherein two variables (education and income) available in both datasets were excluded, indirectly adjusted for, and compared to true models with education and income included to assess the amount of bias correction. An internal validation for objective 1 used only CanCHEC data, whereas an external validation for objective 2 replaced CanCHEC with the CCHS. The two proposed modifications were applied as part of the validation tests, as well as in a final indirect adjustment of four missing risk factor variables (smoking, alcohol use, diet, and exercise) in which adjustment direction and magnitude was compared to models using an equivalent longitudinal cohort with direct adjustment for the same variables.

Results: At baseline (2001) both cohorts had very similar $PM_{2.5}$ distributions across population characteristics, although levels for CCHS participants were consistently 1.8–2.0 $\mu g/m^3$ lower. Applying sample-weighting largely corrected for this discrepancy. The internal validation tests showed minimal downward bias in $PM_{2.5}$ mortality hazard ratios of 0.4–0.6% using a static exposure, and 1.7–3% when a time-varying exposure was used. The external validation of the CCHS as the ancillary dataset showed slight upward bias of −0.7 to −1.1% and downward bias of 1.3–2.3% using the static and time-varying approaches respectively.

Conclusions: The CCHS was found to be fairly well representative of CanCHEC and its use in Canada for indirect adjustment is warranted. Indirect adjustment methods can be used with survival models to correct hazard ratio point estimates and standard errors in models missing key covariates when a representative matching dataset is available. The results of this formal evaluation should encourage other cohorts to assess the suitability of ancillary datasets for the application of the indirect adjustment methodology to address potential residual confounding.

* Corresponding author. The University of British Columbia, 2206 East Mall, Vancouver, BC V6T 1Z3, Canada.
E-mail address: michael.brauer@ubc.ca (M. Brauer).

https://doi.org/10.1016/j.envres.2019.05.010
Received 19 December 2018; Received in revised form 9 April 2019; Accepted 9 May 2019
Available online 11 May 2019
0013-9351/

1. Introduction

The use of large administrative cohorts linked to national mortality registries and environmental exposure data have been important in establishing consistent population-based risk coefficients, such as estimating the air pollution mortality relationship in support of clean air policy (Cesaroni et al., 2013; Di et al., 2017; Pinault et al., 2017). While the large size of these national cohorts provides advantages, their lack of person-level risk factors such as smoking and body mass index (BMI) may bias risk estimates if these factors are correlated with both the exposure and outcome. Indirect adjustment for missing confounding has multiple configurations and incarnations (Gail et al., 1988; Richardson et al., 2014; Villeneuve et al., 2011). In environmental epidemiology, indirect adjustment techniques have included the use of person-level pre-existing comorbidities related to smoking (Cesaroni et al., 2013), adjusting for area-level risk factors (Chen et al., 2013), or area-level comorbidities as a proxy for common lifestyle risk factors (Fischer et al., 2015; Pope et al., 2009; Zeger et al., 2008). Recently Shin and colleagues (Shin et al., 2014) proposed a method based on partitioned regression which has since been applied to several environmental exposure cohort studies (Crouse et al., 2015b, 2015a; Weichenthal et al., 2016).

The Shin et al. (2014) method does not attempt to estimate the missing risk factors directly from ancillary data, but rather uses information contained within a representative ancillary dataset regarding the multivariate relationships between the observed covariates, the exposure, and the missing covariates to produce an adjustment factor which is then applied to the risk estimates from a model with the missing factors. The advantage of this method is that adjustment is at the individual-level and can accommodate multiple missing risk factors simultaneously. Simulation studies performed by Shin et al. (2014) indicated relative bias (HR_{crude}-$HR_{adjusted}/HR_{crude}$) of less than 20% under all realistic testing scenarios. Using a longitudinal cohort and indirectly adjusting for smoking and BMI, they reported a 3% increase in the association between fine particulate matter ($PM_{2.5}$) and ischemic heart disease (IHD) (Shin et al., 2014), compared with no adjustment for smoking and BMI. Other studies have reported both minor (< 1%) and moderate (10%) bias correction after indirect adjustment for smoking and other risk factors in air pollution-mortality analyses (Crouse et al., 2015b, 2015a; Strak et al., 2017; Villeneuve et al., 2013, 2012; Weichenthal et al., 2016).

An important aspect of the indirect adjustment method depends on the representativeness of the ancillary information to the main cohort. Ideally, the ancillary data would be drawn from the same target population as the main cohort and shown to be similar across important characteristics, such as age, sex, health status, and geographic coverage. Further, the method of quantification for matching variables available in both cohorts should be similar (e.g. equivalent group assignment between 'highest level of school' versus 'total years of schooling'). Shin et al. (2014) recommended three criteria to assess the suitability of ancillary health studies in representing the cohort: 1) consistency between the distribution of the primary exposure among subjects across characteristics (e.g. age, sex, marital status); 2) similar direction and magnitude in the correlation amongst the variables available; and 3) evaluation of the magnitude of bias correction for survival models by excluding and indirectly adjusting for specific variables available in both datasets and comparing to models including these variables (i.e. a type of "gold-standard" evaluation).

We applied the above recommendations to evaluate the methodology using non-linear Cox proportional hazard models for the relationship between $PM_{2.5}$ and mortality using 2001 Canadian Census Health and Environment Cohort (CanCHEC) as the primary data cohort and the Canadian Community Health Survey (CCHS) as the ancillary matching dataset. We further incorporated a time-varying exposure measure in the representative dataset and applied a weighting scheme to account for sampling differences between the two datasets as two novel additions. Finally, we applied an indirect adjustment using the CanCHEC and CCHS for missing risk factors (cigarettes/day, alcohol use, fruit and vegetable intake, leisure exercise) and compared adjustment direction and magnitude to models using a third equivalent longitudinal cohort that was not missing those variables (the CCHS-mortality linked cohort).

2. Materials and methods

2.1. Population and air pollution data

The primary dataset used was the 2001 CanCHEC, a longitudinal cohort of 3.5 million Canadian adult respondents to the mandatory 2001 Canadian long-form census (1 in 5 households) linked to the Canadian mortality database and annual income tax filings to obtain residential six-digit postal codes through 2011. Missing postal codes in the historical tax files were imputed based on those reported in adjacent years, using a method where the probability of imputation varies depending on the number of adjacent years missing (Fines et al., 2017). The linkage methodology and cohort description have been provided elsewhere (Pinault et al., 2016a,b; Pinault et al., 2017). Eligibility criteria included: persons between the ages of 25 and 89 years at baseline, Canadian-born, and complete person-year $PM_{2.5}$ estimates and covariate information, for a final baseline sample of 2,468,180 respondents. A total of 196,540 deaths were recorded during the 10 year follow-up period.

The ancillary matching dataset was the CCHS, a national, cross-sectional survey providing information about the health, behaviours, and health care use of the Canadian population aged 12 or older. For consistency with the 2001 CanCHEC, we limited the analysis to the 2001 CCHS (cycle 1.1) and applied the same eligibility criteria as above for a final cohort size of 80,630 respondents. The response rate for the 2001 CCHS was 85%. In contrast to the census long-form used for CanCHEC, the CCHS excludes residents living on reserves and other Aboriginal settlement areas, altogether less than 3% of the target population of Canada (Statistics Canada, 2007). Additional CCHS cycles (2003–2011) were pooled and assessed for sensitivity.

A third dataset used was the CCHS-mortality (mCCHS) longitudinal cohort that includes four pooled cycles of the CCHS linked to the Canadian Mortality Database (Sanmartin et al., 2016). CCHS respondents who gave permission to share and link their information with other administrative datasets at the time of the survey (86% agreement) and died between January 1, 2000 and December 31, 2011 were eligible for linkage. We limited the analytical dataset to the aforementioned eligibility criteria for a final cohort size of 642,000.

$PM_{2.5}$ estimates were derived from a national model that produced annual average estimates (1998–2012) at an approximately 1 km^2 grid (spatial correlation of model estimates with ground measurements: $R^2 = 0.82$, slope = 0.97, n = 1440) (van Donkelaar et al., 2015). These were assigned to individuals based on their residential 6-digit postal codes which were updated for each person-year of follow-up, incorporating annual residential mobility for the CanCHEC and mCCHS cohorts (CCHS survey data was cross-sectional). For consistency with our previous work, we employed a 3-year moving average with a 1-year lag. For example, exposure for 2001 equaled the mean of $PM_{2.5}$ for the years 1998, 1999, and 2000. Canadian six-digit postal codes have positional accuracy of 100–160 m in urban areas, but only about 1–5 km in rural areas (Khan et al., 2018). Postal codes were geocoded using Statistics Canada's Postal Code Conversion File Plus (PCCF + v7) (Statistics Canada, 2017), and used to also assign subjects to census geography units which in turn were used to ascribe time-varying ecological variables (described further below).

2.2. Design of indirect adjustment evaluation

A visual summary of the evaluation process is depicted Fig. 1. Step 1 was to assess the representativeness of the ancillary matching dataset (i.e., CCHS) to the primary dataset (i.e., CanCHEC). We compared absolute and proportional differences in the distribution of $PM_{2.5}$ exposure by demographic and socioeconomic characteristics at the 2001 baseline year. We further assessed temporal changes in the distribution of $PM_{2.5}$ across the 10 years of follow-up between the two datasets. To account for differences in the sampling scheme between the two datasets, sample weights were produced using Health Regions as the sampling unit and applied to the CCHS to emulate the proportions of the CanCHEC. Rural areas with lower $PM_{2.5}$ levels are typically over-sampled in the CCHS and were thus down-weighted, while under-sampled urban areas in the CCHS were up-weighted.

Step 2 was to perform an internal validation to assess the degree of bias in adjusted hazard ratios when applying indirect adjustment to non-linear Cox proportional hazards models. We employed a 'gold-standard' methodology which involved the removal and indirect adjustment for variables available in CanCHEC (education and income) and compared the result to a true model that included both variables and which used the internally derived coefficients and standard errors from the true model in the indirect adjustment formula. To accomplish this, three sets of models were estimated for each mortality outcome. First, the gold-standard hazard ratios and 95% confidence intervals (95% CI) for $PM_{2.5}$ on mortality were obtained from a "True Model" that was age-sex stratified and adjusted for education, income, and the other individual-level covariates in Table 1. Second, the same models were run but with education and income removed to obtain the "Partial Model" $PM_{2.5}$ coefficients and standard errors. Third, the coefficient and variance terms used for education and income within the indirect adjustment formula to calculate the "Internal (validation) Model" were derived from the True Model but with $PM_{2.5}$ excluded. This is the step where one would obtain values (coefficients and standard errors) from the published literature for the missing variables (e.g. see Supplemental Table s4). The X and U matrices (described in detail below) were derived from CanCHEC for the baseline year of 2001 only (no follow-up years included) and employed a static as well as a time-varying $PM_{2.5}$ exposure value. $PM_{2.5}$ – mortality hazard ratios from the True Model (with direct measurement of income and education) and the Internal Model incorporating indirect adjustment for education and income were then compared (i.e. values obtained from the True Model were used to indirectly adjust the Partial Model to calculate the Internal Model which was then compared to the True Model).

Step 3 was the external validation to assess the bias of using the CCHS as the ancillary matching dataset to indirectly adjust for the CanCHEC. We applied a similar approach to the internal validation by using variables available in both datasets (education and income), removing and indirectly adjusting for them. The only difference is the CCHS, not CanCHEC, is used to create the X and U matrices. We also tested using both a static and a time-varying $PM_{2.5}$ value in the X-matrix. The exact same mortality outcomes and related education and income coefficients used in the interval validation were applied here in order to determine the true bias of using the CCHS in place of the CanCHEC for the removed variables.

The X and U matrices were constructed to represent the covariance structure between the missing (U-matrix) and non-missing (X-matrix) variables, including the exposure variable. The stratification of age and sex are incorporated into the X-matrix by creating a series of 5-year age-sex dummy codes with the reference category (males 25 to 29) given a value of all '1s'. The remaining variables are categorized into 0/1 dummy codes with the reference group as '0' along with the continuous $PM_{2.5}$ values as separate columns in the X-matrix. For example, a 3-category marital status variable would be represented by two columns in the matrix. To account for the time-varying nature of $PM_{2.5}$ in the models, an X-matrix was created for each year of follow-up, transposed and summed. The U-matrix represents the missing covariates and is set up in a similar manner as the X-matrix, except it is time invariant. A new addition to this method was to incorporate a sampling weights matrix (W-matrix) to adjust for urban-rural sampling differences between the CanCHEC and the CCHS. This matrix contained only one column of values, the ratio of the proportion of CanCHEC subjects to the proportion of CCHS subjects by Health Region (the CCHS sampling unit) for each individual in the CCHS. The goal was to make the CCHS more like the CanCHEC by giving more weight to urban respondents and less weight to rural respondents. The indirect adjustment formula

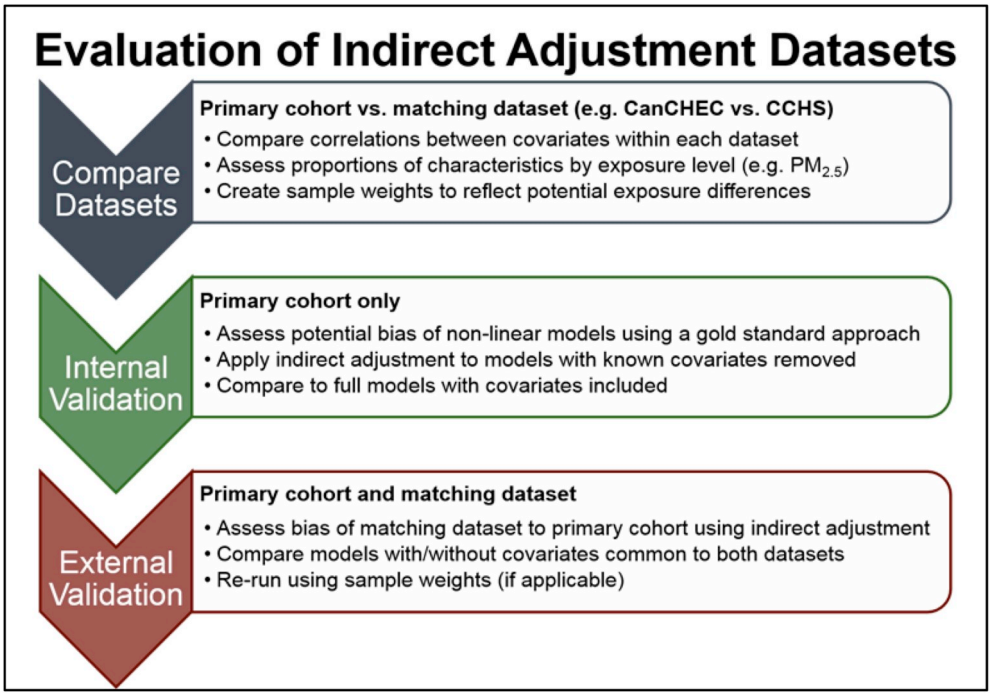

Fig. 1. Schematic showing the steps involved to evaluate the datasets used for indirect adjustment.

Table 1
Descriptive Statistics and $PM_{2.5}$ exposure (μg/m^3) by demographic and socioeconomic characteristics for the 2001 CanCHEC and 2001 CCHS cohorts.

	CanCHEC		CCHS	
	%	$PM_{2.5}$ mean (SE)	%	$PM_{2.5}$ mean (SE)
Full data (N)	2,468,190	8.40 (2.8)	80,630	6.70 (3.1)
Sex				
Male	48.3	8.30 (2.8)	46.2	6.65 (3.1)
Female	51.6	8.37 (2.8)	53.7	6.80 (3.1)
Age group (years)				
25–29	9.0	8.49 (2.7)	9.1	6.93 (3.1)
30–39	23.4	8.28 (2.7)	22.8	6.77 (3.0)
40–49	26.0	8.23 (2.7)	24.2	6.69 (3.0)
50–59	18.2	8.28 (2.7)	17.4	6.61 (3.0)
60–69	11.8	8.32 (2.8)	12.3	6.61 (3.0)
70–79	8.5	8.52 (2.8)	9.8	6.84 (3.1)
80–89	3.2	8.55 (2.8)	4.4	6.84 (3.2)
Visible minority status				
White or Aboriginal	98.6	8.31 (2.8)	95.8	6.78 (3.1)
Visible minority	1.3	9.17 (2.7)	4.1	5.59 (3.0)
Aboriginal status				
Not Aboriginal	94.3	8.4 (2.8)	97.1	6.79 (3.1)
Aboriginal	5.6	7.02 (2.4)	2.9	4.81 (2.5)
Marital status				
Single/Never married	73	8.18 (2.7)	62.1	6.5 (3.0)
Married/Common-law	13.8	8.58 (2.8)	22.4	7.0 (3.1)
Divorced/Widowed	13.1	8.82 (2.8)	15.4	7.24 (3.2)
Educational attainment				
No high school	28.6	8.07 (2.8)	27.9	6.38 (3.1)
High school or higher	71.3	8.42 (2.7)	72	6.86 (3.1)
Income quintile				
1st quintile - lowest	15.3	8.43 (2.8)	21.8	6.83 (3.1)
2nd quintile	19.0	8.33 (2.8)	19.5	6.72 (3.1)
3rd quintile	20.8	8.32 (2.8)	18.8	6.76 (3.1)
4th quintile	21.9	8.28 (2.8)	19.3	6.71 (3.0)
5th quintile - highest	22.9	8.27 (2.7)	20.3	6.61 (3.1)
Labour force status				
Employed	64.5	8.07 (2.8)	62.0	6.75 (3.1)
Unemployed	4.1	8.28 (2.8)	2.6	6.47 (3.0)
Not in labour force	31.2	8.56 (2.7)	35.2	6.71 (3.1)
CMA-Size				
> 1.5 Million	24.1	10.29 (2.4)	11.0	9.73 (2.5)
500,000–1.5M	17.7	8.34 (2.0)	9.9	7.92 (1.9)
100,000–499,999	18.7	8.43 (3.0)	18.8	8.67 (3.2)
30,000–99,999	8.0	7.57 (2.9)	13.5	6.57 (2.9)
10,000–29,999	5.1	6.54 (2.1)	9.7	5.89 (2.1)
< 10,000	26.4	6.99 (2.2)	36.9	4.79 (2.1)
Airshed				
Western	10.8	6.95 (1.9)	12.1	6.07 (2.2)
Prairie	13.7	7.14 (1.7)	16.2	5.29 (2.0)
West Central	6.7	6.52 (1.9)	9.8	4.7 (1.7)
South Atlantic	10.8	5.98 (2.0)	17.9	4.65 (1.6)
East Central	56.1	9.6 (2.6)	40.9	9.08 (2.9)
Northern	1.7	6.44 (2.3)	2.8	4.01 (1.6)
Can-Marg Index				
Residential Instability				
1st quintile - lowest	23.8	7.89 (2.5)	23.8	5.77 (2.8)
2nd quintile	25.7	7.75 (2.7)	25.8	6.23 (2.8)
3rd quintile	20.6	8.14 (2.9)	21.6	6.57 (3.1)
4th quintile	17.2	8.97 (2.8)	17.4	7.69 (3.0)
5th quintile - highest	12.6	9.7 (2.7)	11.2	8.75 (3.0)
Material Deprivation				
1st quintile – lowest	15.5	8.62 (2.6)	10.6	7.62 (2.8)
2nd quintile	20.5	8.4 (2.6)	18.7	7.07 (2.9)
3rd quintile	19.3	8.53 (2.6)	18.5	7.38 (3.0)
4th quintile	18.8	8.44 (2.8)	18.3	6.88 (3.2)
5th quintile – highest	25.7	7.82 (3.0)	33.7	5.82 (3.0)
Dependency				
1st quintile – lowest	15.8	8.09 (2.5)	15.0	6.17 (2.8)
2nd quintile	16.9	8.41 (2.6)	12.9	6.9 (3.1)
3rd quintile	16.3	8.58 (2.8)	14.7	7.38 (3.1)
4th quintile	21.5	8.57 (2.9)	22.5	7.16 (3.2)
5th quintile – highest	29.2	8.06 (2.8)	34.8	6.35 (3.0)
Ethnic Concentration				
1st quintile – lowest	36.0	7.54 (2.5)	42.9	5.82 (2.7)
2nd quintile	26.2	8.29 (2.7)	28.1	7.07 (3.0)
3rd quintile	17.6	8.6 (2.9)	15.9	7.13 (3.1)
4th quintile	12.4	9.33 (2.8)	8.7	7.99 (3.4)
5th quintile – highest	7.5	9.8 (2.3)	4.2	9.58 (2.6)

and associated methodology is detailed in the Supplemental materials, Appendix A).

Finally, we applied the above indirect adjustment to a real missing data scenario to estimate adjusted $PM_{2.5}$ – mortality hazard ratios and compared the results to those using the mCCHS in which smoking, alcohol consumption, fruit and vegetable intake and physical activity were directly measured. Here, the CCHS was used to create the X, U, and W-matrices with time-varying $PM_{2.5}$ to indirectly adjust for the above missing behavioural risk factors not available in the CanCHEC. We obtained risk estimates from published meta-analyses for the specific risk factors on mortality, including smoking intensity (Thun et al., 2013), alcohol consumption (Xi et al., 2017), BMI (Yu et al., 2017), fruit and vegetable intake (Leenders et al., 2014), and physical activity (Hupin et al., 2015). The specific risk estimates are summarized in Supplemental Table s4.

2.3. Statistical analysis

We fit Cox proportional hazard models to examine the association between ambient $PM_{2.5}$ exposure with four causes of death: non-accidental (ICD-10 codes A to R), cardiovascular (ICD-10: I10 to I69), ischemic heart disease (ICD-10: I20 to I25), and lung cancer (ICD-10: C33 to C34). Respondents were followed until death or the end of follow-up. All models were stratified by sex and 5-year age categories. Models were further adjusted for the individual covariates of marital status, Aboriginal identity, visible minority identity, and employment status. Education and income were the two variables that were removed and indirectly adjusted for in the validation tests as both were available in the CanCHEC and CCHS datasets. Education was categorized into a dichotomous variable, those with or without a high school education. Additional educational attainment groupings were considered but proportional comparability between the CanCHEC and CCHS were less favourable. Income adequacy quintiles are based on the ratio between pre-tax income of economic families or unattached individuals to the Statistics Canada low-income cut-off for family and community size, and adjusted for regional differences in economy (Pinault et al., 2016a).

In the final indirect adjustment, we further adjusted the models by contextual ecological covariates. The Canadian Marginalization (CAN-Marg) Index is a census-based, empirically derived, and theoretically informed tool designed to reflect four dimensions of marginalization that characterize inequalities in health and social well-being: residential instability, material deprivation, dependency, and ethnic concentration (Matheson et al., 2012). We assigned the CAN-Marg factors based on neighbourhood-scale census tracts (CTs) in medium and large cities (core population of 50,000 or more), and municipal-scale census subdivisions (CSDs) everywhere else outside of these metropolitan areas. CAN-Marg values were available for two census years (2001 and 2006), and were applied to all datasets based on the closest corresponding year. The other ecological adjustment covariates included Census Metropolitan Area Size (CMA size) categorized into six groups based on population (< 10,000; 10,000–29,999; 30,000–99,999; 100,000–499,999; 500,000–1,499,999; and 1.5 million +), and a geographic identifier for airshed which divides the country into six large geographic areas to adjust for broad scale spatial variation in mortality rates not captured by other risk factors.

3. Results

The representativeness of the CCHS to CanCHEC with respect to the distribution of characteristics and $PM_{2.5}$ exposures is presented in Table 1, Fig. 2, and Supplemental Table s1. Overall, the two datasets were quite similar across the individual variables, with some slight differences among the ecological variables. The largest proportional differences were for CMA-size and airshed, showing a greater proportion of CCHS respondents in rural locations. While the levels of $PM_{2.5}$ for the CCHS were consistently lower than for CanCHEC, the relative differences were fairly uniform across the demographic, socioeconomic, and ecological variable groups (Fig. 2). The aim of Fig. 2 was to help reveal absolute differences as well as similar relative differences across variable groups demonstrated by approximate parallel lines. In general the two datasets track reasonably well in their exposure distributions. Visible minority and Aboriginal identity had the largest absolute differences of 4.3 and 4.0 $\mu g/m^3$ respectively, while the parallel qualities of the ecological variables were less consistent compared to the individual variables but still displayed similar overall trends. Larger differences tended to be in the middle of the $PM_{2.5}$ distribution, while the tails were more similar. Further examination of the representativeness between the CCHS and CanCHEC is available in Supplemental Table s1 which compared the proportions of characteristics across $PM_{2.5}$ quintiles (e.g. the proportion of males in both the CCHS and CanCHEC

Fig. 2. Absolute differences in $PM_{2.5}$ ($\mu g/m^3$) distribution by demographic, socioeconomic, and ecological characteristics between the 2001 CanCHEC and 2001 CCHS cohorts (CanCHEC – CCHS).

decrease with increasing $PM_{2.5}$ exposure). Overall $PM_{2.5}$ differences between CanCHEC and CCHS become smaller over time (Supplemental Fig. 1). Correlation coefficients showed consistency in both the magnitude and direction between all the variables in both datasets (supplemental Table s2).

The results of the validation tests are presented in Fig. 3for four different cause of mortality, non-accidental (N deaths = 196,540), cardiovascular (55,720), ischemic heart disease (33,425), and lung cancer (22,200). The True Model is the gold-standard model showing hazard ratios adjusted for education and income, whereas the Partial Model shows hazard ratios with education and income removed. Using the static $PM_{2.5}$ scenario (Fig. 3a), the True versus Partial adjustment bias ranged from 1.7% to 3.3% depending on the cause of death. The Internal validation model in which education and income were indirectly adjusted for using CanCHEC had an adjustment bias less than 1%. The external validation model replaces the CanCHEC with the CCHS as the ancillary dataset and showed a small over-adjustment bias between −0.7% and −1.2%. Using the time-varying scenario (Fig. 3b), the overall bias caused by the missing covariates (education and income) was larger (Partial Model bias of 3%–5.6%), with the Internal and External validation models showing improved adjustment bias of 1.7%–2.9% and 1.3–2.3% respectively. The inclusion of the sample weights using either the static or time-varying approach did not improve the adjustments (data not shown).

The adjustment correction of indirectly adjusted models missing four common confounding risk factors (smoking, diet, exercise, and alcohol use) are shown in Fig. 4 and are compared to equivalent models using the CCHS-mortality linked cohort (mCCHS) which are directly adjusted by the same risk factors. The Individual covariate models indicate that indirect adjustment for the missing risk factors increases the hazard ratios consistent with that from the mCCHS, except for the unweighted lung cancer estimate. The Individual + Ecological covariate models have the opposite adjustment direction, lowering the hazard ratios after (indirect) adjustment for the missing risk factors, and show similar adjustment direction and magnitude comparable to that from the mCCHS. If using the mCCHS adjustment correction as the guide post, the weighted indirect adjustment performs slightly better than the unweighted version for all mortality outcomes except for IHD. The indirect adjustment for lung cancer was inconsistent. Supplemental Table s3 contains the model hazard ratios and 95% CIs that formed the basis for the adjustment correction results presented in Fig. 4.

4. Discussion

In this paper we demonstrate the application and evaluation of the indirect adjustment method whereby secondary ancillary data is used to adjust for missing covariates in a primary dataset. Using the method developed by Shin and colleagues (Shin et al., 2014), we show that the adjustment bias for non-linear survival models (internal validation) was less than 1% with static $PM_{2.5}$ exposure models and under 3% for time-varying $PM_{2.5}$ models. The external validation assessing the CCHS as the ancillary matching dataset also performed well, indicating small downward (over) adjustment bias for time-varying $PM_{2.5}$ models. These results are comparable to those from Shin et al. (2014) using a similar longitudinal cohort (1991 CanCHEC) that indirectly adjusted for smoking and BMI and reported a 3% increase in the association between $PM_{2.5}$ and IHD following indirect adjustment.

In an analysis of actual missing behavioural risk factors from the CanCHEC (smoking, alcohol use, fruit and vegetable intake, and exercise), the adjustment correction from the indirectly adjusted models

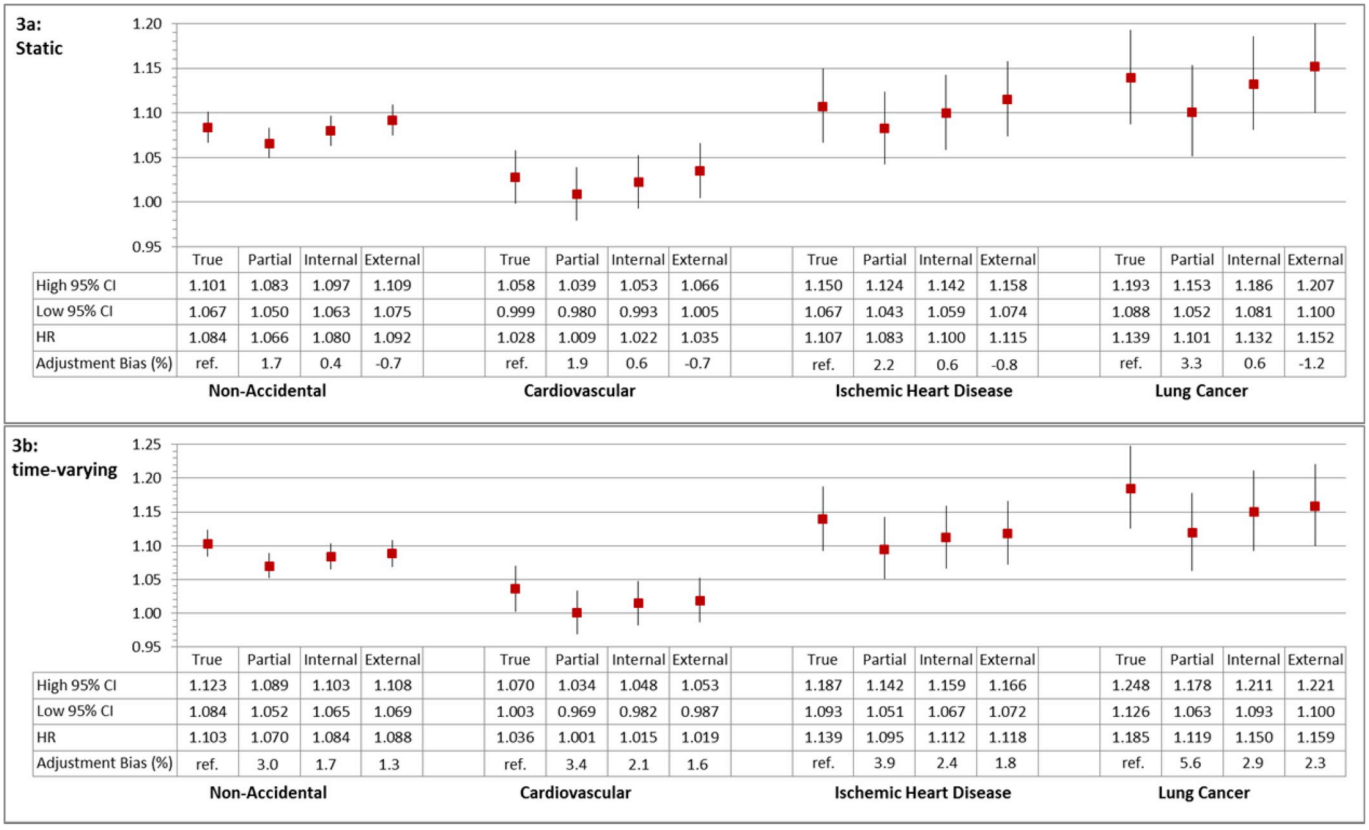

3a: Static	Non-Accidental				Cardiovascular				Ischemic Heart Disease				Lung Cancer			
	True	Partial	Internal	External	True	Partial	Internal	External	True	Partial	Internal	External	True	Partial	Internal	External
High 95% CI	1.101	1.083	1.097	1.109	1.058	1.039	1.053	1.066	1.150	1.124	1.142	1.158	1.193	1.153	1.186	1.207
Low 95% CI	1.067	1.050	1.063	1.075	0.999	0.980	0.993	1.005	1.067	1.043	1.059	1.074	1.088	1.052	1.081	1.100
HR	1.084	1.066	1.080	1.092	1.028	1.009	1.022	1.035	1.107	1.083	1.100	1.115	1.139	1.101	1.132	1.152
Adjustment Bias (%)	ref.	1.7	0.4	-0.7	ref.	1.9	0.6	-0.7	ref.	2.2	0.6	-0.8	ref.	3.3	0.6	-1.2

3b: time-varying	Non-Accidental				Cardiovascular				Ischemic Heart Disease				Lung Cancer			
	True	Partial	Internal	External	True	Partial	Internal	External	True	Partial	Internal	External	True	Partial	Internal	External
High 95% CI	1.123	1.089	1.103	1.108	1.070	1.034	1.048	1.053	1.187	1.142	1.159	1.166	1.248	1.178	1.211	1.221
Low 95% CI	1.084	1.052	1.065	1.069	1.003	0.969	0.982	0.987	1.093	1.051	1.067	1.072	1.126	1.063	1.093	1.100
HR	1.103	1.070	1.084	1.088	1.036	1.001	1.015	1.019	1.139	1.095	1.112	1.118	1.185	1.119	1.150	1.159
Adjustment Bias (%)	ref.	3.0	1.7	1.3	ref.	3.4	2.1	1.6	ref.	3.9	2.4	1.8	ref.	5.6	2.9	2.3

Fig. 3. Internal and External validation model results of $PM_{2.5}$ mortality hazard ratios (HR, 95% CI) True Model: adjusted by marital status, visible minority, Aboriginal identity, employment, education, income; Partial Model: adjusted by marital status, visible minority, Aboriginalidentity, employment; Internal and External validation models are same as Partial Model but indirectly adjusted for education and income using the CanCHEC and CCHS respectively; Adjustment Bias % = $([HR_{true} - HR_{adj}]/HR_{true})*100$; All models stratified by 5-year age-sex groups; hazard ratios are per 10 μg/m^3 increase in $PM_{2.5;}$ *Time-varying internal validation HRs (95%CI) used static $PM_{2.5}$ x-matrix with time-varying coefficients.

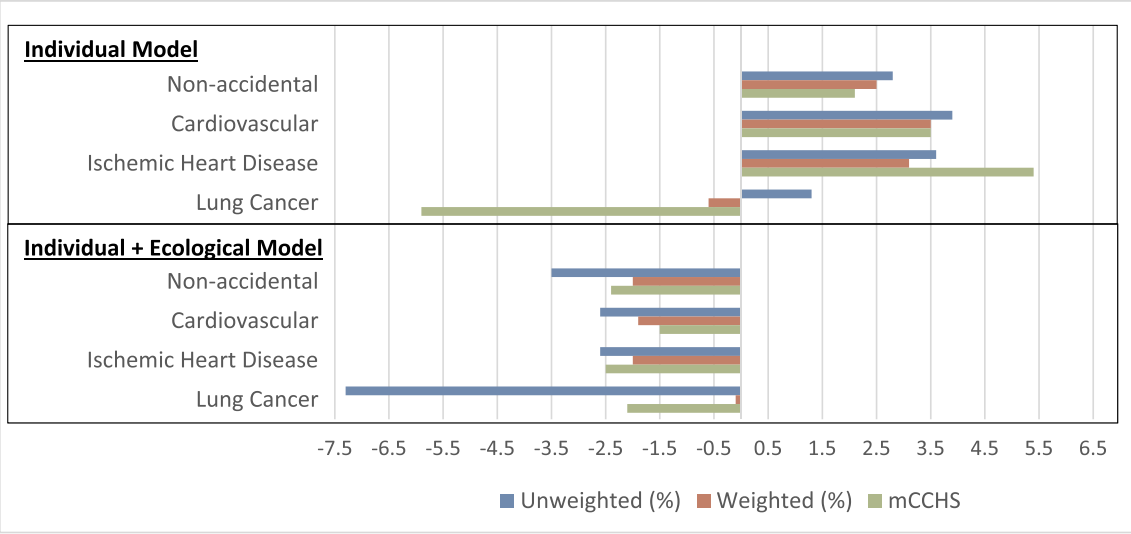

Fig. 4. Adjustment correction (%) of indirect adjustment for missing behavioural risk factors on $PM_{2.5}$ mortality hazard ratios. Individual Model: stratified by 5-year age-sex groups, adjusted by marital status, visible minority, Aboriginal identity, employment, income quintile, education and *indirectly* adjusted by smoking, alcohol use, exercise, diet; Individual + Ecological Model: includes Can-Marg Index, Community Size, Airshed; mCCHS: equivalent models using the CCHS-mortality linked cohort and *directly* adjusted by smoking, alcohol use, exercise, diet; Weighted vs. Unweighted models used sample weights (W-matrix) in the indirect adjustment formula; Adjustment correction % = $([HR_{adjust} - HR_{unadjust}]/HR_{adjust})*100$.

using the CCHS as the ancillary data were comparable to equivalent models using the mCCHS and directly adjusting for the same risk factors. In these analyses the models that applied sample weights performed slightly better overall than the unweighted models, potentially correcting for population sampling differences. As expected, including ecological socioeconomic covariates into the base models reduced the amount of subsequent adjustment required by the indirect adjustment of the individual risk factors. These results indicate that indirect adjustment improves the adjustment by reducing the bias from models missing important confounding (e.g. the Partial Models in Fig. 3), but that internal and external validation tests should be run to assess the magnitude and direction of adjustment prior to running the actual indirect adjustment. Including sampling weights could help improve the adjustments if the proportion of respondents between the primary cohort and ancillary survey data differ geographically between urban and rural areas.

Of the four mortality outcomes assessed, the adjustments for lung cancer were the most inconsistent. This finding could be due to the strong causal relationship between smoking and lung cancer and the potential confounding via regional differences of smoking prevalence in Canada and differential $PM_{2.5}$ exposure (Villeneuve et al., 2011). Interestingly, we showed a similar magnitude but opposite adjustment direction of $PM_{2.5}$ HRs on lung cancer in the mCCHS cohort when adjusting for smoking behaviour compared to Villeneuve et al. (2011). For example, whereas Villeneuve et al. (2011) estimated that $PM_{2.5}$ risk ratios on lung cancer would increase by 6.2%–6.9% when smoking status was included into models; we found that adjustment for smoking, alcohol use, diet, and exercise lower the hazard ratio of $PM_{2.5}$ on lung cancer by −5.9% in the individual covariate model and −2.1% when ecological covariates were included. Our findings are more aligned with those of the ACS CPS II Study (Pope et al., 2002).

We introduced two potential improvements to the Shin et al. (2014) indirect adjustment method by incorporating a time-varying exposure component and a weighting scheme to adjust for sampling differences between the primary and matching datasets. For longitudinal survival models that have a time-varying exposure value, it makes logical sense to include this into the indirect adjustment. Shown in Fig. 3, we assessed both static and time-varying models; however, it's not straightforward to assess which scenario indirect adjustment performed better. Under the static $PM_{2.5}$ scenario, indirect adjustment produced very similar hazard ratios to that of the True Model but the absolute adjustment required was smaller. For example, for non-accidental mortality the bias produced by the missing covariates (education and income) was 1.7% which was over-corrected in the External Model. In the time-varying scenario, the Partial Model bias was nearly double (3%) and was reduced to 1.3% in the External Model, a 57% reduction. We were unable to fully implement the time-varying adaptation for the internal validation due to size restrictions of the matrix algebra required (2.4 million by 2.4 million matrix), therefore the time-varying internal validation is not a direct apples-to-apples comparison with the static scenario. However, the main purpose of the internal validation was to show that indirect adjustment is a viable method with Cox proportional hazard models and is not necessarily a step that others would need to repeat, unlike the external validation step which is highly recommended. That said, it may be possible to take a random sample of the primary cohort to reduce its size and perform a time-varying internal validation.

The second modification we tested was incorporating sampling weights into the formula to adjust for regional (urban-rural) sampling differences between the two datasets. The results were mixed. For the validation tests, including the W-matrix did not improve the adjustments; whereas for the final indirect adjustments in Fig. 4, the weighted results corresponded slightly better to the mCCHS models for non-accidental and CVD mortality, but less so for IHD and lung cancer. Similar to the time-varying modification, in theory, adding sample weights makes logical sense. As this additional adjustment was sensitive to the formula calculating the sample weights, different formulations may improve the results.

This exercise confirms that confounding bias is not unidirectional across models. Our initial hypothesis was that by including the three sets of ecological variables (CAN-Marg, CMA-size, and airshed) they would dramatically reduce the potential bias from the missing risk factors prior to (indirect) adjustment. That was not necessarily the case. In Fig. 4 (and supplemental Table s3), adjustment magnitude was only marginally larger for the individual covariate model compared to the individual plus ecological covariate model, but in opposite directions. This trend was supported by direct adjustment of risk factors using the mCCHS cohort data.

Confounding is data specific, thus the results have been mixed regarding the magnitude of the adjusted bias on the final risk estimates in

the few studies to have used this method. The direction and magnitude of the potential confounding bias in risk estimates depends on, 1) the degree of correlation between omitted and exposure variables, 2) the magnitude of their parameter estimates on the outcome, and 3) whether confounding can be partially accounted for by other extraneous variables in the model (e.g. education, income, occupation, neighbourhood factors) (Villeneuve et al., 2011). Using the 1991 CanCHEC, Crouse et al. and Weichenthal et al. report that indirect adjustment for smoking behaviour and obesity had very little impact (1–2%) on the hazard ratios between air pollutants and various mortality outcomes (Crouse et al., 2015a, 2015b; Weichenthal et al., 2016). Similarly, using Ontario Tax Cohort data, Villeneuve et al. found small attenuations of exposure risk ratios after indirectly adjusting for smoking and other risk factors (Villeneuve et al., 2013, 2012). Conversely, Strak et al. showed that the potential bias for excluding smoking was substantial (up to 10%) on air pollution mortality estimates for CVD and particularly lung cancer (Strak et al., 2017). What has become apparent is that the direction and magnitude of the potential bias is largely dependent on the direction and magnitude of the correlation between air pollution and the missing risk factors, and will thus be population dependent. In Canada, the addition of SES risk factors largely explain much of the impact of smoking and other risk factors on air pollution effect estimates (Pinault et al., 2016b).

The generalizability of the indirect adjustment method to other cohorts could be considered universal, however its effectiveness will depend on the availability of suitably representative ancillary data. Specifically, researchers can assess the appropriateness of available ancillary matching data to use for indirect adjustment by following the evaluation methodology we have described here. In addition to the descriptive and visual comparisons, we suggest running external validation tests to quantify the representativeness of the ancillary dataset by determining the magnitude and direction of adjustment bias when important variables available in both primary and ancillary dataset are removed and indirectly adjusted for. An ideal ancillary matching dataset would be drawn from the same target population as the main cohort and have similar geographic coverage, common variables to match on such as age, sex, income, and education, and similar exposure-to-characteristic proportions (Fig. 2, Supplemental Table s1 & s2). If the primary cohort and ancillary data have differing population sampling schemes, applying custom sample weights may correct for this discrepancy. For example, we categorized education into a dichotomous variable since the proportional comparability between the CanCHEC and CCHS among the higher education groups were less favourable. Simulation tests to examine under what conditions the primary and ancillary data can differ before the results produced by indirect adjustment are no longer acceptable would be a valuable contribution to the literature.

5. Conclusion

Our results show promise in applying indirect adjustment methods with Cox proportional hazard models, and that hazard ratio point estimates and standard errors in models missing key covariates can be reliably adjusted when using a representative matching dataset. Relevant to Canada, these results show that the CCHS can be used as an ancillary dataset to indirectly adjust for missing risk factors in the CanCHEC data. While the method itself is universally generalizable to other cohorts, its effectiveness will depend on the availability of suitably representative ancillary data, as evaluated in an approach similar to that describe here. This formal evaluation will help establish protocols that others can follow to assess the suitability of their data.

Funding

Research described in this article was conducted under contract to the Health Effects Institute (HEI), an organization jointly funded by the United States Environmental Protection Agency (EPA) (Assistance Award No. R-82811201) and certain motor vehicle and engine manufacturers. The contents of this article do not necessarily reflect the views of HEI, or its sponsors, nor do they necessarily reflect the views and policies of the EPA or motor vehicle and engine manufacturers.

The analysis presented in this paper was conducted at the University of British Columbia Research Data Centre, which is part of the Canadian Research Data Centre Network (CRDCN). The services and activities provided by the University of British Columbia Research Data Centre are made possible by the financial or in-kind support of the Social Sciences and Humanities Research Council of Canada (SSHRC), the Canadian Institutes of Health Research (CIHR), the Canada Foundation for Innovation (CFI), Statistics Canada, and The University of British Columbia. The views expressed in this paper do not represent those of the CRDCN or of its partners.

Data Access: Both of the analytical cohorts used (2001 CanCHEC and 2001 CCHS-mortality cohort) are available to researchers to access through Statistics Canada's Research Data Centre program. The programs used to assign environmental exposures (PCCF+ and postal code imputation) are also available to researchers through subscription/request. Environmental exposures are available upon request to the original authors of the data. The analytical codes used were all standard SAS code (e.g., data steps, proc phreg).

The authors have no competing interests to declare.

CRediT authorship contribution statement

Anders C. Erickson: Conceptualization, Formal analysis, Investigation, Visualization, Writing - original draft. **Michael Brauer:** Conceptualization, Writing - review & editing, Supervision, Funding acquisition. **Tanya Christidis:** Resources, Data curation, Writing - review & editing. **Lauren Pinault:** Resources, Data curation. **Daniel L. Crouse:** Software, Resources, Writing - review & editing. **Aaron van Donkelaar:** Resources, Data curation. **Scott Weichenthal:** Conceptualization, Writing - review & editing. **Amanda Pappin:** Resources, Data curation, Writing - review & editing. **Michael Tjepkema:** Resources, Data curation, Supervision. **Randall V. Martin:** Resources, Data curation. **Jeffrey R. Brook:** Resources, Data curation, Funding acquisition. **Perry Hystad:** Resources, Data curation. **Richard T. Burnett:** Conceptualization, Methodology, Supervision, Funding acquisition.

Appendix A. Supplementary data

Supplementary data to this article can be found online at https://doi.org/10.1016/j.envres.2019.05.010.

References

Cesaroni, G., Badaloni, C., Gariazzo, C., Stafoggia, M., Sozzi, R., Davoli, M., Forastiere, F., 2013. Long-term exposure to urban air pollution and mortality in a cohort of more than a million adults in Rome. Environ. Health Perspect. 121, 324–331. https://doi.org/10.1289/ehp.1205862.

Chen, H., Goldberg, M.S., Burnett, R.T., Jerrett, M., Wheeler, A.J., Villeneuve, P.J., 2013. Long-Term exposure to traffic-related air pollution and cardiovascular mortality. Epidemiology 24, 35–43. https://doi.org/10.1097/EDE.0b013e318276c005.

Crouse, D.L., Peters, P.A., Hystad, P., Brook, J.R., van Donkelaar, A., Martin, R.V.,, Villeneuve, P.J., Jerrett, M., Goldberg, M.S., Pope III, C.A., Brauer, M., Brook, R.D., Robichaud, A., Menard, R., Burnett, R.T., 2015a. Ambient PM2.5, O3, and NO2 exposures and associations with mortality over 16 years of follow-up in the canadian census health and environment cohort (CanCHEC). Environ. Health Perspect. 123, 1180–1186. https://doi.org/10.1289/ehp.1409276.

Crouse, D.L., Peters, P.A., Villeneuve, P.J., Proux, M.-O., Shin, H.H., Goldberg, M.S., Johnson, M., Wheeler, A.J., Allen, R.W., Atari, D.O., Jerrett, M., Brauer, M., Brook, J.R., Cakmak, S., Burnett, R.T., 2015b. Within- and between-city contrasts in nitrogen dioxide and mortality in 10 Canadian cities; a subset of the Canadian Census Health and Environment Cohort (CanCHEC). J. Expo. Sci. Environ. Epidemiol. 25, 482–489. https://doi.org/10.1038/jes.2014.89.

Di, Q., Wang, Y., Zanobetti, A., Wang, Y., Koutrakis, P., Choirat, C., Dominici, F., Schwartz, J.D., 2017. Air pollution and mortality in the medicare population. N. Engl. J. Med. 376, 2513–2522. https://doi.org/10.1056/NEJMoa1702747.

Fines, P., Pinault, L., Tjepkema, M., 2017. Imputing Postal Codes to Analyze Ecological Variables in Longitudinal Cohorts: Exposure to Particulate Matter in the Canadian Census Health and Environment Cohort Database. Analytical Studies: Methods and Paper Series. Cat. No. 11-633-X-No. 006 (No. 11–633–X — No. 006), Analytical Studies: Methods and References Imputing. (Ottawa).

Fischer, P.H., Marra, M., Ameling, C.B., Hoek, G., Beelen, R., de Hoogh, K., Breugelmans, O., Kruize, H., Janssen, N.A.H., Houthuijs, D., 2015. Air pollution and mortality in seven million adults: the Dutch environmental longitudinal study (DUELS). Environ. Health Perspect. 123, 697–704. https://doi.org/10.1289/ehp.1408254.

Gail, M.H., Wacholder, S., Lubin, J.H., 1988. Indirect corrections for confounding under multiplicative and additive risk models. Am. J. Ind. Med. 13, 119–130. https://doi.org/10.1002/ajim.4700130108.

Hupin, D., Roche, F., Gremeaux, V., Chatard, J.-C., Oriol, M., Gaspoz, J.-M., Barthélémy, J.-C., Edouard, P., 2015. Even a low-dose of moderate-to-vigorous physical activity reduces mortality by 22% in adults aged ≥60 years: a systematic review and meta-analysis. Br. J. Sports Med. 49, 1262–1267. https://doi.org/10.1136/bjsports-2014-094306.

Khan, S., Pinault, L., Tjepkema, M., Wilkins, R., 2018. Positional Accuracy of Geocoding from Residential Postal Codes versus Full Street Addresses. Heal. Reports 82–033–X.

Leenders, M., Boshuizen, H.C., Ferrari, P., Siersema, P.D., Overvad, K., Tjønneland, A., Olsen, A., Boutron-Ruault, M.-C., Dossus, L., Dartois, L., Kaaks, R., Li, K., Boeing, H., Bergmann, M.M., Trichopoulou, A., Lagiou, P., Trichopoulos, D., Palli, D., Krogh, V., Panico, S., Tumino, R., Vineis, P., Peeters, P.H.M., Weiderpass, E., Engeset, D., Braaten, T., Redondo, M.L., Agudo, A., Sánchez, M.-J., Amiano, P., Huerta, J.-M., Ardanaz, E., Drake, I., Sonestedt, E., Johansson, I., Winkvist, A., Khaw, K.-T., Wareham, N.J., Key, T.J., Bradbury, K.E., Johansson, M., Licaj, I., Gunter, M.J., Murphy, N., Riboli, E., Bueno-de-Mesquita, H.B., 2014. Fruit and vegetable intake and cause-specific mortality in the EPIC study. Eur. J. Epidemiol. 29, 639–652. https://doi.org/10.1007/s10654-014-9945-9.

Matheson, F.I., Dunn, J.R., Smith, K.L.W., Moineddin, R., Glazier, R.H., 2012. Development of the Canadian Marginalization Index: a new tool for the study of inequality. Can. J. Public Health 103, S12–S16.

Pinault, L., Fines, P., Labrecque-Synnott, F., Saidi, A., Tjepkema, M., 2016a. The 2001 Canadian Census-Tax-Mortality cohort: a 10-year follow-up. Anal. Stud. Methods Ref 11–633–X.

Pinault, L., Tjepkema, M., Crouse, D.L., Weichenthal, S., van Donkelaar, A., Martin, R.V., Brauer, M., Chen, H., Burnett, R.T., 2016b. Risk estimates of mortality attributed to low concentrations of ambient fine particulate matter in the Canadian community health survey cohort. Environ. Health 15, 18. https://doi.org/10.1186/s12940-016-0111-6.

Pinault, L., Weichenthal, S., Crouse, D.L., Brauer, M., Erickson, A., van Donkelaar, A., Martin, R.V., Hystad, P., Chen, H., Finès, P., Brook, J.R., Tjepkema, M., Burnett, R.T., 2017. Associations between fine particulate matter and mortality in the 2001 Canadian census health and environment cohort. Environ. Res. 159, 406–415. https://doi.org/10.1016/j.envres.2017.08.037.

Pope III, C.A., Ezzati, M., Dockery, D.W., 2009. Fine-particulate air pollution and life expectancy in the United States. N. Engl. J. Med. 360, 376–386. https://doi.org/10.1056/NEJMsa0805646.

Pope III, C.A., Burnett, R.T., Thun, M.J., Calle, E.E., Krewski, D., Ito, K., Thurston, G.D., 2002. Lung cancer, cardiopulmonary mortality, and long-term exposure to fine particulate air pollution. JAMA 287, 1132. https://doi.org/10.1001/jama.287.9.1132.

Richardson, D.B., Laurier, D., Schubauer-Berigan, M.K., Tchetgen, E.T., Cole, S.R., 2014. Assessment and indirect adjustment for confounding by smoking in cohort studies using relative hazards models. Am. J. Epidemiol. 180, 933–940. https://doi.org/10.1093/aje/kwu211.

Sanmartin, C., Decady, Y., Trudeau, R., Dasylva, A., Tjepkema, M., Finès, P., Burnett, R., Ross, N., Manuel, D.G., 2016. Linking the Canadian community health survey and the canadian mortality database: an enhanced data source for the study of mortality. Heal. Rep. 27, 10–18.

Shin, H.H., Cakmak, S., Brion, O., Villeneuve, P., Turner, M.C., Goldberg, M.S., Jerrett, M., Chen, H., Crouse, D., Peters, P., Pope III, C.A., Burnett, R.T., 2014. Indirect adjustment for multiple missing variables applicable to environmental epidemiology. Environ. Res. 134, 482–487. https://doi.org/10.1016/j.envres.2014.05.016.

Statistics Canada, 2017. Postal Code Conversion File Plus (PCCF+) Reference Guide.

Statistics Canada, 2007. Canadian Community Health Survey (CCHS) - Detailed Information for 2000-2001 (Cycle 1.1). [WWW Document]. http://www23.statcan.gc.ca/imdb/p2SV.pl?Function=getSurvey&Id=3359 (accessed 11.29.18).

Strak, M., Janssen, N., Beelen, R., Schmitz, O., Karssenberg, D., Houthuijs, D., van den Brink, C., Dijst, M., Brunekreef, B., Hoek, G., 2017. Associations between lifestyle and air pollution exposure: potential for confounding in large administrative data cohorts. Environ. Res. 156, 364–373. https://doi.org/10.1016/j.envres.2017.03.050.

Thun, M.J., Carter, B.D., Feskanich, D., Freedman, N.D., Prentice, R., Lopez, A.D., Hartge, P., Gapstur, S.M., 2013. 50-year trends in smoking-related mortality in the United States. N. Engl. J. Med. 368, 351–364. https://doi.org/10.1056/NEJMsa1211127.

van Donkelaar, A., Martin, R.V., Spurr, R.J.D., Burnett, R.T., 2015. High-resolution satellite-derived PM 2.5 from optimal estimation and geographically weighted regression over north America. Environ. Sci. Technol. 49, 10482–10491. https://doi.org/10.1021/acs.est.5b02076.

Villeneuve, P.J., Goldberg, M.S., Burnett, R.T., van Donkelaar, A., Chen, H., Martin, R.V., 2011. Associations between cigarette smoking, obesity, sociodemographic characteristics and remote-sensing-derived estimates of ambient PM2.5: results from a Canadian population-based survey. Occup. Environ. Med. 68, 920–927. https://doi.org/10.1136/oem.2010.062521.

Villeneuve, P.J., Jerrett, M., Su, J., Burnett, R.T., Chen, H., Brook, J., Wheeler, A.J., Cakmak, S., Goldberg, M.S., 2013. A cohort study of intra-urban variations in volatile organic compounds and mortality, Toronto, Canada. Environ. Pollut. 183, 30–39. https://doi.org/10.1016/j.envpol.2012.12.022.

Villeneuve, P.J., Jerrett, M., Su, J.G., Burnett, R.T., Chen, H., Wheeler, A.J., Goldberg, M.S., 2012. A cohort study relating urban green space with mortality in Ontario, Canada. Environ. Res. 115, 51–58. https://doi.org/10.1016/j.envres.2012.03.003.

Weichenthal, S., Crouse, D.L., Pinault, L., Godri-Pollitt, K., Lavigne, E., Evans, G., van Donkelaar, A., Martin, R.V., Burnett, R.T., 2016. Oxidative burden of fine particulate air pollution and risk of cause-specific mortality in the Canadian Census Health and Environment Cohort (CanCHEC). Environ. Res. 146, 92–99. https://doi.org/10.1016/j.envres.2015.12.013.

Xi, B., Veeranki, S.P., Zhao, M., Ma, C., Yan, Y., Mi, J., 2017. Relationship of alcohol consumption to all-cause, cardiovascular, and cancer-related mortality in U.S. Adults. J. Am. Coll. Cardiol. 70, 913–922. https://doi.org/10.1016/J.JACC.2017.06.054.

Yu, E., Ley, S.H., Manson, J.E., Willett, W., Satija, A., Hu, F.B., Stokes, A., 2017. Weight history and all-cause and cause-specific mortality in three prospective cohort studies. Ann. Intern. Med. 166, 613–620. https://doi.org/10.7326/M16-1390.

Zeger, S.L., Dominici, F., McDermott, A., Samet, J.M., 2008. Mortality in the Medicare population and chronic exposure to fine particulate air pollution in urban centers (2000-2005). Environ. Health Perspect. 116, 1614–1619. https://doi.org/10.1289/ehp.11449.

Environmental Research 159 (2017) 406–415

Contents lists available at ScienceDirect

Environmental Research

journal homepage: www.elsevier.com/locate/envres

Associations between fine particulate matter and mortality in the 2001 Canadian Census Health and Environment Cohort

Lauren L. Pinault[a,*], Scott Weichenthal[b,c], Daniel L. Crouse[d], Michael Brauer[e], Anders Erickson[e], Aaron van Donkelaar[f], Randall V. Martin[f,g], Perry Hystad[h], Hong Chen[i,j], Philippe Finès[a], Jeffrey R. Brook[k], Michael Tjepkema[a], Richard T. Burnett[l]

[a] Health Analysis Division, Statistics Canada, Ottawa, ON, Canada
[b] McGill University, Montreal, QC, Canada
[c] Air Health Science Division, Health Canada, Ottawa, ON, Canada
[d] University of New Brunswick, Fredericton, NB, Canada
[e] University of British Columbia, BC, Canada
[f] Dalhousie University, Halifax, NS, Canada
[g] Harvard-Smithsonian Center for Astrophysics, Cambridge, MA, USA
[h] Oregon State University, Corvallis, OR, USA
[i] Public Health Ontario, Toronto, ON, Canada
[j] Institute for Clinical Evaluative Sciences, Toronto, ON, Canada
[k] University of Toronto, Toronto, ON, Canada
[l] Population Studies Division, Health Canada, Ottawa, ON, Canada

ARTICLE INFO

Keywords:
$PM_{2.5}$
Mortality
Cardiovascular
Respiratory
Cohort

ABSTRACT

Background: Large cohort studies have been used to characterise the association between long-term exposure to fine particulate matter ($PM_{2.5}$) air pollution with non-accidental, and cause-specific mortality. However, there has been no consensus as to the shape of the association between concentration and response.

Methods: To examine the shape of this association, we developed a new cohort based on respondents to the 2001 Canadian census long-form. We applied new annual $PM_{2.5}$ concentration estimates based on remote sensing and ground measurements for Canada at a 1 km spatial scale from 1998 to 2011. We followed 2.4 million respondents who were non-immigrants aged 25–90 years and did not reside in an institution over a 10 year period for mortality. Exposures were assigned as a 3-year mean prior to the follow-up year. Income tax files were used to account for residential mobility among respondents using postal codes, with probabilistic imputation used for missing postal codes in the tax data. We used Cox survival models to determine hazard ratios (HRs) for cause-specific mortality. We also estimated Shape Constrained Health Impact Functions (a concentration-response function) for selected causes of death.

Results: In models stratified by age, sex, airshed, and population centre size, and adjusted for individual and neighbourhood socioeconomic variables, HR estimates for non-accidental mortality were HR = 1.18 (95% CI: 1.15–1.21) per 10 $\mu g/m^3$ increase in concentration. We observed higher HRs for cardiovascular disease (HR = 1.25; 95% CI: 1.19–1.31), cardio-metabolic disease (HR = 1.27; 95% CI: 1.21–1.33), ischemic heart disease (HR = 1.36; 95% CI: 1.28–1.44) and chronic obstructive pulmonary disease (COPD) mortality (HR = 1.24; 95% CI: 1.11–1.39) compared to HR for all non-accidental causes of death. For non-accidental, cardio-metabolic, ischemic heart disease, respiratory and COPD mortality, the shape of the concentration-response curve was supra-linear, with larger differences in relative risk for lower concentrations. For both pneumonia and lung cancer, there was some suggestion that the curves were sub-linear.

Abbreviations: AMDB, Amalgamated Mortality Database (Statistics Canada); AQMS, Air Quality Management System; CanCHEC, Canadian Census Health and Environment Cohort (1991 and 2001); CD, Census Division; COPD, Chronic obstructive pulmonary disease; DA, Dissemination area; DB, Dissemination block; GEOS, Goddard Earth Observing System; MODIS, Moderate Resolution Imaging Spectroradiometer; NAC, Non-Accidental; PCCF+, Postal Code Conversion File Plus (Statistics Canada); SCHIF, Shape-Constrained Health Impact Function; SIN, Social insurance number

* Correspondence to: Health Analysis Division, Statistics Canada, 100 Tunney's Pasture Drive, Ottawa, Ontario, Canada K1A 0T6.
E-mail address: Lauren.Pinault@Canada.ca (L.L. Pinault).

http://dx.doi.org/10.1016/j.envres.2017.08.037
Received 22 March 2017; Received in revised form 17 August 2017; Accepted 18 August 2017
Available online 18 September 2017
0013-9351/

Conclusions: Associations between ambient concentrations of fine particulate matter and several causes of death were non-linear for each cause of death examined.

1. Introduction

Fine particulate matter ($PM_{2.5}$) is a complex mixture of particles (e.g., sulfate, smoke, and dust) smaller than 2.5 μm in aerodynamic diameter, and is one of the main components of ambient air pollution. Exposure to $PM_{2.5}$ air pollution was estimated by the Global Burden of Disease study to be responsible for 4.2 million deaths and 108 million disability-adjusted life years in 2015 (GBD, 2016). Several large epidemiological cohort studies have linked long-term exposure to $PM_{2.5}$ to mortality. In the United States, for example, the American Cancer Society cohort study estimated increased relative risks of non-accidental mortality (RR = 1.06, 95% CI: 1.02–1.11 per 10 $\mu g/m^3$ increase), as well as cardiopulmonary and lung cancer mortality associated with exposures to $PM_{2.5}$ (Pope et al., 2002). In an analysis of 22 European cohorts (European Study of Cohorts for Air Pollution Effects: ESCAPE), pooled hazard ratios (HRs) for non-accidental mortality were 1.07 (95% CI: 1.02–1.13) per increase of 5 $\mu g/m^3$ (Beelen et al., 2014).

Despite relatively lower concentrations of air pollution in Canada, previous studies have also indicated that exposure to $PM_{2.5}$ is associated with increased risk of non-accidental and cardiovascular mortality. In Crouse et al. (2012), the 1991 Canadian Census Health and Environment Cohort (1991 CanCHEC) followed 2.1 million census respondents during a 10 year follow-up period, and observed associations between ambient $PM_{2.5}$ and non-accidental and cardiovascular mortality. However, there were several limitations of this study. First, $PM_{2.5}$ estimates were based on a model that had relatively coarse (approximately 10 km grid) spatial resolution, thereby possibly contributing to exposure misclassification, particularly in smaller cities (i.e., less than 10 km across). Second, estimates of exposure were assigned based on postal codes at baseline, therefore not accounting for residential mobility during follow-up. Third, exposure estimates were based on a 2001–2006 average, meaning that changes over time were not considered, and the vintage of the exposure data did not match that of the follow-up period. Fourth, behavioural covariates such as smoking were not considered in the model. To overcome some of these limitations, a follow-up study of the same cohort followed respondent mobility and assigned a 7-year moving average of $PM_{2.5}$ exposure to respondents, based on year-adjusted $PM_{2.5}$ estimates (Crouse et al., 2015). Restricted cubic splines with three knots were used to examine the association between $PM_{2.5}$ and non-accidental mortality. These relative risk predictions suggested that differences in risk were greater for lower concentrations compared to higher concentrations, suggesting a supra-linear association. A separate study using the Canadian Community Health Survey-Mortality cohort accounted for behavioural covariates (e.g., smoking) directly, and reported only a small effect upon hazard ratio estimates for the association between $PM_{2.5}$ and mortality (Pinault et al., 2016a). Again using restricted cubic splines with three knots, a supra-linear association was observed. There was no suggestion of a sub-linear association at lower concentrations in either study.

The purpose of the present study is to provide an updated analysis using a larger and more recent cohort: the 2001 Canadian Census Health and Environment Cohort (2001 CanCHEC), which overcomes many of the remaining limitations of previous studies. We assigned exposures based on a relatively fine-scale $PM_{2.5}$ model (approximately 1 km grid), which incorporated both remote sensing estimates and ground observations. Then, we generated a complete annual residential history for all cohort members from a linkage to postal codes in tax records (as in Crouse et al., 2015). As a novel contribution, we imputed missing postal codes in the residential history with a probabilistic algorithm. As in Crouse et al., 2015, exposures were based on year-adjusted estimates from 1998 onwards, and the vintage of the exposure data matched that of the follow-up period. We also sought to more thoroughly examine the shape of the concentration-response curve beyond using restricted cubic splines with a pre-specified small number of knots (i.e. 3). This analysis also builds on the previous work by Nasari et al. (2016), where an older (1991) CanCHEC was used with coarsely-scaled exposure data and where multiple causes of death were not examined. There is specific interest in the shape of the association at very low concentration in order to conduct burden analysis (GBD, 2016). The concentration-response relationship at low levels is an issue of particular interest in Canada, as a country with relatively low levels of $PM_{2.5}$, and in many global regions that are approaching these lower ranges of exposure.

2. Materials and methods

2.1. Data

The 2001 CanCHEC is an analytical dataset that was formed through the linkage of the 2001 Census long-form questionnaire to tax and mortality databases. The 2001 Census long-form questionnaire is distributed to nearly 20% of Canadian households, although it is distributed to nearly 100% of households in remote areas and enumerated Indian reserves (Statistics Canada, 2003). The linkage methodology and cohort have been described elsewhere (Pinault et al., 2016b). Briefly, non-institutionalized respondents to the 2001 Census long-form questionnaire that lived in Canada were considered in scope for linkage (n = 4,500,200). Of these, 78.6% (n = 3,537,500) were linked through standard deterministic and probabilistic linkage techniques (Fellegi and Sunter, 1969) using sex, date of birth, postal code, and marital status to income tax files (T1 Personal Master File, Canada Revenue Agency) to obtain an annual postal code history and a Social Insurance Number (SIN). The proportion of respondents successfully linked to tax files was lower for younger adults, Aboriginal respondents, and persons who had moved in the previous year, possibly due to being less likely to have filed taxes and/or difficulties in matching linkage keys (e.g., postal codes). The false-positive error rate in the linkage was less than 0.2% (Pinault et al., 2016b).

Subsequently, tax-linked Census respondents were deterministically linked to the Amalgamated Mortality Database (AMDB) using SINs. The AMDB is a dataset that includes death records from both the Canadian Mortality Database (which compiles provincial and territorial hospital death registries beginning in 1950) and deaths recorded in tax files. Deaths that occurred between census day (May 15, 2001) and December 31, 2011 were eligible for linkage. A total of 347,000 deaths were recorded during the 10.6 year follow-up period. Mortality statistics for the cohort were broadly consistent with patterns observed in the 1991 CanCHEC and national vital statistics (Wilkins et al., 2008; Pinault et al., 2016b). Members of the final cohort were slightly more likely to be married or common-law, have higher income or higher educational attainment, or be employed than were the general Canadian population (Pinault et al., 2016b).

Respondents were assigned estimates of exposure to fine particulate matter ($PM_{2.5}$), derived from a national model (van Donkelaar et al., 2015). Briefly, total column optical aerosol depth retrievals from the Moderate Resolution Imaging Spectroradiometer (MODIS) were related to near-surface $PM_{2.5}$ using the GEOS-Chem chemical transport model, and a geographically weighted regression applied to incorporate ground-level observations, thereby adjusting for bias in the remote-sensed estimates. Yearly (2004–2012) averages in estimated surface $PM_{2.5}$ at approximately 1 km^2 resolution were obtained (van Donkelaar et al., 2015), and extended back in time to 1998 by applying inter-

annual variation from a previously published $PM_{2.5}$ dataset (Boys et al., 2014). Within North America, these mean bias-adjusted $PM_{2.5}$ estimates were strongly spatially correlated with ground level measurements over areas where the estimated $PM_{2.5}$ was less than 20 μg/m^3 (R^2 = 0.82, slope = 0.97, n = 1440) (van Donkelaar et al., 2015).

2.2. Data preparation

All respondents who were not matched to air pollution estimates due to missing postal codes at entry or residing outside of the boundaries of air pollution models (i.e., in the far north) were excluded (n = 86,100, or 2.4%). Consistent with previous long-term air pollution studies (Crouse et al., 2012; Pinault et al., 2016a), the analytical cohort was limited to adults aged 25–90 years at enrollment (additional n = 319,900 respondents excluded, or 9.0%). All immigrants were excluded from the cohort (additional n = 683,100, or 19.3%) for the following reasons: prior to arrival in Canada, their previous exposure to air pollution was unknown. After immigrants arrive in Canada, their health is generally better than the Canadian-born population, due largely to a screening effect (Newbold, 2005; Ng, 2011). Additionally, mean immigrant exposure to air pollution ($PM_{2.5}$) remains higher than the native-born population for decades following arrival in Canada, never approaching the Canadian-born mean, largely due to a primarily urban residence (Pinault et al., 2017). For these reasons, associations between air pollution and immigrant health require separate analyses. The final analytical sample was 2,448,500 respondents. All sample sizes were rounded to the nearest hundred for institutional confidentiality, and therefore sums may not add up to totals.

The residential location was determined for all respondents based on postal codes reported in tax files between 1998 and 2010, using Statistics Canada's Postal Code Conversion File plus (PCCF+) V.6 C. The program uses a population-weighted random allocation algorithm to determine representative latitude and longitude coordinates for postal codes in Canada based on the centroid of a block-face, dissemination block (DB), or dissemination area (DA) (Statistics Canada, 2016). A block-face represents one side of a street between two consecutive intersecting features of the street. A DB is the smallest geographic area used for population and dwelling counts, and is bounded by roads or boundaries of standard geographic areas. DAs are composed of one or more adjacent dissemination blocks and represent populations of approximately 400 to 700 persons (Statistics Canada, 2016).

Postal code histories from tax files include many gaps in reporting, which makes it difficult to follow respondents over time. Incomplete postal codes histories were imputed using a method developed by Statistics Canada (Finès et al., 2017). Briefly, postal codes were imputed based on reported postal codes in years before and after the time gap in reporting, with a non-null probability that the imputed postal codes did not match. The probability that the same postal code was imputed from neighbouring postal codes decreased with increasing gap length, with a 95%, 80%, and 60% probability of the same postal code being imputed with a gap length of 1 or 2, 3 or 4, or 5 or more years, respectively. Imputed postal codes that did not match those reported before and after were assigned partial postal codes. In general, these were common characters of the first digits of postal codes, which represented a coarser-scaled division of mail delivery service (Finès et al., 2017). In cases where a postal code was not imputed from neighbouring postal codes, the missing postal code was assigned a dummy value, and the exposure was estimated as a national mean. In a validation exercise with the 1991 CanCHEC, when 5% of postal codes were randomly deleted and then imputed using the program, only 4.2% of imputed postal codes had an absolute $PM_{2.5}$ difference greater than 0.1 μg/m^3 (Finès et al., 2017). In the analytical file, 18.0% of all person-years received an imputed postal code through this process.

Based on residential locations from postal codes, all respondents were assigned an exposure estimate for each year from 1998 to 2010 (described above) based on the closest 1 km^2 grid cell of $PM_{2.5}$. In order

Table 1
Descriptive statistics of the 2001 CanCHEC and air pollution exposure, with Cox proportional hazard ratios among levels of each covariate.

Covariate	Persons	HR[a]	95% CI		$PM_{2.5}$[b]	
			Lower	Upper	Mean	SD
All	2,448,500	–	–	–	7.37	2.60
Sex						
Male	1,185,500	–	–	–	7.32	2.59
Female	1,263,000	–	–	–	7.42	2.61
Age group (years)						
25 to 29	222,100	–	–	–	7.43	2.59
30 to 39	574,400	–	–	–	7.31	2.57
40 to 49	634,900	–	–	–	7.30	2.58
50 to 59	446,000	–	–	–	7.30	2.61
60 to 69	286,700	–	–	–	7.40	2.64
70 to 79	206,200	–	–	–	7.72	2.68
80 to 89	78,100	–	–	–	7.89	2.68
Visible minority status						
White or Aboriginal[c]	2,419,700	1.000	–	–	7.36	2.60
Visible minority	28,800	0.868*	0.825	0.913	8.46	2.37
Aboriginal identity						
Not Aboriginal[c]	2,304,700	1.000	–	–	7.46	2.60
Aboriginal	143,700	1.704*	1.673	1.736	5.87	2.13
Marital status						
Single[c]	323,000	1.000	–	–	7.91	2.67
Common-law	294,700	0.788*	0.769	0.807	7.35	2.61
Married	1,491,200	0.676*	0.666	0.686	7.18	2.55
Separated	59,700	0.996	0.966	1.026	7.59	2.62
Divorced	140,700	1.006	0.985	1.028	7.88	2.61
Widowed	139,200	0.898*	0.884	0.913	7.67	2.70
Educational attainment						
Not completed high school[c]	704,400	1.000	–	–	7.08	2.63
High school with/without trades certificate	887,600	0.803*	0.795	0.810	7.31	2.58
Post-secondary non-university	473,600	0.670*	0.660	0.680	7.45	2.55
University degree	382,900	0.551*	0.542	0.561	7.92	2.58
Income adequacy quintile						
1st quintile - lowest[c]	373,600	1.000	–	–	7.49	2.67
2nd quintile	465,100	0.816*	0.807	0.825	7.41	2.64
3rd quintile	509,900	0.711*	0.702	0.720	7.37	2.60
4th quintile	537,400	0.633*	0.625	0.642	7.33	2.57
5th quintile - highest	562,600	0.536*	0.528	0.543	7.30	2.55
Labour force status						
Employed[c]	1,580,900	1.000	–	–	7.39	2.56
Unemployed	103,800	1.608*	1.559	1.659	6.73	2.62
Not in labour force	763,800	1.944*	1.917	1.971	7.43	2.67
Population Centre Size[d]						
Rural area[c]	641,800	1.000	–	–	5.47	1.96
Small pop centre (1000 to 29,999)	387,000	0.982*	0.968	0.996	6.07	2.01
Medium pop centre (30,000 to 99,999)	230,700	0.980*	0.965	0.995	7.57	2.59
Large pop centre (100,000 or more)	1,151,400	0.982*	0.972	0.993	8.74	2.40
Not assigned (dummy variable)	37,600	–	–	–	6.84	1.53
Airshed[d]						
Western[c]	265,800	1.000	–	–	6.55	1.80
Prairie	288,600	1.083*	1.062	1.104	6.39	1.78
West Central	164,900	1.115*	1.091	1.139	5.56	1.56
East Central	1,376,300	1.035*	1.021	1.049	8.45	2.61
South Atlantic	268,200	1.060*	1.041	1.079	4.82	1.57
Northern	42,500	1.121*	1.067	1.178	4.47	1.88
Not assigned (dummy variable)	42,100	–	–	–	6.87	1.60
Ecological covariates - per 10% increase						
% unemployed	–	1.082*	1.056	1.109	–	–
% not graduated high school	–	1.026*	1.020	1.031	–	–
% low income	–	0.959*	0.951	0.967	–	–

* Significant Hazard Ratio ($p < 0.05$).
[a] Hazard ratios stratified by age (5 year categories) and sex.
[b] Calculated for all person-years.
[c] Reference category.
[d] Based on first year of postal code data included or imputed for each respondent.

to ensure that exposure always preceded the event, respondents were assigned a 3-year mean value in the year preceding the follow-up year, as in Pinault et al. (2016a). For example, the mean $PM_{2.5}$ estimates from 1998 to 2000 were used for the 2001 follow-up year.

2.3. Statistical analysis

We fit standard Cox proportional hazards models (Cox, 1972) to explore the associations between exposures to $PM_{2.5}$ and non-accidental and cause-specific mortality, as described in detail below. Respondents were followed from Census year (2001) to either the year of death or the final year of follow-up (2011). All survival models were stratified by age (5-year groups) and sex. Models were adjusted for the following individual demographic and socioeconomic variables at baseline (on Census day): Aboriginal identity, visible minority status, marital status, educational attainment, income adequacy quintile, and labour force status (Table 1). Visible minority status was defined as in the *Employment Equity Act* as "persons, other than Aboriginal persons, who are not white in race or colour" (Statistics Canada, 2003). Income adequacy quintiles were calculated based on the ratio between the pre-tax income of economic families or unattached individuals to the Statistics Canada low-income cut-off for family and community size, and they are adjusted for regional differences in family economic status (e.g., housing costs) (Pinault et al., 2016b). Low-income cut-off values are the income levels at which families or individuals spend 20% more than average on food, shelter and clothing than others in their community (Statistics Canada, 2003). Labour force status was defined as employed, unemployed, or persons not in the labour force, which included persons who had left on disability, had retired, or had never worked, in the week prior to Census day (Statistics Canada, 2003). Finally, models were also stratified by population centre size and airshed. Six airsheds that share air quality characteristics and air movement patterns have been defined in Canada by the Air Quality Management System (AQMS) (Crouse et al., 2016). The east central airshed includes the large cities of Toronto and Montreal, whereas the western airshed includes the city of Vancouver, the prairie airshed includes the cities of Calgary and Edmonton, and the northern airshed includes a broad swath of the northern territories of Canada. Population centre size was derived from the PCCF+ and classified the postal code as being rural or in a small (1000 to 29,999), medium (30,000 to 99,999) or large (100,000 or greater) population centre (Statistics Canada, 2016). The large population centre size includes all Census Metropolitan Areas (the 27 largest cities in Canada, as of 2001). For all years of follow-up, respondents were assigned to one of these airsheds and population centre sizes, though some (<2%) were assigned to dummy values because of missing imputed postal codes for the person-year.

Models were also adjusted for the following contextual (ecological) covariates at the Census Division (CD) scale: the proportion of persons aged 25 or older who were unemployed, the proportion that had not graduated from high school, and the proportion of persons who were in low-income families (Table 2). There were 288 CDs in 2001. CDs represent an intermediate geographic area between province and municipality scales, and are relatively geographically stable areas, allowing their use in longitudinal studies (Statistics Canada, 2003). Covariates were derived from the 2001 Census year for the follow-up years of 2001–2003, from the 2006 Census year for 2004–2008, and from the 2011 Census year for 2009–2011. Covariates (CD means) obtained from Census were calculated using Census weights from the long-form questionnaire in 2001 and 2006, and the National Household Survey in 2011.

Covariates were added to the survival models in a sequential manner: models were created with age and sex as strata, then individual adjustment factors were added, followed by contextual covariates, and finally models were stratified by airshed and population centre size to create the fully adjusted models. The following causes of death were considered: non-accidental (ICD-10 codes A to R), cardiovascular (ICD-10: I10 to I69, with and without diabetes, E10 to E14), ischemic heart disease (ICD-10: I20 to I25), cerebrovascular disease (ICD-10: I60 to I69), non-malignant respiratory disease (ICD-10: J00-J99), chronic obstructive pulmonary disease (COPD) (ICD-10: J19 to J46), pneumonia (ICD-10: J10 to J19), and lung cancer (ICD-10: C33 to C34).

There are several limitations to our previous approach to examining the shape of the concentration-mortality association using restrict cubic splines with three knots (Crouse et al., 2015; Pinault et al., 2016a). The spline definition (number and placement of knots) was not examined to select the most appropriate structure. Second, there is no guarantee that the best fitting spline would be suitable for health impact assessment (i.e. not only monotonically increasing but display an appropriate amount of curvature). We thus turned to an alternative modeling approach using the Shape Constrained Health Impact Function (SCHIF), which characterises the shape of the association between exposure and mortality (Nasari et al., 2016). The method fits several different shapes of association as variations on sigmoidal functions. The relative risk $R(PM_{2.5})$ between concentrations of $PM_{2.5}$ and mortality are described by a family of shapes:

$$R(PM_{2.5}) = \Im(PM_{2.5})^{\eta(PM_{2.5})}.$$

Here, $\Im(PM_{2.5})$ can take on two shapes,$\Im(PM_{2.5}) = e^{PM_{2.5}}$ or $\Im(PM_{2.5}) = 1 + PM_{2.5}$. The parameter $\eta(PM_{2.5})$ is a function of $PM_{2.5}$ and a set of additional unknown parameters, (θ, μ, τ), where

$$\eta(PM_{2.5}) = \frac{\theta}{1 + \exp(-(PM_{2.5} - \mu)/(\tau \times r))},$$

with r the range in $PM_{2.5}$. The parameter τ controls the amount of curvature in η with μ controlling the shape. The magnitude of μ characterises sub-linear shapes over lower concentrations, with larger values related to wider sub-linear concentration range. Here, θ represents the logarithm of the relative risk for a unit change in the transformed concentrations $\log(\Im(PM_{2.5}))/(1 + \exp(-(PM_{2.5} - \mu)/(\tau \times r)))$.

The logarithm of the SCHIF can represent a variety of shapes, including near linear when $\Im(PM_{2.5}) = e^{PM_{2.5}}$ and $\mu < 0$. The SCHIF is supra-linear when $\Im(PM_{2.5}) = 1 + PM_{2.5}$, $\theta < 1$, and $\mu \approx 0$. The SCHIF has a threshold-type shape (no association for low concentrations and a near linear association for higher concentrations) for $\mu > 0$ and $\Im(PM_{2.5}) = e^{PM_{2.5}}$. The larger the value of μ the larger the $PM_{2.5}$ concentration corresponding to $R(PM_{2.5}) > 1$. Finally, the SCHIF can take on a sigmodal shape when $\mu > 0$, $\theta < 1$, and $\Im(PM_{2.5}) = 1 + PM_{2.5}$.

The method to estimate the SCHIF selects multiple values of $(\Im, \mu, \tau)$ and given these values, estimate θ and its standard error using standard computer software that fit the Cox proportional hazards model. In order to reduce the computational burden we perform a limited number of shapes to be examined.

We first perform Cox regressions on 16 shapes defined by the 0th, 25th, 50th, and 75th percentiles of the $PM_{2.5}$ exposure distribution to define values of μ with both specifications of $\Im$ and two values of τ(0.1 and 0.2). We find that the SCHIF displays an unreasonable amount of curvature if $\tau < 0.1$ and does not allow enough curvature when $\tau > 0.2$. We then identify the value of $(\Im, \mu, \tau)$ corresponding to the best fitting model using the log-likelihood function. We then toggle μ up and down by 5 percentile points until we achieve the best fit. Our search algorithm results in a minimum of 16 shapes fit and a maximum of 21. The SCHIF is then defined as a weighted average of the predictions of all models examined at any concentration with weights defined by the likelihood function value. Uncertainty estimates of the ensemble model predictions were obtained by bootstrap methods which incorporate both sampling and model shape uncertainty.

3. Results

A final analytical population of 2,448,500 persons were followed for up to 10.6 years (mean = 10.4 years, or 25,484,400 person-years). The mean (± standard deviation, SD) age of cohort members at baseline

Table 2
Cox proportional hazard ratios for non-accidental mortality (n = 233,300) per 10 μg/m^3 increase in $PM_{2.5}$, with stepwise addition of covariates and strata variables.

Covariate added	HR	95% CI		(−2) Log likelihood
		Lower	Upper	
Stratified by age and sex	*1.043	1.026	1.060	4,979,063
Stratified by age and sex + individual covariates added separately				
Marital status	1.000	0.984	1.016	4,973,718
Educational attainment	*1.126	1.108	1.145	4,971,245
Income adequacy quintiles	*1.024	1.007	1.041	4,970,057
Employment status	*1.051	1.034	1.068	4,969,655
Visible minority status	*1.044	1.027	1.061	4,979,030
Aboriginal identity	*1.097	1.079	1.115	4,976,266
Stratified by age and sex + all individual covariates	*1.102	1.084	1.120	4,955,833
Stratified by age and sex + all individual covariates + ecological covariates added separately				
% unemployed (aged 25 and older)	*1.086	1.068	1.105	4,955,774
% not graduated from high school (aged 25 and older)	*1.060	1.042	1.079	4,955,700
% low income status	*1.129	1.110	1.149	4,955,753
Stratified by age and sex + all individual covariates + all ecological covariates	*1.087	1.068	1.107	4,955,545
Stratified by age and sex + all individual covariates + all ecological covariates + new strata				
Stratified by age, sex, airshed + all individual covariates + all ecological covariates	*1.126	1.102	1.151	4,303,714
Stratified by age, sex, population centre size + all individual covariates + all ecological covariates	*1.081	1.059	1.103	4,301,452
Stratified by age, sex, airshed, population centre size + all individual covariates + all ecological covariates	*1.177	1.148	1.207	3,809,238

* Significant HR ($p < 0.05$).

was 48.4 (± 15.0) years. The mean $PM_{2.5}$ exposure (± SD) of respondents from the 3-year moving average was 7.4 (± 2.6) μg/m^3 (Table 1), with the following percentiles: min < 0.01 μg/m^3, 5th = 3.51 μg/m^3, 25th = 5.37 μg/m^3, 50th = 7.12 μg/m^3, 75th = 9.07 μg/m^3, 95th = 11.97 μg/m^3, max = 20.00 μg/m^3. During the follow-up period, the age/sex adjusted mortality rate was 1012.5 per 100,000. In general, air pollutant mean exposures were similar across most socio-demographic characteristics (Table 1), although they were greater for visible minority and lower for Aboriginal populations, and varied across airsheds. The distribution of $PM_{2.5}$ across different airsheds and population centre size categories is provided in Supplementary Table 1. In general, $PM_{2.5}$ exposures were higher in increasing population centre sizes, and were particularly large in the east central airshed, where two of the largest cities in Canada (i.e., Toronto and Montreal) are located. The contextual covariates at the CD scale did not differ substantially across Census years, representing a median of 4.1–5.8% unemployed, 23.6–27.5% not graduated from high school, and 10.2–14.6% low income status (Supplementary Table 2). The contextual covariates were weakly correlated to $PM_{2.5}$ exposures (Supplementary Table 2). The population characteristics of the cohort are provided by $PM_{2.5}$ quintile in Supplementary Table 3.

Separate Cox survival models for non-accidental mortality were carried out for all covariates used in subsequent survival models (Table 1). In general, lower mortality HRs were observed for persons of visible minority, common-law, married or widowed (versus single), increasingly higher educational attainment, and increasingly higher income. Higher mortality HRs were observed for Aboriginal respondents, and persons who were unemployed or not in the labour force. Hazard ratios also varied across geographical regions, with higher HRs observed in rural areas (vs. population centres) and in certain airsheds.

All individual and contextual covariates, as well as strata variables, were added in a stepwise manner to a model for non-accidental mortality. Additional variables and strata improved model fit, as evidenced by log-likelihood values (Table 2). In general, the addition of individual covariates strengthened the association between $PM_{2.5}$ and non-

Table 3
Cox proportional survival model hazard ratios for different causes of mortality per 10 μg/m^3 increase in $PM_{2.5}$.

	Deaths[a]	Unadjusted[b]			Adjusted: individual covariates[c]			Adjusted: individual + ecological covariates[d]			Fully adjusted[e]		
		HR	95% CI		HR	95% CI		HR	95% CI		HR	95% CI	
			Lower	Upper		Lower	Upper		Lower	Upper		Lower	Upper
Non-accidental	233,300	*1.043	1.026	1.060	*1.102	1.084	1.120	*1.087	1.068	1.107	*1.177	1.148	1.207
Cardiovascular	69,000	0.984	0.955	1.014	*1.037	1.006	1.068	*1.048	1.013	1.083	*1.246	1.190	1.305
Cardiovascular + diabetes	77,000	0.978	0.951	1.006	*1.048	1.019	1.078	*1.068	1.035	1.102	*1.268	1.214	1.325
Ischemic heart disease	40,400	*1.094	1.053	1.137	*1.158	1.114	1.204	*1.184	1.134	1.236	*1.355	1.276	1.439
Cerebrovascular disease	13,300	*0.816	0.762	0.874	*0.855	0.797	0.916	*0.857	0.794	0.926	1.110	0.998	1.235
Respiratory	21,100	0.948	0.898	1.001	1.038	0.982	1.097	1.011	0.951	1.075	*1.216	1.116	1.324
COPD	11,900	*0.888	0.826	0.955	0.962	0.895	1.035	1.001	0.923	1.086	*1.238	1.106	1.386
Pneumonia	4,600	0.915	0.813	1.030	1.006	0.892	1.134	0.918	0.804	1.049	*1.210	1.004	1.457
Lung cancer	23,900	*1.128	1.073	1.186	*1.206	1.146	1.268	*1.168	1.104	1.236	*1.158	1.072	1.252

[a] Rounded to nearest 100.
[b] Stratified by age (5 year categories), sex.
[c] Stratified by age (5 year categories), sex, and adjusted for visible minority identity, Aboriginal identity, marital identity, educational attainment, income quintile, and labour force identity.
[d] Stratified by age (5 year categories), sex, and adjusted for visible minority identity, Aboriginal identity, marital identity, educational attainment, income quintile, and labour force identity, and also for the % unemployed (aged 25 and older), % not graduated from high school (aged 25 and older), and % low income identity, for CDs.
[e] Stratified by age (5 year categories), sex, airshed and population centre size, and adjusted for visible minority status, Aboriginal identity, marital status, educational attainment, income quintile, and labour force status, and also for the % unemployed (aged 25 and older), % not graduated from high school (aged 25 and older), and % low income status, for CDs.

accidental mortality, while the subsequent addition of contextual covariates attenuated this association. Stratifying the model by airshed and population centre size improved model fit substantially, and also inflated HRs when both strata were used together.

Models for the association between $PM_{2.5}$ and mortality were created for nine causes of death. In fully adjusted models, HR estimates for non-accidental mortality were 1.18 (95% C.I.: 1.15–1.21) per 10 μg/m^3 increase in $PM_{2.5}$ (Table 3). Notably high HRs were observed for cardiovascular disease (HR = 1.25; 95% CI: 1.19–1.31), cardio-metabolic disease (HR = 1.27; 95% CI: 1.21–1.33), ischemic heart disease (HR = 1.36; 95% C.I.: 1.28–1.44 per 10 μg/m^3 increase) and COPD mortality (HR = 1.24; 95% C.I.: 1.11–1.39 per 10 μg/m^3 increase). The hazard ratios were smaller for cerebrovascular disease in fully adjusted models.

To illustrate the family of shapes considered we plotted the predicted value of the SCHIF by $PM_{2.5}$ for each curve for COPD (solid blue line in Fig. 1). The thickness of the line is proportional to the weight. There are a variety of shapes examined, from near linear, sub-linear, and supra-linear. In this case, the best fitting shape is supra-linear (thickest solid blue line). The ensemble curve is also displayed (dashed black line) showing less curvature at the origin compared to the best fitting shape. A linear in concentration curve is also displayed (solid red line). The difference in −2LL between the best fitting model and the linear model is 7.5. Since the SCHIF family of curves does not strictly contain a linear model we cannot compare the fit using a likelihood ratio test. However, if we consider the SCHIF to be defined by four unknown parameters ($\Im$, μ, τ, θ) and the linear model with a single parameter, the AIC difference for improved fit would be 6, suggesting that the best fitting shape has improved predictive power over the linear model. The differences in −2LL for non-accidental deaths was 37, cardio-metabolic deaths was 48, cardiovascular was 36, ischemic heart disease was 27, non-malignant respiratory disease was 9, and lung cancer was 7. These results suggested that there is some evidence that the association between long-term $PM_{2.5}$ exposure and mortality is non-linear in this cohort.

The concentration-response curves for various causes of death in fully adjusted models are presented in Fig. 2. The minimum concentration in the models (0 μg/m^3) was used to specify the reference concentration, at which the hazard function was equal to 1. In general, the shape of the curves for most causes of death (other than pneumonia, cerebrovascular disease and lung cancer) was supra-linear, with the greatest increase in the lower ranges of exposure (Fig. 2). Since the concentration-response curves were non-linear, we also provide an alternative method of describing the shape of the $PM_{2.5}$-mortality association by estimating HRs in ranges of $PM_{2.5}$ concentrations (0–5, 5–10, and >10 μg/m^3) for the causes of death outlined in Fig. 2 (Supplementary Table 4) assuming a linear in concentration model within each range. Mortality HRs were larger for the <5 μg/m^3 range than the other two ranges for all causes of death examined expect lung cancer, a pattern also observed using our SCHIF model. For lung cancer, we observed a pattern with a low (negative) HR estimate in the lowest range, a high estimate in the middle range, and a moderate estimate in the highest range. A similar pattern was also observed with our SCHIF model (Fig. 2).

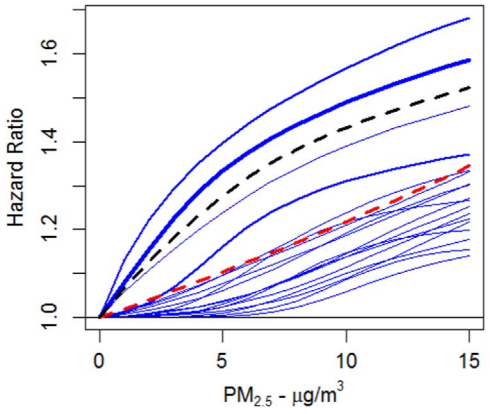

Fig. 1. Predicted values of the family of shapes examined by the Shape Constrained Health Impact Function (solid blue lines) with line thickness proportional to model fit. Ensemble of family of shapes (dashed black line) and linear in concentration (dashed red line) are also displayed. (For interpretation of the references to color in this figure legend, the reader is referred to the web version of this article.)

4. Discussion

In our large Canadian cohort, exposure to ambient $PM_{2.5}$ was associated with an increased risk of non-accidental mortality, with HR = 1.18 per 10 μg/m^3 increase in concentration in a model adjusted for many individual and contextual covariates. The highest HRs were those of associations between $PM_{2.5}$ with ischemic heart disease and cardio-metabolic disease, while weaker associations were observed between $PM_{2.5}$ with cerebrovascular disease. Importantly, the association at the lowest concentrations appeared to be supra-linear for most causes of death.

One notable strength of this study was that it used a large, national cohort based on a census of population, which provides a sample population that is largely representative of the population of Canada. The timing of the cohort and its follow-up period corresponded to annual estimates of air pollution, thus avoiding misalignment in applying more recent estimates for historical exposure. As a result, it was also possible to assign exposures using a 3-year average window, occurring prior to any follow-up year and death event.

An important development in this study over previous ones was the use of a finer-scale and more accurate national $PM_{2.5}$ model that provided estimates on an approximate 1 km^2 grid, and explained 23% more variance (82% vs. 59%) in $PM_{2.5}$ measured by ground-based monitors, compared with previously used models (e.g., van Donkelaar et al., 2010; Crouse et al., 2012). This change in scale was particularly critical for small to large-sized cities, where the previous exposure model often underestimated exposures. For example, in Calgary, Alberta (2011 population = 1,096,833), a typical $PM_{2.5}$ estimate in the city core was approximately 11 μg/m^3 in the new model and 8 μg/m^3 in the previous model, due to estimates in the previous model being averaged over a larger area. In southern Ontario, the small city of Chatham-Kent (2011 population = 101,700), the $PM_{2.5}$ estimate in the city core was 10.5 μg/m^3 in the current model and 13.8 μg/m^3 in the previous model, while just outside the city core it was 6.5 μg/m^3 in the current model and 13.0 μg/m^3 in the previous model (Statistics Canada, 2011). Similarly, our current model more clearly resolved gradients associated with clean air in rural areas. For example, rural areas west of Kitchener, Ontario, were estimated at 10.9 μg/m^3 in the previous model, but only 3.5 μg/m^3 in the our current model.

In our earlier study with coarse-scaled $PM_{2.5}$, incorporating annual residential mobility patterns did not have a significant impact on the results of our survival models, due in part to the fact that differences in exposures related to movements within an urban area may not have been captured (Crouse et al., 2015). For example, subjects would not be assigned different exposure estimates in situations where they moved anywhere within 10 km of their original location. In the case of this study, however, in which we used a finer-scale $PM_{2.5}$ model, we likely reduced exposure misclassification, particularly among subjects who moved during the follow-up period. The addition of a new imputation for missing postal codes allowed these persons to be considered throughout the follow-up period, and a more complete follow-up history to be considered.

Stratifying the analysis by airshed and population centre size, in addition to age and sex, ensured that persons living in similar environments were compared to their peers. This step adjusted for potential confounding from local influences upon health, such as availability of health services, as well as known neighbourhood influences

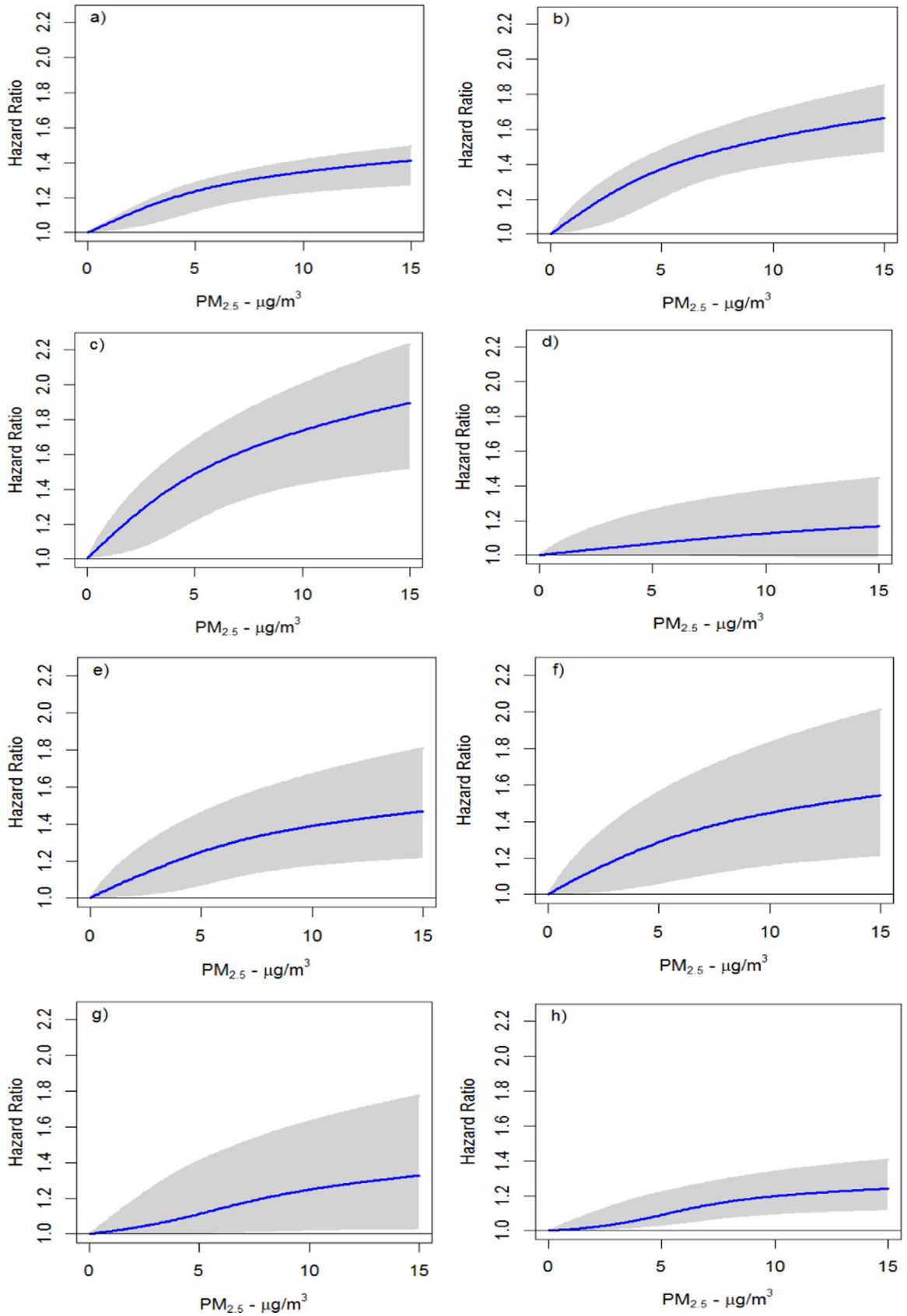

Fig. 2. Ensemble concentration-mortality model predictions (blue solid line) and 95% confidence intervals (grey shaded area) by cause of death: a) non-accidental, b) cardio-metabolic, c) ischemic heart disease, d) cerebrovascular, e) non-malignant respiratory diseases, f) chronic obstructive pulmonary disease, g) pneumonia, h) lung cancer. (For interpretation of the references to color in this figure legend, the reader is referred to the web version of this article.)

upon health. For example, the Ontario Tax Cohort (n = 548,000) was followed for a 22 year follow-up period. After adjusting for individual socioeconomic status, elevated mortality risk was associated with living in the most socially and materially deprived neighbourhoods (HRs ranged between 1.09 and 1.15) (Ross et al., 2013). Similarly, mortality rates are higher in increasingly rural areas that are less influenced by metropolitan areas (Pong et al., 2009). However, it is important to note that stratifying by both airshed and population centre size inflated the HRs substantially from fully adjusted models without these strata.

In comparison to the results of the 1991 CanCHEC analyses, our estimates of HRs were somewhat higher. For non-accidental mortality, HRs reported by Crouse et al. (2015) of HR = 1.04 (95% CI: 1.03–1.04) per 5 μg/m^3 increase (Cochran's Q = 39.5, $p < 0.001$) were lower than our (re-scaled) HR of 1.09 (95% CI: 1.07–1.10). Similarly, our estimate of ischemic heart disease risk (re-scaled HR = 1.16; 95% CI: 1.13–1.20) was significantly greater than that of Crouse et al. (2015) of HR = 1.09 (95% CI: 1.07–1.10) per 5 μg/m^3 increase (Cochran's Q = 16.3, $p < 0.001$). These higher HRs may be due to the addition of the population centre size and airshed as new model strata. Indeed, when we excluded these new strata from our models, our HRs were consistent with those in the literature (i.e., non-accidental mortality HR = 1.08 (95% CI: 1.06–1.10)). Differences in ischemic heart disease mortality have been associated with different sources and mass constituents of $PM_{2.5}$ (Thurston et al., 2016). Changes to the source and type of $PM_{2.5}$ measured over the past decade may also have an influence on the strength of association with mortality.

Our results were broadly consistent with studies conducted elsewhere. Associations between $PM_{2.5}$ and non-accidental mortality were within the same range as that reported by ESCAPE (1.07; 95% CI: 1.02–1.13 per 5 μg/m^3 increase) (Beelen et al., 2014). Non-accidental mortality associations were higher than those reported in older cohort studies, such as the American Cancer Society study (HR = 1.06; 95% CI: 1.02–1.11; Pope et al., 2002), as well as a global pooled meta-analysis (HR = 1.06; 95% CI: 1.04–1.08; Hoek et al., 2013). Associations between cardiovascular mortality and $PM_{2.5}$ air pollution in our cohort (HR = 1.25) were generally also greater than those in other cohorts and meta-analyses, including the global pooled meta-analysis (HR = 1.11; 95% CI: 1.05–1.16) (Hoek et al., 2013), and the Dutch Environmental Longitudinal Study (DUELS) (HR = 1.09; 95% CI: 1.06–1.12) (Fischer et al., 2015). Our higher results may be due to the inclusion of location-specific strata variables as well as the supra-linear nature of $PM_{2.5}$-mortality associations, as suggested by Burnett et al. (2014), since our study exposures are at the extreme lower end of the global exposure distribution (Brauer et al., 2016).

Our estimate for the association between non-malignant respiratory mortality with $PM_{2.5}$ (HR = 1.22) was within the broad range of those reported in the literature, for example, in DUELS (HR = 1.18) and the California Teachers study (HR = 1.21) (Ostro et al., 2010; Fischer et al., 2015). In the ESCAPE cohort, lung cancer associations with $PM_{2.5}$ were stronger than in our study (HR = 1.18; 95% CI: 0.96–1.46 per 5 μg/m^3 increase), though CI were wide and overlapped with ours (Raaschou-Nielsen et al., 2013).

There were some important limitations in this study. First, although estimates of exposure were assigned more accurately than in previous studies, they are still derived by assigning exposures based on a place of residence according to a postal code. We possibly underestimate exposure for the working-age population who live in areas of lower air pollution (i.e., the suburbs) and who commute into regions of higher air pollution exposure. Since the majority of deaths occur among the older population, this difference in exposure may have little effect on overall HR estimates. While the placement of postal codes in urban centres is relatively accurate since it is usually based on a block face, the accuracy in rural areas is likely far less so. We were also unable to account for the exact date where participants may have moved to a different postal code, resulting in further misclassification. However, the misclassification of exposure may be mitigated somewhat by the generally lower variation in exposures across the rural landscape. Second, exposures were based on outdoor estimates at a person's place of residence, and ignore exposures that occur at work or in other locations. Further refinement of models to include place of work might provide a more accurate estimate of exposures. Our models were relatively robust to the imputation of postal codes and $PM_{2.5}$ estimates (non-accidental mortality HR prior to imputation was the same). Third, our cohort included some exclusions, including persons who had not filed any taxes, as well as all immigrants. Although very few persons were excluded based on taxes, the generalizability of these findings is relatively limited to the non-immigrant portion of Canadians, and a follow-up study focusing on immigrant exposures may be warranted.

We observed a near linear association between $PM_{2.5}$ and all non-accidental and several specific causes of death for lower concentrations, with less change in relative risk for higher concentrations. We do not observe any evidence to suggest that the association is sub-linear over the lowest concentrations. A diminished change in relative risk at higher concentrations has been previously suggested (Pope et al., 2009, 2011a, 2011b) and relative risk models have been based on this assumption (Burnett et al., 2014) to create global burden of disease estimates. However, we suggest that the biological mechanism of saturation is unlikely to be the reason for the observed non-linear pattern at the very low concentrations observed in the present study.

We did not have reported information on several behavioural risk factors, such as smoking habits, obesity, diet, and alcohol consumption. In another nationally representative cohort in Canada based on repeated health surveys whose subjects were linked to vital status, we observed a similar supra-linear association, as evidenced by fitting restricted cubic splines (Pinault et al., 2016a). The same follow-up period (2001–2011) and $PM_{2.5}$ exposure model was used as the current study. Although we cannot completely rule out residual confounding by missing risk factors, we suggest that it is unlikely since the Pinault et al. (2016a) study did adjusted for these behavioural risk factors. However, smoking is the strongest risk factor for both malignant and non-malignant respiratory diseases, and a small, positive interaction between smoking and $PM_{2.5}$ exposure has been observed in the American Cancer Society Cancer Prevention Study-II (Turner et al., 2017).

We also note that in a study of 60 million MEDICARE participants in the continental United States (Di et al., 2017), when $PM_{2.5}$ concentrations above 12 μg/m^3 were removed, the effect estimate per 10 μg/m^3 change in $PM_{2.5}$ greatly increased from 7.3% (95% CI: 7.1–7.5%) with all the exposure data, to 13.6% (13.1–14.1%) for exposures less than 12 μg/m^3. The lowest concentration in that study was 5 μg/m^3, and thus these authors could not direct investigate the shape of the concentration-mortality association at lower levels. We observed a similar effect estimate of 13.3 (9.3–17.4) over the 5–12 μg/m^3 exposure range in the current study. However, in our study, 25% of person-years of follow-up were assigned $PM_{2.5}$ exposures below 5 μg/m^3, enabling us to examine the association at these lower levels (Supplementary Table 4). The effect estimate over the 0–5 μg/m^3 range for all non-accidental deaths in our study was 23.7% (8.7–49.1%), a much larger value than in the 5–12 μg/m^3 range observed in this study and the MEDICARE cohort. In both the MEDICARE cohort and our study, the supra-linear association could be due to increasing measurement error as concentration increases (Sheppard et al., 2012) and thus this possibility cannot also be ruled out.

However, we suggest the most likely reason for the observed non-linear pattern is that the physical and chemical composition of the atmosphere is likely changing, even over the very narrow range in $PM_{2.5}$ concentrations. The chemical composition of the atmosphere has been shown in another Canadian cohort, based on linking the respondents of the 1991 long-form census to vital status up to 2006, to improve predictive power in addition to $PM_{2.5}$ mass (Crouse et al., 2016). Penalized smoothing splines were used to examine the shape of the component-mortality association. Although shapes did vary by component (sulfate, nitrate, carbon, dust, organic matter, and ammonium), there was no

evidence of a sub-linear association, with a supra-linear shape observed for many components.

Another possible explanation for the supra-linear concentration-response curves is that the relative abundance of components and properties of $PM_{2.5}$ responsible for health effects vary across the exposure distribution. For example, we previously reported that oxidative potential can modify both the acute and chronic health impacts of $PM_{2.5}$ (Weichenthal et al., 2016a, 2016b, 2016c), and thus the shape of the relationship between $PM_{2.5}$ and mortality may also depend on the oxidative potential of particles across the gradient of mass concentrations. In turn, the oxidative potential of $PM_{2.5}$ is influenced by components including transition metals, quinones, and polycyclic aromatic hydrocarbons (Crobeddu et al., 2017) and if the relative abundance of these components (or others) is greater at lower $PM_{2.5}$ mass concentrations this may explain a steeper slope at lower $PM_{2.5}$ levels (i.e. each unit change in $PM_{2.5}$ at low levels may contain more "active" substances compared to a similar change at higher concentrations). Ultimately, more work is needed to understand the specific components and properties of $PM_{2.5}$ that determine health effects before we can arrive at a more complete understanding of the shape of concentration-response curves at low mass concentrations. Given the heterogeneous nature of $PM_{2.5}$, there is no reason to believe that a single shape is appropriate for all studies and populations as spatial differences in components (or properties such as oxidative potential) likely play an important role in determining the functional form of these associations.

Using an updated, large Canadian census cohort, we refined our previous air pollution exposure estimation methods by using a finer-scale exposure model at a 1 km^2 grid, following respondent mobility using a linkage to tax files, and imputing missing postal codes to generate a more complete residential history for cohort members. In general, these improvements in methodology produced greater hazard ratios for non-accidental and specific causes of death, than those previously reported in Canada.

Funding sources

Research described in this article was conducted under contract to the Health Effects Institute (HEI), an organization jointly funded by the United States Environmental Protection Agency (EPA) (Assistance Award No. R-82811201) and certain motor vehicle and engine manufacturers. The contents of this article do not necessarily reflect the views of HEI, or its sponsors, nor do they necessarily reflect the views and policies of the EPA or motor vehicle and engine manufacturers.

Appendix A. Supporting information

Supplementary data associated with this article can be found in the online version at http://dx.doi.org/10.1016/j.envres.2017.08.037.

References

Beelen, R., Raaschou-Nielsen, O., Stafoggia, M., Jovanovic Andersen, Z., Weinmayr, G., Hoffman, B., et al., 2014. Effects of long-term exposure to air pollution on natural-cause mortality: an analysis of 22 European cohorts within the multicentre ESCAPE project. Lancet 383, 785–795.

Boys, B.L., Martin, R.V., van Donkelaar, A., MacDonell, R.J., Hsu, N.C., Cooper, M.J., Yantosca, R.M., Lu, Z., Streets, D.G., Zhang, Q., Wang, S.W., 2014. Fifteen-year global time series of satellite-derived fine particulate matter. Environ. Sci. Technol. 48, 11109–11118.

Brauer, M., Freedman, G., Frostad, J., van Donkelaar, A., Martin, R.V., Dentener, F., et al., 2016. Ambient air pollution exposure estimation for the global burden of disease 2013. Environ. Sci. Technol. 50 (1), 79–88.

Burnett, R.T., Pope, C.A.I.I., Ezzati, M., Olives, C., Lim, S.S., Mehta, S., et al., 2014. An integrated risk function for estimating the global burden of disease attributable to ambient fine particulate matter exposure. Environ. Health Perspect. 122 (4), 397–403.

Cox, D.R., 1972. Regression models and life tables. J. R. Stat. Soc. B 20, 187–220.

Crobeddu, B., Aragao-Santiago, L., Bui, L.C., Boland, S., Squiban, A.B., 2017. Oxidative potential of particulate matter PM2.5 as predictive indicators of cellular stress. Environ. Poll. 230, 125–133.

Crouse, D.L., Peters, P.A., van Donkelaar, A., Goldberg, M.S., Villeneuve, P.J., Brion, O., Khan, S., Odwa Atari, D., Jerrett, M., Pope III, C.A., Brauer, M., Brook, J.R., Martin, R.V., Stieb, D., Burnett, R.T., 2012. Risk of nonaccidental and cardiovascular mortality in relation to long-term exposure to low concentrations of fine particulate matter: a Canadian national-level cohort study. Environ. Health Perspect. 120, 708–714.

Crouse, D.L., Peters, P.A., Hystad, P., Brook, J.R., van Donkelaar, A., Martin, R.V., Villeneuve, P.J., Jerrett, M., Goldberg, M.S., Pope III., C.A., Brauer, M., Brook, R.D., Robichaud, A., Menard, R., Burnett, R., 2015. Ambient PM2.5, O3, and NO2 exposures and associations with mortality over 16 years of follow-up in the Canadian Census Health and Environment Cohort (CanCHEC). Environ. Health Perspect. 123, 1180–1186.

Crouse, D.L., Philip, S., van Donkelaar, A., Martin, R.V., Jessiman, B., Peters, P.A., Weichenthal, S., Brook, J.R., Hubbell, B., Burnett, R.T., 2016. A new method to jointly estimate the mortality risk of long-term exposure to fine particulate matter and its components. Sci. Rep. 6, 18916.

Di, Q., Wang, Y., Zanobetti, A., Wang, Y., Koutrakis, P., Choirat, C., Dominici, F., Schwartz, J.D., 2017. Air pollution and mortality in the Medicare population. N. Engl. J. Med. 376 (26), 2513–2522.

Fellegi, I.P., Sunter, A.B., 1969. A theory for record linkage. J. Am. Stat. Assoc. 64, 1183–1210.

Finès, P., Pinault, L., Tjepkema, 2017. Imputing postal codes to analyze ecological variables in longitudinal cohorts: exposure to particulate matter in the Canadian Census Health and Environment Cohort Database. Analytical Studies: Methods and References. Statistics Canada. Cat. 11-633-X.

Fischer, P.H., Marra, M., Ameling, C.B., Hoek, G., Beelen, R., de Hoogh, K., et al., 2015. Air pollution and mortality in seven million adults: the Dutch Environmental Longitudinal Study (DUELS). Environ. Health Perspect. http://dx.doi.org/10.1289/ehp.1408254.

GBD 2016 Risk Factors Collaborators, 2016. Global, regional, and national comparative risk assessment of 79 behavioural, environmental and occupational, and metabolic risks or clusters of risks, 1990–2015: a systematic analysis for the Global Burden of Disease Study. Lancet 388, 1659–1724.

Hoek, G., Krishnan, R.M., Beelen, R., Peters, A., Ostro, B., Brunekreef, B., Kaufman, J.D., 2013. Long term air pollution exposure and cardio-respiratory mortality: a review. Environ. Health 12, 43.

Nasari, M.M., Szyszkowicz, M., Chen, H., Crouse, D., Turner, M.C., Jerrett, M., Pope III, C.A., Hubbell, B., Fann, N., Cohen, A., Gapstur, S.M., Diver, R., Stieb, D., Forouzanfar, M.H., Kim, S.-Y., Olives, C., Krewski, D., Burnett, R.T., 2016. A class of non-linear exposure-response models suitable for health impact assessment applicable to large cohort studies of ambient air pollution. Air Qual. Atmos. Health 9 (8), 961–972.

Newbold, K.B., 2005. Self-rated health within the Canadian immigrant population: risk and the healthy immigrant effect. Soc. Sci. Med. 60, 1359–1370.

Ng, E., 2011. The healthy immigrant effect and mortality rates. Health Rep. 22, 4.

Ostro, B., Lipsett, M., Reynolds, P., Goldberg, D., Hertz, A., Garcia, C., et al., 2010. Long term exposure to constituents of fine particulate air pollution and mortality: results from the California Teachers Study. Environ. Health Perspect. 118, 363–369.

Pinault, L., Tjepkema, M., Crouse, D.L., Weichenthal, S., van Donkelaar, A., Martin, R.V., Brauer, M., Chen, H., Burnett, R.T., 2016a. Risk estimates of mortality attributed to low concentrations of ambient fine particulate matter in the Canadian Community Health Survey cohort. Environ. Health 15, 18.

Pinault, L., Finès, P., Labrecque-Synnott, F., Saidi, A., Tjepkema, M., 2016b. The Canadian Census-Tax-Mortality Cohort: A 10-Year Follow-Up. Anal. Studies: Methods Ref. Statistics Canada. No. 11-633-X. no. 003.

Pinault, L., van Donkelaar, A., Martin, R.V., 2017. Exposure to fine particulate matter air pollution in Canada. Health Rep. 28 (3), 9–16.

Pong, R.W., Desmeules, M., Lagacé, C., 2009. Rural-urban disparities in health: how does Canada fare and how does Canada compare with Australia? Aust. J. Rural Health 17 (1), 58–64.

Pope, C.A., Burnett, R.T., Thun, M.J., Calle, E.E., Krewski, D., Ito, K., Thurston, G.D., 2002. Lung cancer, cardiopulmonary mortality, and long-term exposure to fine particulate air pollution. J. Am. Med. Assoc. 287 (9), 1132–1141.

Pope, C.A., Burnett, R.T., Krewski, D., Jerrett, M., Shi, Y., Calle, E.E., Thun, M.J., 2009. Cardiovascular mortality and exposure to airborne fine particulate matter and cigarette smoke: shape of the exposure-response relationship. Circulation 120, 941–948.

Pope, C.A., Brook, R.D., Burnett, R.T., Dockery, D.W., 2011a. How is cardiovascular disease mortality risk affected by duration and intensity of fine particulate matter exposure? An integration of the epidemiologic evidence. Air Qual. Atmos. Health 4 (1), 5–14.

Pope, C.A., Burnett, R.T., Turner, M.C., Cohen, A., Krewski, D., Jerrett, M., Gapstur, S.M., Thun, M.J., 2011b. Lung cancer and cardiovascular disease mortality associated with ambient air pollution and cigarette smoke: shape of the exposure-response relationships. Environ. Health Perspect. 119 (11), 1616–1621.

Raaschou-Nielsen, O., Zorana, A., Beelen, R., Samoli, R., et al., 2013. Air pollution and lung cancer incidence in 17 European cohorts: prospective analyses from the European Study of Cohorts for Air Pollution Effects (ESCAPE). Lancet Oncol. 14, 813–822.

Ross, N.A., Oliver, L.N., Villeneuve, P.J., 2013. The contribution of neighbourhood material and social deprivation to survival: a 22-year follow-up of more than 500,000 Canadians. Int. J. Environ. Res. Publ. Health 10, 1378–1391.

Sheppard, L., Burnett, R.T., Szpiro, A.A., Kim, S.-Y., Jerrett, M., Pope, C.A., Brunekreef, B., 2012. Confounding and exposure measurement error in air pollution epidemiology. Air Qual. Atmos. Health 5 (2), 203–216.

Statistics Canada, 2003. 2001 Census Dictionary. Statistics Canada (Cat No. 92-378-XIE).

Statistics Canada, 2011. Census of Population, Highlight Tables, 2011 Census.

Statistics Canada, 2016. Postal CodeOM Conversion File Plus (PCCF+) Version 6C, Reference Guide. Statistics Canada (Cat no. 82-F0086-XDB).
Thurston, G.D., Burnett, R.T., Turner, M.C., Shi, Y., Krewski, D., Lall, R., Ito, K., Jerrett, M., Gapstur, S.M., Diver, W.R., Pope III, C.A., 2016. Ischemic heart disease mortality and long-term exposure to source-related components of U.S. fine particle air pollution. Environ. Health Perspect. 124, 785–794.
Turner, M.C., Cohen, M., Burnett, R.T., Jerrett, M., Diver, W.R., Gapstur, S.M., 2017. Interactions between cigarette smoking and ambient PM2.5 for cardiovascular mortality. Environ. Res. 154, 304–310.
van Donkelaar, A., Martin, R.V., Brauer, M., Kahn, R., Levy, R., Verduzco, C., et al., 2010. Global estimates of ambient fine particulate matter concentrations from satellite-based aerosol optical depth: development and application. Environ. Health Perspect. 118, 847–855.
van Donkelaar, A., Martin, R.V., Spurr, R.J.D., Burnett, R.T., 2015. High resolution satellite-derived PM2.5 from optical estimation and geographically weighted regression over North America. Environ. Sci. Technol. 49 (17), 10482–10491.
Weichenthal, S., Lavigne, E., Evans, G., Godri-Pollitt, K.J., Burnett, R., 2016a. Ambient PM2.5 and risk of emergency room visits for myocardial infarction: impact of regional PM2.5 oxidative potential: a case-crossover study. Environ. Health 15, 46.
Weichenthal, S., Lavigne, E., Evans, G., Godri-Pollitt, K.J., Burnett, R., 2016b. PM2.5 and risk of emergency room visits for respiratory illness: Effect modification by oxidative potential. Am. J. Respir. Crit. Care Med. 94, 577–586.
Weichenthal, S., Crouse, D.L., Godri-Pollitt, K., Evans, G., van Donkelaar, A., Martin, R., Burnett, R., 2016c. Oxidative burden of fine particulate air pollution and risk of cause-specific mortality in the Canadian Census Health and Environment Cohort (CanCHEC). Environ. Res. 146, 92–99.
Wilkins, R., Tjepkema, M., Mustard, C., Choinière, R., 2008. The Canadian census mortality follow-up study, 1991 through 2001. Health Rep. 19, 25–43.